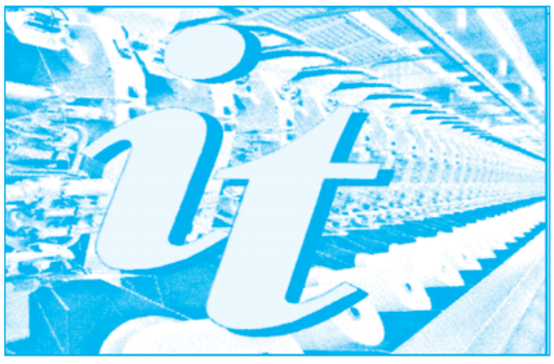

Industria Textilă

ISSN 1222–5347

3/2026

ISI rated *journal, included in the* ***ISI Master Journal List*** *of the Institute of Science Information, Philadelphia, USA, starting with vol. 58, no. 1/2007, with* ***impact factor 1.0 and AIS 0.091 in 2025.***

The journal is indexed by CrossRef, starting with no. 1/2017 having the title DOI: https://doi.org/10.35530/IT.

Edited in 6 issues per year, indexed and abstracted in:

Science Citation Index Expanded (SCIE), Materials Science Citation Index®, Journal Citation Reports/Science Edition, World Textile Abstracts, Chemical Abstracts, VINITI, Scopus, Toga FIZ technik, EBSCO, ProQuest Central, Crossref

EDITORIAL STAFF

General Manager: Dr. Eng. Alexandra-Gabriela Ene
Editor-in-chief: Dr. Eng. Sabina Olaru
Onorific editor: Dr. Eng. Emilia Visileanu
Graphic designer: Florin Prisecaru
Translator: Cătălina Costea
Site administrator: Constantin Dragomir
e-mail: industriatextila@incdtp.ro

INDUSTRIA TEXTILA journal, edited by INCDTP BUCHAREST, implements and respects Regulation 2016/679/EU on the protection of individuals with regard to the processing of personal data and on the free movement of such data ("RGPD"). For information, please visit the Personal Data Processing Protection Policy link or e-mail to DPO rpd@incdtp.ro

Aknowledged in Romania, in the Engineering sciences domain, by the National Council of the Scientific Research from the Higher Education (CNCSIS), in group A
Journal edited in colaboration with **Editura AGIR**, 118 Calea Victoriei, sector 1, Bucharest, tel./fax: 021-316.89.92; 021-316.89.93; e-mail: editura@agir.ro, www.edituraagir.ro

China's textile export potential to South Asian countries and its determinants

DOI: 10.35530/IT.077.03.202562

LIQIN WEN
JIE XU
WENXUE ZOU
XUE LEI
SHENGLIN MA

ABSTRACT – REZUMAT

China's textile export potential to South Asian countries and its determinants

Against the backdrop of the Belt and Road Initiative and the restructuring of the global textile supply chain, this paper analyses textile trade patterns between China and the seven South Asian countries, using China's textile export data to these countries from 2010 to 2023, with a focus on textile exports. It employs a stochastic frontier gravity model for empirical analysis to assess the potential and influencing factors of textile trade between China and the seven South Asian countries, and provides feasible suggestions for the development of textile trade between China and South Asian nations. The study finds that the scale of textile trade between China and South Asian countries has been expanding, with trade relations becoming increasingly close. However, the scale of imports and exports remains relatively small. In terms of influencing factors, the study finds that China's economic size has a significant inhibitory effect on textile exports. In contrast, China's population size, the economic development level and population size of South Asian countries, as well as straight-line distance and whether they share a common border, have a positive impact on textile exports. However, the influence of the Shanghai Cooperation Organisation on China's textile exports is relatively weak, with limited promotional effects; government efficiency indices, free trade agreements, currency flexibility, and economic freedom scores all have a positive promotional effect on textile export efficiency. However, trade freedom has a negative impact on trade efficiency; although China's textile export trade efficiency with the seven South Asian countries remains at a relatively low level, there is significant trade potential and room for expansion, with broad prospects for future development.

Keywords: *China, South Asia, textiles, stochastic frontier gravity model, export trade efficiency*

Potențialul Chinei în materie de exporturi textile către țările din Asia de Sud și factorii determinanți

În contextul Inițiativei „Belt and Road" și al restructurării lanțului global de aprovizionare cu produse textile, lucrarea de față analizează modelele comerțului cu produse textile dintre China și cele șapte țări din Asia de Sud, pe baza datelor privind exporturile de produse textile ale Chinei către aceste țări în perioada 2010-2023, punând accentul pe exporturile de produse textile. Studiul utilizează un model de gravitație stocastică de frontieră pentru analiza empirică, în scopul evaluării potențialului și a factorilor care influențează comerțul cu textile între China și cele șapte țări din Asia de Sud și oferă sugestii fezabile pentru dezvoltarea comerțului de produse textile între China și națiunile din Asia de Sud. Studiul constată că amploarea comerțului cu textile între China și țările din Asia de Sud a crescut, iar relațiile comerciale au devenit din ce în ce mai strânse. Cu toate acestea, amploarea importurilor și a exporturilor rămâne relativ redusă. În ceea ce privește factorii de influență, studiul constată că dimensiunea economică a Chinei are un efect inhibitor semnificativ asupra exporturilor de textile. În schimb, dimensiunea populației Chinei, nivelul de dezvoltare economică și dimensiunea populației țărilor din Asia de Sud, precum și distanța în linie dreaptă și existența unei frontiere comune au un impact pozitiv asupra exporturilor de textile. Cu toate acestea, influența Organizației de Cooperare de la Shanghai asupra exporturilor de textile ale Chinei este relativ redusă, cu efecte de promovare limitate; indicii de eficiență guvernamentală, acordurile de liber schimb, flexibilitatea valutară și scorurile privind libertatea economică au toate un efect pozitiv de promovare asupra eficienței exporturilor de textile. Cu toate acestea, libertatea comercială are un impact negativ asupra eficienței comerțului. Deși eficiența comerțului cu exporturi de textile ale Chinei către cele șapte țări din Asia de Sud rămâne la un nivel relativ scăzut, există un potențial comercial semnificativ și spațiu de expansiune, cu perspective largi de dezvoltare viitoare.

Cuvinte-cheie*: China, Asia de Sud, textile, modelul stocastic de gravitație de frontier, eficiența comerțului de export*

INTRODUCTION

In recent years, China and South Asian countries have deepened trade cooperation in the textile industry through multi-level policy coordination, forming a three-dimensional policy system based on free trade agreements, centred on industrial chain synergy, and driven by technology output. China and the South Asian region have taken the upgrading of free trade agreements as a breakthrough. China and Bangladesh launched free trade agreement negotiations in 2024 and clearly proposed in September 2024 to grant Bangladesh a zero-tariff transition period for 98% of tariff items. According to statistics from the General Administration of Customs of China, since the upgrading of the China-Pakistan Free

Trade Agreement, China's exports of textile yarn to Pakistan reached 1.12 billion USD in 2024, a year-on-year increase of 46.9%, and exports of textile machinery to Pakistan increased by 22%. In terms of in-depth integration of the industrial chain, China has invested in the construction of textile and garment industrial parks in Pakistan, with supporting power projects to solve energy bottlenecks; in Bangladesh, it has promoted the construction of garment accessories factories. According to the 2023 annual report data of the Bangladesh Garment Manufacturers Association, there are 1,200 garment accessories factories in Bangladesh, forming a closed loop of "Chinese raw materials – South Asian processing". In addition, technology output and green transformation have become new highlights. Chinese textile machinery enterprises have promoted Internet of Things spinning equipment in South Asia; at the same time, the 2024 report of the China Textile Industry Federation shows that the Sino-Bangladeshi cooperative environmental protection printing and dyeing project will adopt low-carbon technologies. Moreover, trade facilitation measures have further released potential. After the entry into force of the China-Nepal Transit Transport Agreement, the growth of China's exports of wool products to Nepal stems from the optimisation of cross-border logistics, while Myanmar and other countries under the RCEP framework have implemented tariff reductions, promoting a reduction in the circulation costs of regional textile raw materials. Although India still imposes high tariffs and anti-dumping measures on Chinese textiles, through strategies such as transferring factories to Pakistan and Bangladesh, the scale of China's textile exports to India through third countries has expanded. In the future, the two sides will rely on mechanisms such as the China-Pakistan Economic Corridor and the China-Myanmar-India-Bangladesh Economic Corridor to deepen cooperation in intelligent equipment and green technologies and promote industrial chain upgrading.

The textile trade between China and South Asian countries has seen steady growth. According to statistics from the UN Comtrade database, China's textile export value to South Asia increased from approximately 8.4 billion USD in 2010 to over 18.8 billion USD in 2023. However, a notable trade imbalance persists within the region. India, Pakistan, and Bangladesh account for over 90% of China's textile exports to South Asia, characterised by significant volatility, while markets like Bhutan and the Maldives remain smaller with minimal fluctuations. Meanwhile, Deardorff's trade cost theory manifests prominently in the South Asian context: transportation costs posed by the geographical barrier of the Himalayas, technical trade barriers arising from disparities in animal and plant quarantine standards across nations, and market risks triggered by exchange rate fluctuations in some countries directly impact textile trade [1]. In a specialised study on Sino-Indian textile trade, Karackattu (2013) found that India's non-tariff barriers significantly constrained China's exports of fruits, vegetables, and processed foods, whereas the Bangladeshi market's demand for Chinese grains and aquatic products continued to expand with population growth and income improvement, findings that validate the differential impacts of market scale and institutional factors [2].

In summary, existing studies universally acknowledge the global competitiveness of China's textile trade and the growth potential of Sino-South Asian trade under the Belt and Road Initiative, while also highlighting challenges such as cost pressures, non-tariff barriers, and geoeconomic risks. Future research could further integrate the impacts of the latest regional trade agreements and digital transformation on supply chains to provide more time-sensitive references for policy optimisation. However, bilateral trade still confronts challenges, including geographical barriers, technical trade barriers, and institutional differences, necessitating systematic research to uncover trade potential and key influencing factors. To promote the healthy and sustainable development of bilateral textile trade, it is imperative to remove obstacles to China's textile exports to the seven South Asian countries, enhance China's market share in these markets, expand export volume, and reverse the long-term trade deficit. In short, expanding textile exports to the seven South Asian nations, i.e., achieving export growth, remains China's primary task in the coming period. Regarding whether there is room for growth in China's textile exports to the seven South Asian countries, what major factors hinder export growth, and how to tap export potential, answering these questions requires examining the gap between the current level of China's textile exports to the seven South Asian nations and their potential, measuring export efficiency, and conducting an in-depth analysis of influencing factors.

Existing literature has conducted limited research on the textile trade between China and South Asia, with notable gaps in regional studies and analyses of the textile industry. Most literature applies the gravity model solely in its traditional form, offering insufficient analysis of emerging factors such as institutional elements when introducing inefficiency factors. In response, this paper constructs an extended gravity model based on China's textile export data to seven South Asian countries from 2010 to 2023: Bangladesh, Bhutan, India, the Maldives, Nepal, Pakistan, and Sri Lanka. It empirically examines the direction and intensity of traditional factors, including economic scale, geographic distance, and trade facilitation level, alongside emerging variables such as digital trade infrastructure and regional trade agreements. The study estimates each country's trade potential and identifies key constraining factors. Aiming to address: What are the primary driving forces behind China's textile exports to South Asian nations? Has the current trade level reached its potential ceiling? Which structural factors hinder the improvement of trade efficiency? This research not only provides empirical evidence for optimising China's textile export strategies to South Asia but

also enriches the application of the gravity model in regional textile trade studies. It offers theoretical references for precision policymaking in international textile cooperation under the Belt and Road Initiative.

LITERATURE REVIEW

The gravity model of trade, as a classic tool for analysing bilateral trade flows, has undergone a developmental process from empirical hypotheses to a systematic theory. Tinbergen was the first to introduce Newton's law of universal gravitation into trade research, proposing the core hypothesis that trade flows are positively correlated with economic size and negatively correlated with distance [3]. Anderson provided a micro-theoretical foundation for the model from the perspective of maximising consumer utility, emphasising the impact of product differentiation on trade [4]. Anderson and Van Wincoop solved the "border puzzle" by introducing the "multilateral resistance term", enabling the model to more accurately reflect the structural impact of trade costs, while Egger (2000) revised the econometric specification of the model, emphasising the importance of panel data and fixed effects [5, 6]. In research on the textile trade, the application of the gravity model has become relatively mature. Chen et al. used the gravity model to analyse the factors influencing exports of major global textile-producing countries, finding that economic size, trade agreements, and logistics efficiency are key variables [7]. Shekhawat and Shastri, in their study on India's textile exports, showed that per capita income, trade freedom, and regional trade arrangements significantly enhance export potential [8]. Rahman et al., in their analysis of Bangladesh's textile industry, pointed out that exchange rate fluctuations and infrastructure levels are important factors restricting exports [9]. It is worth noting that Wen et al. used a time-varying coefficient stochastic frontier gravity model to measure export efficiency, providing a methodological reference for the dynamic evaluation of trade potential [10]. This is highly consistent with the analysis of "trade potential and influencing factors" focused on in this paper, and is particularly suitable for capturing efficiency losses and room for improvement in textile trade between China and South Asian countries.

As a vital segment of the global textile trade, South Asia's bilateral trade relations with China have become a focus of academic attention. From a historical perspective, Janaway and Coningham's research on archaeological evidence of South Asian textiles revealed the region's long-standing textile traditions and trade networks [11]. Riello and Roy noted that South Asian textiles dominated the global market between 1500 and 1850, and contemporary textile trade between China and South Asia can be seen as a continuation and transformation of this historical context [12]. Although Maxwell focused on Southeast Asia, his analytical framework of "trade-tradition-transformation" in textiles provides insights for understanding the cultural attributes and economic functions of South Asian textiles [13]. In studies specifically on China-South Asia trade practices, existing research exhibits multi-perspective characteristics. Karackattu analysed the challenges and opportunities in Sino-Indian border trade, identifying insufficient policy coordination as the main obstacle [2]. Tsang and Au compared the textile export competitiveness of South Asian and Southeast Asian countries, finding that China holds significant advantages in mid-to-high-end markets, while South Asian countries have greater potential in labour costs [14]. Guan et al.'s research based on the diamond model showed that the international competitiveness of China's textile industry stems from its complete industrial chain and technological innovation capabilities, which have laid the foundation for exploring the South Asian market [15]. At the regional cooperation level, Zhou et al. studied the Belt and Road Initiative's role in promoting China-South Asia trade, finding that infrastructure connectivity and trade facilitation measures have achieved significant effects [16]. Dastgeer et al.'s analysis of the China-Pakistan Free Trade Agreement, Razzaque et al.'s discussion on China-Bangladesh trade, and Sikder and Dou's research on China-Bangladesh export structures all confirmed the positive impact of free trade agreements on bilateral trade [17–19]. Additionally, Jain pointed out that the textile trade serves as an important carrier in China's economic expansion in South Asia [20]. The rapid growth of China's textile exports to South Asia since the 21st century not only reflects complementarity but also implies the complex dynamics of regional competition and cooperation.

Research on the influencing factors of textile trade has expanded from traditional variables to institutions, policies, and emerging issues. In terms of human factors, the roles of government efficiency, economic freedom, and regional organisations have become increasingly prominent. For example, Shekhawat and Shastri incorporated trade freedom into the gravity model and found that its elasticity coefficient for India's textile exports reached 0.32 [8]. Li et al.'s research on ESG performance and enterprise growth showed that environmental compliance and social responsibility can enhance enterprises' competitiveness in the international market, which is enlightening for Chinese textile enterprises to explore the South Asian market, especially in the context where South Asian countries are paying increasing attention to green trade barriers [21]. Ma and Appolloni pointed out that financial flexibility can improve enterprises' green innovation performance, implying that Chinese textile enterprises can break through trade restrictions through technological upgrading, such as the research and development of environmentally friendly fabrics [22]. In addition, the role of digital transformation in promoting trade efficiency has been verified. Liu et al. found that the digitalisation of construction enterprises can improve innovation efficiency, and this logic is equally applicable to supply chain optimisation and cross-border

e-commerce development in the textile industry [23]. The impact of environmental and policy factors cannot be ignored either. Zhang et al.'s research on the impact of air pollution control on enterprises' green innovation revealed the forcing effect of environmental regulations on industrial upgrading, which may affect the export structure of Chinese textiles [24]. In addition, Zhang et al.'s research on the impact of carbon emissions, green energy, and high-tech policy uncertainty on financial markets uncovered the complex transmission paths of policy variables through market expectations, indicating the potential impact of the macro policy environment on the development of the textile industry [25]. Ma et al.'s analysis of climate change and human activities suggested that differences in natural resource endowments may indirectly affect textile trade through raw material costs [26]. Moreover, Ma et al.'s research on the impact of agricultural mechanisation on agricultural carbon emission intensity analysed, from the upstream of the industrial chain, the mechanism by which agricultural production methods affect carbon emissions, providing an important supplement to understanding the carbon emission reduction path across the entire industrial chain [27]. These studies collectively construct a multi-dimensional analytical framework ranging from micro-enterprises to macro-ecology, and from technological innovation to policy regulations, offering rich theoretical and empirical support for exploring industrial transformation and ecological governance under the goal of sustainable development. Overall, these multi-dimensional factors together constitute the complex influence mechanism of China's textile export potential to South Asia, providing a theoretical and empirical basis for this study to include variables such as government efficiency and economic freedom.

In summary, existing studies have laid the foundation for this paper in terms of the application of the gravity model, regional trade characteristics, and influencing factors, but there are still two shortcomings: first, there are few specialized studies on textile trade between China and South Asian countries, especially a lack of potential measurement based on the stochastic frontier model; second, the analysis of institutional factors such as government efficiency and economic freedom is not systematic. The scarcity of studies on the South Asian region stems from the following factors: geographically, due to the barrier of the Himalayas, transportation costs in South Asia are higher than those in Southeast Asia, and the land transportation cycle is longer than that of maritime transportation in Southeast Asia, while Central Asia has reduced railway transportation costs through the China-Europe Railway Express. Institutionally, the intensity of non-tariff barriers in South Asian countries is much higher than that in Southeast Asia, and India conducts anti-dumping investigations against Chinese textiles more frequently than Southeast Asian countries; Southeast Asia has achieved textile tariff reductions relying on RCEP, and Central Asia has simplified customs clearance procedures through the Shanghai Cooperation Organization, while the role of South Asian regional cooperation mechanisms in promoting trade is significantly weaker. This paper takes textiles as the research object of trade, with the following innovations: first, methodological innovation. This paper applies the time-varying stochastic frontier gravity model to the study of China's textile exports to South Asia, breaking through the "constant trade cost" assumption of the traditional gravity model. Second, expansion of core variables. This paper introduces emerging variables such as digital trade, regional trade agreements, and regional policies, changing the impact of traditional human factors on trade efficiency in the past. Third, a breakthrough in research scope. This paper systematically measures the trade efficiency of the seven South Asian countries for the first time and subdivides the trade efficiency and expansion space of each country in the South Asian region. The study breaks through the "one-size-fits-all" analytical framework of existing literature on the South Asian region, provides a quantitative basis for China to formulate country-specific textile export strategies under the Belt and Road Initiative, and enriches the application scenarios of the gravity model in populous regions. This paper will combine data from 2010 to 2023 and use the stochastic frontier gravity model to fill the above gaps, providing policy references for the development of bilateral trade.

CHINA'S TEXTILE EXPORTS TO THE SEVEN SOUTH ASIAN COUNTRIES

With the deepening of cross-regional economic and trade cooperation, trade between China and the seven South Asian countries has developed rapidly, especially since the deepening of textile trade cooperation through multi-level policy coordination between China and South Asia, and the scale of textile trade has grown rapidly. Figures 1 and 2, respectively, show the scale of China's textile trade with South Asia and the scale of textile exports. Due to data availability, China's import data of textiles from Bhutan and the Maldives are missing in some years, and the total import and export trade data are calculated using estimated values. Overall, between 2020 and 2023, textile trade between China and South Asia showed a growing trend with a good development scenario. From 2010 to 2019, the total textile trade volume between China and the seven South Asian countries increased from 8.466 billion USD to 16.631 billion USD, with an average annual growth rate of 6.34%, showing a significant growth trend, indicating that the scale of textile trade between China and South Asia is gradually expanding. Affected by the new epidemic in 2020, the textile trade volume decreased, but it recovered rapidly and continued to grow from 2021 to 2023, reaching 18.825 billion USD in 2023. From 2010 to 2023, exports increased from 8.412 billion USD to 18.727 billion USD, accounting for more than 99%, while

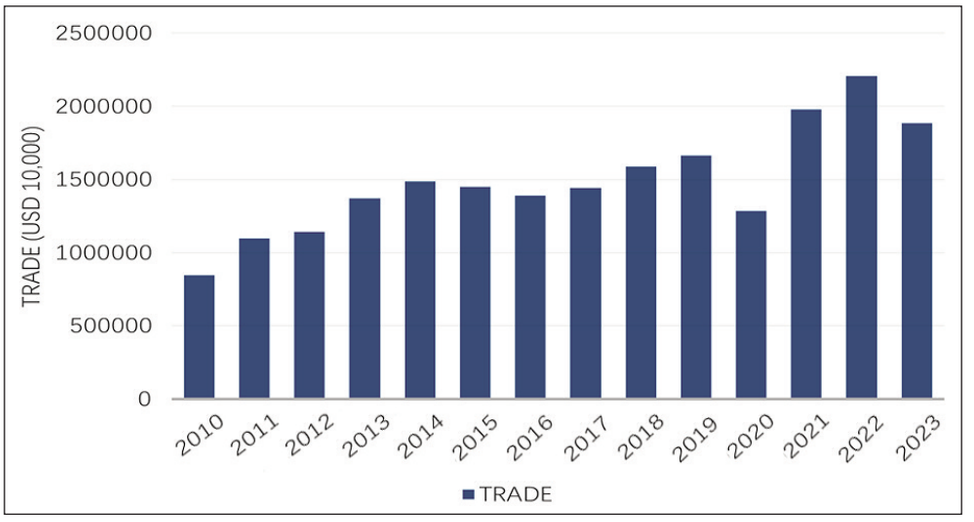

Fig. 1. China's Total import and export of textile products to 7 South Asian countries, 2010–2023 (based on UN Comtrade data)

imports increased from 54 million USD to 98 million USD, reflecting that China occupies a dominant position in the textile trade with South Asia.

Between 2010 and 2023, China's textile exports to South Asian countries demonstrated an overall characteristic of "fluctuating growth with market divergence", though significant variations existed in market performance across different nations. By 2023, the total textile export volume from China to the seven South Asian countries had more than tripled compared to 2010. Except for Bhutan and the Maldives, where export growth was slow, the other five countries experienced relatively satisfactory export growth, as shown in figure 2. From 2010 to 2019, the export value increased from 8.412 billion USD to 16.528 billion USD, doubling in size. However, in 2020, exports declined rapidly, dropping by 23.14% compared to 2019. Following 2020, exports recovered and grew, reaching their peak in 2022 with the total export value exceeding 20 billion USD amid fluctuations. Nevertheless, market divergence intensified across South Asian countries. The textile imports of Bangladesh, India, and Pakistan were severely impacted due to the combined effects of multiple factors in 2020, including supply-demand imbalances caused by the pandemic, heightened trade barriers, and short-term industrial chain restructuring. Bangladesh's export value plummeted from 6.963 billion USD in 2018 to 5.46 billion USD in 2020, a 27.53% decrease from 2018. India's export value fell by 38.55% year-on-year in 2019, while Pakistan's textile import volume decreased by 1.212 billion USD compared to 2019. In contrast, Sri Lanka and Nepal experienced relatively stable export performances with only short-term declines during the pandemic. Post-2020, countries gradually recovered.

Bangladesh, India, and Pakistan reached their export peaks in 2022, with values of 9.369 billion USD, 6.677 billion USD, and 4.367 billion USD, respectively, while the other four countries showed steady recovery.

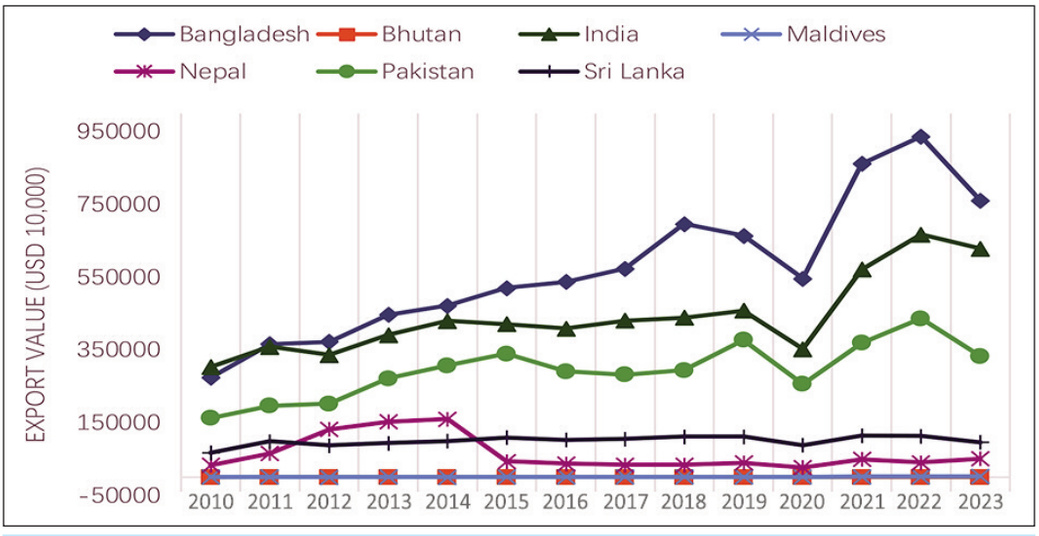

Fig. 2. China's Textile exports to 7 South Asian countries, 2010–2023 (based on UN Comtrade data)

China's textile exports to the seven South Asian countries exhibit significant market concentration, with Bangladesh, India and Pakistan accounting for the largest shares, followed by Sri Lanka and Nepal, whilst exports to Bhutan and the Maldives are relatively small, as shown in table 1. In terms of export share, Bangladesh is China's largest textile export market in South Asia, and its market position continues to strengthen. Between 2010 and 2023, the share of China's textile exports to Bangladesh rose from 25.66% to 34.04%, an increase of 8.38 percentage points, demonstrating the sustained expansion of the country's demand for Chinese textiles. India's market share, however, has shown a fluctuating downward trend. In 2010, China's share of textile exports to India stood at 31.57%, falling to 27.95% by 2023, a decrease of 3.62 percentage points. Despite this decline, India remains one of China's key export markets in South Asia. It is worth noting that, as shown in figure 2, the value of China's textile exports to India has not decreased but has, in fact, increased. This indicates that the overall growth rate of India's textile imports has outpaced the growth rate of imports from China. The change in market share was most pronounced in Pakistan. In 2010, China's share of textile exports to Pakistan stood at 29.52 per cent, falling sharply to 19.36 per cent by 2023, a decline of 10.16 percentage points. This downward trend reflects the diversification of Pakistan's textile import sources or a relative weakening of China's export competitiveness in this market. China's market share in Sri Lanka remained stable, whilst its share in the Nepalese market showed an overall upward trend. Between 2010 and 2023, China's share of textile exports to Sri Lanka fluctuated between 9.39% and 7.79%, whereas its share in Nepal rose from 3.56% to 10.30%, indicating a marked increase in demand for Chinese textiles in the Nepalese market.

THEORETICAL MODEL AND DATA SOURCES

Theoretical model

In the field of international trade research, the gravity model is widely used by most scholars. Tin Bergen was the first scholar to apply the gravity model to international trade research [28]. The basic theory of this model is that the total trade volume between two countries is directly proportional to their economic scale and inversely proportional to the distance between them. However, over time, the gravity model has gradually developed from its original traditional form to the stochastic frontier gravity model, and its theory has been continuously improved. The traditional trade gravity model, while canonical in trade potential estimation, harbours an inherent limitation: it overlooks endogenous trade resistances stemming from institutional frictions, policy barriers, and logistical inefficiencies. In contrast, the SFG model incorporates a trade inefficiency term, a construct rooted in Meeusen and van den Broeck's technical inefficiency formulation, that explicitly accounts for such anthropogenic resistances [29]. Compared with the traditional gravity model, the stochastic frontier gravity model decomposes trade resistance into random errors and optimizable artificial factors by introducing the trade inefficiency term. This not only allows for the quantification of the boundaries of trade potential but also identifies the time-varying characteristics of remediable resistances, such as institutional and logistical factors. Therefore, this paper uses the stochastic frontier gravity model to analyse how the development level of digital service trade in countries along the route affects China's exports.

The stochastic frontier gravity model was formulated as follows:

$$T_{ijt} = f(X_{ijt}, \beta) \exp(v_{ijt}) \exp(-u_{ijt}), \quad u_{ijt} \geq 0 \qquad (1)$$

It is obtained after taking the logarithm:

Table 1

PROPORTION OF CHINA'S TEXTILE EXPORTS TO THE SEVEN SOUTH ASIAN COUNTRIES FROM 2010 TO 2023

Year	Bangladesh	Bhutan	India	Maldives	Nepal	Pakistan	Sri Lanka
2010	25.66%	0.03%	31.57%	0.29%	3.56%	29.52%	9.39%
2011	23.61%	0.01%	31.95%	0.42%	5.29%	27.99%	10.72%
2012	21.09%	0.03%	36.45%	0.29%	4.57%	25.40%	12.17%
2013	22.70%	0.03%	37.57%	0.33%	5.19%	21.62%	12.57%
2014	23.93%	0.01%	34.22%	0.31%	3.60%	23.01%	14.92%
2015	22.66%	0.05%	26.80%	0.34%	3.53%	24.97%	21.65%
2016	22.30%	0.03%	30.10%	0.47%	4.76%	23.01%	19.33%
2017	21.33%	0.02%	31.86%	0.44%	5.33%	24.62%	16.40%
2018	28.90%	0.02%	27.56%	0.42%	6.58%	23.59%	12.93%
2019	37.37%	0.01%	20.74%	0.45%	5.91%	22.65%	12.87%
2020	40.93%	0.01%	18.22%	0.26%	4.61%	23.92%	12.04%
2021	39.67%	0.01%	19.03%	0.41%	9.17%	22.19%	9.52%
2022	36.64%	0.00%	24.33%	0.51%	7.76%	23.90%	6.85%
2023	34.04%	0.01%	27.95%	0.55%	10.30%	19.36%	7.79%

$$\ln T_{ijt} = \ln f(X_{ijt}, \beta) + v_{ijt} - u_{ijt}, \quad u_{ijt} \geq 0 \qquad (2)$$

In the above equation, T_{ijt} represents the total trade volume between country i and country j in period t; X_{ijt} represents the natural factors such as economic size, population size, straight-line distance between the capitals, whether there is a border and language that affect the trade volume between the two sides in period t; β is a parameter; v_{ijt} represents the random error, which obeys the normal distribution with a mean value of 0 and a variance of σ^2, and is independent of the trade inefficiency term u_{ijt}; u_{ijt} obeys a kinked normal or half-normal distribution and contains the human factors that affect the trade volume between the two parties. The trade inefficiency term adds human resistance factors when the trade inefficiency term $u_{ijt} = 0$, that is, there is no trade inefficiency term, the two countries maximise the trade size, and at this time, the two countries reach the trade potential T_{ijt}^*, expressed as:

$$T_{ijt}^* = f(X_{ijt}, \beta) \exp(v_{ijt}) \qquad (3)$$

The efficiency of trade between the two sides is indicated as:

$$TE_{ijt} = \frac{T_{ijt}}{T_{ijt}^*} = \exp(-u_{ijt}) \qquad (4)$$

When there are artificial resistance factors, i.e., $u_{ijt} > 0$, $T_{ijt}^* < 1$, the trade volume of the two countries is less than the trade potential; when there are no artificial resistance factors, i.e., $u_{ijt} = 0$, $T_{ijt}^* = 1$, the trade volume of the two countries reaches the trade potential. Based on researchers' observations of the mean value of trade inefficiency terms changing over time, the gravity model can be classified into the time-varying stochastic frontier gravity model and the time-invariant stochastic frontier gravity model. Initially, most scholars believed that the trade inefficiency term remained constant over time, thus adopting the time-invariant stochastic frontier gravity model to estimate trade efficiency. However, this assumption was clearly unreasonable. Battese and Coelli pointed out that with the increase in the time dimension, the trade inefficiency term might change, and its expression is as follows [30]:

$$u_{ijt} = \{\exp[-\eta(t - T)]\} u_{ij} \qquad (5)$$

The time-varying model posits that u_{ijt} is nonlinearly related to time. The time variable t and the base period T constitute the temporal framework for dynamic analysis. When t approaches T, the "stubborn resistance" not intervened by policies becomes prominent. The inefficiency term u_{ijt} reflects the inherent trade resistance at the initial stage of the sample period, and u_{ijt} follows a truncated normal distribution. η is the parameter to be estimated, characterising the decay rate of trade inefficiency over time.

Specifically, η indicates that u_{ijt} does not change with time; η implies that the trade inefficiency term, increasing with time, can reduce trade resistance; η signifies that the trade inefficiency term escalating over time leads to an increase in trade resistance.

The analysis of the impact of human resistance factors in trade inefficiency models involves two approaches: the "one-step method" and the "two-step method". The one-step method integrates the trade inefficiency model into the stochastic frontier gravity model for analysis, whereas the two-step method constructs an independent model using the trade inefficiency term as the dependent variable.

However, the two-step method assumes that the trade inefficiency term remains constant, which contradicts the premise of treating it as a dependent variable in an independent model. Therefore, this study draws on Battese and Coelli's (1995) application of the one-step method for trade efficiency research, simultaneously conducting regression on both the stochastic frontier gravity model and the trade inefficiency term [31].

The expression for the trade inefficiency term u_{ijt} was as follows:

$$u_{ijt} = \alpha' z_{ijt} + \varepsilon_{ijt} \qquad (6)$$

In the above equation, α' is the parameter to be estimated, and $\alpha' > 0$ indicates that the exogenous variable z_{ijt} is positively correlated with the trade inefficiency term; z_{ijt} is the exogenous variable affecting u_{ijt}; ε_{ijt} indicates the random error term obeying the normal truncated-tailed distribution with a mean of 0 and a variance of σ^2, and it is assumed that $u_{ijt} > 0$. According to the "one-step method, equation 6 can be obtained by substituting equation 2:

$$\ln T_{ijt} = \ln f(X_{ijt}, \beta) + v_{ijt} - (\alpha' z_{ijt} + \varepsilon_{ijt}) \qquad (7)$$

Model construction and variable selection

Time-varying stochastic frontier gravity model

This paper referenced Armstrong's suggestions, introducing natural factors affecting trade volume into the stochastic frontier gravity model, such as economic scale, population size, and whether there is a common language [32]. In the trade inefficiency model, artificial factors were introduced, including the government efficiency index, economic freedom score, monetary freedom, trade freedom, and whether a free trade agreement was signed between the trading parties or whether they belonged to the Shanghai Cooperation Organisation. On this basis, this paper constructed a time-varying stochastic frontier gravity model to study the trade potential and influencing factors of China's textile exports to South Asia.

The specific equation setting is as follows:

$$\begin{aligned} \ln EXP_{ijt} = {} & \beta_0 + \beta_1 \ln GDP_{it} + \beta_2 \ln GDP_{jt} + \\ & + \beta_3 \ln POP_{it} + \beta_4 \ln POP_{jt} + \beta_5 \ln DIS_{ij} + \\ & + \beta_6 \ln LANG_{ij} + v_{ijt} - u_{ijt} \end{aligned} \qquad (8)$$

In the model, i denoted China, while j represented one of the seven South Asian countries. The dependent variable EXP_{ijt} referred to the actual level of textile exports from country i to country j in period t, measured by the real value of textile exports. The explanatory variables were primarily derived from

factors that influenced export volumes, including characteristics of the exporting country, the importing country, and bilateral features. The economic meanings of these variables were explained as follows: GDP_{it} and POP_{it} denoted China's total GDP and population size in the period t, respectively. These variables represented China's level of economic development and demographic scale. Generally, a country's economic development determined its position in the international market and was positively correlated with its export volume. The higher the total GDP of the exporting country, the higher the level of economic development, and the stronger its production capacity and supply capacity for the international market. Therefore, GDP_{it} was expected to have a positive effect on EXP_{ijt}. The population size of a country was typically proportional to its domestic demand for textiles. Given China's relatively large population, a considerable portion of textile production was allocated to meeting domestic demand, potentially limiting its external supply capacity. Hence, POP_{it} was expected to have a negative impact on EXP_{ijt}.

GDP_{jt} and POP_{jt} were characteristics of the importing countries, representing, respectively, the GDP and population size of the country j in period t. GDP_{jt} reflected the economic development level of the importing country, while POP_{jt} indicated its population size. Higher economic development and a larger population typically implied stronger purchasing power and greater market demand for textiles, which, in turn, promoted exports from China. Therefore, both GDP_{jt} and POP_{jt} were expected to have a positive influence on China's textile export trade.

DIS_{ij} referred to a bilateral characteristic variable representing the geographical distance between countries i and j, serving as a proxy for transportation costs between the exporting and importing countries. In general, the greater the geographical distance, the higher the transportation costs, thereby reducing trade feasibility. Thus, DIS_{ij} was expected to have a negative effect on EXP_{ijt}.

$LANG_{ij}$ was a dummy variable indicating whether a common language was shared between the two countries. A value of 1 was assigned if a common language existed, and 0 otherwise. The presence of a common language facilitated communication and reduced trade information costs, thereby providing a natural advantage in conducting export trade. Accordingly, $LANG_{ij}$ was expected to have a positive impact on EXP_{ijt}.

Model of export trade inefficiency

To further explore the trade potential of China's textile exports to the seven South Asian countries, this paper refers to the research by Wen Liqin et al. on the impact of the development level of digital service trade in Belt and Road countries on China's green building commodity exports [25]. It introduces human factors affecting bilateral trade – the government efficiency index, economic freedom score, monetary freedom, trade freedom, whether a free trade agreement is signed between the trading parties, and whether they are members of the Shanghai Cooperation Organization – into the inefficiency term, and further constructs a trade inefficiency model. The specific equation is as follows:

$$u_{ijt} = \alpha_0 + \alpha_1 GEI_{jt} + \alpha_2 EFI_{jt} + \alpha_3 TRA_{jt} + \\ + \alpha_4 MON_{jt} + \alpha_5 FTA_{ijt} + \alpha_5 SCO_{ijt} + \varepsilon_{ijt} \quad (9)$$

In this model, the dependent variable u_{ijt} represented export trade inefficiency, while α_0 denoted the parameter to be estimated. The explanatory variables were defined as follows: GEI_{jt} represented policy communication and was measured by the Government Effectiveness Index. This index reflected the government's capacity and efficiency in policy implementation. A higher value of this index indicated lower administrative communication costs and, consequently, greater efficiency in textile exports. Thus, GEI_{jt} was expected to be positively correlated with export efficiency and negatively associated with the inefficiency term.

Trade facilitation was measured by trade freedom, denoted as TRA_{jt}. A higher value indicated fewer institutional restrictions on international trade, such as lower tariffs and non-tariff barriers. Therefore, TRA_{jt} was anticipated to be negatively related to trade inefficiency.

Financial integration was proxied by monetary freedom, represented by MON_{jt}, which measured the degree of currency circulation freedom and price stability. A higher score suggested greater monetary stability and liberalisation, which was expected to be positively related to trade efficiency, and thus negatively related to inefficiency.

Economic mobility was assessed using the Economic Freedom Index EFI_{jt}, which captured a country's reliance on market mechanisms and the degree to which the government had transitioned from being an economic participant to a rule-setter. Higher levels of economic freedom were associated with greater international trade openness and capital flow liberalisation. Countries with greater economic freedom typically exhibited stronger export competitiveness and greater appeal to foreign investment. Therefore, EFI_{jt} was expected to reduce export inefficiency.

FTA_{ijt} and SCO_{ijt} were both dummy variables. FTA_{ijt} indicated whether a free trade agreement had been signed between countries i and j in period t; SCO_{ijt} denoted whether both countries were members of the Shanghai Cooperation Organisation during the same period. Each variable equalled 1 if the condition was satisfied, and 0 otherwise. Free trade agreements played a key role in reducing trade barriers and uncertainty, while regional cooperation frameworks such as the SCO facilitated institutional arrangements and trade among member states. Both mechanisms contributed to improving export efficiency.

The freedom indices used in this study were developed by the Heritage Foundation and provided a comprehensive assessment of a country's economic institutional environment. These indices were scored on a scale of 0 to 100, with higher scores indicating better institutional quality, greater market orientation, and reduced export barriers for exporting countries. As such, MON_{jt}, EFI_{jt}, FTA_{ijt}, and SCO_{ijt} were all expected to exert a negative influence on u_{ijt}.

Sample selection and data sources

To avoid the adverse effects of heteroscedasticity and autocorrelation, and considering the reliability of regression results and data availability, this paper selected sample data from China and seven South Asian countries for empirical analysis. The seven South Asian countries include Bangladesh, Bhutan, India, the Maldives, Pakistan, Nepal, and Sri Lanka. Empirical analysis of panel data from 2010 to 2023 was conducted using Frontier 4.1 software.

Data on China's textile exports to partner countries (*ExPit*) are sourced from the UN Comtrade database. The scope of textiles includes various fabrics made from natural fibres and chemical fibres, with specific HS codes for textiles as follows: 5601-5604, 5607-5609, 57, 5807-5808, 5810-5811, 59, 63, 6501-6502. Data on GDP and population (GDP_{it} and POP_{it}) for both China and its trading partners, data were sourced from the World Bank. The geographic distance (DIS_{ij}) between China and its trading partners was derived from the CEPII database. Information on the Shanghai Cooperation Organisation (SCO_{ijt}) was retrieved from the official website of the SCO. Within the trade inefficiency model, the Government Effectiveness Index (GEI_{jt}) was sourced from the World Development Indicators (WDI), while the Trade Freedom Index (TRA_{jt}) and Monetary Freedom Index (MON_{jt}) were obtained from the Index of Economic Freedom. Where data were missing, interpolation methods were used to supplement the dataset.

EMPIRICAL TESTING AND RESULT ANALYSIS

Before estimating the model using the stochastic frontier gravity approach, it was necessary to conduct likelihood ratio (LR) tests to ensure model validity. These tests included assessments of whether trade inefficiency existed and whether the inefficiency term varied over time. By comparing the log-likelihood values of the restricted and unrestricted models, the LR statistic was calculated and compared against the 1% critical value. The results are presented in table 2. At the 1% significance level, the LR statistics were greater than the critical values from the chi-squared distribution. Therefore, the null hypothesis H_0: $\gamma = 0$, which suggested the absence of inefficiency, was rejected. Similarly, the null hypothesis H_0: $\eta = 0$, which assumed time-invariant inefficiency, was also rejected. These results indicated that trade inefficiency did exist and varied over time. Accordingly, the time-varying stochastic frontier model was adopted for estimation. This confirmed the presence of export trade inefficiencies between China and the seven South Asian countries and demonstrated that such inefficiencies exhibited time variation over the period 2010–2023.

Analysis of results from the stochastic frontier gravity model

According to the estimation results presented in table 3, China's total economic output ($\ln GDP_{it}$) exhibited a statistically significant negative impact on textile exports, passing the 1% significance level. This finding was contrary to expectations. Several possible explanations may account for this result.

The growth of China's total economic output was accompanied by an increase in per capita income, causing the domestic textile demand structure to shift from "quantity-oriented" to "quality-oriented". The surging demand for high-protein products and characteristic organic textiles led to partial textiles prioritising domestic market satisfaction, demonstrating the adverse selection of "domestic demand crowding out exports" (Deaton and Muellbauer, 1980) [33]. From the perspective of industrial structure adjustment, the expansion of China's total economic output promoted the transformation of industrial structure toward high-end and service-oriented sectors [34, 35]. As a traditional manufacturing industry, the textile industry, under the dual influence of rising factor costs and optimised resource allocation, had part of its production capacity reallocated to emerging industries with higher added value, such as information technology and high-end equipment manufacturing [36]. This squeezed the raw material supply, labour resources, and capital investment of textile export enterprises, correspondingly weakening their export capabilities [37, 38]. Meanwhile, economic growth prompted the continuous improvement of domestic environmental protection standards and labour rights

Table 2

STOCHASTIC FRONTIER GRAVITY MODEL APPLICABILITY RESULTS

Original hypothesis	Constrained model log-likelihood	Unconstrained model log-likelihood	LR statistic	1% critical value	Test result
Absence of the trade inefficiency term	–69.847	–38.536	62.622	14.325	Rejection
Trade inefficiency term is non-time varying	–38.536	–29.854	17.346	12.483	Rejection

Table 3

REGRESSION RESULTS OF THE STOCHASTIC FRONTIER GRAVITY MODEL

Variable	Time-invariant model		Time-varying model	
	Coefficient value	T value	Coefficient value	T value
Constant	–501.238***	–93.298	–476.500***	–14.135
ln GDP_{it}	–1.736***	–9.902	–1.283***	–6.055
ln GDP_{jt}	0.950***	4.323	0.998***	4.154
ln POP_{it}	24.879***	62.640	24.386***	15.958
ln POP_{jt}	0.328*	1.857	0.055	0.263
ln DIS_{ij}	2.305***	5.722	0.610	0.452
ln $LANG_{ij}$	1.983***	7.614	0.831**	2.367
σ^2	2.709	1.506	12.969	1.110
γ	0.962***	33.941	0.994***	168.390
μ	–3.229**	–2.433	–7.181**	–2.059
η	-	-	–0.039***	–4.344
Log-likelihood value	–38.536		–29.854	
LR test	62.621		79.985	

protection regulations [39, 40]. Textile production enterprises needed to invest more costs in energy conservation, emission reduction, and compliant operations, further compressing export profit margins and inhibiting enterprises' export enthusiasm [41, 42].

In addition, China's population size (ln POP_{it}) exerted a statistically significant positive effect on textile exports to South Asia, also passing the 1% significance threshold. This result contradicted traditional theoretical expectations, which suggest that population growth generally increases domestic consumption demand and suppresses exports. On one hand, the labour-intensive nature of China's textile processing sector allowed population growth to enhance production through increased labour supply elasticity and industrial clustering effects. On the other hand, the rigid demand for mid- to low-end textiles in South Asia was well-aligned with China's economies of scale and competitive pricing, indicating that population growth facilitated textile development and promoted textile exports to the region.

The economic scale of the seven South Asian countries (ln GDP_{jt}) had a significant and positive effect on China's textile exports, with results significant at the 1% level. That is, GDP growth was positively correlated with import demand elasticity: a 1% increase in GDP led to a 0.998% growth in textile import demand. When the economic consumption capacity of South Asian countries improved, Chinese enterprises had greater motivation to break through trade barriers and enhance export efficiency, with such investment decisions directly related to local GDP growth rates. Moreover, countries with higher economic levels typically have more complete infrastructure and lower trade costs. The population size of South Asian countries (ln POP_{jt}) had a positive impact on textile exports but failed to pass the significance test, indicating that an increase in the total population of South Asian countries might promote China's textile exports.

Geographical distance between China and South Asian countries (ln DIS_{ij}) had a positive influence on textile exports, but the effect was statistically insignificant. This could be attributed to the diminishing role of spatial distance as regional integration efforts advanced.

Whether the trading partners shared a common language under the Shanghai Cooperation Organisation framework ($LANG_{ij}$) had a positive and statistically significant effect on Chinese textile exports, at the 5% level. This outcome highlighted the role of linguistic and cultural connections in reducing transaction costs and fostering trust in international trade. From the perspective of transaction cost theory, a shared language could reduce information asymmetry and lower communication costs associated with business negotiations, contract enforcement, and market research. Culturally, linguistic similarities often correlated with converging consumer preferences. This also demonstrates the indispensable role of shared language in facilitating textile trade between China and the seven South Asian nations.

Analysis of results from the trade inefficiency model

The estimation results in table 4 indicate that the γ value (0.999) was significant at the 1% level, and the LR value reached 105.703. This suggests that the overall estimation effect was good, and the presence of the trade inefficiency term in the model was an important factor hindering smooth trade. Analysing the empirical results, the government efficiency index (GEI_{jt}) had a negative impact on trade inefficiency, with a coefficient of –2.931, which promoted the textile trade exports of the exporting country. This indicates that strengthening policy coordination and communication among partner countries is conducive to improving the export efficiency of China's textiles to South Asian countries. Therefore, with the full support of various government departments, the export efficiency of China's textiles to South Asian countries would naturally be enhanced.

The result shows whether China has signed a Free Trade Agreement (FTA_{jt}) with the seven South Asian countries passed the significance test at the 10% level and had a negative impact on trade inefficiency, which was in line with the theoretical expectation of the gravity model that "institutional arrangements reduce trade costs". This indicates that the signing of free trade agreements between China and South Asian countries can promote China's textile exports to South Asian countries to a certain extent. The main reason is that free trade agreements remove trade barriers and release policy dividends through a multidimensional mechanism: first, tariff reduction directly reduces the market access cost of Chinese textiles; second, the transparency and simplification of

non-tariff barriers reduce compliance costs, shorten customs clearance time and reduce enterprise testing fees; third, trade facilitation measures directly improve cross-border circulation efficiency; fourth, the enhancement of policy stability reduces market risks. The clear rules of origin, dispute settlement mechanism and other provisions in the agreement provide enterprises with a predictable trade environment and stimulate long-term export investment.

The Shanghai Cooperation Organisation (SCO_{jt}) exhibited an inhibitory effect on the trade inefficiency term of China's textile exports to the seven South Asian countries, i.e., it promoted textile exports, but failed to pass the significance test. This indicates that the role of the Shanghai Cooperation Organisation in textile trade between China and the seven South Asian countries was not particularly prominent. The possible reasons are as follows: the focus of SCO cooperation has been more concentrated on areas such as security and energy, with fewer implemented mechanisms and arrangements related to textile trade, leading to weak direct policy impacts. Additionally, within the data time frame, some cooperation initiatives might not have been fully translated into trade effectiveness, or were interfered with by factors such as geopolitics and other trade agreements, causing the promotion effect of this variable on textile exports to fail to be statistically significant.

The Economic Freedom Index (EFI_{jt}) of the seven South Asian countries exhibited an inhibitory effect on the inefficiency of China's textile trade and passed the significance test at the 1% level. That is, economic freedom was directly proportional to China's textile exports to South Asia. The main reason is that countries with higher economic freedom have lower trade barriers and a more stable and transparent policy environment, reducing the institutional costs for Chinese textiles to enter local markets.

Simultaneously, economies with a higher degree of marketisation have more elastic demand for textiles, and their private sectors are more dynamic, making it easier to form stable import demands and supply chain collaborations. This aligns with the logic in the gravity model that "institutional quality enhances trade flows".

The Monetary Freedom Index (MON_{jt}) exerted a negative impact on trade inefficiency, with a coefficient of –0.039, and passed the significance test at the 10% level. This indicates that the free flow of currency can effectively enhance the export efficiency of Chinese textiles. The primary reasons are as follows: fewer currency exchange restrictions and relaxed foreign exchange controls reduce cross-border settlement costs and exchange rate risks, enabling Chinese exporters to more easily determine prices and receive payments. Simultaneously, countries with a higher degree of monetary freedom have more open financial environments, facilitating the establishment of flexible trade settlement mechanisms, improving transaction efficiency, and strengthening enterprises' willingness to export. This reflects the positive impact of financial institutional convenience on textile trade.

Table 4

REGRESSION RESULTS OF THE TRADE INEFFICIENCY TERM MODEL

Function	Variable	Coefficients	T-value
Stochastic front function	Constant	–458.004	–458.243
	ln GDP_{it}	–1.315	–15.767
	ln GDP_{jt}	0.658	8.730
	ln POP_{it}	22.380	183.047
	ln POP_{jt}	0.533	9.187
	ln DIS_{ij}	2.383	26.630
	ln $LANG_{ij}$	1.035	14.256
Trade inefficiency function	Constant	13.061	8.055
	GEi_{jt}	–2.931	–11.240
	FTA_{jt}	–0.545	–1.733
	SCO_{jt}	–0.064	–0.098
	EFI_{jt}	–0.244	–6.630
	MON_{jt}	–0.039	–1.708
	TRA_{jt}	0.071	4.721
	σ^2	0.706	5.869
	γ	0.999	154.626
Log-likelihood value	–74.031		
LR test	105.703		

The Trade Freedom Index (TRA_{jt}) exerted a significant positive impact on trade inefficiency at the 1% level, which contradicted expectations. This indicates that increasing trade freedom did not promote China's textile exports. Possible reasons include: countries with high trade freedom might rely more on protective policies for their domestic textile industries, setting implicit barriers to textiles despite overall openness; high trade freedom was accompanied by fierce international competition, and Chinese textiles might face squeezing from similar products in regions such as Southeast Asia and Australia, leading to a diversion of market share; the indicator measurement might not have accurately distinguished the characteristics of the textile sector, as overall trade freedom did not necessarily equate to textile trade facilitation, causing the results to deviate from theoretical expectations.

Export trade efficiency and potential

Tables 5 and 6 present the textile export efficiency and expansion potential of China to the seven South Asian countries from 2010 to 2023. As shown in table 5, the average export efficiency of China to South Asia demonstrated a steady growth trend during 2010–2023. The average efficiency of China's textile exports to South Asian countries was 0.3864 in 2010, rising to 0.5403 by 2023. After the Belt and Road Initiative was proposed in 2013, the average textile export efficiency reached a peak of 0.5767 in 2015, followed by a slight decline from 2016 to 2018, dropping to 0.3784 in 2018. The direct cause of the

recent decline in average export efficiency to the seven South Asian countries was the significant reduction in textile imports from China by India and Pakistan. For example, India's textile imports from China decreased by $9.5123 million in 2018 compared to 2017, and Pakistan's imports decreased by $4.5261 million, with the import reduction from these two countries accounting for over 80% of the total decline. Overall, China's textile export efficiency to South Asia showed an upward trend but with large fluctuations. Except for Bhutan, India, and Pakistan, the annual average export efficiency exceeded 0.5. The highest annual average efficiency was observed in exports to Bangladesh at 0.7633, followed by the Maldives, Sri Lanka, and Nepal at 0.7360, 0.5845, and 0.5303, respectively, while the efficiency of exports to India was the lowest at 0.0973.

China and the seven South Asian countries demonstrated substantial potential in textile export trade, and this potential showed a steady upward trend, as presented in table 6. An in-depth analysis of trade potential differences across countries revealed that China's textile export potential to Bangladesh, India, Pakistan, and Sri Lanka was at a relatively high level, while that to Bhutan and the Maldives was relatively low. In terms of specific trade potential values, under the ideal assumption of no trade resistance or frictions, the average textile export potential from China to the seven South Asian countries in 2023 was approximately 2.1 billion USD. In the same year, China's export potential to India reached about 12.6 billion USD, which was closely related to India's huge population base, strong demand for textiles, and the long-standing good cooperation foundation between the two countries in the textile industry. As the most populous and largest economy in South Asia, India has a huge demand for textiles. China's wide variety of textile products can meet the diversified needs of the Indian market, ranging from grains to various textile products. In 2023, the export potentials of Bangladesh and Pakistan were approximately 0.6 billion USD and 1.1 billion USD respectively. These two countries have vast textile markets and growing consumption capacity, and China has strong complementarity with them in textile trade.

Meanwhile, Sri Lanka's export potential was about 0.2 billion USD. Although its market size was relatively small, the demand for some speciality textiles was stable. In contrast, China's textile export potential to Bhutan and the Maldives was low, at about 1.09 million USD and 8.35 million USD, respectively. This was mainly because Bhutan, located in the Himalayan mountains, had a relatively closed geographical environment, a small-scale textile industry, and limited domestic market demand.

The Maldives, an archipelagic country with scarce land resources, faced significant constraints in textile industry development and mainly relied on imports. However, restricted by its own economic scale and market capacity, its import demand for textiles was relatively small. Such differences in trade potential reflected the disparities between China and South Asian countries in terms of textile resource endowments, market demand structures, and trade cooperation foundations. With the in-depth advancement of the Belt and Road Initiative, cooperation between China and South Asian countries in infrastructure construction and trade facilitation has been continuously strengthened, which will help further unleash trade potential, reduce trade resistance, and promote the development of textile export trade between China and the seven South Asian countries to a higher level. In the future, through measures such as strengthening scientific and technological exchanges

Table 5

EFFICIENCY OF CHINA'S EXPORTS TO SEVEN SOUTH ASIAN COUNTRIES, 2010–2023

Year	Bangladesh	Bhutan	India	Maldives	Nepal	Pakistan	Sri Lanka	Mean (USD)
2010	0.7989	0.3043	0.0324	0.5658	0.3270	0.3082	0.3681	0.3864
2011	0.8522	0.1259	0.0385	0.9731	0.4994	0.3256	0.4769	0.4702
2012	0.7184	0.3444	0.0423	0.6199	0.4168	0.2693	0.5101	0.4173
2013	0.7650	0.3485	0.0461	0.6912	0.5006	0.2388	0.5423	0.4475
2014	0.7894	0.1614	0.0423	0.6348	0.3681	0.2639	0.6610	0.4173
2015	0.7345	0.6232	0.3452	0.6815	0.3679	0.2846	0.9998	0.5767
2016	0.5954	0.3794	0.0368	0.8915	0.4990	0.2561	0.8794	0.5054
2017	0.5042	0.1698	0.0335	0.7440	0.4755	0.2456	0.6733	0.4066
2018	0.6115	0.1602	0.0271	0.6193	0.5120	0.2155	0.5034	0.3784
2019	0.8696	0.1411	0.2306	0.7241	0.5243	0.2573	0.6083	0.4793
2020	0.8632	0.1389	0.1987	0.5266	0.3899	0.2667	0.5579	0.4203
2021	0.9607	0.1135	0.2288	0.8080	0.8905	0.2749	0.5255	0.5431
2022	0.7810	0.0469	0.0265	0.8447	0.6601	0.2643	0.4015	0.4321
2023	0.8425	0.1984	0.0329	0.9798	0.9954	0.2570	0.4759	0.5403
Mean	0.7633	0.2326	0.0973	0.7360	0.5305	0.2663	0.5845	0.4586

Table 6

ESTIMATED EXPORT TRADE POTENTIAL OF SEVEN SOUTH ASIAN COUNTRIES, 2010–2023

Year	Bangladesh	Bhutan	India	Maldives	Nepal	Pakistan	Sri Lanka	Mean
2010	292237604	879648	8865652994	4607047	98975040	871531204	232114789	1480856904
2011	268622695	828832	8044682182	4181548	102790288	833514189	217965024	1353226394
2012	274037553	825494	8043498132	4333588	102440917	880529740	222623292	1361184102
2013	297049179	820660	8159251649	4804657	103774586	906329012	232082318	1386301723
2014	335117326	884758	8942739480	5394625	108066582	964147806	249595502	1515135154
2015	386673003	972378	9733979900	6265680	120267043	1099831859	271474990	408411849
2016	529605339	1143919	11569697935	7425328	134896172	1270679520	310961701	1974915702
2017	577616244	1241137	12982879821	8131220	152984414	1368740428	332452243	2203435072
2018	582866481	1177428	12538856753	8447802	158384750	1349893838	316828802	2136636551
2019	648310657	1281545	1357245317	9314411	169994850	1328233964	319194588	547653618.8
2020	689814403	1218474	1334193659	7229070	172019787	1304898950	313910645	546183569.7
2021	588135369	1046652	1184976543	7292621	146638056	1149812710	258102700	476572093
2022	626987041	1073390	12270693811	8120471	157063562	1208702694	227977758	2071516961
2023	600199742	1091351	12618677720	8348898	153722194	1119121374	243178132	2106334202
Mean	478376617	1034690	8403358993	6706926	134429874	1118283378	267747320	-

in the textile industry, optimising the textile trade structure, and improving trade service levels, textile trade between China and South Asian countries is expected to achieve greater growth, bringing more opportunities for the development of the textile industry and economic cooperation between both sides.

According to the level of trade potential, South Asian countries can be categorised into “high-potential low-efficiency countries”, “medium-potential high-efficiency countries”, “medium-potential medium-efficiency countries”, and “small-scale markets”. The high-potential low-efficiency group includes India and Pakistan. From 2010 to 2023, their textile export efficiencies were 0.0973 and 0.2663, respectively, significantly lower than the South Asian average (0.4586), but their trade potentials reached 7.7 billion USD and 1.1 billion USD, ranking top two in South Asia. India’s high potential stems from the consumption demand of its 1.4 billion population, while Pakistan relies on its textile processing industry foundation. However, trade inefficiencies in both countries are primarily constrained by non-tariff barriers and infrastructure bottlenecks, necessitating breakthroughs in inefficiency bottlenecks to unleash trade potential. Medium-potential high-efficiency countries such as Bangladesh and Sri Lanka have export efficiencies of 0.7633 and 0.5845, respectively, significantly higher than the South Asian average, with trade potentials of 480 million USD and 270 million USD, classifying them as “mature markets”. Bangladesh, relying on its garment processing industry, has become a major importer of Chinese fabrics, while Sri Lanka demonstrates stable demand for speciality textiles but faces competition from Southeast Asian products, requiring deepened industrial collaboration to enhance trade quality. Small-scale markets include the Maldives and Bhutan, where strategies should focus on precise demand positioning and niche potential exploration. Nepal, a medium-potential medium-efficiency country with an export efficiency of 0.5305 (slightly above the South Asian average) and a trade potential of 0.134 billion USD, is a “growth market” that can activate its regional hub value through infrastructure connectivity. The final category, small-scale markets (Maldives and Bhutan), has export efficiencies of 0.7360 and 0.2326, with trade potentials of only 6.7 million USD and 1.03 million USD. The Maldives, constrained by its island economy, primarily demands tourism-related textiles, while Bhutan, geographically isolated with a weak textile foundation, shows growing demand for environmental products.

The export expansion space of Chinese textiles to South Asian countries showed significant country-specific differentiation, as presented in table 7, which was closely related to export efficiency. The largest expansion spaces were observed in Bhutan and India, reaching 2132.20% and 3773.58%, respectively. Although China’s textile export efficiency to these countries was low, the expandable space released was the largest, indicating broad cooperation prospects for future textile trade. The formation of such high expansion space stemmed from both the high logistics costs caused by Bhutan’s geographical isolation and India’s textile industry protection policies. In contrast, the smallest expansion spaces were in Bangladesh, the Maldives, and Sri Lanka, at 134.77%, 140.72%, and 183.36%, respectively. While the import expansion space in these countries was limited, the low expansion space did not imply exhausted trade potential but directly reflected market maturity. From 2010 to 2023, the overall export expansion space of Chinese textiles to South Asia

Table 7

EXPORT EXPANSION POTENTIAL OF THE SEVEN SOUTH ASIAN COUNTRIES, 2010–2023

Year	Bangladesh	Bhutan	India	Maldives	Nepal	Pakistan	Sri Lanka	Mean
2010	125.17%	328.62%	3086.42%	176.74%	305.81%	324.46%	271.67%	659.84%
2011	117.34%	794.28%	2597.40%	102.76%	200.24%	307.13%	209.69%	618.41%
2012	139.20%	290.36%	2364.07%	161.32%	239.92%	371.33%	196.04%	537.46%
2013	130.72%	286.94%	2169.20%	144.68%	199.76%	418.76%	184.40%	504.92%
2014	126.68%	619.58%	2364.07%	157.53%	271.67%	378.93%	151.29%	581.39%
2015	136.15%	160.46%	289.69%	146.74%	271.81%	351.37%	100.02%	208.03%
2016	167.95%	263.57%	2717.39%	112.17%	200.40%	390.47%	113.71%	566.53%
2017	198.33%	588.93%	2985.07%	134.41%	210.30%	407.17%	148.52%	667.53%
2018	163.53%	624.22%	3690.04%	161.47%	195.31%	464.04%	198.65%	785.32%
2019	115.00%	708.72%	433.65%	138.10%	190.73%	388.65%	164.39%	305.61%
2020	115.85%	719.94%	503.27%	189.90%	256.48%	374.95%	179.24%	334.23%
2021	104.09%	881.06%	437.06%	123.76%	112.30%	363.77%	190.29%	316.05%
2022	128.04%	2132.20%	3773.58%	118.39%	151.49%	378.36%	249.07%	990.16%
2023	118.69%	504.03%	3039.51%	102.06%	100.46%	389.11%	210.13%	637.71%
Mean	134.77%	635.92%	2175.03%	140.72%	207.62%	379.18%	183.36%	550.94%

decreased from 659.84% to 550.94%, indicating a gradual improvement in the prospects of textile trade between China and South Asia. Despite short-term fluctuations due to external shocks such as India's trade policy adjustment in 2014 and the COVID-19 pandemic in 2020, the continuous convergence trend was of clear positive significance. The decline in expansion space essentially represented the process of actual trade volume approaching trade potential, reflecting the effectiveness of policy tools such as the second-phase implementation of the China-Pakistan Free Trade Agreement and the launch of the China-Bangladesh cross-border textile industrial park. The improvement of regional trade facilitation gradually dismantled tariff and non-tariff barriers.

CONCLUSION AND POLICY RECOMMENDATIONS

Conclusion

Expansion of textile trade and efficiency trends (2010–2023)

Between 2010 and 2023, China's textile exports to South Asian countries experienced significant growth, enhancing China's position within the regional textile trade. Overall, trade efficiency exhibited an upward trajectory; however, export volumes remained relatively modest, and efficiency levels were generally low, with notable disparities among countries. While there was substantial room for improvement in trade potential and expansion capacity, these opportunities varied considerably across different nations.

Impact of objective factors on export efficiency

China's domestic economic development level imposed certain constraints on textile exports, indicating that it was no longer a primary driver for exports to South Asia and, in some respects, may have acted as a limiting factor. Conversely, the growth in China's textile exports to South Asian countries was primarily attributed to China's large population, the economic advancement of South Asian nations, and the influence of shared languages. Although the expansion of South Asian populations and the geographical proximity between capitals somewhat facilitated textile trade, their impact was not pronounced. Therefore, it was imperative for China and South Asian countries to enhance the role of common languages and for South Asian nations to focus on economic development to further elevate bilateral textile trade cooperation.

Influence of institutional and policy factors

Key institutional factors, such as government effectiveness, free trade agreements, participation in the Shanghai Cooperation Organisation (SCO), and monetary freedom, played significant roles in reducing inefficiencies in China's textile exports to South Asia. These elements substantially promoted export efficiency. However, trade freedom exerted a positive effect on export inefficiency, potentially hindering the development of textile trade between China and South Asian countries. This phenomenon might be attributed to the strong protective measures for domestic textile industries within South Asian nations, which adversely affected China's export markets. Consequently, both parties needed to implement measures to reduce tariff and non-tariff barriers, thereby expanding marketing flexibility and mitigating inefficiencies.

From the empirical results, the promoting effect of human factors is significantly greater than that of natural factors, which answers the question in the introduction: the main driving force for China's textile exports to South Asian countries is human factors, and the current trade level has not reached the upper limit of potential.

Policy recommendations and future outlook

Policy recommendations

(1) At the national level

China and South Asian countries need to establish a long-term intergovernmental cooperation framework for the textile industry, focusing on promoting institutional coordination in three aspects. First, establish the "China-South Asia Textile Standards Joint Committee" to unify textile safety certifications, testing methods, and labelling specifications, reducing trade barriers caused by standard discrepancies. For example, in major markets such as Bangladesh and Pakistan, pilot mechanisms for mutual recognition of indicators like formaldehyde content and colour fastness in textile fabrics can be prioritised to lower corporate compliance costs. Second, accelerate the upgrading negotiations of free trade agreements (FTAs). In the second-phase implementation of the China-Pakistan Free Trade Agreement, expand the coverage of textile items with zero tariffs, and launch feasibility studies on FTAs with countries such as India and Sri Lanka to directly reduce the market access costs for Chinese textiles through tariff reductions. Third, establish a "Textile Industry Policy Communication Platform" to regularly release trade policy updates of South Asian countries and provide policy risk assessment services for enterprises.

Relying on the Belt and Road Initiative, a multi-dimensional infrastructure network should be constructed. Accelerate the construction of the main line of the China-Nepal Railway, the Gwadar Port section of the China-Pakistan Railway, and the extension of the China-Laos Railway to form a three-dimensional transportation system of "railway-highway-port", shortening the transportation cycle and reducing costs for textiles from China to South Asia. Meanwhile, launch intermodal routes for the "China-South Asia Railway Express", establish bonded logistics centres in Kathmandu (Nepal) and Lahore (Pakistan), and achieve "one inspection, full-domain clearance" for textiles. Additionally, promote South Asian countries' access to China's cross-border e-commerce comprehensive pilot zones, establish online textile trading markets via platforms such as Alibaba.com and AliExpress, and compress customs clearance time for small and medium orders through digital technologies to enhance trade efficiency.

(2) At the enterprise level

Chinese textile enterprises need to adjust their strategies according to the characteristics of South Asian markets. On the one hand, strengthen the industrial chain collaboration model of "Chinese raw materials, South Asian processing", such as expanding investment in Pakistan's Sahiwal Textile and Garment Industrial Park and constructing supporting chemical fibre raw material production lines to meet local garment manufacturers' demand for high-elasticity fabrics. On the other hand, develop a cost-effective product matrix for the rigid demand of mid-to-low-end textiles in South Asia. Meanwhile, establish a Southeast Asia-South Asia entrepot trade network by setting up distribution centres in Yangon (Myanmar) and Colombo (Sri Lanka) to evade India's anti-dumping restrictions on Chinese polyester fibres.

Furthermore, promote digital transformation and green production reforms to accelerate textile technology export and standard upgrading. Popularise IoT spinning equipment to help South Asian enterprises improve production efficiency while reducing energy consumption. Deploy intelligent printing and dyeing factories in Bangladesh and Nepal, adopt zero-emission technologies, obtain EU eco-labels, and break through green trade barriers in developed countries. Additionally, develop products compliant with South Asian environmental standards: launch degradable textile packaging materials in response to India's "Clean India" initiative, and research and develop plant fibre-based textiles to meet the Maldives' plastic ban, thereby enhancing product premium.

(3) At the international cooperation level

China should strengthen multilateral mechanisms and cultural integration bonds, activate the trade promotion function of the Shanghai Cooperation Organisation (SCO), and build a textile trade coordination system with the SCO as the platform. Establish an "SCO Textile Trade Working Group" including members from India, Pakistan, China, etc., focus on formulating regional rules of origin mutual recognition schemes, and promote the establishment of a "South Asian Textile Trade Database" to share supply and demand information among countries. Meanwhile, jointly issue a "White Paper on South Asian Textile Trade Facilitation" to unify customs codes and inspection and quarantine procedures, reducing corporate customs clearance costs. In response to the SCO's current focus on security-related cooperation, initiate an "SCO Textile Industry Innovation Forum" focusing on topics such as green textiles and digital technology applications to enhance the direct impact of policies on trade.

Moreover, construct a language-culture-trade integration ecosystem to promote deep trade integration through language interoperability. Establish "China-Pakistan Bilingual Talent Training Bases for the Textile Industry" in Lahore (Pakistan) and Kathmandu (Nepal), collaborate with local universities to offer specialised courses in Urdu, Nepali, and textile engineering, cultivate interdisciplinary talent, and reduce business negotiation costs. Meanwhile, carry out "Chinese Textile Culture Exhibition Tours" through Confucius Institutes, display traditional craftsmanship such as Su embroidery and Xiang embroidery in Sri Lanka and Bhutan, promote the integration of Chinese embroidery with local clothing cultures, develop "Belt and Road"-themed textiles, and enhance product premium derived from cultural identity. Additionally, leverage the advantage of common languages to optimise trade negotiation efficiency: form bilingual negotiation teams in the upgrading negotiations of the China-Pakistan Free Trade Agreement, shorten the consultation cycle for technical trade barriers, and promote the implementation of

the China-Bangladesh textile fast-track customs clearance agreement.

Research limitations and future directions

This study reveals the potential landscape of textile trade between China and South Asia, covering only seven South Asian countries and excluding Central Asia or Southeast Asia, so the conclusions do not apply to other regions. The stochastic frontier model is used to reveal the multidimensional influencing factors of trade potential, but there are still many limitations. The policy recommendations proposed in this paper aim to promote textile trade between China and South Asia, but their effectiveness may be constrained by practical obstacles, especially trade protectionism and geopolitical risks in the region. These limitations highlight the necessity of adjusting policies according to local conditions and formulating risk mitigation strategies. Moreover, due to the limitations of data dimensions and availability, this paper does not include domestic logistics costs and consumer preference data of South Asian countries, which may lead to incomplete identification of trade inefficiency factors. The trade characteristics of textile subcategories differ significantly, but the model does not conduct category-specific estimations, making it difficult to accurately locate the potential release paths of different products. In addition, this paper fails to consider spatial spillover effects; for example, the competitive relationship between India and Pakistan may affect China's export decisions through third-country markets, thus requiring the introduction of spatial econometric models to analyse the interactive effects of intra-regional trade. Future research could explore and promote practices from the following dimensions:

(1) Inclusion of emerging variables and dynamic mechanism analysis

Due to data constraints, variables such as domestic logistics costs and consumer preferences in South Asian countries were not incorporated, potentially leading to an incomplete identification of trade inefficiency factors. Additionally, significant differences existed in the trade characteristics of various textile subcategories, but the model did not estimate these separately, hindering the precise identification of potential release pathways for different products. Future research could introduce emerging variables, such as a "Digital Trade Intensity Index", to quantitatively assess the marginal contributions of innovations like live-streaming e-commerce and smart logistics to trade efficiency, particularly in countries like the Maldives and Bhutan, which were in the early stages of digital development. Furthermore, climate change impacts, such as monsoon anomalies in India leading to reduced grain production, could reshape trade structures, necessitating the inclusion of climate risk indices to dynamically evaluate the effects of extreme weather on export potential.

(2) Deepening regional institutional coordination

The positive impact of the SCO on trade efficiency had not yet been fully realised. Future studies could focus on the synergistic mechanisms between the Belt and Road Initiative and the SCO, such as examining the effects of textile tariffs within the SCO framework on trade dynamics. Additionally, the policy spillover effects of the Regional Comprehensive Economic Partnership (RCEP) on South Asian countries warranted investigation, with analyses of its long-term influence on textile trade volumes and structures.

(3) Expanding research from a microenterprise perspective

Current analyses were based on macro-level data, lacking in-depth insights into enterprise behaviours. Future research could employ surveys or case studies to explore the practical challenges faced by small and medium-sized export enterprises in South Asian markets, particularly strategies to navigate non-tariff barriers in India. Moreover, examining how the supply chain configurations of multinational textile enterprises influenced trade efficiency could provide valuable empirical insights at the enterprise level.

(4) Integrating green trade and sustainable development:

The rising demand for environmentally friendly products in South Asian countries, such as the Maldives' plastic ban, highlighted the need to incorporate variables like green certifications and carbon footprints into analyses. Future studies could develop a "Textile Green Trade Index" to assess the impact of organic certification, mutual recognition, and low-carbon packaging technologies on export premiums.

Additionally, evaluating the trade creation effects of China's promotion of green technologies, such as photovoltaic irrigation and smart greenhouses, in South Asia would offer theoretical support for "climate-smart agricultural cooperation".

This study provided a quantitative analysis framework based on the gravity model for examining China's textile trade with South Asia. Future research should aim to enhance data richness, model sophistication, and policy relevance to comprehensively elucidate the dynamic evolution of regional trade patterns and offer targeted theoretical support for precise policy formulation within the context of Belt and Road textile cooperation.

REFERENCES

[1] Deardorff, A.V., *Determinants of bilateral trade: does gravity work in a neoclassical world?* Cambridge, MA, USA: National Bureau of Economic Research, 1995, 5377,1–30

[2] Karackattu, J.T., *India–China Trade at the Borders: challenges and opportunities*, In: Journal of Contemporary China, 2013, 22, 82, 691–711

[3] Tinbergen, J., *An analysis of world trade flows*, In: Shaping the World Economy, 1962, 3, 1–117

[4] Anderson, J.E., *A theoretical foundation for the gravity equation*, In: The American Economic Review, 1979, 69, 1, 106–116
[5] Anderson, J.E., Van Wincoop, E., *Gravity with gravitas: A solution to the border puzzle*, In: American Economic Review, 2003, 93, 1, 170–192
[6] Egger, P., *A note on the proper econometric specification of the gravity equation*, In: Economics Letters, 2000, 66, 1, 25–31
[7] Chen, F., Ahmad, S., Jiang, G., Chen, J., *Factors Affecting Textiles Products Exports of Major Producers: A Gravity Model Approach*, In: SAGE Open, 2023, 13, 4, 21582440231213688
[8] Shekhawat, K.K., Shastri, S., *The Determinants and Potentials of India's Textiles Exports: A Gravity Model Approach*, In: Journal of Economic Cooperation & Development, 2023, 44, 4, 17–46
[9] Rahman, R., Shahriar, S., Kea, S., *Determinants of exports: A gravity model analysis of the Bangladeshi textile and clothing industries*, In: FIIB Business Review, 2019, 8, 3, 229–244
[10] Wen, L., Xu, J., Zeng, H., Ma, S., *The impact of digital services trade in belt and road countries on China's construction green goods export efficiency: a time-varying stochastic frontier gravity model analysis*, In: Journal of Asian Architecture and Building Engineering, 2025, 1–24
[11] Janaway, R.C., Coningham, R.A.E., *A review of archaeological textile evidence from South Asia*, South Asian Studies, 1995, 11, 1, 157–174
[12] Riello, G., Roy, T., *How India Clothed the World: The World of South Asian Textiles*, 2009, 4, 1500–1850
[13] Maxwell, R., *Textiles of Southeast Asia: Trade, tradition and transformation*, Tuttle Publishing, 2012
[14] Tsang, W.Y., Au, K.F., *Textile and clothing exports of selected South and Southeast Asian countries: A challenge to NAFTA trading,* In: Journal of Fashion Marketing and Management: An International Journal, 2008, 12, 4, 565–578
[15] Guan, Z., Xu, Y., Jiang, H., Jiang, G., *International competitiveness of Chinese textile and clothing industry – a diamond model approach,* In: Journal of Chinese Economic and Foreign Trade Studies, 2019, 12, 1, 2–19
[16] Zhou, L., Mao, Y., Fu, Q., Xu, D., Zhou, J., Zeng, S., *A study on the Belt and Road Initiative's trade and its influencing factors: Evidence of China-South Asia's panel data*, In: PloS one, 2023, 18, 4, e0282167
[17] Dastgeer, A., Hassan, A., Husnain, M.A., Bhatti, M.K., Javed, A., *The impact of the China-Pakistan free trade agreement (FTA) on the economic growth of Pakistan,* In: Russian Law Journal, 2023, 11, 3, 2288–2299
[18] Razzaque, M.A., Rahman, J., Akib, H., *Bangladesh-China trade and economic cooperation: issues and perspectives. Navigating new waters: unleashing Bangladesh's export potential for smooth LDC graduation*, 2020, 193–228
[19] Sikder, M., Dou, X., *Bilateral Export Trading Analysis between Bangladesh and China: Opportunities and Prospects*, In: American International Journal of Business and Management Studies, 2020, 2, 2, 1–10
[20] Jain, R., *China's economic expansion in South Asia*, In: Indian Journal of Asian Affairs, 2018, 31, 1/2, 21–36
[21] Li, D., Yan, H., Ma, S., *ESG performance drivers and corporate growth: a life-cycle-based fsQCA–PSM study of China's construction and manufacturing enterprises*, In: Journal of Asian Architecture and Building Engineering, 2025, 1–18
[22] Ma, S., Appolloni, A., *Can financial flexibility enhance corporate green innovation performance? Evidence from an ESG approach in China*, In: Journal of Environmental Management, 2025, 387, 125869
[23] Liu, H., Cong, R., Liu, L., Li, P., Ma, S., *The impact of digital transformation on innovation efficiency in construction enterprises under the dual carbon background*, In: Journal of Asian Architecture and Building Engineering, 2025, 1–18
[24] Zhang, X., Li, D., Yan, H., Ma, S., *Does Air pollution affect the green innovation of industrial enterprises? Insights from Urban Sewage Control Policies in China*, In: Global NEST Journal, 2025
[25] Zhang, X., Li, G., Wu, R., Zeng, H., Ma, S., *Impact of Carbon Emissions, Green Energy, Artificial Intelligence and High-Tech Policy Uncertainty on China's Financial Market*, In: Finance Research Letters, 2025, 107599
[26] Ma, S., Liu, H., Li, S., Lyu, S., Zeng, H., *Quantifying the relative contributions of climate change and human activities to vegetation recovery in Shandong Province of China,* In: Global NEST Journal, 2025
[27] Ma, S., Yan, H., Li, D., Liu, H., Zeng, H., *The Impact of Agricultural Mechanisation on Agriculture Carbon Emission Intensity: Evidence from China,* In: Pakistan Journal of Agricultural Sciences, 2025, 62, 1
[28] Tinbergen, J., *Shaping the world economy; suggestions for an international economic policy*, 1962
[29] Meeusen, W., van Den Broeck, J., *Efficiency estimation from Cobb-Douglas production functions with composed error*, In: International Economic Review, 1977, 435–444
[30] Battese, G.E., Coelli, T.J., *Frontier production functions, technical efficiency and panel data: with application to paddy farmers in India*, In: Journal of Productivity Analysis, 1992, 3, 153–169
[31] Battese, G.E., Coelli, T.J., *A model for technical inefficiency effects in a stochastic frontier production function for panel data*, In: Empirical Economics, 1995, 20, 325–332
[32] Armstrong, S.P., *Measuring trade and trade potential: A survey*, In: Crawford School Asia Pacific Economic Paper, 2007, 368
[33] Deaton, A., Muellbauer, J., *An almost ideal demand system,* In: The American economic review, 1980, 70, 3, 312–326
[34] Liu, H., He, Q., Cong, R., Ma, S., Gong, J., *Exploring the Dynamic Linkages between Carbon Trading Market and Smart Technology Indices: A Multi-dimensional Analysis of China's Case*, In: International Review of Economics & Finance, 2025,104360
[35] Sun, D., Li, Y., *Carbon peaking pressure and corporate R&D investment*, In: Economics Letters, 2025, 251, 112328

[36] Wu, Y., Zeng, H., Hao, N., Ma, S., *The impact of economic policy uncertainty on the domestic value added rate of construction enterprise exports – evidence from China*, In: Journal of Asian Architecture and Building Engineering, 2025,1–15

[37] Shen, D., Guo, X., Ma, S., *Study on the Coupled and Coordinated Development of Climate Investment and Financing and Green Finance of China*, In: Sustainability, 2024,16, 24, 11008

[38] Ma, S., Zeng, H., Abedin, M.Z., *The impact of the reforms in the Chinese equities exchange and quotations on innovation in cross-border e-commerce enterprises*, In: Asia Pacific Business Review, 2025, 1–41

[39] Wang, Z., Wang, F., Ma, S., *Research on the Coupled and Coordinated Relationship Between Ecological Environment and Economic Development in China and its Evolution in Time and Space,* In: Polish Journal of Environmental Studies, 2025, 34, 3

[40] Wang, Z., Ma, S., *Research on the impact of digital inclusive finance development on carbon emissions – Based on the double fixed effects model*, In: Global NEST Journal, 2024, 26, 7

[41] Ding, Y., Guo, J., Ji, Y., Guo, K., Ma, S., *The digital economy and city innovation convergence – an empirical research based on the innovation value chain theory*, In: Technological and Economic Development of Economy, 2025, 1–36

[42] Zhang, G., Ma, S., Zheng, M., Li, C., Chang, F., Zhang, F., *Impact of Digitization and Artificial Intelligence on Carbon Emissions Considering Variable Interaction and Heterogeneity: An Interpretable Deep Learning Modeling Framework*, In: Sustainable Cities and Society, 2025, 106333

[43] Sun, D., Luo, Q., *Green transition under carbon peak pressure: beyond greenwashing*, In: Applied Economics, 2026, 1–17

Authors:

LIQIN WEN[1], JIE XU[1], WENXUE ZOU[2], XUE LEI[3], SHENGLIN MA[1]

[1]School of Economics and Management, North University of China, Taiyuan, China

[2]Financial Interbank Department, Beijing Rural Commercial Bank, Beijing, China

[3]School of Management, Shanghai University, Shanghai, China

Corresponding author:

SHENGLIN MA
e-mail: sz202209002@st.nuc.edu.cn

Enhancing textile industry efficiency using data mining and business intelligence for optimal supply chain management

DOI: 10.35530/IT.077.03.202554

P. VIJAYALAKSHMI
MANIMARAN S
KISHORE KUNAL
VAIRAVEL MADESHWAREN

ABSTRACT – REZUMAT

Enhancing textile industry efficiency using data mining and business intelligence for optimal supply chain management

In the modern textile industry, the integration of Business Intelligence (BI) through advanced Business Analytics (BA) and Data Mining (DM) techniques is crucial for enhancing supply chain management, optimising production efficiency, reducing operational costs and improving market responsiveness. By using data-driven decision-making techniques, clothing manufacturers can improve their production planning, inventory control and demand forecasting. Nonetheless, the textile industry frequently faces challenges such as unstructured data supply chain inefficiencies and unpredictable market trends, which can lead to increased waste and production delays. This study's main goal is to create a Python-based analytical framework that makes use of data mining methods to improve business intelligence and optimise production processes in the clothing industry. Over six months, production data quality control records and supply chain information were collected from three textile manufacturing facilities located in Trippur from SouthIndia. The gathered dataset was meticulously analysed using Python-based tools, including Pandas, Scikit-learn, and TensorFlow. Various techniques, such as clustering classification, association rule mining and predictive analytics, were employed to extract valuable insights. The research tested four key hypotheses that concentrated on production efficiency, demand prediction, raw material utilisation, and inventory optimisation. Machine learning models were applied to identify production bottlenecks, forecast sales trends and enhance inventory planning. The study's conclusions offer practical suggestions for raising operational effectiveness and profitability in the textile industry. Overall, this research highlights the transformative potential of business analytics in revolutionising textile manufacturing, fostering data-driven growth and strengthening competitiveness in the industry.

Keywords: *textile industry, business intelligence, data mining, predictive analytics, Python, supply chain optimisation*

Creșterea eficienței industriei textile prin utilizarea tehnicilor de explorare a datelor și Business Intelligence pentru o gestionare optimă a lanțului de aprovizionare

În industria textilă modernă, integrarea Business Intelligence (BI) prin intermediul tehnicilor avansate de Business Analytics (BA) și Data Mining (DM) este esențială pentru îmbunătățirea gestionării lanțului de aprovizionare, optimizarea eficienței producției, reducerea costurilor operaționale și îmbunătățirea capacității de reacție la cerințele pieței. Prin utilizarea tehnicilor de luare a deciziilor bazate pe date, producătorii de îmbrăcăminte își pot îmbunătăți planificarea producției, controlul stocurilor și previziunile privind cererea. Cu toate acestea, industria textilă se confruntă frecvent cu provocări precum datele nestructurate, ineficiențele lanțului de aprovizionare și tendințele imprevizibile ale pieței, care pot duce la creșterea deșeurilor și la întârzieri în producție. Obiectivul principal al acestui studiu este de a crea un cadru analitic bazat pe Python care utilizează metode de explorare a datelor pentru a îmbunătăți Business Intelligence și a optimiza procesele de producție în industria de îmbrăcăminte. Pe o perioadă de șase luni, au fost colectate date de producție, înregistrări de control al calității și informații privind lanțul de aprovizionare de la trei unități de producție textilă situate în Trippur, din sudul Indiei. Setul de date colectat a fost analizat meticulos folosind instrumente bazate pe Python, inclusiv Pandas, Scikit-learn și TensorFlow. Au fost utilizate diverse tehnici, precum clasificarea prin clustering, extragerea regulilor de asociere și analiza predictivă, pentru a extrage informații valoroase. Cercetarea a testat patru ipoteze cheie care s-au concentrat pe eficiența producției, previziunea cererii, utilizarea materiilor prime și optimizarea stocurilor. Au fost aplicate modele de învățare automată pentru a identifica blocajele din producție, a prognoza tendințele de vânzări și a îmbunătăți planificarea stocurilor. Concluziile studiului oferă sugestii practice pentru creșterea eficienței operaționale și a profitabilității în industria textilă. În ansamblu, această cercetare evidențiază potențialul transformator al analizei de afaceri în revoluționarea producției textile, în stimularea creșterii bazate pe date și în consolidarea competitivității în cadrul industriei.

Cuvinte-cheie*: industria textilă, Business Intelligence, explorarea datelor, analiza predictivă, Python, optimizarea lanțului de aprovizionare*

INTRODUCTION

The Indian garment business is seeing a very attractive market with a huge young consuming population of the fastest-growing nations in the world. The textile clothing sector plays a key part in developing countries like India, employing a large number of both unskilled and semiskilled people. The challenges in automating garment sewing due to constant alterations

in patterns and stitching techniques have resulted in the industry's reliance on manual labour, rendering the clothing sector a typical entry-level industry that provides employment opportunities for developing nations due to its low fixed costs. In the 21st century, individuals focus more on self and social elements, which requires much of the (EQ) Emotional quotient than the (IQ) Intellectual quotient [1]. Every employee of a business at one point in time has to interact with their supervisors, subordinates, clients, colleagues, as well as other stakeholders on executing their tasks [2, 3]. It is crucial to recruit, maintain and motivate the most appropriate personnel inside the firm in order to achieve the corporate goals and objectives [4]. Supply chains serve two primary purposes: a market broker function that balances supply and demand, and a physical one centred on inventory management and transportation. Effective communication between suppliers and consumers is vital, acting as the foundation for Electronic Data Interchange (EDI), which promotes computer-to-computer transactions. Companies must know customer wants to build systems that link supply with demand [5].

To meet the growing demands of stakeholders for sustainability and the circular economy, fashion companies are rethinking their value chain, with a focus on how the transition from prompt to slower fashion business prototypes can result in an important change in the value they provide through development and distribution processes [6]. The multi-trillion-dollar textile and apparel business is increasingly globalised, with a focus on how the area may enhance various aspects of its GVC involvement to become a significant competitor in the industry's reconfiguration [7].

The textile and apparel (TandA) sector is widely acknowledged as a vital component of the global economy, making a substantial contribution to economic growth and job opportunities in low- and middle-income nations [8]. The epsilon-based measure (EBM) and the DEA-Malmquist productivity index (MPI) model were used to evaluate the performance of Vietnam's ten textile and apparel companies between 2017 and 2020. The proposed model was used to determine which companies performed the best and to increase their operational efficiency [9]. The textile, apparel, and fashion (TAF) sectors are a major contributor to worldwide pollution of the environment at every level of the supply chain, with stakeholders becoming increasingly aware of the impact these industries have on human rights and the climate [10].

A systematic analysis of 127 articles on sustainable supply chain management in the textile and apparel (T&A) industry focused on managing both economic and non-economic risks. Social and environmental ones are distinct [11]. In the examination of data-driven sustainable supply chain management (SSCM) indicators under industrial disruption and ambidexterity, the most important components were found to be resilience, financial vulnerability, and supply chain uncertainty risk assessment [12].

Utilising the revealed comparative advantage approach, the competitiveness of the Turkish textile industry was assessed, emphasising that export volume alone does not adequately determine an industry's competitiveness [13]. To investigate potential avenues for future research in the development of sustainable supply chain management (SSCM) in Indonesia's T&A industry, specifically in the small- and medium-sized enterprise (SME) sector, a systematic review was carried out [14]. A summary of sustainability assessment methods used in the textile and clothing industry was given, emphasising how most product-related assessment methods only considered environmental factors [15]. To lessen their environmental impact and obtain a competitive edge, producers of textiles and modern clothing are embracing and incorporating cutting-edge technologies. Most previous studies have ignored business intelligence systems (BIS) and instead concentrated on the larger picture of how big data might affect retail and distribution inside a firm, especially in the textile and apparel (T&A) industry [16].

METHODOLOGY

Data collection

Data was collected from three textile manufacturing facilities located in Trippur, Tamil Nadu, India, over six months (January 2023 – June 2023). The data encompassed three key areas: production data, quality control records, and supply chain information. Production data included details such as machine output, production time, downtime reasons, and resource utilisation. Quality control records comprised data on defects, rejection rates, and quality parameters. Supply chain information included data on raw material procurement, supplier details, delivery times, and inventory levels, which is explained in table 1. The data was collected in CSV format and stored in a secure database.

Table 1

DEMOGRAPHIC PROFILE OF DATA COLLECTION

Facility ID	Location (city)	Product specialization	Workforce size	Annual revenue (INR)
F001	Tirupur	Knitted garments	500	50 Crores
F002	Erode	Woven fabrics	350	30 Crores
F003	Karur	Home textiles	600	70 Crores

Research methodology

The primary components of the apparel global value chain are shown in the figure 1 below, which will aid in our analysis of all the processes involved in obtaining clothing from its inception through the phases of design, raw materials and intermediate inputs, marketing, and distribution to the end user. The garment

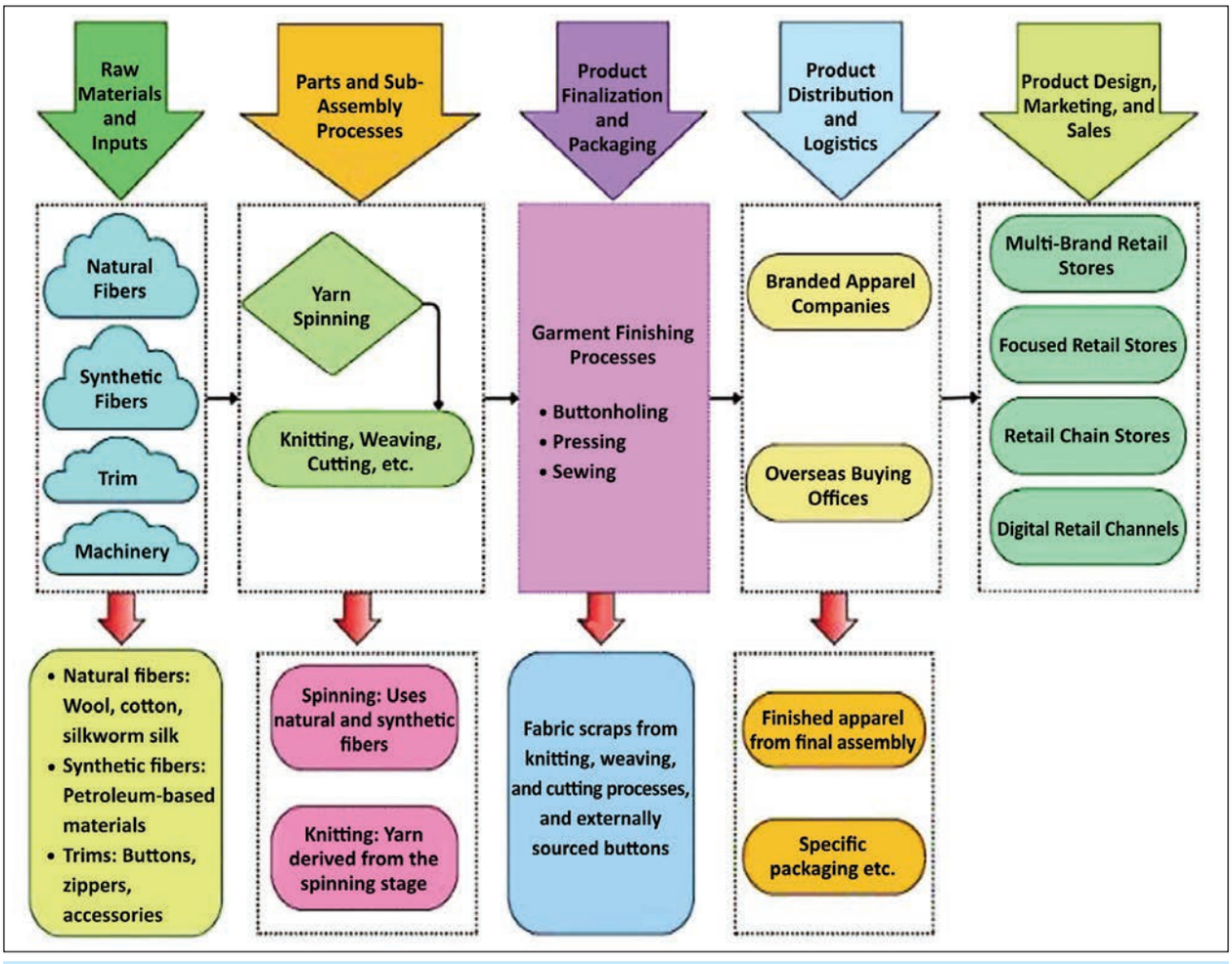

Fig. 1. Manufacturing and supply chain operations in Tamil Nadu's textile and apparel sector

chain often originates with huge stores holding established companies and distribution networks in countries that import them, which produce clothing ideas for approaching seasons. They then outsource operations to firms in developing countries to minimise costs. These manufacturers lack the brands and distribution methods to come to markets directly, which makes them reliant on the leading retailers, referred to as lead businesses. In the garment sector, innovation is generally focused on product design and marketing rather than manufacturing skills, enabling lead businesses to easily outsource production and keep substantial influence over the value chain. This dynamic describes the sector as a "buyer-driven" chain.

PROPOSED TECHNIQUES

Production batches were divided according to lead times, production efficiency and defect rates using clustering techniques, particularly K-Means clustering. The intention was to identify high-risk production categories and improve resource management by combining similar production batches

The K-Means algorithm iteratively assigns each data point x_i to one of K clusters by minimising the intra-cluster variance, represented as equation 1:

$$J = \sum_i = 1K\sum_{x_j} \in C_i||x_j - \mu_i||2 \quad (1)$$

where x_j represents individual data points (e.g., production batches), μ_i is the centroid of cluster C_i, $||x_j - \mu_i||2$ is the squared Euclidean distance between a data point and the cluster centroid, and J is the total intra-cluster variance that the algorithm minimises. Figure 2 shows the production process of apparel.

By using K-Means clustering, the textile industry could optimise inventory planning and schedule maintenance more effectively by analysing trends in defect rates.

Classification

To predict defective batches based on historical inspection records, Decision Tree and Random Forest classifiers were implemented. Automated defect prediction was made possible by these classification techniques, which enhanced quality control and decreased the need for manual inspections. A tree-like structure is created by the Decision Tree algorithm to classify production batches, with each node representing a decision rule based on input features like machine temperature, humidity, raw material quality and operator skill. The following equation 2 is used to determine the likelihood that a batch falls into a particular defect category:

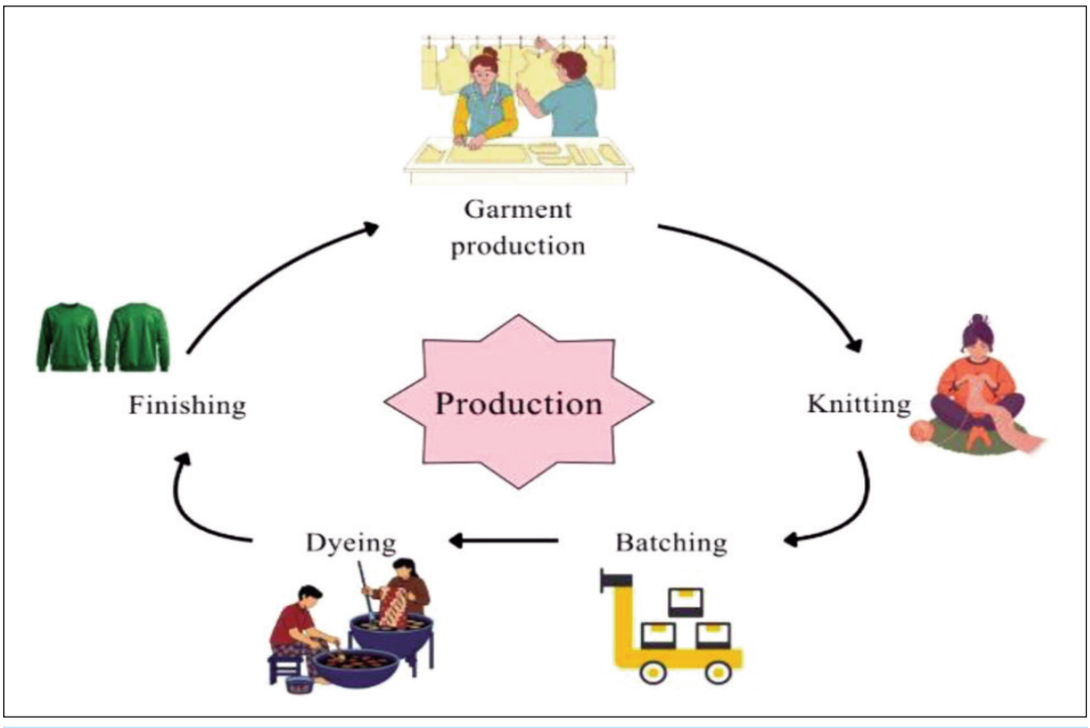

Fig. 2. Production process of apparel

$$P(C_k \mid X) = \frac{N_{C_k}}{N} \quad (2)$$

where $P(C_k \mid X)$ is the probability of class C_k (defective or non-defective) given feature set X, N_{C_k} is the number of instances belonging to class C_k, and N is the total number of instances in the dataset.

LSTM technique

The LSTM has three controllers or gates: IOF, in addition to a long memory cell. The input gate is responsible for determining what extra information should be retained in the cell state. It uses the current input data from the previous period and removes data about irrelevant factors. Finding data that is no longer necessary in the unit state allows the forget gate to calculate the forget vector. Lastly, the output gate determines the output. The following are the main LSTM equations. The forget gate decides which data should be removed from the cell state, which is expressed in equation 3.

$$f_t = \sigma(W_f \cdot [h_{t-1}, x_t] + b_f) \quad (3)$$

Equation 4 chooses which newly acquired data should be kept in the cell state.

$$i_t = \sigma(W_i \cdot [h_{t-1}, x_t] + b_i) \quad (4)$$

Equation 5 adds new information to the cell state.

$$C_t = f_t * C_{t-1} + i_t * \tilde{C}_t \quad (5)$$

Equation 6 figures out the current time steps output.

$$o_t = \sigma(W_o \cdot [h_{t-1}, x_t] + b_o) \quad (6)$$

where x_t represents the input at time t, h_{t-1} is the hidden state from the previous time step, W_f, W_i, W_o are weight matrices, b_o are bias terms, and σ is the sigmoid activation function.

The textile industry could enhance supply chain efficiency, predict changes in market demand and optimise inventory management by putting LSTM-based predictive analytics into practice. In the textile industry, the application of cutting-edge data mining techniques greatly enhanced quality control, production efficiency and decision-making.

Classification improved defect prediction, association rule mining revealed important machine failure patterns, clustering made resource allocation easier and predictive analytics improved sales forecasting. Textile producers increased operational effectiveness, decreased waste and increased profitability by utilising these strategies.

Validation of the model

Standard evaluation metrics were used to evaluate the predictive models' performance. The Scikit-learn metrics library was used to compute the classification models' accuracy, precision, recall and F1-score (equation 7):

$$RMSE = \sqrt{\frac{1}{n}\sum_{i=1}^{n}(y_i - \hat{y}_i)^2} \quad (7)$$

where y_i is the actual value and $\hat{y}_i$ is the predicted value.

Hypotheses

The hypothesis used for this research was:

- *H1: Data-driven decision-making significantly improves operational efficiency in textile manufacturing.*

- *H2: Enhanced business intelligence frameworks contribute to better demand forecasting and inventory management.*
- *H3: The adoption of business analytics reduces raw material wastage and optimises supply chain efficiency.*
- *H4: Predictive insights lead to improved production planning and reduced market response delays.*

RESULTS

Hypothesis 1 analysis

Table 2 analysed the impact of Business Intelligence on production efficiency for hypothesis 1. The metric used for this research was Average Machine Utilisation (%), Downtime Reduction, Production Cycle Time, Defect Rate Reduction (%), and Energy Consumption Reduction (%). These metrics were analysed for facility F001 (knitted garments), Facility F002 (Woven Fabrics), and Facility F003 (Home Textiles). Facility F002 had a lower utilisation of 78.3% and a longer cycle of 14.8 hours, while Facility F001 had the highest machine utilisation of 85.6% with a production cycle of 12.2 hours. Facility F003 demonstrated an 82.1% utilization rate, the most effective downtime reduction of 18.2%, and a 13.3% energy savings. With F003 at 10.5%, F001 at 9.7%, and F002 at 8.3% defect rates also improved.

Hypothesis 2 analysis

Table 3 illustrates the forecast accuracy for demand prediction for hypothesis 2. Here, the LSTM neural network has 2.15 MAE, 3.28 RMSE, and 4.6% MAPE, which outperformed the best compared to the other 2 techniques. The random forest regression model effectively captured nonlinear historical relationships and had moderate error rates. On the other hand, the traditional moving average approach performed the worst, failing to take seasonality into account, and the ARIMA model showed higher error rates, indicating difficulty adjusting to demand fluctuations. Overall, the findings support Hypothesis 2, demonstrating that more accurate demand projections are produced by sophisticated forecasting models.

Hypothesis 3 analysis

Optimisation strategies driven by Business Intelligence (BI) have significantly improved raw material efficiency across various categories, which is shown in table 4 and figure 3. Cotton utilisation was highest in facility F003 at 90.2%, indicating reduced

Table 2

IMPACT OF BUSINESS INTELLIGENCE ON PRODUCTION EFFICIENCY (HYPOTHESIS 1)

Metric	Facility F001 (Knitted garments)	Facility F002 (Woven fabrics)	Facility F003 (Home textiles)
Average machine utilisation (%)	85.6%	78.3%	82.1%
Downtime reduction (%)	15.4%	12.8%	18.2%
Production cycle time (hrs)	12.2	14.8	13.1
Defect rate reduction (%)	9.7%	8.3%	10.5%
Energy consumption reduction (%)	12.1%	10.5%	13.3%

Table 3

FORECAST ACCURACY FOR DEMAND PREDICTION (HYPOTHESIS 2)

Forecasting model	MAE (Mean Absolute Error)	RMSE (Root Mean Square Error)	MAPE (Mean Absolute Percentage Error)
LSTM Neural Network	2.15	3.28	4.6%
ARIMA Model	3.42	4.86	6.1%
Random Forest Regression	2.87	4.02	5.3%
Traditional Moving Average	5.23	7.41	8.9%

Table 4

OPTIMIZATION OF RAW MATERIAL UTILIZATION (HYPOTHESIS 3)

Raw material	Facility F001 – Utilization efficiency (%)	Facility F002 – Utilization efficiency (%)	Facility F003 – Utilization efficiency (%)
Cotton	89.4	86.1	90.2
Polyester	84.2	80.5	85.6
Rayon	88.1	82.7	89.5
Wool	81.3	79.2	84.1
Blended fibers	87.8	84.9	88.2

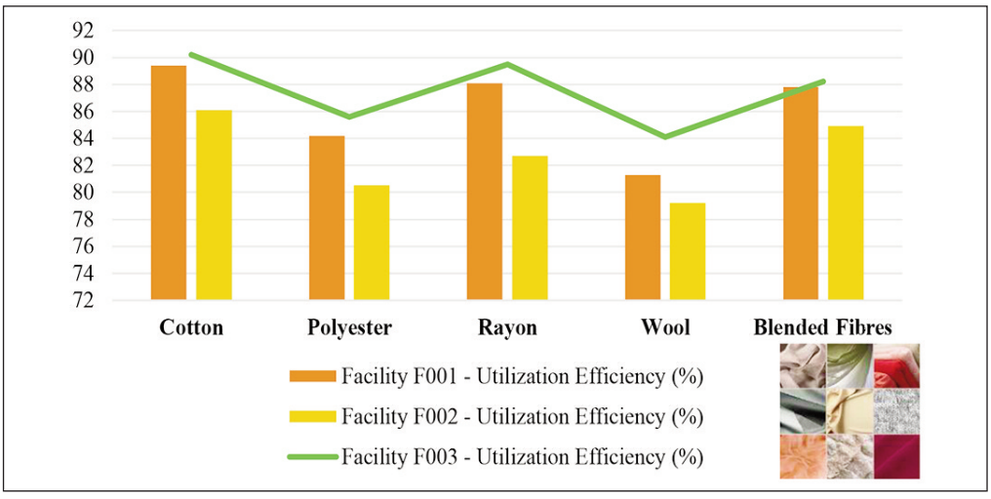

Fig. 3. Optimization process

wastage in home textile production. Polyester utilisation showed a marked improvement, particularly in F003 at 85.6%. Rayon also performed well with efficiencies of 88.1% and 89.5% in F001 and F003, respectively.

In F002, wool utilisation was lower at 79.2%, but the system handled variability well. Blended fibres achieved high efficiencies with F001 at 87.8% and F003 at 88.2%. Overall, BI has notably enhanced raw material utilisation, affirming hypothesis 3.

Hypothesis 4 analysis

The effectiveness of inventory optimisation for hypothesis 4 was explained in table 5. Here, the stock turnover ratio was 5.2% in before Business Intelligence implementation, and 7.8% in after BI implementation. So totally the improvement % was 50% for the stock turnover ratio. Then 1.2 M and 850 K for holding cost reduction (INR) for both before and after BI implementation. The improvement of Holding Cost Reduction was 29.2%. Lead time (days) was reduced from 14 to 10 before and after BI implementation. The range improvement was 28.6%. And finally, the overstock reduction of before and after was 18.2% and 9.4%, and the overall improvement was 48.4%.

Process-wise performance evaluation in textile manufacturing

Table 6 illustrates the significant operational variation found in the evaluation of textile manufacturing processes. Important results show that knitting took an average of 11.5 hours with a 5.2% defect rate, while dying took the longest at 14.2 hours with a 7.8% defect rate. Printing required 12.7 hours with a 6.3% defect rate, and cutting proved efficient with just 9.8 hours and 4.9% defects. It took 13. 4 hours to sew with a 5.6% defect rate and 10.9 hours to finish with a 4.1% defect rate. Packaging was the fastest at 8.6 hours, achieving the lowest defect rate of 3.5%. Different efficiency and quality metrics are highlighted in the assessment, suggesting areas for process optimisation.

Business intelligence impact on supply chain metrics

Table 7 demonstrates the Business Intelligence Impact on Supply Chain Metrics. Supplier Lead Time (days), On-time Delivery (%), Procurement Cost Reduction (INR), and Order Fulfilment Rate (%) were the supply chain parameters utilised in this study. The supplier lead time was 12 days before BI installation and 8 days after BI implementation, which have 33.3% improvement. The on-time was better after BI installation, which 91% and 78% in before BI deployment. The procurement cost reduction has improved by 24%, and it was 1.9 million before and 2.5 million after BI adoption. And lastly, the order fulfilment rate fared best after BI deployment, which has 14.6% improvement.

Table 5

EFFECTIVENESS OF INVENTORY OPTIMIZATION (HYPOTHESIS 4)			
Inventory parameter	**Before BI implementation**	**After BI implementation**	**Improvement (%)**
Stock turnover ratio	5.2	7.8	50%
Holding cost reduction (INR)	1.2 M	850 K	29.2%
Lead time (days)	14	10	28.6%
Overstock reduction (%)	18.2%	9.4%	48.4%

Table 6

PROCESS-WISE PERFORMANCE EVALUATION IN TEXTILE MANUFACTURING				
Process	**Picture**	**Avg. production time (hrs)**	**Defect rate (%)**	**Resource utilization (%)**
Knitting		11.5	5.2	87.3
Dyeing		14.2	7.8	82.5
Printing		12.7	6.3	85.2
Cutting		9.8	4.9	89.7
Sewing		13.4	5.6	86.1
Finishing		10.9	4.1	90.2
Packaging		8.6	3.5	91.3

Table 7

BUSINESS INTELLIGENCE IMPACT ON SUPPLY CHAIN METRICS			
Supply chain parameter	**Before BI implementation**	**After BI implementation**	**Improvement (%)**
Supplier lead time (days)	12	8	33.3
On-time delivery (%)	78	91	16.7
Procurement cost reduction (INR)	2.5 M	1.9 M	24
Order fulfilment rate (%)	82	94	14.6

CONCLUSION

The implementation of business intelligence (BI) in the textile sector has led to significant improvements in production and supply chain operations. Facility F001 achieved higher machine utilisation rates and shorter production cycle times, indicating more effective operational procedures according to analysis. Facility F003 experienced notable reductions in energy consumption and equipment downtime, illustrating BI's effectiveness in detecting and resolving hidden inefficiencies. Optimisation of material usage was particularly pronounced in Facility F003, especially for cotton and rayon, while Facility F002 identified further improvement opportunities. In terms of inventory management, BI-driven predictive analytics, especially LSTM-based demand forecasting, allowed for more efficient stock turnover, lower inventory holding costs and lower levels of excess inventory. In examining production processes, packaging was found to be highly efficient; however, dyeing processes require further refinement to lessen defects and energy usage. Enhancements in procurement strategies, shorter lead times, and improved reliability in deliveries have collectively bolstered supply chain performance, leading to faster and more dependable order fulfilment. Overall, the adoption of BI has not only enhanced operational efficiency but also fostered a more agile, cost-effective and future-oriented manufacturing environment, thereby reinforcing long-term competitiveness.

ACKNOWLEDGEMENT

I would express my gratitude to my guide, co-authors and institutions for their continual support in writing this research.

REFERENCES

[1] Sumera, A., Miskon, S., Alabdan, R., Tlili, I., *Statistical assessment of business intelligence system adoption model for sustainable textile and apparel industry*, In: IEEE Access, 2025, 9, 106560-106574

[2] Sumera, A., Miskon, S., Alabdan, R., Tlili, I., *Towards sustainable textile and apparel industry: Exploring the role of business intelligence systems in the era of industry 4.0*, In: Sustainability, 2020, 12, 7, 2632

[3] Waleed Hassan, A., Watanabe, C., Tou, Y., Neittaanmäki, P., *A new perspective on the textile and apparel industry in the digital transformation era*, In: Textiles, 2025, 2, 4, 633–656

[4] Nazma, B., Karim, S.R., Ali, M.M., *Enhancing Managerial Effectiveness with Business Analytics in Sustainable Textile Supply Chains*, 2024

[5] Iranjali, S., Liyanage, P., *Impact of Data Analytics on Operations Success of Apparel Sector ABC Clothing Pvt Limited (Sri Lanka)*, In: International Journal of Computer Applications, 975, 8887

[6] Stefano, A., Centobelli, P., Cerchione, R., *From fast to slow: An exploratory analysis of circular business models in the Italian apparel industry*, In: International Journal of Production Economics, 2023, 260, 108824

[7] Fernandez-Stark, K., Penny, B., Vivian, C., *Analysis of the Textile and Clothing Industry Global Value Chains*, 2024

[8] Weilin, X., Jeff Jia, F., Chen, L., Schoenherr, T., *Sustainable transition in the textile and apparel industry*, In: Journal of Cleaner Production, 2024, 443, 141081

[9] Chia-Nan, W., Phuong-Thuy, T.N., Yen-Hui, W., Thanh-Tuan, D., *A study of performance evaluation for textile and garment enterprises*, In: Processes, 2022, 10, 11, 2381

[10] Stefano, A., Centobelli, P., Cerchione, R., Nadeem, S.P., Riccio, E., *Sustainability trends and gaps in the textile, apparel and fashion industries*, In: Environment, Development and Sustainability, 2024, 26, 2, 2837–2864

[11] Ronak, W., Brandenburg, M., Seuring, S., *Sustainability, risk and performance in textile and apparel supply chains*, In: Cleaner Logistics and Supply Chain, 2022, 5, 100069

[12] Ming-Lang, T., Tat-Dat Bui, M., Lim, K., Fujii, M., Umakanta, M., *Assessing data-driven sustainable supply chain management indicators for the textile industry under industrial disruption and ambidexterity*,b In: International Journal of Production Economics, 2022, 245, 108401

[13] Halife, H., *Competitiveness analysis of textile industry of Turkey: Revealed comparative advantage approach*, In: International Journal of Global Business and Competitiveness, 2022, 17, Suppl 1, 25–30

[14] Vita, S., Primiana, I., Harsanto, B., Satyakti, Y., *Sustainable supply chain of Indonesia's textile & apparel industry: opportunities and challenges*, In: Research Journal of Textile and Apparel, 2024, 28, 4, 819–838

[15] Fadara, T.G., Wong, K.Y., Maulana, M.I., *Sustainability assessment of textile and apparel sector: a review of current approaches and tools*, In: Nigerian Journal of Technological Development, 2023, 20, 3, 1–20

[16] Zurong, C., Zhao, J., Jin, C., *Business intelligence for Industry 4.0: predictive models for retail and distribution*, In: International Journal of Retail & Distribution Management, 2023

Authors:

P. VIJAYALAKSHMI[1], MANIMARAN S[1], KISHORE KUNAL[2], VAIRAVEL MADESHWAREN[3]

[1]Department of Management Studies, PSNA College of Engineering and Technology, Kadiranampatti, Dindigul, Tamil Nadu, India

[2]Professor and Dean of Online Education, Loyola Institute of Business Administration (LIBA), Loyola College Campus, Nungambakkam, Chennai, Tamil Nadu, India

[3]Department of Agriculture Engineering, Dhanalakshmi Srinivasan College of Engineering, Coimbatore, Tamil Nadu, India

Corresponding author:

P. VIJAYALAKSHMI
e-mail: Viji2025guide@induniversityedu.org

Optimising ancient costume image generation using the stable diffusion model: a focus on dynastic characteristics

DOI: 10.35530/IT.077.03.202570

JIAN HUA
ZHI LI
RUIHONG CHEN
YU CHEN

ABSTRACT – REZUMAT

Optimising ancient costume image generation using the stable diffusion model: a focus on dynastic characteristics

The source of the generated images of ancient costumes is misplaced because the process of generating ancient costume effect images cannot accurately capture the distinctive features of different dynasties. By leveraging the Stable Diffusion model, this study organises costume characteristics across different dynasties into 163 textual prompts, drawing on historical literature and classical scrolls. By matching these prompts with image feature vectors, a new token embedding layer V is introduced, which is optimised together with the cross-attention layer parameters W^k and W^v. Then, the model was fine-tuned using the Low-Rank Adaptation (LoRA) model to reduce training costs while maintaining historical fidelity. The results demonstrate that the optimised model can generate costume images that align with the corresponding dynastic and ethnic characteristics based on textual prompts. Validation experiments across the Tang, Song, and Ming dynasties show that the model achieves relatively low Kernel Inception Distance (KID) and Maximum Mean Discrepancy (MMD) values, indicating its effectiveness in generating ancient costume images. This study not only optimises the generation of ancient costume effect images but also holds reference value for the digital preservation and protection of costume cultures from other dynasties and ethnic regions.*

Keywords: *ancient costumes, image generation, intelligent design, stable diffusion model, text-to-image*

Optimizarea generării imaginilor cu costume antice folosind modelul Stable Diffusion: un accent pe caracteristicile dinastice

Sursa imaginilor cu costume antice generate este eronată din cauza incapacității de a surprinde cu precizie trăsăturile distinctive ale diferitelor dinastii în timpul procesului de generare a imaginilor cu efecte de costume antice. Folosind modelul Stable Diffusion, acest studiu organizează caracteristicile costumelor din diferite dinastii în 163 de prompturi textuale, pe baza analizei literaturii istorice și a pergamentelor clasice. Prin potrivirea acestor prompturi cu vectorii de caracteristici ai imaginilor, este introdus un nou strat de încorporare a token-urilor V, care este optimizat împreună cu parametrii stratului de atenție încrucișată Wk și Wv. Apoi, modelul a fost ajustat folosind modelul Low-Rank Adaptation (LoRA) pentru a reduce costurile de antrenare, menținând în același timp fidelitatea istorică. Rezultatele demonstrează că modelul optimizat poate genera imagini cu costume care se aliniază cu caracteristicile dinastice și etnice corespunzătoare, pe baza prompturilor textuale. Experimentele de validare din dinastiile Tang, Song și Ming arată că modelul atinge valori relativ scăzute ale Kernel Inception Distance (KID) și Maximum Mean Discrepancy (MMD), indicând eficacitatea sa în generarea de imagini cu costume antice. Acest studiu nu numai că optimizează generarea de imagini cu efecte de costume antice, ci are și o valoare de referință pentru conservarea digitală și protecția culturilor vestimentare din alte dinastii și regiuni etnice.*

Cuvinte-cheie*: costume antice, generarea de imagini, proiectare inteligentă, modelul Stable Difussion, text-imagine*

INTRODUCTION

As an important part of the world's cultural heritage, costumes contain historical narratives and cultural significance. In the digital era, the digital reproduction of ancient costumes has become an essential strategy for preserving and sharing traditional history and culture [1]. The text-to-image model generates semantically compliant image content based on textual prompts, achieving semantic mapping across different modalities. This new method has become a powerful means of generating images of costumes [2–4]. However, it is difficult for existing models to capture the complex details and temporal nuances of ancient costumes, especially in representing dynasty-specific design elements, fabric textures, and chronological changes in costume construction, which limits their effectiveness in cultural preservation.

Although models such as Generative Adversarial Networks (GANs) [5] and CLIP [6] have demonstrated exceptional capabilities in general image synthesis, their application in generating specific ancient costumes is limited. For example, Patashnik et al. [7] proposed a joint embedding method based on GAN and CLIP for text-driven image generation,

constraining the matching of geometric relations between the text vector difference (Δt) and the image vector difference (Δs). This method performs well regarding global semantic alignment but still suffers from distortion in generating high-frequency details. ClothGAN [3] improved the generation of Dunhuang mural costumes but requires more training data than the Stable Diffusion (SD) model [8]. A similar problem was addressed by Avrahami et al. [9], who segmented image regions based on localised textual descriptions, thus enabling finer spatial control. While this approach improves spatial coherence, it can miss or incorrectly infer key historical features of costumes. In addition, Saito et al. [10] proposed a Compressed Image Retrieval (CIR) model that improves text-image matching without labelling training data, but sacrifices computational efficiency and restricts scalability and accessibility.

In recent years, advances in generative artificial intelligence have had a significant impact on various fields, including textile digitisation. In particular, it has been applied in the preservation and digital reconstruction of cultural heritage [1]. Liu et al. [11] used deep learning and virtual fitting to reconstruct costumes from the Five Dynasties period, revealing historical fashion trends. The image generation model was applied to the restoration and design of specific costumes [12], contributing to the authenticity of digital collections. Zhuo Shi et al. [13] refined diffusion models to generate accurate depictions of traditional Yao costumes. In contrast to traditional generative models, such as GANs and VQ-VAE [14], SD has emerged as a dominant framework for text-to-image generation, particularly in terms of its denoising-based stability [8] compared to GANs [15]. One of its main advantages lies in its conditional generation and noise-guided optimisation, which enable precise control over image features based on specific textual prompts and enhance the fine details and fidelity of the generated images [16]. SD's noise-guided optimisation enables finer control over historical details, such as textures and colour patterns, making it a promising candidate for ancient costume generation. Nevertheless, current models often struggle to capture the complex and context-specific features of ancient costume, particularly those tied to regional or temporal variations. While the integration of textual conditional control embedding layers has shown good potential for application, SD's reliance on pre-trained generators and the CLIP algorithm limits its ability to adequately capture the complex and diverse characteristics inherent in ancient costumes [17, 18].

As a consequence, this paper proposes two synergistic innovations:

(1) A V* token embedding layer that dynamically maps dynasty-specific textual prompts to latent space markers for more accurate generation of era-identifying features.
(2) A parameter-efficient fine-tuning framework based on the Low-Rank Adaptation (LoRA), which reduces computational requirements while maintaining the performance of multi-dynasty costume generation.

MODEL FOR COSTUME IMAGE GENERATION

This section outlines the proposed approach, which consists of several key steps: analysis and extraction of prompts, optimisation of feature parameters, and image generation model improvement.

Dataset construction and textual prompts

The formulation of textual prompts is key to guiding text-to-image models in generating contextually accurate costume images. The framework employs a dual-prompt composition that utilises positive prompts to specify desired attributes such as colour, style, material, and accessories to ensure historical accuracy. Negative prompts are also used to filter out inappropriate elements, such as modern zippers and synthetic fabrics, to eliminate inconsistencies that greatly affect the model's ability to generate visually and contextually appropriate images.

Aiming at the issues of multi-dynasty costume style changes and data scarcity in ancient costume research, this study constructs a multi-dynasty figure costume image dataset. The dataset systematically integrates 2031 image samples (each image contains more than five attributes, such as collar shape and fabric texture) from digital archives of museum collections, illustrations of historical literature, and paintings of ancient figures, covering the three key periods of costume changes in typical Chinese traditional culture, namely the Tang, Song, and Ming. The specific dataset processing is described in the section below. For example, the Song Dynasty dataset (figure 1) includes a round-collared robe, a spread-feet scarf, and the holding of a ceremonial tablet, which are key to the historical accuracy of costumes. In addition, we compiled 163 textual prompts from historical scrolls and literature, covering the key features of these dynasties' costumes (table 1). This specialised dataset, along with detailed prompts focusing on collar styles, fabric types, and accessory

Fig. 1. Representative training images of Song Dynasty men's costumes showing key attributes such as round-collared robes, ceremonial tablets, and period-specific footwear

Table 1

DESCRIPTION OF PROMPTS FOR CHINESE SONG DYNASTY COSTUMES (MALE)

Category	Examples	Key features
Head ornament	scarf	spread feet scarf
		stiff feet scarf
	kerchief	kerchief
	chignon	chignon
	coronet	coronet
Under-garment	belly lock	belly lock
	undergarment	undergarment
Pant	pleated skirt	pleated skirt
Footwear	gleditsia boots	gleditsia boots
	bow shoes	bow shoes
	toe shoes	toe shoes
	square-toe shoes	square-toe shoes

details, was incorporated into the model training process to improve its ability to generate accurate and contextually appropriate descriptions of ancient costumes.

Token embedding (V*) for era-discriminative control

In the diffusion model, the cross-attention layer is important for ensuring that textual prompts are consistent with visual features [8]. Nupur et al. [19] studied the tuning of model parameters for introducing new features and observed significant variation in the parameter change rates across layers of the U-Net [20] in the SD model. These parameters were derived from three types of training layers: the cross-attention layer (for interaction between images and text), the self-attention layer (for correlation within images), and the remaining parameters (convolutional blocks and normalisation layer in the LDM model U-Net). Analysis of the rate of change in parameter weights of the loss function across different layers $\Delta t = \|\theta_t' - \theta_t\| / \|\theta_t\|$ (where θ_t' and θ_t represent model parameters for the first layer update and pre-training, respectively) reveals that the cross-attention layer undergoes substantial Δ change during model tuning, despite constituting only 5% of the total parameters. This observation motivated us to focus on optimising these layers for era-discriminative control.

Therefore, in this study, we adjusted the input costume text feature condition to modify the image features of the U-network based on the cross-attention layer $Attention(Q,K,V)$ [21]. Given the text $c \in \mathbb{R}^{s\times d}$ and image $f \in \mathbb{R}^{(h\times w)\times l}$ features, the single-head cross-attention operation involves $Q = W^q f$, $K = W^k c$, $V = W^v c$ and a weighted sum of value features.

$$Attention(Q,K,V) = \text{softmax}\left(\frac{QK^T}{\sqrt{d'}}\right)\cdot V \qquad (1)$$

where W^q, W^k, and W^v map inputs to the query, key, and value features, respectively, and d' is the output dimension of the key and query features. The purpose of tuning is to update the mapping from custom text features to the distribution of custom-image features, which are only input into the key-values (KV) layer of the cross-attention layer, and thus optimised by injecting new costume text features along with the W^k and W^v parameters of the cross-attention layer in the SD model when tuning the model in this study. This procedure effectively updates the model to incorporate new costume text-image pairs.

To address the problem of temporal feature obfuscation, this study introduces the V^* token embedding. This is a trainable layer inspired by Abdal et al. [22] that injects dynasty-specific semantic tokens into the cross-attention mechanism. V^* was optimised as a textual conditional embedding layer and integrated with the relevant parameters of the cross-attention layers W^k and W^v. The implementation of V^* involves three key steps:

Token initialisation

A single collected costume image contains multiple new costume features in different categories. Therefore, the joint training of each costume text feature is required to tune the model. Different token symbols Vi^* are used during token initialisation to represent different costume text features. The token V^* is initiated using the mean and standard deviation of the CLIP text embeddings extracted from historical references to ensure their semantic relevance to the target dynasty.

$$V^*_{init} = \mu_{CLIP} + \sigma_{CLIP} \odot \epsilon,\ \epsilon \sim N(0,1) \qquad (2)$$

where μ_{CLIP} denotes the mean value of the CLIP text embedding of the costume description for a specific historical period. σ_{CLIP} is the standard deviation of the CLIP embedding, reflecting the degree of feature discretisation of the textual description.

Feature augmentation

Given the text $c \in \mathbb{R}^{s\times d}$, and image feature $f \in \mathbb{R}^{(h\times w)\times l}$, the cross-attention operation is enhanced by connecting V^* with c.

$$K = W^k \cdot [c \oplus V^*],\ V = W^v \cdot [c \oplus V^*] \qquad (3)$$

where $[c \oplus V^*]$ denotes the channel connection. The tandem features are then processed by the key matrix (W^k) and value matrix (W^v) to form the key (K) and value (V) vectors of the attention mechanism.

Layer-specific adaptation

For each cross-attention layer y, only the key and value matrices associated with the costume text features are updated to form a unified parameter set $\{W^k_{0,y}, W^v_{0,y}\}^L_{y=1}$. If n new costume features are added ($n \in \{1...n\}$), the corresponding update matrix is defined as $\{W^k_{n,y}, W^v_{n,y}\}^L_{y=1}$. The subscript y is omitted below and denoted by $W^{K,V}$ which only the mapped text features are modified. The training objective combines the denoising loss with a forgetting penalty.

$$\min_{W^{K,V}_t \in \theta} \mathcal{L}_{diff}(x,\theta) + \lambda \mathcal{L}_{forget}(W^{K,V}_{t-1}, W^{K,V}_t) \qquad (4)$$

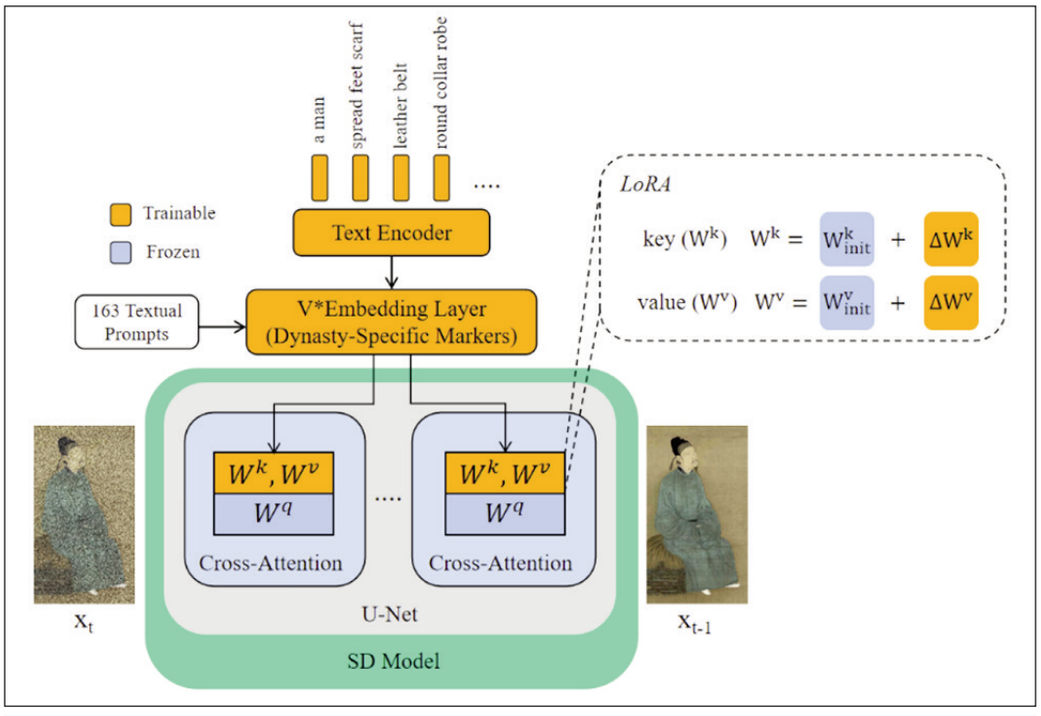

Fig. 2. Proposed model architecture with *V** embedding and LoRA module

where x is the new text feature data, and $\mathcal{L}_{diff}$ is the updated SD model loss function, which is the standard denoising objective for image generation. Model θ is not modified, and $\mathcal{L}_{forget} = \| W_t^{K,V} - W_{t-1}^{K,V} \|_2^2$ prevents disastrous forgetting by limiting the deviation from the pre-training weights. λ is the hyper-parameter chosen by exponential random search ($\lambda \in [0.1,1.0]$).

The proposed architecture integrates the CLIP text encoder and token embedding (*V**) to condition the cross-attention layers of U-Net, as illustrated in figure 2. The CLIP encoder first converts the input text prompts into semantic embeddings, which are connected to trainable *V** tokens to form enhanced text features. These features interact with the latent images through the cross-attention mechanism, where the key and value matrices are adaptively updated using the LoRA decomposition ($W = W_0 + BA$) to inject era-specific features.

Training proceeds in two phases:

1) Warm-up Phase: In the first five epochs, only the *V** embedding is trained with a forgetting penalty factor λ = 0.1 to ensure a stable initialisation while preserving the pre-training knowledge.
2) Joint Phase: 20 joint optimisations of *V**, W^k, and W^v using the AdamW-8bit optimiser with a learning rate of 5×10−4 and cosine decay scheduling. This V*-enhanced cross-attention was further optimised by LoRA, as detailed below.

Cross-attention optimization with LoRA

Full fine-tuning of large-scale diffusion models generated by ancient costumes incurs excessive computational costs. Therefore, we adopted LoRA [23], a parameter-efficient fine-tuning strategy that restricts weight updates to low-rank subspaces. For a pre-trained weight matrix $W_0 \in \mathbb{R}^{d\times k}$, the update decomposition is

$$W = W_0 + \Delta W = W_0 + BA$$
$$B \in \mathbb{R}^{d\times r},\ A \in \mathbb{R}^{r\times k},\ r \ll \min(d,k) \quad (5)$$

where ΔW is the parameter to be updated.

In the implementation mechanism, the original SD parameters (W_0) are frozen to preserve pre-trained knowledge and reduce catastrophic forgetting. During the training process, only low-rank matrices *A* and *B* are updated to achieve an efficient adaptation. The modified output for the input x is calculated as

$$h = W_0 x + \Delta W x = W_0 x + BAx \quad (6)$$

where $\Delta W = BA$ denotes the weight update, and h denotes the final feature embedding.

Subsequently, we applied LoRA to the key and value matrices of the cross-attention layer to strengthen era-specific feature alignment. The incremental update formula for layer t is

$$W_t^{K,V} = W_{init}^{K,V} + \sum_{t'=1}^{t-1} A_{t'}^{K,V} B_{t'}^{K,V} + A_t^{K,V} B_t^{K,V} \quad (7)$$

where $W_{init}^{K,V}$ denotes the pre-trained weights and $A_t^{K,V} \in \mathbb{R}^{D_1\times r}$, $B_t^{K,V} \in \mathbb{R}^{r\times D_2}$ are low-rank adapters.

Meanwhile, we imposed the L2 regularisation penalty $\| A_t^{K,V} B_t^{K,V} \|_F$ with a coefficient λ = 0.01 to mitigate overfitting on the limited training data.

The optimisation method of the LoRA-enhanced cross-attention mechanism dynamically integrates era-specific textual prompts and visual features, which can effectively adapt to ancient costume features and maintain the generalisation ability of the base model.

EXPERIMENTS AND RESULTS

To evaluate the performance of the model for generating costume renderings of ancient Chinese costumes, qualitative and quantitative evaluation analyses were conducted.

Training set preparation

We proposed a specialised dataset of 2,031 high-resolution images (512 × 768 pixels) divided into Tang (643 images), Song (744 images), and Ming (643 images) dynasties. Training set (1625 images), validation set (203 images), and test set (203 images).
We further used data augmentation approaches to increase the diversity and robustness of the dataset. First, we simulated the performance of costumes from different viewpoints and poses through geometric transformations, such as random cropping, rotation, and scaling. Second, the colour space was adjusted (brightness, contrast, and saturation) to improve the ability of our model to adapt to lighting changes. Finally, a slight noise was introduced into the image to improve the robustness of the model for low-quality input data. In addition, we introduce a regularisation term in Section 2.3 to prevent the model from over-relying on specific features. Although the data augmentation approach mitigates the limitations of the small dataset to some extent, we will still analyse the risk of overfitting in Section 4 and explore the importance of expanding the size of the dataset in future studies.

Experiment details

The experiments were conducted on an NVIDIA RTX 4090 GPU (24GB VRAM) using PyTorch 2.1.2 with CUDA 12.1 acceleration. Based on the community-validated chilloutmix_NiPrunedFp32Fix basic model, we implemented our adaptation framework using the Kohya-ss toolkit. Only 75MB of model weights are updated, which requires less memory for the model. In the specific model parameter tuning experiments, we determined the parameters dim = 32, alpha = 32, optimiser type (AdamW8bit), and a batch size of 1 as the optimal parameters for the model by comparing the clarity, the restoration of costume texture details, and the differentiation of dynastic features of the ancient costume images generated by the model. The number of repetition steps (repeat = 10), the number of training rounds (epoch = 20), the U-Net learning rate (5e–4), and the text learning rate (5e–5) were determined by comparing the loss function size of the model. These parameter settings ensure that the model achieves better results in learning costume features, and the generated images have the advantages of high clarity and obvious dynastic costume features.

Evaluation metrics

The evaluation protocol uses three key metrics: CLIP Alignment Scores for semantic consistency between generated images and text prompts, Kernel Inception Distance (KID) to quantify divergence from real images in the feature space, and Maximum Mean Discrepancy (MMD) to evaluate distributional similarity. Metric selection followed recent advances in text-to-image evaluation [24–26], with lower KID/MMD and higher CLIP scores indicating better performance. All metrics were calculated using five random seeds on a standardised test set to ensure statistical significance.

Fig. 3. Qualitative comparison of generated costumes across dynasties (From left to right: Real image, This model, Dreambooth, Textual Inversion, StyleCLIP)

Comparative experiments

In the comparative experiments, we chose to make a comprehensive comparison with three representative customised generation methods: Dreambooth [27], Textual Inversion [28], and StyleCLIP [7]. All models were based on the same training data, hardware configuration, and hyperparameter settings. Figure 3 shows the results of generating Tang, Song, and Ming dynasty costumes using real images as a reference. Despite Dreambooth's high parametric efficiency (32MB model size), the generated costumes have anatomical flaws (such as oversized heads and distorted hand proportions) owing to the single-task design. Textual Inversion introduces colour artefacts, especially the wrong shade of white in Ming costumes (figure 3, row 3), and unintentionally incorporates modern design elements. StyleCLIP suffers from severe detail degradation, producing blurred patterns and unnatural fabric transitions owing to unstable text

guidance. In contrast, our model successfully reproduces the iconic features of dynastic costumes through *V** embedding and LoRA optimisation.

Quantitative assessments

Text-image alignment analysis

The cross-model evaluation (table 2) shows different performance characteristics for the models. Although Textual Inversion achieves the highest text alignment, this comes at the cost of a severe drop in image alignment and an elevated KID/MMD score, suggesting that the erroneous presence of modern elements in the dynastic costumes resulted in semantic bias. Dreambooth demonstrates a balanced but suboptimal alignment. Our model achieves an optimal balance, achieving competitive text alignment along with excellent image fidelity while reducing the KID and MMD by 13% and 8%, respectively, compared to Dreambooth. This balance stems from the V*-guided attention mechanism, which dynamically weights dynasty-specific textual prompts during cross-attention operations, specifically enhancing the preservation of dynasty-specific structures and continuity of costume patterns.

Ablation experiments

The initialisation strategy analysis (table 3) highlights the critical trade-offs in feature anchoring. Fixed V* initialisation produced excellent text alignment but exhibited high KID and MMD owing to rigid semantic constraints that hindered adaptive feature fusion. The optimised V* initialisation matches the text alignment degree of the random initialisation, while there is an improvement in image alignment and a lower MMD, which effectively mitigates problems such as historical inaccuracy. The component contribution tests (table 4) show the necessity of a dual adaptation mechanism. The removal of LoRA reduces model alignment, with significant increases in the KID and MMD. The complete removal of V* and LoRA further exacerbates these problems, reflecting significant deviations from historical distribution. The results suggest that the synergy between the optimised V* (managing epoch-specific semantics) and LoRA (enabling parameter-efficient feature adaptation) is effective for reconstructing complex and specific details.

Table 2

CROSS-MODEL TEXT-IMAGE ALIGNMENT PERFORMANCE

Model	Text alignment ↑	Image alignment ↑	KID ↓	MMD ↓
Dreambooth	0.77	0.76	16.82	3.21
Textual inversion	0.80	0.69	18.95	4.05
Our model	0.79	0.78	14.64	2.96

Table 3

ABLATION STUDY ON V* INITIALIZATION STRATEGIES

Condition	Text alignment ↑	Image alignment ↑	KID ↓	MMD ↓
Random init	0.80	0.76	15.57	4.08
Fixed V*	0.83	0.75	16.44	5.06
Optimised V*	0.80	0.77	15.57	3.43

Table 4

CROSS-MODEL TEXT-IMAGE ALIGNMENT PERFORMANCE

Configuration	Text alignment ↑	Image alignment ↑	KID ↓	MMD ↓
Full model	0.79	0.78	14.64	2.96
w/o LoRA	0.75	0.76	15.57	3.43
w/o V* + LoRA	0.77	0.71	17.74	5.61

CONCLUSIONS

In conclusion, this study proposes an enhanced lightweight framework based on SD for generating historically accurate images of ancient costumes. Compared with the baseline model, the proposed method demonstrates excellent performance in restoring multi-dynasty costume features, especially in achieving higher historical fidelity in key details. The quantitative assessment further confirms the better match between the generated images and the reference historical sources. Despite the success of our method in generating ancient costumes, we recognise the main limitations that must be addressed. Primarily, the current dataset, while focused on core Han-style costumes, is limited in scope (encompassing only the Tang, Song, and Ming dynasties) and size (2,031 images). Limited by the scarcity of authoritative historical documents and the complexity of multi-dynastic costume form examinations, this scale remains small compared to large-scale benchmark datasets. Although we have adopted technical measures such as data augmentation, the risk of overfitting has not been eliminated in small sample fine-tuning. Furthermore, the labelling scheme treats each dynasty as a single entity and does not account for stylistic evolution within different periods of a dynasty, which may reduce the historical accuracy of the generated results. It is worth noting that data scarcity and detailed historical representation are common challenges in the field of textile artefact digitisation. In future research, we will prioritise the construction of an expanded dataset covering more dynasties and diverse ethnic costumes. At the same time, we will consider more detailed time labels (such as early/mid/late Tang Dynasty) to better capture the evolution within each dynasty. Additionally, we will develop a feature decoupling module for fabric features based on high-resolution 3D scanning and promote the application of digital reconstruction and innovative design of ancient costumes by relying on the multimodal semantic understanding advantages of models like DeepSeek Janus-Pro [29].

REFERENCES

[1] Ding, Q.-K., Liang, H.-E., *Digital restoration and reconstruction of heritage clothing: a review*, In: Herit Sci, 2024, 12, 1, 225, https://doi.org/10.1186/s40494-024-01349-4

[2] Liu, L., Zhang, H., Li, Q., Ma, J., Zhang, Z., *Collocated Clothing Synthesis with GANs Aided by Textual Information: A Multi-Modal Framework*, In: ACM Trans. Multimedia Comput. Commun. Appl., 2024, 20, 1, 1–25, https://doi.org/10.1145/3614097

[3] Wu, Q., et al., *ClothGAN: generation of fashionable Dunhuang clothes using generative adversarial networks*, In: Connection Science, 2021, 33, 2, 341–358, https://doi.org/10.1080/09540091.2020.1822780

[4] Wu, X., Li, L., *An application of generative AI for knitted textile design in fashion*, In: The Design Journal, 2024, 27, 2, 270–290, https://doi.org/10.1080/14606925.2024.2303236

[5] Goodfellow, I., et al., *Generative adversarial networks*, In: Commun. ACM, 2020, 63, 11, 139–144, https://doi.org/10.1145/3422622

[6] Radford, A. et al., *Learning Transferable Visual Models From Natural Language Supervision*, 2021, arXiv, https://doi.org/10.48550/ARXIV.2103.00020

[7] Patashnik, O., Wu, Z., Shechtman, E., Cohen-Or, D., Lischinski, D., *StyleCLIP: Text-Driven Manipulation of StyleGAN Imagery,* 2021, arXiv: arXiv:2103.17249, https://doi.org/10.48550/arXiv.2103.17249

[8] Rombach, R., Blattmann, A., Lorenz, D., Esser, P., Ommer, B., *High-Resolution Image Synthesis with Latent Diffusion Models*, 2021, arXiv, https://doi.org/10.48550/ARXIV.2112.10752

[9] Avrahami, O., et al., *SpaText: Spatio-Textual Representation for Controllable Image Generation*, In: 2023 IEEE/CVF Conference on Computer Vision and Pattern Recognition (CVPR), Vancouver, BC, Canada: IEEE, Jun. 2023, 18370–18380, https://doi.org/10.1109/CVPR52729.2023.01762

[10] Saito, K., et al., *Pic2Word: Mapping Pictures to Words for Zero-shot Composed Image Retrieval*, 2023, arXiv, https://doi.org/10.48550/ARXIV.2302.03084

[11] Liu, K., Wu, H., Ji, Y., Zhu, C., *Archaeology and Restoration of Costumes in Tang Tomb Murals Based on Reverse Engineering and Human-Computer Interaction Technology*, In: Sustainability, 2022, 14, 10, 6232, https://doi.org/10.3390/su14106232

[12] Liu, K., Gao, Y., Zhang, J., Zhu, C., *Study on digital protection and innovative design of Qin opera costumes*, In: Herit Sci, 2022, 10, 1, 127, https://doi.org/10.1186/s40494-022-00762-x

[13] Shi, Z., Xiong, B., *Fine-Tuning Text-to-Image Generation Models Using Curriculum Learning for Yao Costume Image Generation*, In: 5th International Seminar on Artificial Intelligence, Networking and Information Technology (AINIT), Nanjing, China: IEEE, Mar. 2024, 1305–1311, https://doi.org/10.1109/AINIT61980.2024.10581585

[14] van den Oord, A., Vinyals, O., Kavukcuoglu, K., *Neural Discrete Representation Learning*, 2017, arXiv, https://doi.org/10.48550/ARXIV.1711.00937

[15] Creswell, A., White, T., Dumoulin, V., Arulkumaran, K., Sengupta, B., Bharath, A.A., *Generative Adversarial Networks: An Overview*, In: IEEE Signal Process. Mag., 2018, 35, 1, 53–65, https://doi.org/10.1109/MSP.2017.2765202

[16] Huang, Y., et al., *Diffusion Model-Based Image Editing: A Survey*, 2024, https://doi.org/10.48550/ARXIV.2402.17525

[17] Xiong, S., Pan, L., Ma, X., Hu, Q., Beckman, E., *Unsupervised deep hashing with multiple similarity preservation for cross-modal image-text retrieval*, In: Int. J. Mach. Learn. & Cyber., 2024, 15, 10, 4423–4434, https://doi.org/10.1007/s13042-024-02154-y

[18] Ramesh, A., Dhariwal, P., Nichol, A., Chu, C., Chen, M., *Hierarchical Text-Conditional Image Generation with CLIP Latents*, 2022, arXiv, https://doi.org/10.48550/ARXIV.2204.06125

[19] Kumari, N., Zhang, B., Zhang, R., Shechtman, E., Zhu, J.-Y., *Multi-Concept Customization of Text-to-Image Diffusion*, 2023, arXiv: arXiv:2212.04488, https://doi.org/10.48550/arXiv.2212.04488

[20] Ronneberger, O., Fischer, P., Brox, T., *U-Net: Convolutional Networks for Biomedical Image Segmentation*, In: Medical Image Computing and Computer-Assisted Intervention – MICCAI 2015, Navab, N., Hornegger, J., Wells, W.M. and Frangi, A.F. Eds., Cham: Springer International Publishing, 2015, 234–241, https://doi.org/10.1007/978-3-319-24574-4_28

[21] Vaswani, A. et al., Attention Is All You Need, 2017, arXiv, https://doi.org/10.48550/ARXIV.1706.03762

[22] Abdal, R., Qin, Y., Wonka, P., *Image2StyleGAN: How to Embed Images Into the StyleGAN Latent Space?*, In: 2019 IEEE/CVF International Conference on Computer Vision (ICCV), Seoul, Korea (South): IEEE, Oct. 2019, 4431–4440, https://doi.org/10.1109/ICCV.2019.00453

[23] Hu, E.J., et al., *LoRA: Low-Rank Adaptation of Large Language Models*, 2021, arXiv, https://doi.org/10.48550/ARXIV.2106.09685

[24] Hessel, J., Holtzman, A., Forbes, M., Bras, R.L., Choi, Y., *CLIPScore: A Reference-free Evaluation Metric for Image Captioning*, 2021, https://doi.org/10.48550/ARXIV.2104.08718

[25] Bińkowski, M., Sutherland, D.J., Arbel, M., Gretton, A., *Demystifying MMD GANs,* 2018, arXiv, https://doi.org/10.48550/ARXIV.1801.01401

[26] Gretton, A., Borgwardt, K.M., Rasch, M.J., Schölkopf, B., Smola, A., *A kernel two-sample test*, In: J. Mach. Learn. Res., 2012, 13, 723–773

[27] Ruiz, N., Li, Y., Jampani, V., Pritch, Y., Rubinstein, M., Aberman, K., *DreamBooth: Fine Tuning Text-to-Image Diffusion Models for Subject-Driven Generation*, In: 2023 IEEE/CVF Conference on Computer Vision and Pattern

Recognition (CVPR), Vancouver, BC, Canada: IEEE, Jun. 2023, 22500–22510, https://doi.org/10.1109/CVPR52729.2023.02155

[28] Gal, R., et al., *An Image is Worth One Word: Personalizing Text-to-Image Generation using Textual Inversion*, 2022, arXiv, https://doi.org/10.48550/ARXIV.2208.01618

[29] Chen, X., et al., *Janus-Pro: Unified Multimodal Understanding and Generation with Data and Model Scaling*, 2025, 2025, arXiv: arXiv:2501.17811, https://doi.org/10.48550/arXiv.2501.17

Authors:

JIAN HUA[1], ZHI LI[2], RUIHONG CHEN[2], YU CHEN[2]

[1]School of Textiles and Fashion, Shanghai University of Engineering Science, China

[2]Shanghai University of Engineering Science, 333 Longteng Road, Shanghai 201620, China

Corresponding author:

YU CHEN
e-mail: ychen0918@sues.edu.cn

Research on the recycling of sulfuric acid waste liquid in textile composition detection based on the ISO 1833-11 standard

DOI: 10.35530/IT.077.03.2025119

GUANJIE CHEN
YU ZHANG
DAN ZOU

BEI CHENG
SHUANGYING ZHA
CHEN YANG

ABSTRACT – REZUMAT

Research on the recycling of sulfuric acid waste liquid in textile composition detection based on the ISO 1833-11 standard

In the field of textile quantitative component analysis, the 75 wt% sulfuric acid solution dissolution method, a globally adopted standard, generates substantial acidic waste solution, imposing both environmental burden and economic costs. To address this, this study selected white knitted fabric (cotton/polyester blended fabric) and red knitted fabric (viscose/polyester blended fabric) as research subjects based on ISO 1833-11, conducting experiments with 0–8 cycles of waste liquid recycling to compare dissolution efficiency, residual fibre morphology, and quantitative determination results between fresh and recycled dissolution agents. Results indicated that within eight reuse cycles, the measurement deviation between fresh and recycled acid remained minimal, with relative deviation generally below 2%, while microscopic observation confirmed structurally intact polyester fibres in residues across all cycles, though minor surface deposits emerged only after higher cycle counts without significantly affecting quantitative outcomes. Further assessment revealed that this recycling strategy could reduce acid consumption and waste discharge by approximately 80%, offering both environmental benefit and economic benefit, thereby validating the feasibility of multi-cycle waste liquid recycling of concentrated sulfuric acid in textile detection and providing a practical foundation for green testing laboratories.

Keywords: *textile detection, quantitative chemical analysis, sulfuric acid method, waste liquid recycling, sustainability*

Cercetare privind reciclarea deșeurilor lichide de acid sulfuric în cadrul procesului de detectare a compoziției materialelor textile, în conformitate cu standardul ISO 1833-11

În domeniul analizei cantitative a componentelor textile, metoda de dizolvare cu soluție de acid sulfuric 75% în greutate, printr-un standard adoptat la nivel mondial, generează o cantitate considerabilă de deșeuri acide, ceea ce implică atât un impact asupra mediului, cât și costuri economice. Pentru a aborda această problemă, studiul de față a selectat un tricot alb (tricot din amestec de bumbac/poliester) și un tricot roșu (tricot din amestec de viscoză/poliester) ca subiecte de cercetare, în conformitate cu ISO 1833-11, efectuând experimente cu 0–8 cicluri de reciclare a lichidului rezidual pentru a compara eficiența dizolvării, morfologia fibrelor reziduale și rezultatele determinării cantitative între agenții de dizolvare proaspeți și cei reciclați. Rezultatele au indicat că, în cadrul a opt cicluri de reutilizare, abaterea de măsurare între acidul proaspăt și cel reciclat a rămas minimă, cu o abatere relativă în general sub 2%, în timp ce evaluarea microscopică a confirmat fibrele de poliester intacte din punct de vedere structural în reziduuri în toate ciclurile, deși au apărut depozite superficiale minore doar după un număr mai mare de cicluri, fără a afecta în mod semnificativ rezultatele cantitative. O evaluare suplimentară a relevat că această strategie de reciclare ar putea reduce consumul de acid și deversarea deșeurilor cu aproximativ 80%, oferind atât beneficii de mediu, cât și beneficii economice, validând astfel fezabilitatea reciclării în mai multe cicluri a deșeurilor lichide de acid sulfuric concentrat în detectarea textilelor și oferind o bază practică pentru laboratoarele de testare ecologice.

Cuvinte-cheie*: detectarea materialelor textile, analiza chimică cantitativă, metoda cu acid sulfuric, reciclarea deșeurilor lichide, sustenabilitate*

INTRODUCTION

The rapid expansion of the global textile industry, combined with the prevailing fast fashion model, has led to a continuous surge in textile waste. Each year, over 92 million tons of discarded textiles are generated, with a substantial portion ultimately ending up in landfills or incineration, imposing a severe environmental burden [1]. Among these wastes, cotton/polyester blended fabrics (polycotton) are predominant, accounting for nearly 50% of disposed textiles due to their combined advantages of cotton fibre comfort and polyester fibre durability, making them widely used in both apparel and home textiles [2]. However, the intimate binding between cotton and polyester presents a significant challenge to separation and recycling, resulting in over 80% of textile waste being excluded from high-value recovery pathways [3, 4]. Thus, developing efficient and eco-friendly separation and recycling use methods is vital for promoting the circular economy and advancing the sustainability of the textile sector.

At present, the primary approach to recycling polycotton fabrics involves chemical separation, particularly acid hydrolysis, which selectively dissolves cellulose-based fibres while preserving polyester fibres. This technique has been widely studied and applied in both laboratory research and industrial pilot processes [5–7]. Leenders et al. [8], for instance, employed a 43 wt% hydrochloric acid solution to achieve effective hydrolysis of the cotton component, yielding up to 75% glucose, while the retained polyester was further depolymerised to produce high-purity bis(2-hydroxyethyl) terephthalate (BHET), enabling cascade recycling of the blended textile/fabric. Similarly, Costa et al. [5] utilised the sulfuric acid method to recover cellulose powder from blended textile waste with yields ranging from 65 88%, which was subsequently converted into carboxymethyl cellulose, cellulose acetate, and other derivatives to serve as regenerated raw materials for the textile industry. Emerging alternatives such as hydrothermal treatment [9], high-ethanol alkaline hydrolysis [4], and switchable solvent systems [10] also demonstrate promising separation capabilities, yet still face limitations including high energy demands, challenges in solvent recovery, and inadequate scalability.

Beyond material recovery, increasing attention has been drawn to the release of microplastics from textile waste during usage and processing. Studies have shown that polyester fibres embedded within blended fabrics release more microplastic particles compared to those in pure polyester textiles, posing substantial threats to aquatic systems and ecological health [11, 12]. Therefore, the development of separation techniques that are not only efficient and value-added but also environmentally benign is becoming a central focus in textile waste management research [13–15].

In the field of quantitative component analysis for textiles, the ISO 1833-11 and its Chinese National Standard GB/T 2910.11 equivalent recommend the use of the 75 wt% sulfuric acid solution method for determining the composition ratio in polycotton blends [16]. This approach enables rapid and accurate dissolution of cotton fibres, preserving the polyester component for quantitative determination results. However, the process generates large volumes of concentrated acidic waste solution, increasing both treatment costs and environmental risks [17, 18]. While current research often focuses on novel separation technologies, studies on waste liquid recycling within standardised testing processes remain limited. Notably, industries have already adopted various recycling use strategies for acidic solutions, such as membrane separation technology, electrodialysis, and diffusion dialysis, with encouraging results [19–23]. Translating such circular utilisation strategies to textile testing scenarios offers significant environmental and economic benefits.

Against this backdrop, the present study, grounded in the ISO 1833-11 [16], investigates the waste liquid recycling potential of 75 wt% sulfuric acid solution in the context of quantitative component analysis. Two representative fabrics were selected: a white knitted fabric composed of cotton/polyester blended fabric, and a red knitted fabric composed of viscose/polyester blended fabric. A series of controlled experiments was conducted across 0–8 reuse cycles, assessing variations in dissolution efficiency, residual fibre morphology, and quantitative determination results. Through combined microscopic observation and analytical evaluation, the study aims to validate the feasibility and reliability of acid recycling use, while also evaluating the sustainability and environmental benefit of such an approach. The findings are expected to contribute practical methodologies for green testing laboratory development and provide theoretical and empirical support for the resource-saving and waste acid reduction in the reuse of blended textile materials.

MATERIALS AND METHODS

Textile samples

Two types of textile specimens were selected in this study: a white knitted fabric composed of a typical cotton/polyester blended fabric (polycotton), and a red knitted fabric composed of a viscose/polyester blended fabric. The former, being the most commonly discarded textile type, was used to systematically evaluate the dissolution efficiency and quantitative determination results under different waste liquid recycling conditions. The latter served to verify the applicability of the method to viscose-based blended textile/fabric systems, assessing its performance in terms of fibre separation and analytical accuracy.

To ensure result comparability, both fabric types were cut into samples weighing 0.8–1.0 g. For each type, experiments were grouped into a fresh acid group (0 cycles of reuse) and waste liquid recycling groups spanning 1 to 8 reuse cycles. This design enabled systematic analysis of the effect of recycling frequency on dissolution performance and fibre composition measurements.

Dye/finish specification of the T/R red fabric. The viscose/polyester (T/R) red knitted fabric used in this study is a commercially dyed jersey. Consistent with standard mill practice for these fibres, the polyester component was dyed with disperse dyes, and the viscose component with reactive dyes (medium red shade, approximately standard depth; mill label: Disperse Red 60 / Reactive Red 195, shade code TR-Red-3, nominal 2.0% o.w.f.). According to the supplier's note, the fabric carried a conventional silicone softener (nonionic amino-modified silicone softener, nominal 1.0% o.w.f.) and no functional/ resin/ fluorochemical finishing was declared. These specifications are provided to contextualise the "dyes/finishes" limitation noted later in the 4th section.

Sample scope and representativeness. This study evaluates two representative blended fabrics under ISO 1833-11 conditions: a white cotton/polyester (C/T) knitted fabric and a red viscose/polyester (T/R) knitted fabric. Across 0-8 reuse cycles, both systems maintained quantitative stability within ±2%, with T/R

showing a lower inter-cycle RSD (~0.13%). The moisture-corrected compositions are approximately C/T: cotton ~61% / polyester ~39% and T/R: polyester ~64% / viscose ~36%, providing two distinct cellulose polyester ratios and one dyed system for stability comparison. Future extensions will include additional fibre ratios and construction styles. Scope extension and challenging-case triage. Beyond the two representative blends evaluated here (C/T white; T/R red), the protocol is designed to handle challenging cases often encountered in practice, such as elastane-containing blends, resin-finished fabrics, and dark, reactive-dyed cellulosics, without altering the core dissolution and QC steps.

Reagents and instruments

The dissolution agent used in the experiments was a 75 wt% sulfuric acid solution, which is prescribed by the ISO 1833-11 for the selective dissolution of cellulose-based fibres [16], allowing for reliable quantitative component analysis of blended textiles. All sulfuric acid used was of analytical grade, freshly prepared, and stored in airtight containers to prevent concentration fluctuation.

Perform all acid work in a fume hood and use appropriate personal protective equipment. Required PPE includes chemical splash goggles, a face shield for pouring, acid-resistant gloves, a lab coat paired with an apron, and closed-toe shoes. For any dilution, add the acid to water slowly. Use external cooling and gentle stirring during this process. Prepare in advance a labelled container for acidic rinsates and a base solution. Suitable base solutions include 5–10 wt% sodium carbonate or dilute ammonia. After use, collect and cool the acidic rinsates. Neutralise them gradually under stirring while monitoring pH, allowing pauses to accommodate effervescence and heat. Stop neutralisation when the pH reaches 6.5–8.5 and manage the neutralised waste in accordance with institutional standard operating procedures and local regulations. This quick note is intended to facilitate direct adoption. It aligns with the process rinse endpoint specified in the 2nd section, which requires a filtrate pH of ≥ 6.8.

The key laboratory equipment included:

- constant temperature water bath (20–100 °C), set to 130 rpm, for maintaining the experimental temperature at 50 ± 5 °C;
- analytical balance (accuracy: 0.1 mg) for determining the dry mass of samples and residues;
- optical microscope equipped with a digital imaging system for conducting microscopic observation of residual polyester fibre morphology and potential surface deposits;
- standard glassware and consumables, including sealed Erlenmeyer flasks, glass rods, filter papers, and a vacuum filtration device;
- acid reuse system consisting of an acid storage container and a liquid separation module, allowing controlled waste liquid recycling of the 75 wt% sulfuric acid solution;
- digital densimeter or 20 ml Gay-Lussac pycnometer, operated at 20.0 ± 0.1°C, for per-cycle density measurement of the recycled acid;
- acid-base titration setup (class-A burette; standardised NaOH; phenolphthalein or potentiometric endpoint) for titrated acidity checks on a defined dilution.

Uncertainty alignment

The narrative budget indicates that filtration/drying repeatability is the dominant contributor, whereas balance precision and moisture correction are minor–to–moderate; this is consistent with the small inter-cycle RSDs (C/T ≈ 0.55%; T/R ≈ 0.13%) and the ≤±2% deviations already observed across 0–8 cycles.

Experimental basis and principles

All experimental procedures in this study were based on the ISO 1833-11:2017 Standard [16], which specifies a method for quantitative component analysis of blended textile/fabric by selectively dissolving cellulose-based fibres using a 75 wt% sulfuric acid solution. The underlying principle lies in the ability of concentrated sulfuric acid to rapidly disrupt the β-1,4-glycosidic bonds within cellulose, hydrolysing and dissolving the cellulose into soluble sugars and oligosaccharides. Under such strong-acid conditions, partial dehydration by-products may also form. Meanwhile, polyester fibres and other insoluble components remain structurally intact under these conditions [6, 8, 9, 24]. By measuring the dry weight of the remaining residue after dissolution, the percentage content of polyester fibre can be accurately quantified, and the proportion of cellulose-based fibres can be calculated accordingly [25].

In the experimental setup concerning waste liquid recycling, this study assumed that the dissolution agent would exhibit minimal variation in performance over multiple cycles of reuse. Previous research has demonstrated that although the accumulation of by-products, such as soluble sugars and dye-related/dehydration products, during acidic waste-solution recycling is inevitable, their influence on the cellulose-hydrolysis/dissolution rate and on the structural integrity of polyester fibres remains relatively minor [8, 12]. Based on this premise, comparative experiments using both fresh acid and recycled acid over 1–8 reuse cycles were conducted to evaluate the feasibility and stability of waste liquid recycling in this context. The ultimate goal was to provide experimental evidence supporting the advancement of a green testing laboratory and promote low-carbon, sustainable practices within the field of textile quantitative component analysis.

Experimental procedure

To ensure operational consistency and experimental reproducibility, this study strictly followed the standard protocol outlined in the ISO 1833-11:2017 Standard [16], while incorporating an additional investigation into waste liquid recycling. The overall experimental procedure is illustrated in figure 1.

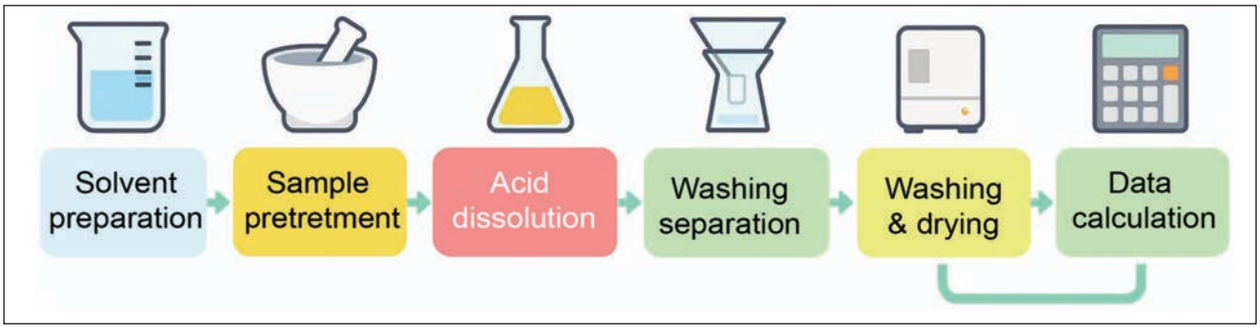

Fig. 1. Overview of the experimental procedure

As depicted in figure 1, the process begins with sample pre-treatment and solution preparation, followed by acid dissolution, residue separation, and residue weighing, ultimately leading to the calculation of the percentage content of each fibre component. While aligned with the ISO standard methodology, this procedure introduces a dedicated branch for waste liquid recycling, assessing the performance of acidic waste solutions reused from 0 to 8 cycles. This modification ensures compliance with international standards while advancing the practical implementation of green testing laboratory practices.

To disentangle the independent effects of dyes and finishing auxiliaries on experimental stability without altering the core workflow, this study adopts a paired-control approach for future datasets:

Test undyed (greige) and piece-dyed fabrics of identical construction and fibre ratio to isolate dye class/level effects from matrix effects.

Compare mass-coloured (dope-dyed) yarns against disperse-dyed yarns of matched linear density.

Spike the recycled solution with representative levels of softener/resin used on the fabric to screen whether deposits/variance increase relative to the greige baseline.

Include higher-cellulose and higher-polyester blends to probe composition-dependent variance.

Elastane-blended textiles will be handled following the relevant ISO 1833 series guidance for such systems and then evaluated under the same recycling QC, recognising this class as outside the present C/T or T/R scope.

Sample pre-treatment

Selected samples of cotton/polyester blended fabric (polycotton) and viscose/polyester blended fabric, referred to as white knitted fabric (C/T) and red knitted fabric (T/R), respectively, were cut into test pieces weighing 0.8–1.0 g, ensuring consistent mass across both sample types. The specimens were dried in a drying oven at 105°C to constant weight (validated such that the C/T white knitted fabric showed a mass change < 0.05% within 60 min after 5 h of drying, and the T/R red knitted fabric showed a mass change < 0.05% within 60 min after 6 h of drying) to remove moisture, then cooled to room temperature and stored in a desiccator before use. This step minimised the influence of initial moisture content differences on subsequent dissolution outcomes.

Solution preparation and experimental grouping

A 75 wt% sulfuric acid solution was employed as the dissolution agent, and samples were divided into three experimental groups:

- fresh acid group (0 cycles): utilising newly prepared concentrated sulfuric acid;
- recycling group (1–8 cycles): using acidic waste solution recovered from the previous cycle.

Each experimental condition was conducted in duplicate to ensure the reliability and reproducibility of the data.

Dissolution and residue separation

Following pre-treatment, each sample was placed into a stoppered Erlenmeyer flask; 200 ml of the acid solution per gram of specimen was added, and the mixture was maintained in a constant-temperature water bath at 50 ± 0.5°C for approximately 1 h with mechanical shaking. After completion of the hydrolytic dissolution of the cellulose-based fibres, the undissolved polyester fibre residue was separated using a vacuum filtration device.

The collected residue was thoroughly rinsed with distilled water until the filtrate pH was ≥ 6.8, and then dried in a drying oven at 105°C to constant weight. The collected residue was first drained by vacuum suction, then the remaining solids were washed several times with cold water, washed twice with dilute ammonia solution, and finally thoroughly rinsed with cold water.

To visualise the transformation in fibre morphology before and after dissolution, tables 1 and 2 present direct comparisons of C/T white knitted fabric and T/R red knitted fabric, respectively, across the three key stages: original state, post-dissolution, and microscopic observation using an optical microscope equipped with a digital imaging system. For trace-colour carryover checks specific to dyed substrates, laboratories may optionally record the visual colour of the recycled acid and keep a brief note; any progressive reddening across cycles can be used as a practical trigger for make-up/replacement, alongside the density checks already reported. This note is intended for dyed systems such as the T/R red fabric.

Filtration was performed with acid-resistant hardware and a staged capture strategy to minimize blinding

while preserving mass balance: glass-fibre filter, 1.6 µm (47 mm, binder-free) in a PTFE holder; pre-exposed to working acid before use; 100–150 µm stainless-mesh basket at the funnel entrance to retain lint clumps/large fragments; upstream 2.7 µm glass-fibre disc when heavy finish or dark-dye particulates are present; the final 1.6 µm layer remains the quantitative collection stage; where crucibles are preferred, a borosilicate sintered-glass support, porosity P3–P4 (~40–10 µm) may be used beneath the 1.6 µm disc to spread flow on high-load samples.
Maintain 50 ± 0.5°C during transfer to reduce viscosity; use wide-bore funnels, short pulses of moderate vacuum (−20 → −60 kPa) to avoid cake compaction; gently re-suspend the residue with small aliquots of working acid if local sealing occurs; enlarge filter area (25 → 47 mm) when needed.

Triage notes

Elastane-containing blends: process as usual if elastane is a minor fraction and does not form persistent gels under these study conditions; otherwise, route via the relevant ISO-1833 elastane procedure first, then apply this acid-reuse workflow to the non-elastomeric fraction under the same QC gates.
Resin-finished fabrics: do not pre-extract finishes; rely on the staged filtration above. If rinsing to pH ≥ 6.8 requires non-routine volumes or if repeated blinding occurs, treat as an early replacement/top-up trigger.
Dark, reactive-dyed cellulosics: use the optional pre-filter and pulsed-vacuum mode to limit compacting; monitor the diluted-conductivity/visual-colour cue as an early-warning for replacement if ionic/organic build-up accelerates.

Table 1

C/T WHITE KNITTED FABRIC BEFORE AND AFTER DISSOLUTION UNDER DIFFERENT ACID RECYCLING CONDITIONS

Dissolution agent	Original sample	Residue after dissolution	Microscopic image 2 (500X)
75 wt% H_2SO_4 (0-cycle, fresh) ρ(20°C) 1.682 g/ml	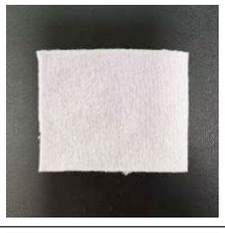		
1-cycle ρ(20°C) 1.678 g/ml	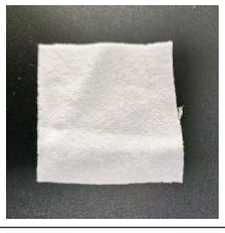		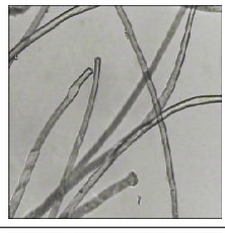
2-cycle ρ(20°C) 1.676 g/ml			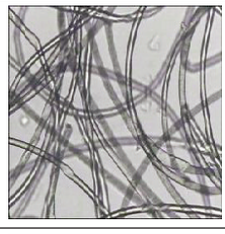
3-cycle ρ(20°C) 1.676 g/ml			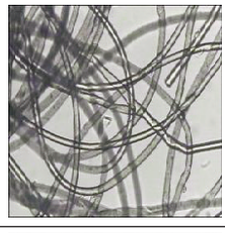
4-cycle ρ(20°C) 1.668 g/ml			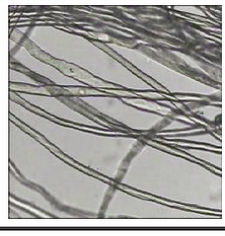

Table 1 (continuation)

Dissolution agent	Original sample	Residue after dissolution	Microscopic image 2 (500X)
5-cycle ρ(20°C) 1.668 g/ml			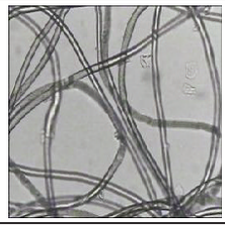
6-cycle ρ(20°C) 1.662 g/ml			
7-cycle ρ(20°C) 1.652 g/ml			
8-cycle ρ(20°C) 1.652 g/ml	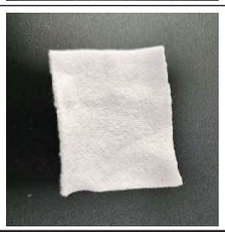		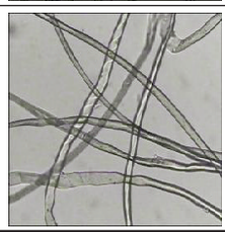

Table 2

T/R RED KNITTED FABRIC BEFORE AND AFTER DISSOLUTION UNDER DIFFERENT ACID RECYCLING CONDITIONS			
Dissolution agent	**Original sample**	**Residue after dissolution**	**Microscopic image 2 (500X)**
75 wt% H_2SO_4 (0-cycle, fresh) ρ(20°C) 1.686 g/ml			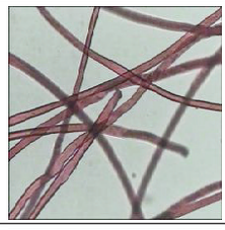
1-cycle ρ(20°C) 1.684 g/ml			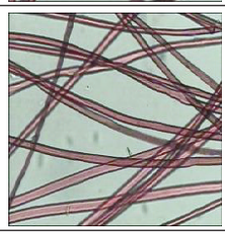
2-cycle ρ(20°C) 1.682 g/ml			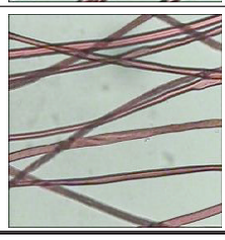

Table 2 (continuation)

Dissolution agent	Original sample	Residue after dissolution	Microscopic image 2 (500X)
3-cycle ρ(20°C) 1.674 g/ml			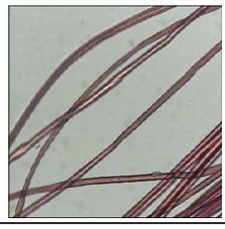
4-cycle ρ(20°C) 1.674 g/ml			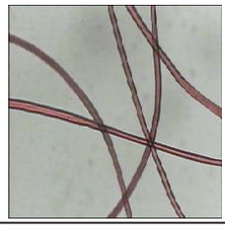
5-cycle ρ(20°C) 1.670 g/ml			
6-cycle ρ(20°C) 1.668 g/ml	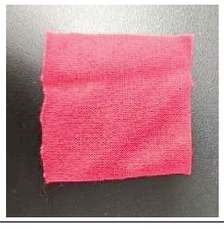		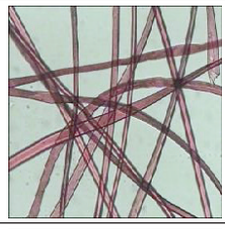
7-cycle ρ(20°C) 1.662 g/ml			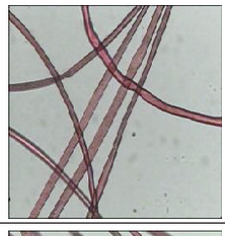
8-cycle ρ(20°C) 1.660 g/ml			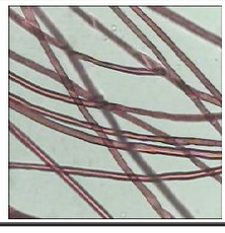

As illustrated in table 1, the residues of the C/T white knitted fabric after dissolution appear as smooth and structurally intact polyester fibres with uniform diameter, indicating that the 75 wt% sulfuric acid solution offers strong selectivity towards cellulose fibres while exerting minimal effect on the polyester fibre structure. In table 2, partial surface roughness is observed on the residue fibres of the T/R red knitted fabric following dissolution, yet the overall fibre morphology remains intact. This suggests that the use of acidic waste solution, particularly under extended waste liquid recycling conditions, may result in minor surface deposits on polyester fibres, but does not significantly affect the quantitative determination results.

For each reuse cycle, the working acid was routinely checked to contextualise minor deposits and variance:

- density at 20°C was recorded to confirm restoration to the 75 wt% target;
- conductivity was measured on a defined dilution using a conductivity meter as a qualitative indicator of ionic build-up.

Dissolved organics were assessed on a neutralised, diluted aliquot by simple qualitative checks suitable for routine labs, e.g., a reducing-sugar colour check

and a quick UV vis scan including the HMF region, to flag any progressive presence of hydrolysis-related species without adding new figures/tables. These checks are intended as practice-oriented flags; numerical speciation is beyond the scope of this study.

QC thresholds and replacement criteria

To enable conditional extension beyond eight reuse cycles while maintaining data quality, this study defines the following routine QC checks and decision rules:

- Primary control – 20°C density window; after make-up, the working acid must fall within 1.66–1.69 g ml^{-1} at 20°C. If the density cannot be restored to this window, replace the solution.
- Diluted conductivity (25°C, defined dilution) is used as a qualitative indicator of ionic build-up. Warning if conductivity rises by >30% vs. fresh; action/replace if >60% or if warnings persist for two consecutive cycles.
- Quick screen of dissolved organics: reducing-sugar colour check and a UV-Vis scan including the HMF region. Warning if the 280 290 nm absorbance increases by ≈0.10 (1 cm path) vs. fresh; action/replace if ≈0.20 or if a monotonic rise is seen across two cycles.
- Process performance checks: the standard rinse sequence should still achieve filtrate pH ≥ 6.8 without exceeding the routine volumes; if not, replace. Marked process slowdowns also trigger replacement.
- Top-up vs. replace: a single warning allows top-up and continue; any action criterion, or ≥2 warnings in the same cycle, triggers replacement.
- Operational cap: unless an action criterion is reached earlier, this study set a conservative pilot cap of 12 cycles for routine practice, after which replacement is recommended.

Full raw weighing entries for every cycle (0–8) and for all replicates (parallel sample 1–3) are provided in table 3.

For microscopic observations, this study additionally acquired higher-magnification micrographs and performed a minimal image-analysis routine to quantify deposit area-fraction: (i) calibrate pixel size from the scale bar; (ii) select a fixed ROI (≥0.04 mm^2) avoiding edges; (iii) convert to grayscale and apply Otsu global threshold; (iv) apply a 3×3 opening to suppress isolated pixels; (v) compute area-fraction (%) = 100 × (foreground pixels / ROI pixels). The procedure was repeated on three replicate images (n = 3) per condition. Raw masks and a CSV of area fractions are provided in the Supplementary Dataset; higher-magnification images are provided in the Supplementary Image Set.

Safety and waste neutralisation

All work with concentrated sulfuric acid was performed in a fume hood with appropriate personal protective equipment: chemical splash goggles, face shield during pouring, acid-resistant gloves, lab coat with acid-resistant apron, long pants, and closed-toe shoes. Secondary containment and spill kits were kept at hand. For any dilution, acid was added into water slowly with cooling and gentle stirring to control heat release. Acidic rinsates and used solutions were collected separately, allowed to cool to room temperature, and neutralised gradually with an aqueous base under stirring while monitoring pH; additions were paced to control exotherm and avoid localised boiling or splashing. Neutralisation was stopped once the bulk pH reached approximately 6.5–8.5. Resulting neutral salts and any precipitates were handled and disposed of as hazardous waste in accordance with institutional SOPs and local regulations; no neutralised liquids were discharged without authorisation. Waste streams were segregated and kept away from incompatible reagents.

Per-sample "green lab" metrics and sensitivity

The detailed derivation of the "~80% saving at 8 reuse cycles" and the definitions of all loss/Make-up terms have been moved to the Supplementary Note. Calculations are normalised to one specimen (≈1.0 g) dissolved at 200 $ml \cdot g^{-1}$ of 75 wt% H_2SO_4 (20°C density target), with the batch restored to the 75 wt% density after each cycle. Loss terms include evaporation, entrainment/carryover moisture on glassware/filter and wet residue before rinsing, and neutralisation equivalents required to reach filtrate pH ≥ 6.8; measured rinse volumes and titration-derived neutralisation equivalents per cycle are summarised in the SI table. The nominal outcome is a ≈80% reduction of fresh-acid consumption and acid-equivalent discharge at N=8; a one-page sensitivity shows this outcome is robust within a ~70–85% band over the measured loss ranges.

Residue weighing and data calculation

The dried residues were cooled to room temperature and weighed using an analytical balance with a precision of 0.1 mg. According to the ISO 1833-11 [16], the content of insoluble fibres (i.e., polyester fibres) in the fabric was calculated, and the proportion of dissolved fibres (i.e., cellulosic components) was deduced by difference.

The quantitative determination results were recorded in tabular form. The residue mass and component content of the C/T white knitted fabric and the T/R red knitted fabric under 0–8 cycles of waste acid reuse are presented in table 3.

Mass-balance basis

Calculations are normalised to a 1.0-g specimen dissolved at a fixed acid-to-fibre ratio of 200 ml per gram using 75 wt% H_2SO_4. A single 200 ml charge is reused for eight consecutive cycles. Between cycles, the working solution is restored to the 75 wt% target based on its density at 20°C. The small per-cycle make-up accounts for three routine losses observed in the workflow: minor evaporative loss of about 1 ml per cycle with stoppered flasks, entrainment and carryover on glassware and in the wet cake before rinsing of about 12 ml per cycle, and the acid consumed during the ammonia rinse to reach a filtrate pH ≥ 6.8,

Table 3

RESIDUE MASS AND QUANTITATIVE DETERMINATION RESULTS OF C/T WHITE KNITTED FABRIC AND T/R RED KNITTED FABRIC UNDER DIFFERENT RECYCLING CYCLES

Fabric type	Reagent	Sample parameters		Parallel sample 1	Parallel sample 2	Parallel sample 3
A piece of white fabric (C/T)	75 wt% H_2SO_4 (0-cycle, fresh)	Net dry total weight (g)		0.9914	0.8852	1.0226
		Net dry weight of insoluble fibres (g)		0.3981	0.3553	0.4106
		Net dry content percentage (%)	Cotton	59.84	59.86	59.85
			Polyester fibres	40.16	40.14	40.15
		Content adjusted by standard moisture regain (%)		Cotton: 61.4%; Polyester fibres: 38.6%		
	1-cycle	Net dry total weight (g)		0.9411	0.9522	0.9761
		Net dry weight of insoluble fibres (g)		0.3779	0.3814	0.3920
		Net dry content percentage (%)	Cotton	59.84	59.95	59.84
			Polyester fibres	40.16	40.05	40.16
		Content adjusted by standard moisture regain (%)		Cotton: 61.4%; Polyester fibres: 38.6%		
	2-cycle	Net dry total weight (g)		1.0182	0.9286	0.8156
		Net dry weight of insoluble fibres (g)		0.4089	0.3709	0.3275
		Net dry content percentage (%)	Cotton	59.84	60.06	59.85
			Polyester fibres	40.16	39.94	40.15
		Content adjusted by standard moisture regain (%)		Cotton: 61.5%; Polyester fibres: 38.5%		
	3-cycle	Net dry total weight (g)		0.9131	1.0074	0.9258
		Net dry weight of insoluble fibres (g)		0.3678	0.4044	0.3718
		Net dry content percentage (%)	Cotton	59.72	59.86	59.84
			Polyester fibres	40.28	40.14	40.16
		Content adjusted by standard moisture regain (%)		Cotton: 61.4% Polyester fibres: 38.6%		
	4-cycle	Net dry total weight (g)		0.8928	0.9151	0.8763
		Net dry weight of insoluble fibres (g)		0.3585	0.3661	0.3519
		Net dry content percentage (%)	Cotton	59.85	59.99	59.84
			Polyester fibres	40.15	40.01	40.16
		Content adjusted by standard moisture regain (%)		Cotton: 61.4%; Polyester fibres: 38.6%		
	5-cycle	Net dry total weight (g)		0.8692	0.8645	0.9522
		Net dry weight of insoluble fibres (g)		0.3453	0.3440	0.3824
		Net dry content percentage (%)	Cotton	60.27	60.21	59.84
			Polyester fibres	39.73	39.79	40.16
		Content adjusted by standard moisture regain (%)		Cotton: 61.7%; Polyester fibres: 38.3%		
	6-cycle	Net dry total weight (g)		0.8611	0.8704	0.9874
		Net dry weight of insoluble fibres (g)		0.3455	0.3484	0.3965
		Net dry content percentage (%)	Cotton	59.88	59.97	59.84
			Polyester fibres	40.12	40.03	40.16
		Content adjusted by standard moisture regain (%)		Cotton: 61.4%; Polyester fibres: 38.6%		
	7-cycle	Net dry total weight (g)		0.8459	0.7879	0.8914
		Net dry weight of insoluble fibres (g)		0.3400	0.3160	0.3579
		Net dry content percentage (%)	Cotton	59.81	59.89	59.85
			Polyester fibres	40.19	40.11	40.15
		Content adjusted by standard moisture regain (%)		Cotton: 61.4%; Polyester fibres: 38.6%		
	8-cycle	Net dry total weight (g)		0.8092	0.8141	0.8674
		Net dry weight of insoluble fibres (g)		0.3193	0.3225	0.3497
		Net dry content percentage (%)	Cotton	60.54	60.39	59.68
			Polyester fibres	39.46	39.61	40.32
		Content adjusted by standard moisture regain (%)		Cotton: 61.8%; Polyester fibres: 38.2%		

Table 3 (continuation)

Fabric type	Reagent	Sample parameters		Parallel sample 1	Parallel sample 2	Parallel sample 3
A piece of white fabric (C/T)	75 wt% H_2SO_4 (0-cycle, fresh)	Net dry total weight (g)		0.9805	0.9838	0.9981
		Net dry weight of insoluble fibres (g)		0.6493	0.6507	0.6609
		Net dry content percentage (%)	Polyester fibres	66.22	66.14	66.22
			Viscose fibres	33.78	33.86	33.78
		Content adjusted by standard moisture regain (%)		Polyester fibres: 63.8%; Viscose fibres: 36.2%		
	1-cycle	Net dry total weight (g)		0.9742	0.8966	0.8969
		Net dry weight of insoluble fibres (g)		0.6461	0.5927	0.5939
		Net dry content percentage (%)	Polyester fibres	66.32	66.11	66.22
			Viscose fibres	33.68	33.89	33.78
		Content adjusted by standard moisture regain (%)		Polyester fibres: 63.8%; Viscose fibres: 36.2%		
	2-cycle	Net dry total weight (g)		0.9431	0.8728	0.9731
		Net dry weight of insoluble fibres (g)		0.6226	0.5780	0.6444
		Net dry content percentage (%)	Polyester fibres	66.02	66.22	66.22
			Viscose fibres	33.98	33.78	33.78
		Content adjusted by standard moisture regain (%)		Polyester fibres: 63.8%; Viscose fibres: 36.2%		
	3-cycle	Net dry total weight (g)		0.9928	0.9145	1.0009
		Net dry weight of insoluble fibres (g)		0.6578	0.6036	0.6662
		Net dry content percentage (%)	Polyester fibres	66.23	66.00	66.56
			Viscose fibres	33.77	34.00	33.44
		Content adjusted by standard moisture regain (%)		Polyester fibres: 63.8%; Viscose fibres: 36.2%		
	4-cycle	Net dry total weight (g)		0.9672	1.0351	0.9188
		Net dry weight of insoluble fibres (g)		0.6402	0.6839	0.6074
		Net dry content percentage (%)	Polyester fibres	66.19	66.07	66.11
			Viscose fibres	33.81	33.93	33.89
		Content adjusted by standard moisture regain (%)		Polyester fibres: 63.7%; Viscose fibres: 36.3%		
	5-cycle	Net dry total weight (g)		0.9033	0.9567	0.9763
		Net dry weight of insoluble fibres (g)		0.5962	0.6307	0.6442
		Net dry content percentage (%)	Polyester fibres	66.00	65.92	65.98
			Viscose fibres	34.00	34.08	34.02
		Content adjusted by standard moisture regain (%)		Polyester fibres: 63.6%; Viscose fibres: 36.4%		
	6-cycle	Net dry total weight (g)		0.9532	1.0068	1.0084
		Net dry weight of insoluble fibres (g)		0.6286	0.6648	0.6658
		Net dry content percentage (%)	Polyester fibres	65.95	66.03	66.03
			Viscose fibres	34.05	33.97	33.97
		Content adjusted by standard moisture regain (%)		Polyester fibres: 63.6%; Viscose fibres: 36.4%		
	7-cycle	Net dry total weight (g)		1.0648	1.0012	0.8364
		Net dry weight of insoluble fibres (g)		0.7032	0.6611	0.5529
		Net dry content percentage (%)	Polyester fibres	66.04	66.03	66.10
			Viscose fibres	33.96	33.97	33.90
		Content adjusted by standard moisture regain (%)		Polyester fibres: 63.7%; Viscose fibres: 36.3%		
	8-cycle	Net dry total weight (g)		0.8551	0.8604	1.0036
		Net dry weight of insoluble fibres (g)		0.5639	0.5690	0.6613
		Net dry content percentage (%)	Polyester fibres	65.95	66.13	65.89
			Viscose fibres	34.05	33.87	34.11
		Content adjusted by standard moisture regain (%)		Polyester fibres: 63.6%; Viscose fibres: 36.4%		

this consumption is reported as the equivalent volume of the working acid, about 3 ml per cycle. The standard rinsing sequence per cycle includes two cold water rinses of ~100 ml each, two dilute ammonia rinses of ~50 ml each, and two final cold-water rinses of ~100 ml each, continuing until the filtrate reaches pH ≥ 6.8. With these inputs, the cumulative fresh-acid requirement after eight cycles is about one-fifth of the no-reuse baseline, which aligns with the ~80% saving, and the acid-equivalent discharge is of the same order.

Based on table 3, it is evident that both fabric types exhibited minimal variation in residue mass and fibre content across 0–8 cycles of acid reuse. The test results remained highly consistent with those of the fresh acid group, with relative deviations within ±2%. These findings demonstrate that even after multiple reuse cycles, the 75 wt% sulfuric acid solution maintained reliable dissolution efficiency and analytical accuracy. This outcome validates the feasibility and environmental value of waste liquid recycling in quantitative fibre analysis.

Safety, corrosion, and materials of construction

All handling was performed in a fume hood with appropriate PPE (goggles/face shield during pouring, acid-resistant gloves, lab coat with apron). For any dilution, acid was added to water slowly with cooling and gentle stirring. Corrosion-related notes for 75 wt% H_2SO_4 at 50°C: (i) prefer glass/borosilicate vessels and PTFE/PVDF wetted parts; (ii) avoid unlined carbon steel and aluminum; (iii) 316L stainless steel hardware is not recommended under these conditions; Hastelloy-class alloys may be acceptable for short-contact fittings if lined parts are not feasible; (iv) choose elastomers cautiously, PTFE/FFKM preferred, EPDM/NR unsuitable; (v) minimize chloride ingress to avoid pitting, and rinse/neutralize contact surfaces promptly after use.

EXPERIMENTAL RESULTS

Microscopic observation

To visually assess the effect of waste liquid recycling on fibre morphology, this study conducted a comparative microscopic observation of white knitted fabric (cotton/polyester blended fabric) and red knitted fabric (viscose/polyester blended fabric) under different recycling conditions. Tables 4 and 5 present representative images of both fabric types under the original condition (0 cycles) and after eight reuse cycles.

Table 4

MICROSCOPIC IMAGES OF WHITE KNITTED FABRIC BEFORE AND AFTER DISSOLUTION

Dissolution agent	Original sample	Microscopic image 1 (500X)	Microscopic image 2 (500X)	Microscopic image 3 (500X)
75 wt% H_2SO_4 (0-cycle, fresh)	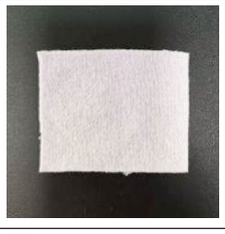	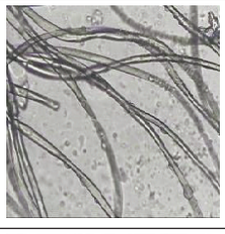		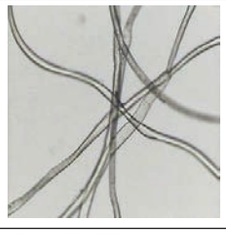
1-cycle		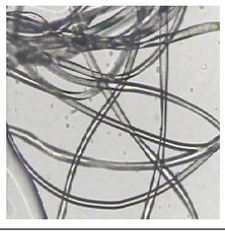		
2-cycle		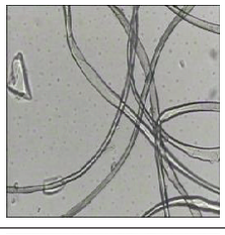	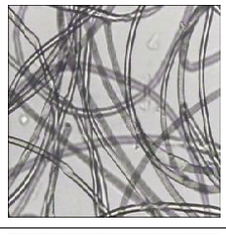	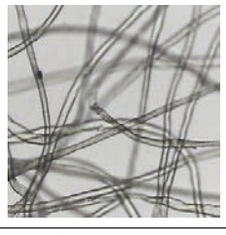
3-cycle		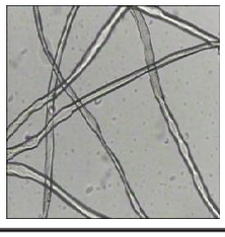	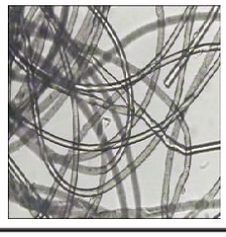	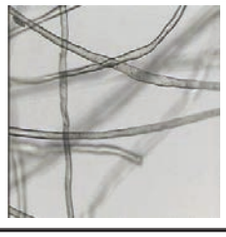

Table 4 (continuation)

Dissolution agent	Original sample	Microscopic image 1 (500X)	Microscopic image 2 (500X)	Microscopic image 3 (500X)
4-cycle		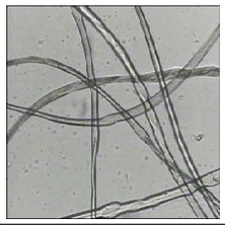	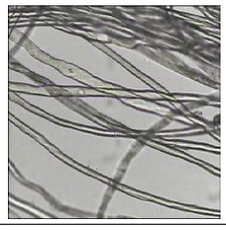	
5-cycle		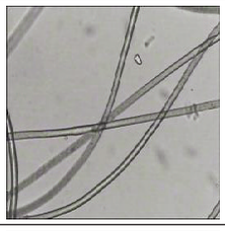	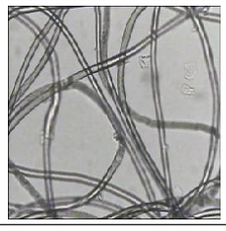	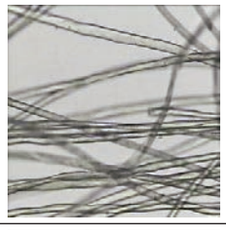
6-cycle				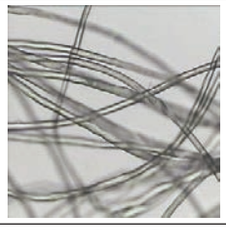
7-cycle		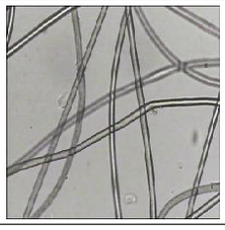		
8-cycle		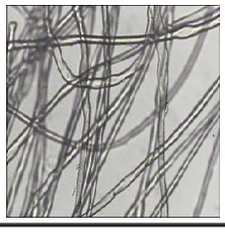	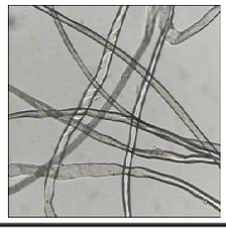	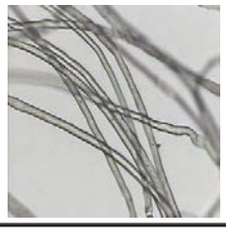

Note: Left: Original sample; Centre: Residue after 0-cycle dissolution; Right: Residue after 8-cycle dissolution.

Table 5

MICROSCOPIC IMAGES OF RED KNITTED FABRIC BEFORE AND AFTER DISSOLUTION				
Dissolution agent	**Original sample**	**Microscopic image 1 (500X)**	**Microscopic image 2 (500X)**	**Microscopic image 3 (500X)**
75 wt% H_2SO_4 (0-cycle, fresh)		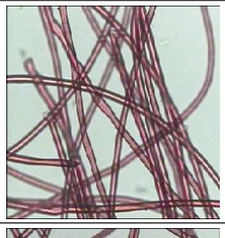	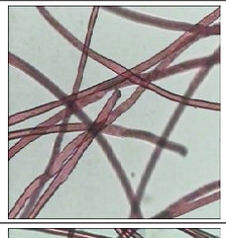	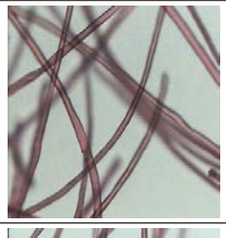
1-cycle		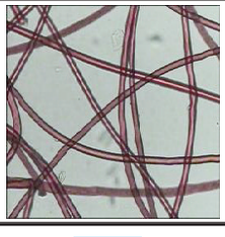	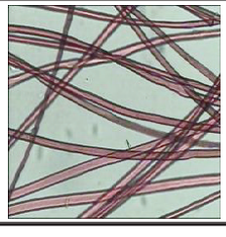	

Table 5 (continuation)

Dissolution agent	Original sample	Microscopic image 1 (500X)	Microscopic image 2 (500X)	Microscopic image 3 (500X)
2-cycle			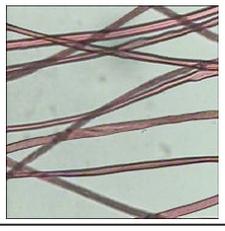	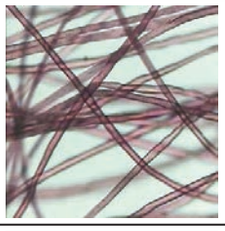
3-cycle	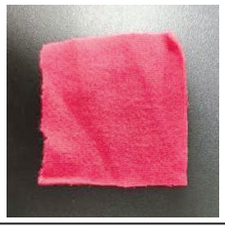	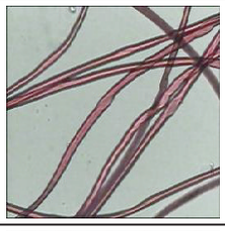		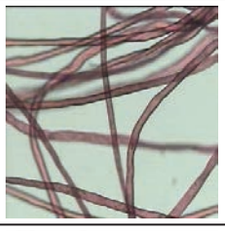
4-cycle			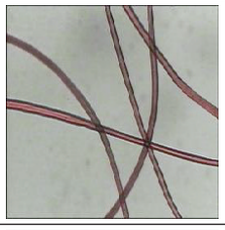	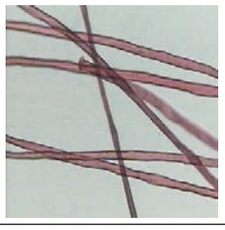
5-cycle				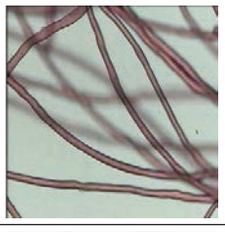
6-cycle		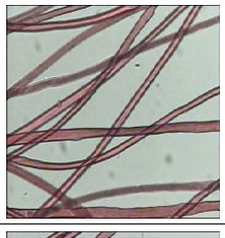	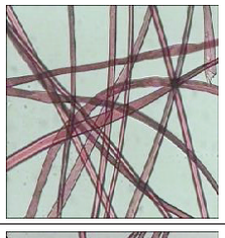	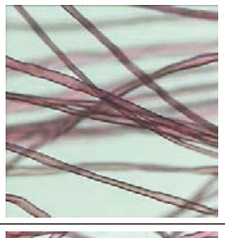
7-cycle		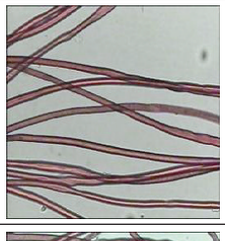	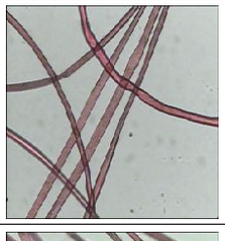	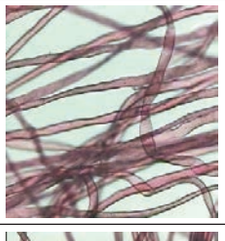
8-cycle		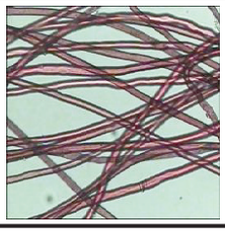		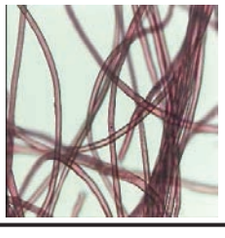

Note: Left – Original Sample; Centre – Residue after 0-cycle Dissolution; Right – Residue after 8-cycle Dissolution.

As illustrated in table 4, the post-dissolution residues of white knitted fabric mainly consisted of uniformly sized, smooth-surfaced polyester fibre, with negligible differences in morphology between 0 and 8 reuse cycles. No evident fibre breakage or surface damage was observed, indicating that both fresh acid and recycled acidic waste solution retained excellent cellulose-selective dissolution agent performance.

In contrast, table 5 shows that the red knitted fabric exhibited minor surface deposits and surface roughness

on some polyester fibre strands after eight cycles. These features are likely attributable to the accumulation of byproducts or viscose fibre residues generated during acid hydrolysis. Nevertheless, the fibres largely maintained their structural continuity and integrity, with no signs of extensive degradation, confirming that waste liquid recycling does not compromise the accuracy of quantitative component analysis.

Quantitative determination results

To further verify the quantitative accuracy of waste liquid recycling, this study measured the residue mass and Percentage Content of components in the two fabric types under 0–8 cycles of reuse of the 75 wt% sulfuric acid solution. The quantitative determination results are presented in table 3.

To facilitate a more intuitive Cross-comparison of the variation under different recycling conditions, figures 2 and 3 illustrate the changes in polyester fibre content with increasing recycling cycles for the white knitted fabric and red knitted fabric, respectively.

Points whose 95% CIs lie entirely within ±2 percentage points are described as equivalent within margin; reported effect sizes include Δpp and the tolerance-scaled effect e = |Δpp|/2.

Impact of waste liquid recycling on analytical accuracy

As shown in figures 2 and 3, the polyester contents of both textile types under 0–8 cycles of waste liquid recycling remain highly consistent with the results obtained using the fresh 75 wt% sulfuric acid solution. The relative deviation is controlled within ±2%, demonstrating excellent experimental reproducibility.

The polyester content in the cotton/polyester blended fabric (C/T white knitted fabric) remains approximately 39–40% (moisture-corrected value: 38.6%), with

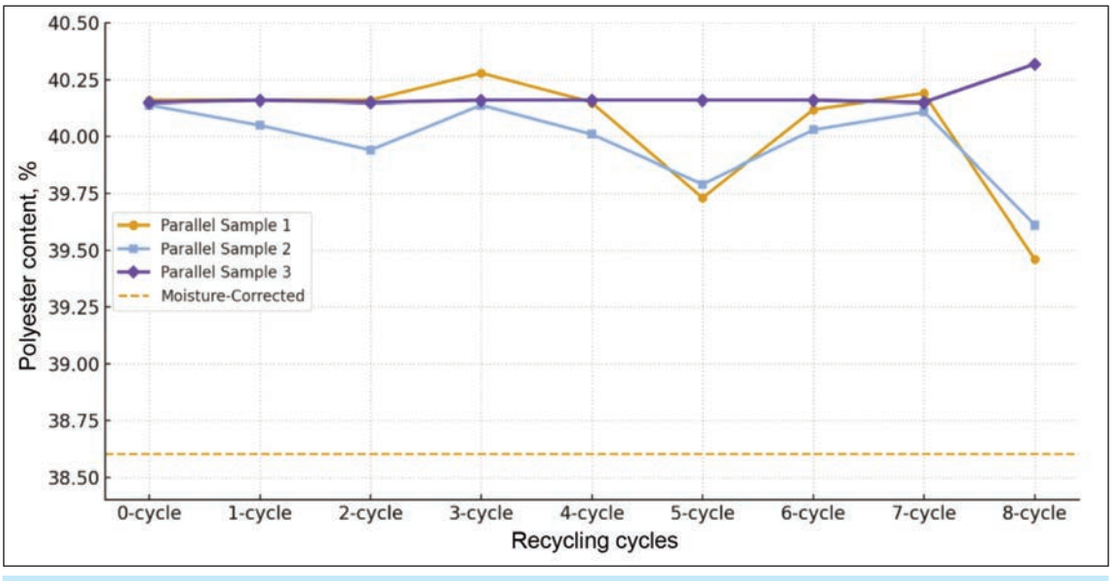

Fig. 2. Variation in polyester content of C/T white knitted fabric under different recycling cycles

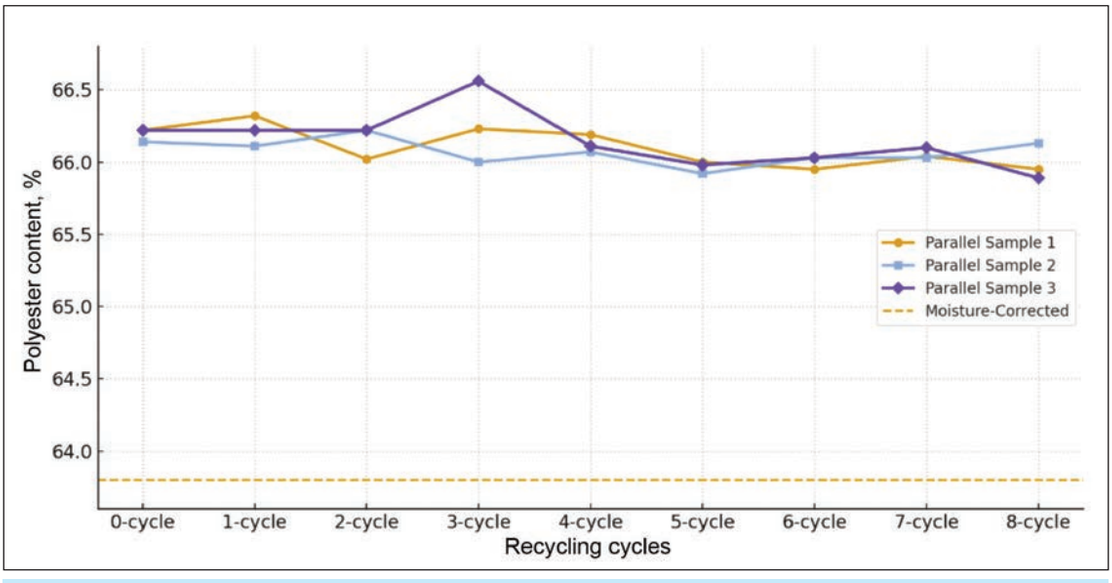

Fig. 3. Variation in polyester content of T/R red knitted fabric under different recycling cycles

minimal data fluctuation across cycles. Similarly, the viscose/polyester blended fabric (T/R red knitted fabric) maintains a stable polyester content around 66% (moisture-corrected value: 63.8%), even after eight consecutive cycles, which matches the quantitative determination results of the fresh solution group.
These findings indicate that even at high recycling frequencies, the accumulation of impurities in the acidic waste solution has a limited impact on the Dissolution efficiency of cellulose and the preservation of polyester residues. When combined with the microscopic observation data, it can be concluded that the 75 wt% sulfuric acid solution maintains excellent selectivity and analytical precision within eight cycles. This ensures reliable quantitative component analysis while significantly reducing both fresh acid consumption and waste acid reduction.

Cross-comparison and deviation analysis

To comprehensively evaluate the influence of waste liquid recycling on analytical accuracy, a Cross-comparison was conducted between the fresh solution group and various recycling groups. Corresponding relative deviations were calculated to assess experimental variability. This study now reports n=3 per cycle with mean ± 95% CI and per-cycle RSD in figures 2 and 3 (table 3). Across 0–8 cycles, all results remained within ±2%, with inter-cycle RSDs of ≈0.55% (C/T) and ≈0.13% (T/R), supporting high repeatability under the disclosed QC. For transparency and independent verification, the raw replicate weighings and calculated contents for each cycle are compiled in table 3.

Cotton/polyester blended fabric (C/T white knitted fabric)

As shown in table 3 and supported by the experimental data, the polyester content of the C/T white knitted fabric remains consistently around 39–40% across 0–8 recycling cycles (moisture-corrected value: 38.6%), with relative deviation typically within ±0.5% to ±1.5% (and within ±2% overall). The content curve in figure 2 is nearly horizontal, confirming that the residue-weighing results after repeated recycling are highly consistent with those obtained using the fresh acid.
Microscopic observations for the C/T fabric are presented in table 1. The polyester fibre surfaces remain smooth and intact throughout the recycling cycles. Any minor surface deposits observed under extended recycling do not compromise the quantitative outcomes, indicating that impurity accumulation has a negligible impact on cellulose-dissolution selectivity or on the integrity of polyester residues.

Viscose/polyester blended fabric (T/R red knitted fabric)

For the T/R red knitted fabric, the polyester content remains essentially stable at ≈66% across 0–8 recycling cycles (moisture-corrected value: 63.8%), with relative deviations controlled within ±2%. Compared with C/T, T/R shows slightly lower inter-cycle variability (RSD ≈0.13% for T/R vs. ≈0.55% for C/T; table 3). The slight variability observed is plausibly linked to by-products from viscose acid hydrolysis at higher recycling cycles, which can lead to minor surface deposits on polyester fibres.
This interpretation is supported by the microscopy images in table 5. After the eighth cycle, the polyester fibres exhibit slight surface roughness/deposition while the overall morphology remains intact, no rupture or significant degradation, so the deviations stay well within acceptable limits for quantitative component analysis.
Consistent with these observations, the content-versus-cycle curve for T/R in figure 3 is nearly horizontal, in line with the ISO-compatible ±2% precision demonstrated across cycles.
Despite the dyed nature of T/R, no monotonic drift was observed in the polyester content across 0–8 cycles; relative deviations remained within ±2%, and the inter-cycle RSD for T/R was approximately 0.13%, arguing against a progressive build-up that would bias quantification. Microscopy after eight cycles shows minor surface deposits on polyester residues, plausibly linked to dye-related fragments or cellulose hydrolysis products, yet these did not compromise the analytical outcome within eight cycles. About the link to deposits and variance, consistent with tables 1 and 2, the slight drift in 20°C density across cycles and the qualitative conductivity/organic-screening flags are in line with minor ionic/organic build-up expected under reuse and with the occasional light deposits observed for the dyed T/R fabric at later cycles. Importantly, polyester contents remained within ±2%, and inter-cycle RSD for T/R was ~0.13%, indicating that such build-up did not translate into systematic bias within eight cycles.

Cross-comparison between textile types

When comparing both fabric types, it is evident that despite repeated recycling, both maintain high consistency in quantitative determination results.
Nevertheless, the T/R red knitted fabric demonstrates marginally lower inter-cycle variability than the C/T white knitted fabric (inter-cycle RSD: C/T ≈ 0.55% vs. T/R ≈ 0.13%; table 3), leading to the following insights:
The viscose/polyester (T/R) blended fabric exhibits slightly superior stability under waste-liquid recycling (lower inter-cycle RSD), while both fabric types remain within ±2%.
The viscose/polyester blended fabric is more susceptible to interference from by-products generated during cellulose dissolution, but still maintains relative deviations within ±2%, aligning with analytical precision standards.

Comprehensive deviation analysis

Integrating results from both the C/T white knitted fabric and the T/R red knitted fabric, it is evident that all polyester content measurements across eight recycling cycles remain within ±2% relative deviation. This fully satisfies the accuracy requirements of quantitative component analysis as defined in the ISO 1833-11 [16].
The primary sources of deviation are identified as follows:

1) Accumulation of impurities in the acidic waste solution, leading to localised surface deposits.
2) Minor inconsistencies in Residue Weighing due to experimental handling.
3) Variations in fabric structure, such as dye composition or viscose fibre content, which affect Dissolution byproducts.
The results demonstrate that the impact of waste liquid recycling on analytical precision is minimal and well-controlled, ensuring methodological reliability and reproducibility across different textile types [15]. For both C/T and T/R, the 95% CIs of cycle-to-cycle differences and of the fresh-vs-cycle-8 contrast lie within the ±2 pp acceptance band; the estimates are equivalent within a margin. The corresponding tolerance-scaled effects ($e = |\Delta pp|/2$) are < 1, and standardised effects (Hedges' g) fall in the small range, in line with the observed inter-cycle RSDs (≈ 0.55% for C/T; ≈ 0.13% for T/R) and the ±2% stability already documented (figures 2 and 3; table 3).

DISCUSSION

Impact of waste liquid recycling on analytical accuracy

Per-sample perspective. Interpreted per specimen, the eight-cycle scheme reduces fresh-acid use and acid-equivalent discharge to ~20% of the no-reuse baseline, while dissolution and drying energy per specimen remain essentially unchanged; the time spent on neutralisation and hazardous-waste handling decreases in proportion to the reduced residual stream. A short sensitivity check indicates that these conclusions are robust within a ~70–85% saving window.
The results of this study demonstrate that within 0–8 cycles of reuse, the quantitative determination results for different blended textile/fabric types remained highly consistent with those obtained using fresh solution, with the relative deviation maintained within ±2% (figure 2 for C/T and figure 3 for T/R; data summarized in table 3). This level of precision not only falls well within the allowable range for experimental reproducibility defined by the ISO 1833-11 [16], but also aligns with precision thresholds reported in both domestic and international literature on quantitative component analysis [18, 26]. Together with the microscopy images (table 4 for C/T; table 5 for T/R), these findings confirm that recycling the waste acid does not significantly compromise cellulose dissolution or the retention of polyester residues, thereby verifying its feasibility for routine fibre analysis.
Additionally, the reliability of the quantification was corroborated through microscopic observation. The surface morphology of polyester fibre in cotton/polyester blended fabric (polycotton) remained smooth and intact under all reuse conditions. Although minor surface deposits were observed on viscose/polyester blended fabric after multiple recycling cycles, no evidence of fibre breakage or degradation was found. This is consistent with previous findings that concentrated sulfuric acid selectively dissolves cellulose fibre while leaving polyester fibre largely unaffected [5, 9]. Hence, it can be inferred that the gradual accumulation of by-products in the acidic waste solution exerts only superficial effects on fibre morphology without altering the fundamental quantification outcome.

Variability among different fibre systems

Notably, the quantification of white knitted fabric (C/T) showed slightly greater data fluctuation under recycling conditions compared to the more stable results observed for red knitted fabric (T/R). This discrepancy is likely due to differences in the proportion of cellulose fibre content. In the polycotton fabric, a higher percentage of cotton fibre leads to increased by-product accumulation during dissolution, thereby causing greater variability in the measurements. Conversely, the lower and more homogeneously dissolving viscose fibre content in the T/R samples likely contributes to more stable data. This is consistent with the lower inter-cycle RSD observed for T/R (≈ 0.13%) relative to C/T (≈ 0.55%).
Furthermore, dyeing processes may also play a role in the observed differences. To operationalise this observation, this study's expansion plan includes greige vs dyed and dope-dyed vs piece-dyed controls, plus auxiliary add-back screens, so that any dye/auxiliary-related contribution to minor deposits can be separated from fibre-ratio effects. The red dye components in T/R fabrics could interact with 75 wt% sulfuric acid solution or its hydrolysis products, leading to increased formation of surface deposits on residual fibres [27]. These changes, reflected as surface roughness under microscopy and minor variations in mass during Residue Weighing, suggest a degree of acid hydrolysis-induced structural transformation in cellulose fibre. Nevertheless, since all variations remain within the acceptable threshold of experimental reproducibility, the findings affirm the applicability of waste liquid recycling even for viscose/polyester blended fabric, though some caution is warranted for long-term operational deployment.

Environmental and economic benefits

Conventional quantitative component analysis requires extensive use of fresh 75 wt% sulfuric acid solution, generating substantial quantities of acidic waste solution that pose a serious environmental burden and increase laboratory operational costs [17]. The results of this study reveal that reliable analytical outcomes can be maintained over eight cycles of reuse/recycling, potentially reducing acid consumption and waste generation by approximately 80%.
This achievement holds significant implications for the development of a Green Testing Laboratory:
- Environmental benefits: reduction in high-concentration acidic waste solution discharge lowers the risks of water and soil acidification;
- Economic benefits: significant savings in reagent procurement and waste treatment costs, especially valuable for high-throughput testing scenarios;

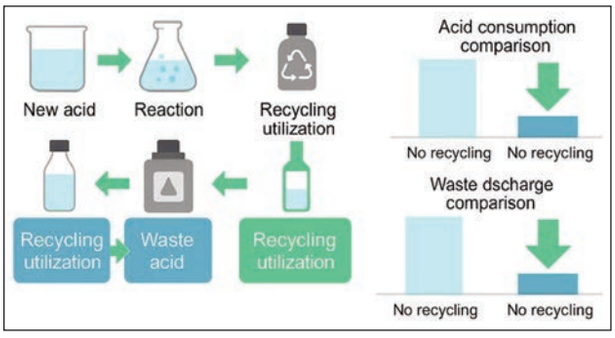

Fig. 4. Illustrates the projected resource conservation and waste acid reduction potential brought about by the proposed waste liquid recycling protocol

- Sustainability impacts: demonstrates a model for sustainable practices in analytical laboratories, in alignment with the national Dual Carbon Strategy [19–21]. Under the disclosed mass-balance basis, the eight-cycle workflow uses ~20% of the fresh acid and leads to an acid-equivalent discharge of the same order relative to a no-reuse baseline, aligning with the ~80% saving shown in figure 4.

For each cycle, the recycled acid met the 20°C density window (1.65–1.69 g ml^{-1}), and the titration-equivalent 75 ± 0.5 wt% band before use; filtrate pH ≥ 6.8 was confirmed.

From figure 4, it is evident that when the number of reuse/recycling cycles reaches eight, both 75 wt% sulfuric acid solution consumption and acidic waste solution discharge decrease to approximately 20% of the original volume, reflecting substantial gains in resource saving and waste acid reduction. Combined with the stability of quantitative determination results across cycles, this trend highlights the strong potential of the proposed method for practical implementation in quantitative component analysis of blended textile/fabric.

Application prospects and limitations

While the results of this study are consistent across 0–8 cycles (±2%; T/R inter-cycle RSD ~0.13%), this study now provides explicit QC thresholds and stopping rules so that reuse can be extended conditionally. In practice, continuation beyond eight cycles is permitted only if the QC window is met; otherwise, early top-up or replacement is performed.

A concise practitioner safety note summarises fume-hood/PPE practice, acid-into-water dilution, segregated collection, and gradual neutralisation to pH ≈ 6.5–8.5, aligning with this study rinse endpoint (filtrate pH ≥ 6.8).

From an application perspective, the method proposed in this study is not only well-suited for use in Green Testing Laboratory environments but may also serve as a reference framework for the separation and recovery of textile waste. However, several limitations must be acknowledged:

1) The current study validates up to eight cycles of waste liquid recycling. Whether further cycling will lead to increased data fluctuation due to by-product accumulation remains to be explored.

2) Beyond the two systems tested here (C/T and dyed T/R), additional fibre ratios, dye/finish systems, and elastane-containing textiles should be examined. This study, therefore specify a paired-control and add-back design to isolate dye/auxiliary effects from substrate effects. These studies will determine whether the ±2% stability observed over 0–8 cycles generalises across challenging cases and will refine actions if deposits/variance become material.

3) As the current analysis is based on laboratory-scale testing, extending the method to large-scale or industrial applications will necessitate additional consideration of acid management systems, recycling use technology, and process safety.

Addressing these issues will be crucial in advancing the practical value of concentrated sulfuric acid recycling within the textile industry, thereby promoting both sustainability and alignment with the broader goals of the national Dual Carbon Strategy.

This study now discloses the dye/finish information of the T/R red fabric to ground this limitation. Within eight cycles, this study did not find evidence of dye-hydrolysate accumulation at a level that alters analytical stability: contents stayed within ±2%, and T/R exhibited a low RSD (~0.13%). Minor deposits seen under microscopy likely reflect trace by-products but do not translate into systematic bias.

For practice, a simple visual colour check of the recycled acid can serve as an early-warning flag in dyed systems.

In routine use, laboratories may keep the density-to-target control as primary QC and add the diluted-conductivity and quick organic-screening notes above as qualitative early-warning cues for replacement/top-up decisions in dyed or heavily finished systems.

About regeneration options vs direct neutralisation, qualitative cost-benefit framing. With eight-cycle reuse, fresh-acid demand and acid-equivalent discharge fall to ~20% of the no-reuse baseline, leaving a smaller residual stream to manage. Direct neutralisation/disposal involves no CAPEX and is simple, but incurs ongoing base/neutralisation and hazardous-waste fees, well-suited to low-throughput labs. Diffusion dialysis (DD) is energy-lean, recovering free H_2SO_4 using anion-exchange membranes; CAPEX is moderate, and OPEX low, and acid purity can suffice for make-up after density restoration. Electrodialysis (ED/BMED) has higher power/control needs but can co-recover acid/base, cutting neutral-salt waste. Membrane-based impurity removal can extend reuse lifetime by removing dyes/particulates or polishing streams upstream of DD/ED; it is less about free-acid recovery per se but valuable as a life-extension step. References on DD/ED/hybrid economics and performance are listed in this study's bibliography.

CONCLUSION

This study, based on the ISO 1833-11 [16], investigated the waste liquid recycling of concentrated sulfuric acid in the quantitative component analysis of cotton/polyester blended fabric (polycotton) and viscose/

polyester blended fabric, specifically targeting white knitted fabric and red knitted fabric, respectively. Through a combination of microscopic observation and quantitative assessment across 0–8 recycling cycles, the following conclusions were drawn:

1) Stable analytical accuracy: within eight cycles, the Percentage Content of polyester fibre in both fabric types remained highly consistent with results from fresh acid usage, with relative deviation controlled within ±2%, thereby fulfilling the precision requirements of textile quantitative component analysis.

2) Intact fibre morphology: polyester fibre in polycotton retained its structural integrity throughout all cycles, while viscose/polyester blended fabric exhibited minor surface deposits at higher cycles, without compromising quantitative determination results.

3) Significant environmental and economic benefits: acid reuse resulted in a reduction of approximately 80% in both reagent consumption and acidic waste solution generation, effectively alleviating both the environmental burden and associated laboratory costs.

4) Broad applicability: the proposed method proved effective not only for cotton/polyester blended fabric but also for viscose/polyester blended fabric, indicating promising generalizability across multiple blended textile/fabric systems.

Collectively, these findings confirm the feasibility and efficiency of multi-cycle reuse of 75 wt% sulfuric acid solution in textile component testing. The method balances analytical rigour with sustainability, providing a scientific foundation for the development of green testing laboratories and offering practical insights for the textile industry's transition toward waste liquid recycling and low-carbon operations.

ACKNOWLEDGEMENTS

This paper was financially supported by the United Testing Services (Jiangxi) Co., Ltd. Research Project (CN) (RD202504). This paper was financially supported by the Science and Technology Research Project of Jiangxi Provincial Department of Education (CN) (GJJ250XXXX).

REFERENCES

[1] Xing, L., Gu, J., Zhang, W., Tu, D., Hu, C., *Cellulose I and II nanocrystals produced by sulfuric acid hydrolysis of Tetra pak cellulose I*, In: Carbohydrate Polymers, 2018, 192, 184 192, http://doi.org/10.1016/j.carbpol.2018.03.042

[2] Leenders, N., van Klink, G.P., Gruter, G.J., *Towards polycotton waste valorisation: depolymerisation of cotton to glucose with polyester preservation*, In: RSC Sustainability, 2025, http://doi.org/10.1039/D5SU00230C

[3] Kahoush, M., Kadi, N., *Towards sustainable textile sector: Fractionation and separation of cotton/polyester fibres from blended textile waste*, In: Sustainable Materials and Technologies, 2022, 34, e00513, http://doi.org/10.1016/j.susmat.2022.e00513

[4] Pavlopoulou, K.E., Hrůzová, K., Kahoush, M., Kadi, N., Patel, A., Rova, U., Matsakas, L., Christakopoulos, P., *Textile Recycling: Efficient Polyester Recovery from Polycotton Blends Using the Heated High-Ethanol Alkaline Aqueous Process*, In: Polymers, 2024, 16, 21, 3008, http://doi.org/10.3390/polym16213008

[5] Costa, C., Viana, A., Silva, C., Marques, E.F., Azoia, N.G., *Recycling of textile wastes, by acid hydrolysis, into new cellulosic raw materials*, In: Waste Management, 2022, 153, 99 109, http://doi.org/10.1016/j.wasman.2022.08.019

[6] Ling, C., Shi, S., Hou, W., Yan, Z., *Separation of waste polyester/cotton blended fabrics by phosphotungstic acid and preparation of terephthalic acid*, In: Polymer Degradation and Stability, 2019, 161, 157 65, http://doi.org/10.1016/j.polymdegradstab.2019.01.022

[7] Rosson, L., Wang, X., Byrne, N., *Investigating how the dye colour is impacted when chemically separating polyester-cotton blends*, In: The Journal of the Textile Institute, 2024, 115, 4, 656–666, http://doi.org/10.1080/00405000.2023.2201977

[8] Leenders, N., Moerbeek, R.M., Puijk, M.J., Bronkhorst, R.J., Bueno Morón, J., van Klink, G.P., Gruter, G.J., *Polycotton waste textile recycling by sequential hydrolysis and glycolysis*, In: Nature Communications, 2025, 16, 1, 738, http://doi.org/10.1038/s41467-025-55935-6

[9] Matsumura, M., Inagaki, J., Yamada, R., Tashiro, N., Ito, K., Sasaki, M., *Material separation from polyester/cotton blended fabrics using hydrothermal treatment*, In: ACS Omega, 2024, 9, 11, 13125 33, http://doi.org/10.1021/acsomega.3c09350

[10] Jungbluth, M., Beuermann, S., *Separation of Polycotton for Textile Recycling Using the DBU/DMSO/CO2 Switchable Solvent System*, In: ACS Sustainable Chemistry & Engineering, 2025, 13, 11, 4341–4348, http://doi.org/10.1021/acssuschemeng.4c07633

[11] Zhang, Y., Haque, A.N., Ranjbar, S., Tester, D., Naebe, M., *Decoding microplastic shedding from cotton/polyester blends: An analysis through fibre identification*, In: Environmental Pollution, 2025, 126909, http://doi.org/10.1016/j.envpol.2025.126909

[12] Chandra Manivannan, A., Panneerselvan, L., Kandaiah, R., Ravindran, A., Nachimuthu, G., Conaty, M., Palanisami, T., *Textile Recycling's Hidden Problem: Surface-Modified Fibre Fragments Emitted at Every Stage*, In: Environmental Science & Technology, 2025, 59, 17, 8766–76, http://doi.org/10.1021/acs.est.5c01854

[13] Moreno-Marrodán, C., Brandi, F., Barbaro, P., Liguori, F., *Advances in catalytic chemical recycling of synthetic textiles*, In: Green Chemistry, 2024, http://doi.org/10.1039/D4GC04768K

[14] Manivannan, C., Panneerselvan, L., Nachimuthu, G., Conaty, M., Palanisami, T., *Eco-innovative approaches for recycling non-polyester/cotton blended textiles*, In: Waste Management Bulletin, 2025, 3, 1, 255–270, http://doi.org/10.1016/j.wmb.2025.02.001

[15] Choudhury, K., Tsianou, M., Alexandridis, P., *Recycling of Blended Fabrics for a Circular Economy of Textiles: Separation of Cotton, Polyester, and Elastane Fibres*, In: Sustainability, 2024, 16, 14, http://doi.org/10.3390/su16146206

[16] International Organization for Standardization, *Textiles – Quantitative chemical analysis – Part 11: Mixtures of certain cellulose fibres with certain other fibres (method using sulfuric acid)*, 2nd ed., Geneva: ISO, 2017 (ISO 1833-11:2017), Available at: https://www.iso.org/standard/70286.html [Accessed on May 2025]

[17] Agarwal, C., Pandey, A.K., *Remediation and recycling of inorganic acids and their green alternatives for sustainable industrial chemical processes*, In: Environmental Science: Advances, 2023, 2, 10, 1306–39, http://doi.org/10.1039/D3VA00112A

[18] Zhang, C., Zhang, W., Wang, Y., *Diffusion dialysis for acid recovery from acidic waste solutions: Anion exchange membranes and technology integration*, In: Membranes, 2020, 10, 8, 169, http://doi.org/10.3390/membranes10080169

[19] Tongwen, X., Weihua, Y., *Sulfuric acid recovery from titanium white (pigment) waste liquor using diffusion dialysis with a new series of anion exchange membranes–static runs*, In: Journal of Membrane Science, 2001, 183, 2, 193–200, http://doi.org/10.1016/S0376-7388(00)00590-1

[20] Song, K., Meng, Q., Shu, F., Ye, Z., *Recovery of high purity sulfuric acid from the waste acid in toluene nitration process by rectification*, In: Chemosphere, 2013, 90, 4, 1558–1562, http://doi.org/10.1016/j.chemosphere.2012.09.043

[21] Loza, S., Loza, N., Korzhov, A., Romanyuk, N., Kovalchuk, N., Melnikov, S., *Hybrid membrane technology for acid recovery from wastewater in coated steel wire production: A pilot scale study*, In: Membranes, 2022, 12, 12, 1196, http://doi.org/10.3390/membranes12121196

[22] Lin, Y.I., Pan, S.Y., Tseng, P.C., Yeh, C.H., *Electrodialysis-based recovery of water and chemicals in recycled polyethylene terephthalate industries: energy, environmental, and economic performance*, In: ACS Sustainable Chemistry & Engineering, 2024, 12, 4, 1584–1594, http://doi.org/10.1021/acssuschemeng.3c06873

[23] Narayen, D., van Berlo, E., van Lier, J.B., Spanjers, H., *Recovery of sulfuric acid and ammonia from scrubber effluents using bipolar membrane electrodialysis: Effect of pH and temperature*, In: Separation and Purification Technology, 2024, 338, 126605, http://doi.org/10.1016/j.seppur.2024.126605

[24] Kunov-Kruse, A.J., Riisager, A., Saravanamurugan, S., Berg, R.W., Kristensen, S.B., Fehrmann, R., *Revisiting the Brønsted acid catalysed hydrolysis kinetics of polymeric carbohydrates in ionic liquids by in situ ATR-FTIR spectroscopy*, In: Green Chemistry, 2013, 15, 10, 2843–2848, http://doi.org/10.1039/C3GC41174E

[25] Becker, M., Ahn, K., Bacher, M., Xu, C., Sundberg, A., Willför, S., Rosenau, T., Potthast, A., *Comparative hydrolysis analysis of cellulose samples and aspects of its application in conservation science*, In: Cellulose, 2021, 28, 13, 8719–8734, http://doi.org/10.1007/s10570-021-04048-6

[26] Saeman, J.F., *Kinetics of wood saccharification-hydrolysis of cellulose and decomposition of sugars in dilute acid at high temperature*, In: Industrial & Engineering Chemistry, 1945, 37, 1, 43–52, http://doi.org/10.1021/ie50421a009

Authors:

GUANJIE CHEN[1], YU ZHANG[2], DAN ZOU[1], BEI CHENG[2], SHUANGYING ZHA[1], CHEN YANG[2,3]

[1]United Testing Services (Jiangxi) Co., Ltd, Floor 4-5, Building 14, Nanchang Light Textile City, No. 666, Changdong Avenue, Qingshan Lake District Hi-tech Industrial Park, 330012, Nanchang City, China
e-mail: 04guanjie@163.com (G.C.), 1052229021@qq.com (D.Z.), 814699598@qq.com (S.Z.)
ORCID: 0009-0008-3234-9916 (G.C.), ORCID: 0009-0004-2682-075X (D.Z.), ORCID: 0009-0001-8870-9430 (S.Z.)

[2]Jiangxi Centre for Modern Apparel Engineering and Technology, Jiangxi Institute of Fashion Technology, No. 108, Lihu Middle Avenue, Xiangtang Economic Development Zone, 330201, Nanchang City, China
e-mail: 3147006101@qq.com (Y.Z.), 345236840@qq.com (B.C.)
ORCID: 0009-0000-3532-3166 (Y.Z.), ORCID: 0009-0005-5440-9148 (B.C.)

[3]Wuhan Textile University Gongqingcheng Textile and Garment Industry Research Institute, 2nd Floor, Down Museum, Yaya Industrial Park, Gongqingcheng Industrial New Area, 332020, Jiujiang City, China

Corresponding author:

CHEN YANG
e-mail: comradeyang@qq.com
ORCID: 0000-0003-1593-7739

The impact of sales promotions on consumers' purchasing behaviour in the clothing industry

DOI: 10.35530/IT.077.03.202587

SIMONA TRIPA
LUCIA ADRIANA PANTEA
FLORIN TRIPA

ABSTRACT – REZUMAT

The impact of sales promotions on consumers' purchasing behaviour in the clothing industry

The fashion industry reflects global economic, technological, and cultural transformations, and consumer behaviour regarding clothing purchases is strongly influenced by these dynamic forces. In today's highly digitalised and competitive market, consumers are more informed, more demanding, and increasingly aware of the social, environmental, and economic implications of their purchasing decisions. They have access to an unprecedented variety of products, and the rise of e-commerce has significantly shaped their preference for convenience, speed, and personalisation. A growing number of consumers prefer quick, online purchases and are attracted to promotions and special offers that provide value for money. In this context, promotional strategies and discount campaigns have become essential tools for fashion retailers, helping them attract new customers, retain existing ones, and stimulate demand in an oversaturated market. These strategies include seasonal sales, "buy two, get one free" offers, flash sales, discount coupons, and loyalty programs. The study on the impact of promotions on consumer behaviour in the clothing sector highlighted aspects related to consumer preferences based on place of residence, level of education, gender, and income. The key factors influencing the decision to purchase clothing were identified, as well as the impact of discounts and special offers on this decision – all of which provide valuable insights for marketing professionals operating in the fashion industry.

Keywords: *promotions, consumers, clothing, fashion, marketing*

Impactul promoțiilor asupra comportamentului de cumpărare al consumatorilor în industria de îmbrăcăminte

Industria modei reflectă transformările economice, tehnologice și culturale înregistrate la nivel global, iar comportamentul consumatorilor în ceea ce privește achizițiile de îmbrăcăminte este puternic influențat de aceste modificări dinamice. În piața actuală, extrem de digitalizată și competitivă, consumatorii sunt mai informați, mai exigenți și din ce în ce mai conștienți de implicațiile sociale, de mediu și economice ale deciziilor lor de cumpărare. Ei au acces la o varietate fără precedent de produse, iar dezvoltarea comerțului electronic a modelat semnificativ preferința lor pentru confort, rapiditate și personalizare.

Un număr tot mai mare de consumatori preferă achizițiile rapide, online și sunt atrași de promoții și oferte speciale care oferă un raport bun calitate-preț. În acest context, strategiile promoționale și campaniile de reduceri au devenit instrumente esențiale pentru retailerii din industria modei, ajutându-i să atragă clienți noi, să-i fidelizeze pe cei existenți și să stimuleze cererea într-o piață suprasaturată. Aceste strategii includ reduceri sezoniere, oferte de tipul „cumperi două, primești unul gratuit", vânzări fulger, cupoane de reducere și programe de loialitate.

Studiul privind impactul promoțiilor asupra comportamentului consumatorilor în sectorul produselor de îmbrăcăminte a evidențiat aspecte legate de preferințele acestora în funcție de locul de reședință, nivelul de educație, gen și venit. Au fost identificați factorii principali care influențează decizia de cumpărare a articolelor de îmbrăcăminte, precum și impactul reducerilor și ofertelor speciale asupra acestei decizii – toate acestea oferind perspective valoroase pentru specialiștii în marketing care activează în industria modei.

Cuvinte-cheie: *promoții, consumatori, îmbrăcăminte, modă, marketing*

INTRODUCTION

The study of consumer behaviour has become a field of interest for marketing specialists, as it helps them understand how buyers choose products and services and the factors that influence these choices. Since the 1960s, the study of consumer behaviour has evolved into a distinct branch of marketing, once the need to understand the complex process through which a need transforms into demand for goods and services was recognised [1].

The way consumers make purchasing decisions is highly varied, as their reactions are strongly influenced by the context of their environment. The complexity of consumer behaviour is also due to the diversity of factors that affect the decision-making process of purchasing and consumption, both directly and indirectly. To understand consumer behaviour, a deep knowledge of the system of interacting and mutually influencing factors is necessary [2].

The increasing complexity of economic life has emphasised the need to study human behaviour in an economic context, divided into two major components: behaviour as a producer and behaviour as a consumer. In contemporary society, where technological progress tends to replace the human producer with

machines, the analysis of consumer behaviour becomes even more important. This analysis is crucial, especially in the context of limited resources, to ensure the production of only necessary goods and services.

The diversification of supply and the increase in purchasing power, associated with a higher level of education and culture, provide consumers with more options and more sophisticated needs. Producers must take these changes into account to respond appropriately to consumer preferences.

A deep understanding of consumer behaviour allows fashion brands to personalise their marketing strategies for specific audience segments. Different categories of consumers (based on age, gender, income level, lifestyle) have different preferences and behaviours when it comes to purchasing clothing products. Understanding these differences helps brands create more effective campaigns and attract consumers through personalised messages and promotions [3].

The objective of this study was to identify how promotions influence clothing purchase decisions, which types of promotions are most appreciated by consumers, and the sources of information through which these promotions reach them. The methodology employed consisted of an online questionnaire developed using the Google Forms platform.

LITERATURE REVIEW

The fashion industry has experienced rapid development in recent decades, marked by globalisation and digitalisation. Technology has had a major impact on how consumers buy clothing and how brands promote their products. E-commerce and social media platforms have transformed the purchasing process, allowing consumers to access brands and products from around the world without geographical limitations. Additionally, data and digital marketing analytics enable companies to better understand consumer behaviour and offer various types of promotions [4].

Over time, promotions have been widely studied due to their significant impact on purchasing decisions. They have been defined as a set of marketing tools used to stimulate consumer interest, trial, or purchase of products or services [5].

In the fashion industry, promotions are particularly important due to the fast pace of product changes, seasonal trends, and intense competition among brands. Promotions play an essential role in the marketing strategy of clothing brands, serving as a key tool for achieving various objectives such as increasing sales, attracting new customers, building customer loyalty, and creating an appealing brand identity. In an industry that is highly competitive and trend-sensitive, promotions provide a distinct advantage to stand out and build a strong connection with consumers.

Promotions also play a crucial role in consumer psychology, influencing both brand loyalty and impulsive buying behaviour. These effects are triggered by various psychological mechanisms such as instant rewards, fear of missing out (FOMO), and immediate gratification [6].

Promotions and discount strategies have become essential tools in the fashion industry, contributing to customer acquisition and retention. These include seasonal discounts, “2+1 free” offers, flash sales, as well as discount coupons and loyalty programs. The most appreciated promotions for clothing products are discounts and coupons [7, 8], while “buy one, get one free” promotions should be used with caution, as they tend to have less impact [9,10]. Promotions have proven effective in increasing short-term sales by creating a sense of urgency and perceived value [11]. Moreover, promotions – especially those with limited duration, monetary discounts, and online reviews – directly influence consumer behaviour, stimulating impulsive purchases, particularly in clothing, where fashion trends and consumer preferences evolve rapidly [12].

Numerous studies have focused on identifying the factors that determine how consumers respond to promotions. Chowdhury and Akter highlight that income level plays a crucial role, pointing out that lower-income consumers are more price-sensitive and more responsive to promotions than higher-income ones [13]. Shukla shows that women are generally more motivated by promotional offers in the fashion sector compared to men [14]. Another factor influencing perception and reaction to promotions is the consumer’s age. Studies have concluded that consumer interest in promotions increases with age [15].

Consumer behaviour has changed significantly in recent years, influenced by factors such as digitalisation, globalisation, and sustainability concerns. Modern consumers are more informed, have access to a wider variety of options, and are more aware of the impact of their purchasing decisions. The digital revolution and the growth of e-commerce have transformed promotional tactics in the fashion industry. Online flash sales, personalised discount codes, and loyalty programs offered through digital channels allow retailers to target consumers more precisely and increase engagement [16]. Furthermore, content creation on social platforms (Instagram, TikTok) plays a major role in shaping trends, influencing buying behaviour, and enhancing the effectiveness of promotions [17]. Zhang and Huang highlight the importance of visual marketing in influencing purchase intentions for fast fashion brands, while also emphasising the role of promotional strategies in the context of e-commerce [18]. Solomon and Rabolt emphasise the psychological factors that influence purchasing decisions and responses to promotions in the fashion sector [19], while Mishra et al. mention that the clothing industry adapts its promotional strategies based on the socio-economic status of consumers, which is closely tied to their market behaviour [8].

RESEARCH METHODOLOGY

The survey study aimed to determine the impact of promotions on consumer behaviour regarding clothing products.

The instrument used for data collection was an online questionnaire developed using the Google Forms platform. It included 18 questions, most of which were closed-ended (with pre-set answers), along with a few open-ended questions designed to capture qualitative nuances of consumer behaviour. The questions addressed aspects such as the frequency of clothing purchases, the budget allocated to them, preferred purchasing channels, factors influencing the purchase decision, the impact of discounts on buying behaviour, types of promotions perceived as attractive, and disadvantages experienced by respondents in relation to promotional offers.

The questionnaire was pre-tested on a small sample of 10 individuals to assess the clarity of the wording, the logical flow of the questions, and the time required to complete it. Following the pre-test, minor adjustments were made to ensure the content validity of the instrument.

Data collection was conducted online over a period of two months by distributing the questionnaire via email, WhatsApp, and social media platforms (Facebook, Instagram). In total, 167 individuals completed the questionnaire voluntarily and anonymously.

The data were analysed using descriptive statistical methods (frequencies, percentages) and highlighted the relationships between various socio-demographic variables and respondents' consumption behaviours, providing relevant and particularly useful insights for stakeholders in the fashion industry.

RESULTS AND DISCUSSION

Demographic characteristics and consumer behaviour

The first part of the questionnaire included several questions aimed at collecting demographic data from respondents, to determine if there are particularities in the behaviour of clothing consumers based on gender, age, education level, income, etc.

No significant differences related to clothing consumer behaviour were identified based on the respondents' gender. Regardless of gender, the average monthly budget allocated for clothing purchases ranged between 100 and 300 RON. Purchase sources included both physical stores and online shops, while the main factors influencing purchase decisions were price, product quality, and promotions/discounts. Percentage discounts (e.g., 30% off) and fixed amount price reductions (e.g., 50 RON off) were preferred. The only difference observed was in purchase frequency, which was monthly for females compared to once every few months for males.

Respondents' income influenced both the purchase frequency and the budget allocated. As income increased, so did both the purchase frequency and the budget dedicated to clothing products.

Education level and place of residence were not influential factors in consumers' clothing purchasing behaviour.

Clothing purchase patterns

The subsequent questions in the questionnaire were designed to identify the main patterns of clothing acquisition, encompassing the frequency of purchases and expenditure levels, as well as the preferred points of purchase and the factors influencing consumer choices.

Regarding the question on the frequency of clothing purchases, most respondents indicated that they buy clothes either once every few months (45.5%) or once a month (40.1%).

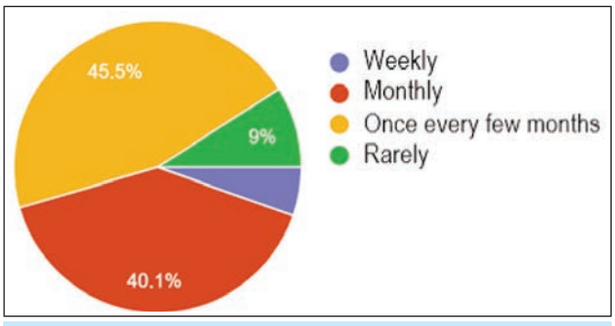

Fig. 1. Frequency of clothing purchases

The average monthly budget allocated for clothing purchases is between 100 and 300 RON for 52.7% of respondents.

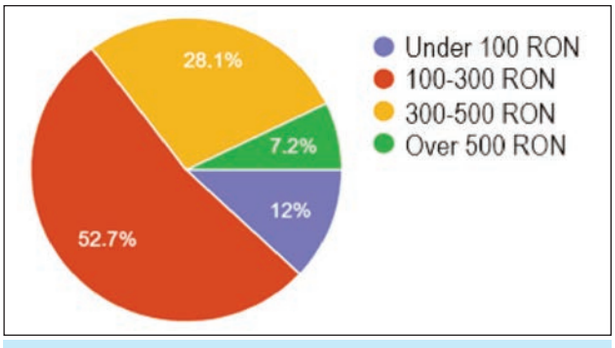

Fig. 2. Average monthly budget allocated for clothing purchases

In response to the question, "Where do you most often purchase your clothing products?" the vast

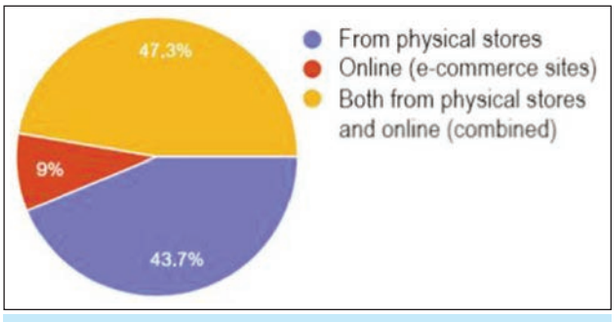

Fig. 3. Preferred place for purchasing clothing

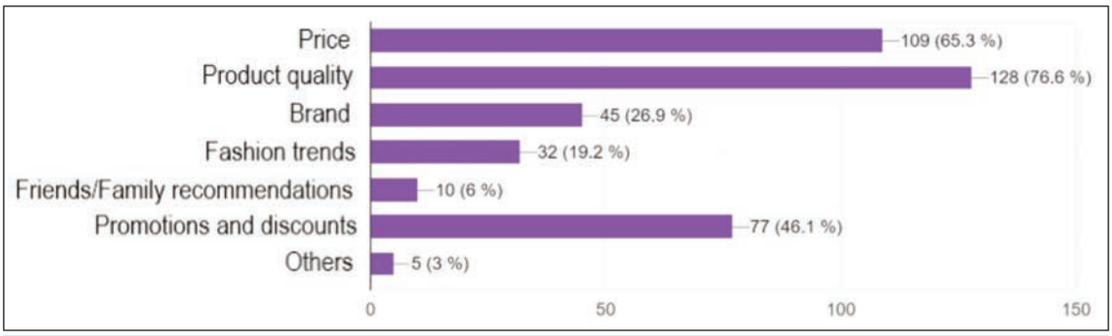

Fig. 4. Factors that most influence the decision to buy clothing

majority of respondents indicated that they prefer to buy clothing from physical stores or through a combination of physical and online options. Only 9% of respondents purchase their clothing exclusively online (figure 3).

The factors that most influence the decision to buy clothing are product quality, price, and promotions or discounts applied to the products (figure 4).

Impact of promotions on consumer behaviour

The final questions of the questionnaire focused on the impact of promotions on clothing purchase decisions.

To the question, "How often are you tempted to buy clothing products when they are promoted through discounts or special offers?" 58.7% of respondents answered "often" or "very often". Only 1.2% stated that they are not interested in purchasing clothing products when there are discounts or special offers (figure 5).The preferred promotions among clothing buyers are percentage discounts, followed by bundle

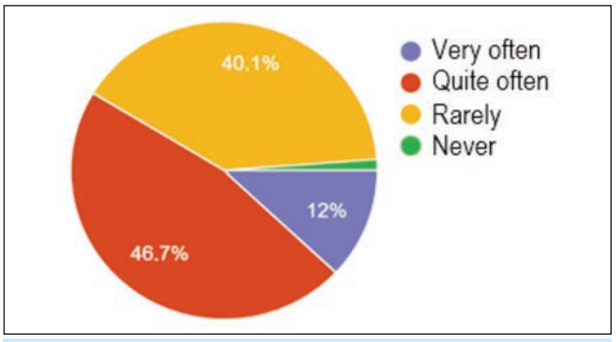

Fig. 5. Impact of discounts and special offers on clothing buyers

offers such as "buy 2, get 1 free", and free shipping (figure 6).

Clothing buyers consider the most attractive promotions to be those during season changes (46.7%) and in established discount periods such as Christmas, Easter, and Black Friday (figure 7).

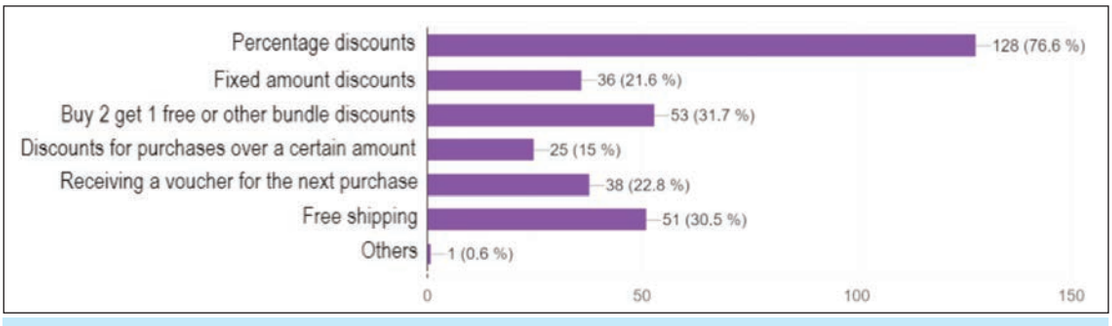

Fig. 6. Types of promotions preferred by clothing buyers

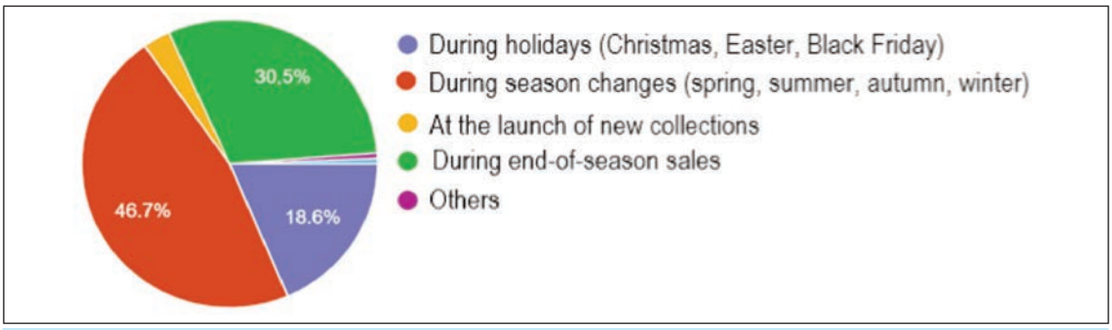

Fig. 7. Periods with the most attractive clothing promotions

Promotions influence 29.3% of respondents to make purchasing decisions more easily, 19.8% to buy more than they initially intended, and 13.8% to purchase a product they otherwise would not have bought (figure 8).

The main sources through which consumers learn about clothing promotions are advertisements on social media platforms (Facebook, Instagram, TikTok), in-store advertisements (e.g., window displays or posters), and recommendations from friends or family. A significant percentage also learn about promotions through clothing store websites and email newsletters (figure 9).

The primary disadvantages of clothing promotions mentioned are limited stock availability, the desired product or size being unavailable, misleading discounts, and promotions encouraging unnecessary or impulsive purchases (figure 10).

Among the survey respondents, 36.5% would like to see larger discounts during promotional periods, 21.6% want promotions dedicated to loyal customers and to be more frequent, and 20.4% desire clearer and easier-to-understand promotions (figure 11).

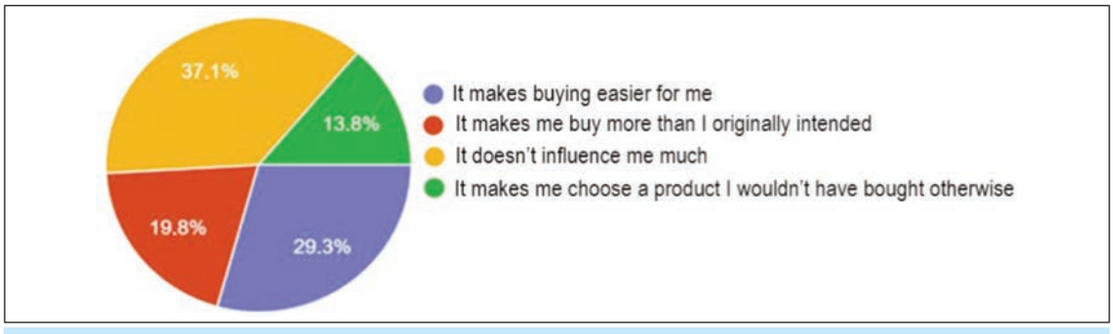

Fig. 8. Influence of promotions on the decision to purchase a clothing product

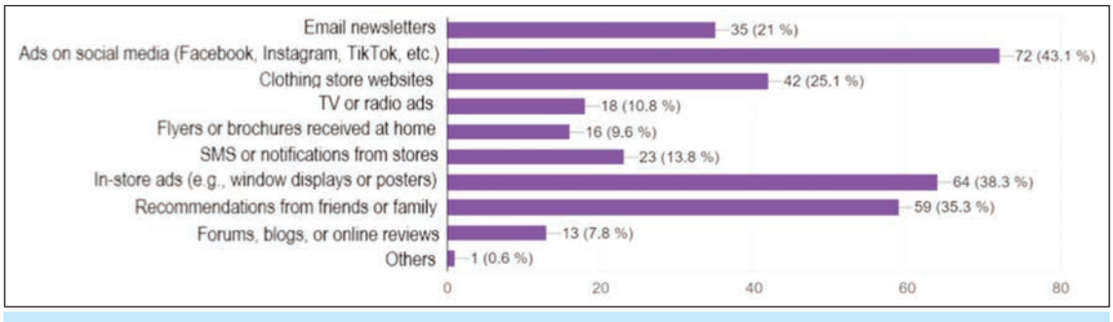

Fig. 9. Main sources of information about clothing promotions

Fig. 10. Main disadvantages of clothing promotions

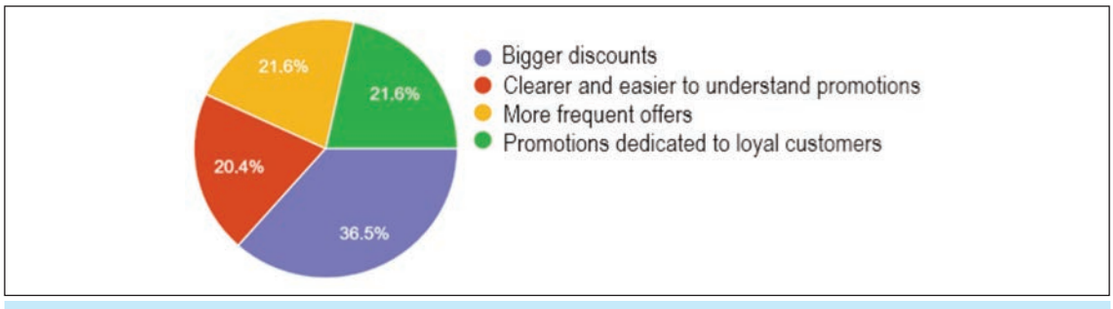

Fig. 11. Suggestions for improving clothing promotions

CONCLUSIONS

This study on consumer behaviour regarding clothing products found no major differences based on place of residence, education level, or gender, except for purchase frequency, which is higher among women. While the literature shows mixed findings regarding gender differences in decision-making styles, motivations, or influencing factors (e.g., higher brand loyalty among men) [20], there is general agreement that women purchase clothing more frequently than men [21, 22].

Respondents' income influences both purchase frequency and the budget allocated for clothing purchases: as income increases, so does purchase frequency and the allocated budget.

The most influential factors in clothing purchase decisions – product quality, price, and applied promotions or discounts – are consistent with findings from previous studies [23, 24].

Promotions influence clothing purchase decisions in various ways, from making the decision easier to buying in larger quantities, or even purchasing products that consumers would not have bought otherwise.

The most appreciated types of promotions are percentage discounts, followed by bundle offers such as "buy 2, get 1 free" and free shipping.

The main sources of information about promotions are social media advertisements, in-store displays, and recommendations from friends or family. Ads on store websites and email newsletters are also significant. These sources are highlighted in the most recent studies, whereas earlier research emphasised direct mail marketing, TV advertisements, and in-store promotions as the primary channels for communicating promotions [25].

The primary disadvantages of clothing promotions mentioned are limited stock availability, the desired product or size being out of stock, misleading discounts, and promotions that encourage unnecessary or impulsive purchases.

The study demonstrates how promotions affect the purchasing behaviour of clothing consumers. By understanding and leveraging this information, companies can optimise their marketing tactics, enhance brand loyalty, differentiate themselves in a competitive market, and increase sales. In the clothing market, sales promotions can drive sales, customer retention, and business growth. However, companies must carefully balance promotional efforts to avoid undermining brand credibility and long-term profitability.

ACKNOWLEDGEMENTS

The research undertaken was made possible by the equal scientific involvement of all the authors concerned. The research has been funded by the University of Oradea, Romania.

REFERENCES

[1] Stanciu, S., *Bazele generale ale marketingului*, Editura Universității din București, 1999

[2] Antošová, I., Pšurný, M., Štańková, J., *Changes in consumer purchasing decisions: Traditional and emerging factors in the dynamic marketing landscape over 15 years*, In: Marketing and Management of Innovations, 2023, 14, 3, 85–96, https://doi.org/10.21272/mmi.2023.3-08

[3] Gaugaș, T., *Studierea impactului tacticilor de șoc în reclamă asupra comportamentului consumatorului. Teză de doctor în științe economice*, 2024, Available at: https://irek.ase.md/xmlui/handle/123456789/3453 [Accessed on July 3, 2025]

[4] Ungur, S., *Moda în era digitală: Cum tehnologia schimbă industria fashion*, 2024, Available at: https://antreprenorismart.ro/moda-in-era-digitala-cum-tehnologia-schimba-industria-fashion/ [Accessed on June 15, 2025]

[5] Kotler, P., Keller, K.L., Brady, M., Goodman, M., Hansen, T., *Marketing Management*, 3rd edn PDF eBook. Pearson Higher Ed, 2016

[6] Nguyen, D.N., Van Nguyen, D., *FOMO and the Impulsive Purchasing Behaviour of Young People,* In: European Journal of Business and Management Research, 2025, 10, 3, 41–47

[7] Shahzad, K., Bhatti, A., Islam, T., Javaid, A., *Impact of sales promotion on consumer buying behaviour: A case of garments industry of Pakistan*, In: International Journal of Advanced Research in Engineering and Technology, 2020, 11, 10

[8] Mishra, M., Kushwaha, R., Gupta, N., *Impact of sales promotion on consumer buying behaviour in the apparel industry*, In: Cogent Business & Management, 2024, 11, 1, 2310552

[9] Shamsi, M.S., Khan, M.A., *Impact of Sales Promotion on Consumer Behaviour: An Analytical Study of Readymade Garments and Footwear Segments*, In: Al-Barkaat Journal of Finance & Management, 2018, 10, 1, 94–102

[10] Salvi, P., *Effectiveness Of Sales Promotional Tools: A Study On Discount, Price Off And Buy One Get One Free Offers In Branded Apparel Retail Industry,* In: Gujarat. ELK Asia Pacific Journal of Marketing and Retail Management, 2013, 4, 4

[11] Blattberg, R.C., Neslin, S.A., *Sales Promotion: Concepts, Methods, and Strategies*, Prentice Hall, 1990

[12] Liang, C.C., Lin, Y.W., *Online promotion effects under time limitation-A study of survey and physiological signals,* In: Decision support systems, 2023, 170, 113963, https://doi.org/10.1016/j.dss.2023.113963

[13] Chowdhury, T.A., Akter, T., *Fashion attributes preferred by young Bangladeshi consumers while buying casual clothes: A multi-dimensional approach*, In: Journal of Fashion Marketing and Management: An International Journal, 2018, 22, 4, 540–556

[14] Shukla, S., *A study on effect of gender differences on apparels buying decision*, In: International Journal of Advanced Research in Commerce, Management & Social Science, 2019, 02, 03, 203–211

[15] Khare, A., Achtani, D., Khattar, M., *Influence of price perception and shopping motives on Indian consumers' attitude towards retailer promotions in malls*, In: Asia Pacific Journal of Marketing and Logistics, 2014, 26, 2, 272–295

[16] Wilson, G., Brown, W., Johnson, O., *The Impact of Mobile Technologies on Consumer Behaviour in Retail Marketing*, 2024, Available at: https://www.preprints.org/manuscript/202407.2030/v1 [Accessed on May 11, 2025]

[17] Kumar, V., Mirchandani, R., *Increasing the ROI of social media marketing*, In: MIT Sloan Management Review, 2012, 54, 1, 55-61

[18] Zhang, Y., Huang, S., *The influence of visual marketing on consumers' purchase intention of fast fashion brands in China*, In: Frontiers in Psychology, 2024, 15, 11033480

[19] Solomon, M.R., Rabolt, N.J., *Consumer Behaviour in Fashion*, Pearson, 2008

[20] Žukina, I., Hunjet, A., Vuković, D., *A Comparative Analysis between Male and Female Consumer Behaviour toward Purchasing Items of Clothing*. In: Social and Economic Studies within the Framework of Emerging Global Developments, 2023, 2, 43

[21] Koca, E., Vural, T., Koç, F., *The evaluation of consumer tendencies towards hedonistic shopping for clothes*, In: European Journal of Research on Education, 2013, 54, 64

[22] Millan, E., Wright, L.T., *Gender effects on consumers' symbolic and hedonic preferences and actual clothing consumption in the Czech Republic*. In: International Journal of Consumer Studies, 2018, 42, 5, 478–488

[23] Wulandari, T.R., Suzanto, B., Fitria, B.T., Coenraad, D.P., *The Influence of Product Quality and Promotion on Purchase Decisions: A Study of a Fashion Store in Bandung*, In: Jurnal Ekonomi, Bisnis & Entrepreneurship (e-Journal), 2025, 19, 1, 101–111

[24] Saragih, R.B., *The influence of price, promotion, and product quality on fashion product purchase decisions at Irian supermarket Tanjung Morawa*, In: Mount Hope Economic Global Journal, 2025, 3, 2, 152–165

[25] Hultén, P., Vanyushyn, V., *Promotion and shoppers' impulse purchases: the example of clothes*, In: Journal of Consumer Marketing, 2014, 31, 2, 94–102

Authors:

SIMONA TRIPA[1], LUCIA ADRIANA PANTEA[1], FLORIN TRIPA[2]

[1]University of Oradea, Faculty of Energy Engineering and Industrial Management, Department of Textiles, Leather and Industrial Management, Universității Str. no. 4, 410087, Oradea, Romania
e-mail:anapantea72@gmail.com

[2]University of Oradea, Doctoral School of Engineering Sciences, Universitatii Str.no.1, 410087 Oradea, Romania
e-mail: florintripa@yahoo.com

Corresponding author:

SIMONA TRIPA
e-mail: tripasimona@yahoo.com

Textile materials for transdermic therapy in neurocognitive disorders

DOI: 10.35530/IT.077.03.2025137

DIANA ANDREEA PLĂCINTĂ
MIRELA BLAGA
ROMEO PETRU DOBRIN
ANA-RAMONA CIOBANU

ABSTRACT – REZUMAT

Textile materials for transdermic therapy in neurocognitive disorders

Neurocognitive disorders are a group of conditions that affect already developed cognitive abilities such as memory, learning capacity, perception, attention, and language. Excluding delirium and amnestic disorders, dementia is currently the seventh leading cause of death, with ten million new patients diagnosed annually. Patients with dementia, especially those with Alzheimer's disease, sooner or later develop neuropsychiatric symptoms that, along with the disease itself, place a significant burden on caregivers and society. Developing alternative methods of drug administration compared to traditional routes (oral, intravenous, intramuscular, inhalation) is essential to increase patient compliance and quality of life. Transdermal drug delivery via patches has become a convenient alternative to other administration routes, evolving from basic patches that simply store and release an active substance to smart and personalised patches that can incorporate sensors and various technologies, allowing them to adjust drug release according to the patient's needs in real time. However, challenges related to precise drug release, adhesion stability, and uniform diffusion control still remain. Unfortunately, for neurocognitive disorders, there are few patches available on the market, highlighting the need for further research. This paper aims to analyse neurocognitive disorders, from symptoms to new approaches using medical textiles in the form of medical patches for transdermal drug delivery.

Keywords: *Alzheimer's disease, dementia, medical textiles, transdermal patch*

Materiale textile pentru terapie transdermică în tulburările neurocognitive

Tulburările neurocognitive reprezintă un grup de afecțiuni care influențează abilitățile cognitive deja dezvoltate, precum memoria, capacitatea de învățare, percepția, atenția și limbajul. Excluzând delirul și tulburările amnestice, demența este în prezent a șaptea cauză principală de deces, cu zece milioane de noi pacienți diagnosticați anual. Pacienții cu demență, în special cei cu boala Alzheimer, dezvoltă mai devreme sau mai târziu simptome neuropsihiatrice care, alături de boala în sine, reprezintă o povară semnificativă pentru aparținători și societate. Dezvoltarea unor metode alternative de administrare a medicamentelor, comparativ cu cele tradiționale (orală, intravenoasă, intramusculară, inhalatorie), este esențială pentru a crește aderența pacienților la tratament și calitatea vieții. Administrarea transdermică a medicamentelor prin intermediul plasturilor a devenit o alternativă convenabilă la alte căi de administrare, evoluând de la plasturii de bază, care doar stochează și eliberează o substanță activă, la cei inteligenți și personalizați care pot încorpora senzori și diverse tehnologii, permițând ajustarea eliberării medicamentului în funcție de nevoile pacientului în timp real. Cu toate acestea, rămân în continuare provocări legate de eliberarea precisă a medicamentului, stabilitatea adeziunii și controlul difuziei uniforme. Pentru tulburările neurocognitive există puțini plasturi disponibili pe piață, ceea ce evidențiază necesitatea unor cercetări suplimentare. Această lucrare își propune să analizeze tulburările neurocognitive, de la simptome până la noi abordări care utilizează textile medicale sub formă de plasturi medicali pentru livrarea transdermică a medicamentelor.

Cuvinte-cheie*: boală Alzheimer, demență, textile medicale, plasturi transdermici*

INTRODUCTION

Neurocognitive disorders represent a group of disorders that affect mainly ones already developed cognitive abilities such as: memory, learning capacity, perception, attention, language. They include delirium, amnestic disorders and dementia.

According to official data from the World Health Organization in 2021 approximately 57 million people had dementia worldwide, over 60% of whom live in low-and middle-income countries. Every year, there are nearly 10 million new cases. Dementia results from a variety of diseases and injuries that affect the brain. Alzheimer's disease is the most common form of dementia and may contribute to 60–70% of cases.

Dementia is currently the seventh leading cause of death and one of the major causes of disability and dependency among older people globally. In 2019, dementia cost economies globally 1.3 trillion dollars, approximately 50% of these costs are attributable to care provided by informal careers (e.g. family members and close friends), who provide on average 5 hours of care and supervision per day. Women are disproportionately affected by dementia, both directly and indirectly. Women experience higher disability-adjusted life years and mortality due to dementia, but also provide 70% of care hours for people living with dementia [1].

Patients with neurocognitive disorders develop, sooner or later, behavioural and neuropsychiatric symptoms, such as depression, anxiety, aggression, psychosis. There is an increased necessity in research for alternative ways of administering medication in order to treat these symptoms. Not only do they affect the independence and quality of life of patients, but they also have a big impact on the life of the caregivers, who tend to develop psychiatric symptoms themselves, such as depression and anxiety, as a response to high levels of stress. This only increases the need for institutional care, posing a great burden on individuals and society.

NEUROCOGNITIVE DISORDERS. DEMENTIA

Delirium represents an acute decline in cognitive function, attention and state of consciousness. It is a common disorder in the elderly, but depending on the etiology (substance abuse, surgical interventions, acute infections, metabolic alterations, withdrawal, medication-induced etc), it can also affect young people [2, 3]. It has an acute onset (hours, days) and may be completely reversible with the right causal treatment.

Amnestic disorders are a group of neurocognitive disorders due to other medical conditions, substance induced or of unknown etiology, with memory impairment as the primary complaint. The prognosis of amnestic disorders is variable, depending on its etiology: it can be reversible, but if it involves brain damage, the lesions become permanent.

Dementia is a term used for multiple neurodegenerative disorders, characterized by loss of cognitive function, memory impairment and a loss of skills and abilities needed to perform daily activities. There are different types of dementia: Alzheimer's dementia (responsible for most cases of dementia), vascular dementia, Lewy bodies dementia, dementia related to other diseases (Parkinson disease, HIV, Prion disease, Huntington disease etc). Usually, Alzheimer dementia coexists with other forms of dementia (vascular dementia or Lewy body's dementia), pure syndromes being less common.

Vascular dementia

Vascular dementia is the most common form of dementia after Alzheime's disease. Depending on its physio pathological mechanism, it can be classified into four subtypes: multi-infarct dementia, post stroke dementia, subcortical ischemic vascular dementia and mixed dementia [4, 5]. Patients can develop, at some point, neuropsychiatric symptoms.

Management focuses mainly on prevention and treatment of the risk factors for cerebrovascular disease: hypertension treatment with antihypertensive medication, especially with angiotensin-converting enzyme (ACE) inhibitors may protect against further cognitive decline in vascular dementia [6].

Hyperlipidemia can be treated using statins, which also have shown to decrease cognitive decline [7, 8]. Diabetes treatment and antithrombotic medication can also be used for influencing cardiovascular risk in dementia. Cholinesterase inhibitors such as donepezil and galantamine may have some beneficial effects on cognition. Donepezil in dose of 10 mg has the best influence on cognition in combination with galantamine 16–24 mg, but also tend to be associated with more adverse effects than placebo. Also, the beneficial effect is unlikely to be of clinical importance. The evidence for rivastigmine is less certain, further research is needed. Although the effect is modest, but in the absence of any other treatments, people living with vascular dementia may still wish to consider the use of these agents [9].

Dementia with Lewy bodies

Dementia with Lewy bodies may account for up to 20% of all dementia cases. Apart from cognitive decline, it also involves neuropsychiatric symptoms such as: early and persistent visual hallucinations, disturbances of consciousness, neuroleptic sensitivity, and motor features Parkinson-like [10]. Both donepezil and rivastigmine are recommended as first-line treatments for dementia with Lewy bodies. The use of galantamine is unclear, and the NDMA receptor antagonist memantine is well tolerated in patients with Lewy body dementia, but evidence for its efficacy remains mixed [11, 12].

Alzheimer dementia

Alzheimer's disease is the most common cause of dementia. It places a significant burden on both individuals and society. It involves irreversible cognitive and memory decline, to the point where a person is unable to carry out daily activities and loses independence.

The main characteristic of the disease is progressive memory loss, especially of episodic memory, with long-term memory only initially preserved.

Neuropsychiatric symptoms are also present or may develop over time (hallucinations, seizures, paranoia, etc.) [13].

Diagnostic and investigations

There are two types of screening tools with high sensitivity and specificity that can be used to diagnose cognitive impairment. The Montreal Cognitive Assessment (MoCA) is widely used neurocognitive dysfunctions. It is easy to use, patient-friendly and lasts several minutes. It tests memory, attention, orientation, language, executive functions etc. A score of 25 points or lower is considered abnormal. For dementia detection it has a sensitivity of 91% and specificity of 81%. The Mini Mental State Examination (MMSE) can also be used for dementia detection. A score of 24 or less is considered abnormal. It has a sensitivity of 81% and specificity of 89%. Blood tests are usually carried out to rule out other causes of dementia (thyroid stimulating hormone, thiamine, vitamin B12, metabolic panel, full blood count etc.). Brain imaging should be obtained. Magnetic resonance imaging (MRI) shows diffuse cortical atrophy, as well as focal atrophy of the medial temporal lobes. A positron emission tomographic scan (PET) can

show reduced metabolic activity, especially in the parietal and temporal lobes [14].

Treatment

Three main inhibitors are approved for mild to moderate forms of Alzheimer disease: *rivastigmine, donezepil and galantamine*, with similar tolerability. Rivastigmine recommended dose is 3.6 mg twice a day. It also comes in form of a patch, with the recommended dose of 9.5 mg/24 hours patch. Donepezil normal treatment dose is 10 mg/24 hours and Galantamine 16–24 mg XL/24 hours. The most common adverse effect of AChE inhibitors are digestive problems, such as diarrhea, vomiting, nausea, abdominal pain. In case of intolerance at one AChe inhibitor, patients may switch to another [15].

Memantine is an antagonist for the N-methyl-D-aspartate (NMDA) receptor that slows neurotoxicity by binding to open calcium channels. The usual treatment dose is 20 mg/24 hours. It should be used with caution in patients with balance disorders, cardiac problems and liver dysfunction. Guidelines and different studies recommend at the moment a combination treatment between an AChE inhibitor and memantine. Donezepil and memantine showed better outcomes for patients with moderate and severe Alzheimer's disease [16, 17].

A systematic review revealed that supplementation with B complex vitamins can delay cognitive decline. Vitamin D supplementation has not been conclusive [18]. Other research found that Ginkgo biloba may slow cognitive decline especially in patients with dementia and neuropsychiatric symptoms [19]. Quercetin, a very popular flavonoid found in fruits and vegetables has shown interesting anti-inflammatory properties and neuroprotective effects.

Unfortunately, it has extensive digestive absorption and metabolism, lowering its efficacy in dementia [20]. The use of saffron in Alzeimer's disease improves cognitive function, and according to systematic reviews and meta-analyses, there is no difference between saffron administration and AChE inhibitors with memantine [21].

MEDICAL PATCHES FOR NEUROCOGNITIVE DISORDERS

Most medications available for neurocognitive disorders have many side effects that reduce patients' tolerability to treatment (digestive problems such as nausea, vomiting, abdominal pain, diarrhea, pain, etc.), as summarised in table 1.

Transdermal patches represent a rapidly growing market as a reliable delivery system, with more consumers seeking an easy, non-invasive way to take their medications. Transdermal patches are topical medications or products that attach to the patient's skin using a skin-friendly adhesive. The active formulation is then absorbed through the skin and enters the bloodstream. Compared to other drug delivery methods, such as oral or intravenous administration, transdermal patches offer several benefits that improve drug efficacy and patient compliance. They

Table 1

TRADITIONAL WAYS OF ADMINISTERING DRUGS

Drug administrations	Side effects
Oral route	Difficult for patients with neurocognitive disorders and swallowing problems requires high dosages, first pass metabolism
Intravenous or Intramuscular route	Possible pain, infection site
Inhalator route	Difficult to adjust the right dosage

are non-invasive, easy and painless to apply, provide controlled and consistent therapeutic dosages, and avoid the first-pass effect, where the drug is metabolised before reaching systemic circulation. Due to these advantages, transdermal patches have become an increasingly popular delivery method for both pharmaceuticals (such as nicotine, fentanyl, buprenorphine, and others) and nutraceuticals for OTC or recreational use (including CBD, caffeine, Vitamin B12).

Medical textiles, in form of transdermal patches have gain much popularity in recent years, because they are patient friendly, less invasive, easy to apply and don't require digestive absorption. A transdermal patch is usually made of four layers (figure 1) consisting of: a backing layer, which is the external layer of a patch, protecting it from the environment, usually made from polyethylene, a drug layer, which contains the pharmacological active substance, a rate controlling membrane layer, which controls the rate at which the drug is released into the system. An adhesive layer is used to attach the patch to the skin. For neurocognitive disorders there are few patches commercially available and are described in table 2.

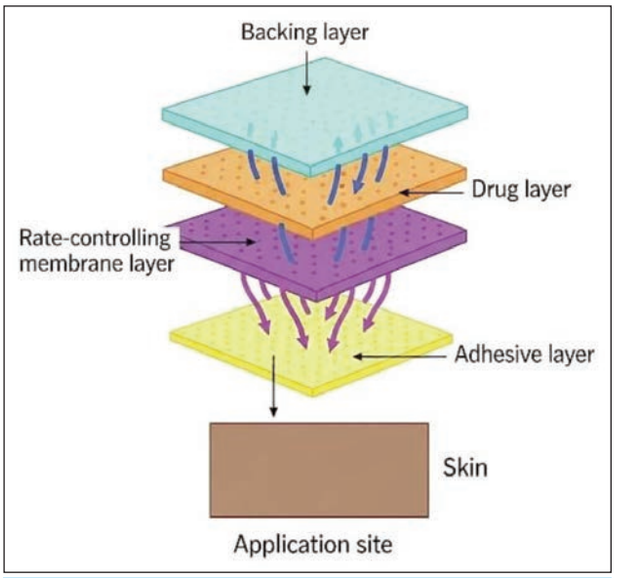

Fig. 1. Transdermal patch structure

Table 2

COMMERCIAL TRANSDERMAL PATCHES	
Transdermal patch name	**Description**
Rivastigmine	In the form of 4.6 mg/24 hours or 9.5 mg/24 hours, has superior tolerability and safety profile compared to oral capsules. It was approved in 2007 and is the only patch available for Alzheimer's dementia.
Rotigotine	A A non-selective dopamine agonist patch, is used for Parkinson's disease treatment, as well as, to treat the restless leg syndrome.
Asenapine	One atypical antipsychotic medication, was approved as a transdermal patch, being the only available patch for schizophrenia and bipolar disorder treatment.
Methylphenidate	A central nervous system stimulant patch is used to treat attention-deficit hyperactivity disorder (ADHD), improving focus and reducing impulsive behaviour.
Nicotine	One of the oldest patches on the market is used for smoking cessation.

The next generation of patches are matrix patches, which contain a solution or suspension of the active ingredient within a polymer or textile pad held in direct contact with the skin. Later, patches combined the drug and adhesive in a single layer. These patches are lighter, thinner, more flexible, and more comfortable to wear, improving the properties of the patches [22].

MEDICAL TEXTILES FOR DRUG DELIVERY

Medical textiles can be designed to gradually release therapeutic agents via diffusion, and some are being explored for their potential to help patients with psychiatric or neurological conditions. These drug-eluting textiles can be divided into three categories: 1. transdermal delivery, where drugs are administered through the skin; 2. controlled-release systems, fabrics designed to dispense medication at precise, sustained rates; 3. clinical applications, used in wound care, tissue repair, and cancer treatment [23–27].

Whether embedded within the fibre or applied as surface coating, the drug is gradually released over time through a diffusion process that follows Fick's law of diffusion. The rate of release depends on key factors such as the fibre structure, the concentration of drug and type of polymer used.

Natural and artificial polymers, chitosan and alginate are preferred due to their biodegradability, biocompatibility and low cost. Fabric characteristics such as thickness and air permeability play an important role in determining functional performance of transdermal delivery systems [23, 27].

Thickness is a decisive factor in ensuring comfort, durability and adaptability, especially when considering the anatomical part and surface area of application. Thicker fabrics are advantageous for prolonged therapeutic delivery, supporting extended wear durations [23], while thinner ones exhibit superior conformability to skin contours, preferred for thin-skinned regions like facial [28].

Air permeability is a critical parameter, essential for maintaining skin integrity during extended wear, as it facilitates moisture exchange and helps prevent maceration [23, 28–37]. On low permeability, the risk of bacterial growth is higher due to the perspiration accumulation, in contrast, whereas excessive permeability can destabilize the drug reservoir by accelerating moisture loss [37, 38]. Open structures, support increased drug loading capacity due to their volumetric porosity, while denser structures act as diffusion-regulating barriers, promoting controlled release profiles [27].

Knitted fabric structure significantly influences both wearer comfort and the controlled release of therapeutic agents. Among these, single jersey structures exhibit inherent elasticity and recovery due to their intermeshing loop configuration. This structural flexibility provides natural conformability and excellent skin contact during movement, making them suitable for application involving sensor integration [36]. In contrast, interlock structures offer superior dimensional stability, with minimal curling effect and smooth surfaces on both sides enhancing patient comfort against sensitive skin [23]. The high surface area promotes uniform coating adhesion for drug carriers. Within laminate hybrid system [28], knitted substrates provide comfort and flexibility while functional membrane controls drug diffusion rate. Double-layer knitted structures represent a good solution for wound care applications. Their unique configuration, independent knitted face and back layers connected by loops or yarns, allows for strategic material pairing: hydrophilic inner layers (cotton, viscose) absorb excess exudate while hydrophobic outer layers (polypropylene) direct liquid movement away from wounds. Open channels designed within double-layer structures guide therapeutic substances across wound surfaces with even distribution, while components maintain moisture and deliver medication effectively [23, 37, 38]. Furthermore, cellular structures demonstrate a greater drug-loading capacity compared to plain configurations. Their open architecture accommodates more drug-loaded microparticles [23, 28], making them suitable to be used for compact patch design.

Material selection for transdermal and wearable therapeutic systems must find the balance between natural fibre that offers biocompatibility and comfort, with functionalities provided by synthetic alternatives [23, 25, 26, 37]. Key considerations in fibre selection

include skin compatibility, long-wear comfort and structural stability to support active pharmaceutical compounds [33].

As natural fibre choice, cotton is valued for its inherent absorbency, which aids in perspiration management. Its breathability prevents skin irritation while hypoallergenic properties are beneficial for sensitive geriatric skin prone to dermatitis, mostly when it is used in direct contact with skin [24, 26, 33]. Synthetic fibres like polypropylene and poly(4-Methyl-1-Pentene) are lightweight, thereby the pressure on skin is reduced [38]. Their excellent chemical resistance ensures structural integrity throughout extended wear periods, while their hydrophobic nature supports efficient fluid management. Additionally, certain synthetic fibres can be engineered for conductivity, enabling integration of sensors when required [25, 30].

In the field of textile used for mental health support with drug-release there is a grown interest in the form of:

- *Transdermal patches* delivering anxiolytics or antipsychotics.
- *Smart textiles* that respond to physiological signals and release calming agents.
- *Wearable fabrics* integrated with therapeutic sensors or drug reservoirs for on-demand delivery.

Alternative to oral routes of drug administration, transdermal delivery has done a considerable contribution to the treatment of various medical diseases. Currently, most *transdermal patches* with drug-release capabilities are done from woven, nonwoven or coated textiles substrates, typically incorporating adhesive matrix systems, microneedle arrays, or laminated layers composed of polymers such as ethylene vinyl acetate or polyurethane [28, 29].

While knitted textiles are still considered an outgoing field in transdermal drug delivery, they are gaining attention due to their flexibility, moisture management and skin compatibility properties [29]. However, they present constant challenges related to precise drug release, adhesion stability, and uniform diffusion control.

Smart textiles are being actively developed for sensor-based monitoring applications [29, 30]. Knitted fabric configurations are often selected for their comfort, tactile sensitivity and breathability, integrating features such as conductive fibres, hardware pockets, and strategically padded areas to enhance wearability and protect sensitive skin. Although these systems typically do not deliver medication directly, they have an important contribution to mental health care through comfort-oriented therapeutic design.

Wearable fabrics with embedded therapeutic systems can be designed to monitor physiological signals and enable precise, on-demand drug delivery. Integration techniques involve: knitting or weaving conductive fibres into fabric; printing or coating drug reservoirs onto textile surfaces; embedding microfluidic channels for drug transport; designed layered textile architecture that combine sensing, actuation and drug release capabilities [32, 33].

Current research direction in drug-delivery medical textile mainly focuses on several key areas: ensuring biocompatibility and optimal skin adhesion; achieving uniform drug diffusion and accurate dosing profiles; improving durability, washability, and scalability of the textile systems; sensor accuracy for clinical use [34]. The main functionalities of their wearable fabrics are: real-time glucose monitoring and insulin/glucagon release; controlled chemotherapy dosing via microneedles; pain relief through transdermal patches with analgesic reservoirs activated by heat or motion; and sensor-based feedback for stress and comfort-enhancing textile design. The main functionalities of their wearable fabrics are: real-time glucose monitoring and insulin/glucagon release; controlled chemotherapy dosing via microneedles; pain relief through transdermal patches with analgesic reservoirs activated by heat or motion; and sensor-based feedback for stress and comfort-enhancing textile design [32, 33, 35]. In their research on wound healing, Arice and Karpagam [24] revealed that using a drug-carrier coated knitted fabrics can effectively reduce wound-related complications. Selected for their flexibility, breathability and suitability for direct skin contact, these fabrics were evaluated for their performance when coated with synergistic drug combinations. The findings confirm that knitted fabrics can serve as promising platforms for drug delivery in wound care, especially when enhanced with antimicrobial agents. Notably, drug-carrier coated knitted fabric has shown to have greater antibacterial efficacy than the drug-coated fabric. The knitted fabrics was a commercial one made of cotton yarn, chosen for its softness, breathability, and compatibility with wound care applications. Cotton's natural absorbency and comfort make it ideal for biomedical textiles, supporting the effectiveness of antibacterial coatings with antibacterial agents like piperacillin-tazobactam and beta-cyclodextrin.

Known for its stretchability and softness, knitted fabrics can be integrated in article for monitoring mental health, as a sensor platform [30, 32]. Their inherent comfort makes them ideal for long-term wear without causing skin irritation, an essential feature for continuous physiological tracking in psychiatric contexts.

Using conductive yarns, directly knitted into the garment, these textiles can form electrodes or sensor capable to detect signals like ECG (electrocardiogram), EEG (electroencephalogram), and EDA (electrodermal activity). The loop architecture of the knitted fabrics ensures close contact with the skin, enhancing signal reliability even during body movement throughout daily activities. The knitting technology allows to use technique to create customizable design for zonal placement of sensors (tighter stitches, shape-conforming zones, loose stiches, different loop architecture inside the structure).

Drug delivery textiles adapted for mental health support through coated fabrics and nanocomposite layers are study also by Ferri et al. [32]. Knitted fabrics is explored in a hybrid system of knitted with laminated drug-release membranes. The surface topology

and the number of fabric-to-skin contact points are those that can influence drug loading and drug release. Knitted structures with open structure such as honeycomb patterns tend to be ideal to host more microparticles of drugs loading on a bio-functional fabric. Most used method for transdermal delivery is the utilization of electrospun nanofibers with core-shell arrangement that allows different drug distribution in the nanofiber. Cotton and wool are natural fibres, good candidates for insect-repellent and antibacterial activity, functionality added trough a dyeing process or microencapsulation of DEET in polymer shells and subsequent surface treatment of fabrics.

Rumon et al. [36] investigate the potential of knitted fabrics as stretch sensors for monitoring physiological parameters such as respiration and body movement. By using embedding silver-based conductive yarns into the knitted surface, to create functional sensors capable of detecting mechanical strain. The intermeshing loops of the single jersey structure, offers natural elasticity and recovery, making it suitable for motion sensing. When stretched, the fabric translates physical movement (like breathing) into measurable electrical signals. The study provides design recommendations to enhance the sensors' durability and accuracy in practical, real-world health monitoring scenarios.

Komisarczyk et al. [37] developed double-layer knitted fabric and a woven one, intro an arrangement made of hydrophilic fibres (cotton, viscose) and hydrophobic fibres (polypropylene). They explore how liquids move through textile materials, especially when used in medical applications like wound dressings. Knitted fabrics showed strong potential as wound dressings due to their ability to manage moisture and potentially deliver drugs. The research highlights the importance of double layer design of the fabric, combining a hydrophobic layer to guide liquid movement with a hydrophilic layer to absorb excess moisture, features used to maintain a moist healing environment while managing exudate overflow. The smart wound dressing proved to be effective thanks to its components that helped the healing process by maintaining moisture, eliminating bacteria and deliver medication through specially designed open channels. Sasirekha et al. [38] explores the role of knitted fabric as a wound dressing application, highlighting their potential to support healing without the use of traditional antimicrobial agents. In the study it is used a knitted Poly (4-Methyl-1-Pentene) (PMP) fabric, a hydrophobic material that encourages bacterial adhesion. The dressing was fabricated using standard textile techniques manufacturing, a melt spinning PMP into multifilaments approximately 30 µm in diameter, followed by knitting. This knitted structure demonstrates excellent fluid management properties, enabling effective moisture control and handling of wound exudate, while leveraging its hydrophobicity to aid in bacterial clearance.

A wearable knitted patch can be a viable soft solution for mental wellness. As a gentle and effective approach that enables on-demand transdermal drug delivery for conditions such as anxiety, depression, or PTSD can be developed. The design can be built around layered functionality, offering both therapeutic impact and comfort. Key components can include:

1. *Knitted base layer* – made out from breathable, skin-friendly yarns such as cotton, bamboo, lyocell or conductive fibres, meant to ensures softness, flexibility, and long-wear comfort.
2. *Controlled-release drug container* – create a specialized matrix embedded within the knit structure, engineered to store and release medication consistently over time.
3. *Integrated channels* – fine distribution channels designed to guide the flow of the therapeutic substances across the skin surface, with even distribution and targeted absorption.
4. *Embedded smart sensors* – biometric sensors monitor key health indicators such as cortisol levels, body temperature, and heart rate. These readings can trigger automated dosing adjustments, offering responsive care.
5. *Comfort and hygiene characteristics*- designed for sensitive skin, the patch should feature moisture-wicking and antimicrobial properties, ensuring hygiene and irritation-free in wear, even during long use.

The design of the transdermal patch should be focused on the fulfilling of their main functions:

- medication released only when needed;
- enhances therapeutic outcomes;
- reduces reliance on oral medication and improves dosing compliance;
- promotes comfort in wear through its design (soft textures and stretchable structure);
- reusable feature through a washable design and pharmacological load.

Overall, biomaterials are integral to advancing drug delivery, offering diverse applications beyond conventional uses. By overcoming the blood–brain barrier, biomaterials enable targeted drug delivery for neurodegenerative diseases such as Alzheimer's and Parkinson's. Biomaterials have also revolutionised pain management through the development of localised, sustained-release drug delivery systems [39–41]. These systems can be implanted or injected near the source of pain, ensuring that analgesic medications are delivered directly to the affected area, reducing the potential for systemic side effects and dependency [42].

CONCLUSIONS

Medical patches and transdermal drug delivery have recently become a trend in the medical field. Owing to their many advantages over traditional routes, medical patches are increasingly attractive, especially for patients with neurocognitive disorders, who already present challenges in treatment compliance and tolerability. The need for alternative methods of administering treatment has led to developments in the medical textile field: the use of knitting technology, hosting micro particles on bio functional fabrics,

embedding micro particles, and using more natural polymers open new possibilities for improved transdermal drug delivery. The use of smart textiles, which incorporate various sensors and technologies, also offers promising solutions. The main goal is to achieve more personalized treatment, guided by real-time monitoring of patients' physiological and psychological needs, to increase compliance with treatment. Improving quality of life for both patients and caregivers may ease the burden of neurocognitive disorders, highlighting the need for further research and solutions.

ACKNOWLEDGEMENT

This paper is published within the framework of the project Centre for Research and Innovation in Textiles and Fashion Industry – SMART-Tex-IS, MySmis code 334492.

REFERENCES

[1] World Health Organization, *Dementia*, Available at: www.who.int/news-room/fact-sheets/detail/dementia [Accessed on August 2025]

[2] Inouye, S.K, Westendorp, R.G, Saczynski, J.S., *Delirium in elderly people*, In: Lancet, 2014, 383, 9920, 9, 11–22, https://doi.org/10.1016/S0140-6736(13)60688-1

[3] Iglseder, B., Frühwald, T., Jagsch, C., *Delirium in geriatric patients*, In: Wiener Medizinische Wochenschrift, 2022, 172, 5-6, 114–121, https://doi.org/10.1007/s10354-021-00904-z

[4] Livingston, G., Huntley, J., Sommerlad, A., et al., *Dementia prevention, intervention, and care: 2020 report of the Lancet Commission*, In: Lancet, 2020, 396, 10248, 413–446, https://doi.org/10.1016/S0140-6736(20)30367-6

[5] Chang Wong, E., Chang Chui, H., *Vascular cognitive impairment and dementia*, In: Continuum (Minneap Minn), 2022, 28, 3, 750–780, https://doi.org/10.1212/CON.0000000000001124

[6] Zhuang, S., Wang, H.F., Wang, X., Li, J., Xing, C.M., *The association of renin-angiotensin system blockade use with the risks of cognitive impairment of aging and Alzheimer's disease: a meta-analysis*, In: Clin Neurosci., 2016, 33, 32–38, https://doi.org/10.1016/j.jocn.2016.02.036

[7] Mishra, N., Mohan, D., Fuad, S., et al., *The Association between hypertension and cognitive Impairment, and the Role of Antihypertensive Medications: A Literature Review*, In: Cureus, 2020, 12, 12, e12035, https://doi.org/10.7759/cureus.12035

[8] Marcum, Z.A, Walker, R., Bobb, J.F., et al., *Serum cholesterol and incident Alzheimer's disease: findings form the adult changes in thought study*, In: J Am Geriatr Soc, 2018, 66, 12, 2344–2352, https://doi.org/ 10.1111/jgs.15581

[9] Battle, C.E, et al., *Cholinesterase inhibitors for vascular dementia and other vascular cognitive impairments: a network meta-analysis*, In: Cochrane Database Syst Rev, 2021, 2, 2, CD013306, https://doi.org/10.1002/14651858.CD013306.pub2

[10] Wild, R., et al., *Cholinesterase inhibitors for dementia with Lewy bodies,* In: Cochrane Database Syst Rev, 2003, 3, CD003672, https://doi.org/10.1002/14651858.CD003672

[11] Taylor, J.P., et al., *New evidence on the management of Lewy body dementia*, Lancet Neurol, 2020, 19, 157–169, https://doi.org/10.1016/S1474-4422(19)30153-X

[12] Wang, H.F., Yu, J.T., Tang, S.W., et al., *Efficacy and safety of cholinesterase inhibitors and memantine in cognitive impairment in Parkinson's disease, Parkinson's disease dementia, and dementia with Lewy bodies: systematic review with meta-analysis and trial sequential analysis*, In: J Neurol Neurosurg Psychiatry, 2015, 86, 135–43, https://doi.org/10.1136/jnnp-2014-307659

[13] Lane, C.A., Hardy J., Schott, J.M., *Alzheimer's disease*, In: Eur. J. Neurol., 2018, 25, 59–70, https://doi.org/10.1111/ene.13439

[14] Mastriani, A.J., Harris, E.A., *Hankets clinical neurology,* In: Dementia. Alzheimer's disease, CRC Press, 2021, 535–536

[15] Massoud, F., et al., Switching cholinesterase inhibitors in older adults with dementia, In: Int Psychogeriatr, 2011, 23, 3, 372–378, https://doi.org/10.1017/S1041610210001985

[16] National Institute for Health and Care Excellence, *Dementia: assessment, management and support for people living with dementia and their careers. NICE Guideline [NG97]*, 2018

[17] Guo, J., et al., *Memantine, donepezil, or combination therapy – what is the best therapy for Alzheimer's disease? A network meta-analysis*, In: Brain Behav, 2020, 10, 11, e01831, https://doi.org/10.1002/brb3.1831

[18] Gil Martínez, V., et al., *Vitamin supplementation and dementia: a systematic review*, In: Nutrients, 2022, 14, 5, 1033, https://doi.org/10.3390/nu14051033

[19] Fan, F., et al., *The efficacy and safety of Alzheimer's disease therapies: an updated umbrella review*, In: J Alzheimers Dis, 2022, 85, 3, 1195–1204, https://doi.org/10.3233/JAD-215423

[20] Khan, H., et al., *Neuroprotective effects of quercetin in Alzheimer's disease*, In: Biomolecules, 2019, 10, 1, 59, https://doi.org/10.3390/biom10010059

[21] Ayati, Z., et al., *Saffron for mild cognitive impairment and dementia: a systematic review and meta-analysis of randomised clinical trials*, In: BMC Complement Med Ther, 2020, 20, 1, 333, https://doi.org/10.1186/s12906-020-03102-3

[22] Atanasova, D., Staneva, D., Grabchev, I., *Textile Materials Modified with Stimuli-Responsive Drug Carrier for Skin Topical and Transdermal Delivery*, In: Materials, 2021, 14, 930, https://doi.org/10.3390/ma14040930

[23] Ahmed, U., Hussain, T., Abid, S. *Role of knitted techniques in recent developments of biomedical applications: A review*, In: Journal of Engineered Fibers and Fabrics, 2023, 18, 1–18, https://doi.org/10.1177/15589250231180

[24] Arice Mary, M., Karpagam Chinnammal, S. *Antibacterial coatings of knitted bio materials against bacterial pathogens using synergistic drugs*, In: Journal of Pharmaceutical and Scientific Innovation, 2018, 7, 4, 156–160, https://europub.co.uk/articles/-A-631494
[25] Gouveia, C.I., Mouro, C., *Development of Drug-Delivery Textiles Using Different Electrospinning Techniques: A Review*, In: IntechOpen, 2024, https://doi.org/10.5772/intechopen.112788
[26] Rostamitabar, M., Abdelgawad, A.M., Jockenhoevel, S., Ghazanfari, S., *Drug-Eluting Medical Textiles: From Fiber Production and Textile Fabrication to Drug Loading and Delivery*, In: Macromolecular Bioscience, 2021, 21, 7, https://doi.org/10.1002/mabi.202100021
[27] Aboli, M.G., Nitin, B.K., Nikita, M.W., Sawarkar, H.S., *A comprehensive review on controlled drug delivery systems (Cdds)*, In: IJNRD, 2024, 9, 11
[28] Wong, W.F., Ang, K.P., Sethi, G., Looi, C.Y., *Recent Advancement of Medical Patch for Transdermal Drug Delivery*, In: Medicina, 2023, 59, 778, https://doi.org/10.3390/medicina59040778
[29] Isaac, M., Holvey, C., *Transdermal patches: the emerging mode of drug delivery system in psychiatry*, In: Therapeutic Advances in Psychopharmacology, 2012, 2, 6, 255–263, https://doi.org/10.1177/2045125312458311
[30] Fernandes, S., Ramos, A., Vega-Barbas, M., García-Vázquez, C., Seoane, F., Pau, I., *Smart Textile Technology for the Monitoring of Mental Health*, In: Sensors, 2025, 25, 1148, https://doi.org/10.3390/s25041148
[31] O'Mahony, M., *Trends in smart textiles for health and wellbeing. Sustainable and accessible wearables are impacting home care, the work place and hospitals*, In: Textile Technology Org., February 27, 2023, Available at: https://textiletechsource.com/2023/02/27/trends-in-smart-textiles-for-health-and-wellbeing [Accessed at July 20, 2025]
[32] Ferri, A., Plutino, M.R., Rosace, G., *Recent trends in smart textiles: Wearable sensors and drug release systems*, In: AIP Conf. Proc. NANOINNOVATION, Rome, Italy, 11–14 September 2018, 2145, 020014, https://doi.org/10.1063/1.5123575
[33] Amjadi, M., Sheykhansari, S., Nelson, B.J., Sitti, M., *Recent Advances in Wearable Transdermal Delivery Systems*, In: Advanced Materials, 2018, https://doi.org/10.1002/adma.201704530
[34] Azeem, M., Shahid, M., Masin, I., Petru, M., *Design and development of textile-based wearable sensors for real-time biomedical monitoring; a review*, In: The Journal of the Textile Institute, 2024, 116, 1, 80–95, https://doi.org/10.1080/00405000.2024.2318500
[35] Hao Wang, et al., *A wearable transdermal device for on-demand drug delivery*, In: Materials, 2025, 8, 4, 102040, https://doi.org/10.1016/j.matt.2025.102040
[36] Rumon, M.A.a., Cay, G., Ravichandran, V., Altekreeti, A., Gitelson-Kahn, A., Constant, N., Solanki, D., Mankodiya, K., *Textile Knitted Stretch Sensors for Wearable Health Monitoring: Design and Performance Evaluation*, In: Biosensors, 2023, 13, 34, https://doi.org/10.3390/bios13010034
[37] Komisarczyk, A., Dziworska, G., Krucinska, I., Michalak, M., Strzembosz, W., Kaflak, A., Kaluza, M., *Visualisation of Liquid Flow Phenomena in Textiles Applied as a Wound Dressing*, In: Autex Research Journal, 2013, 13, 4, 141–149, https://doi.org/10.2478/v10304-012-0035-3
[38] Sasirekha, R., Sona, M.A., Shahanaz, Z., Gokarneshan, N., Ratna, U., Kayalvizhi, C., Lavanya, J., Padma, B., Priya, H.R., *Role of knit fabric as wound dressing*, In: Annals of Medical Case Reports & Reviews, 2025, 1, 1, 1002
[39] Pawar, V., Maske, P., Khan, A., Ghosh, A., Keshari, R., Bhatt, M., Srivastava, R., *Responsive Nanostructure for Targeted Drug Delivery*, In: J. Nanotheranostics, 2023, 4, 4., https://doi.org/10.3390/jnt4010004
[40] Malhotra, N., Joshi, M., Dey, S., Sahoo, R., Verma, S., Asish, K., *Recent Trends in Chronic Pain Medicine*, In: Indian J. Anaesth., 2023, 67, 123–129, https://doi.org/10.4103/ija.ija_31_23
[41] Gu, X., Carroll Turpin, M.A., Romero-Ortega, M.I., *Biomaterials and Regenerative Medicine in Pain Management*, In: Curr. Pain Headache Rep., 2022, 26, 533–541, [https://doi.org/10.1007/s11916-022-01055-5
[42] Trucillo, P., *Biomaterials for Drug Delivery and Human Applications*, In: Materials, 2024, 17, 456, https://doi.org/10.3390/ma17020456

Authors:

DIANA ANDREEA PLĂCINTĂ[1,3], MIRELA BLAGA[1,2], ROMEO PETRU DOBRIN[3], ANA-RAMONA CIOBANU[1]

[1]''Gheorghe Asachi'' Technical University of Iasi, Romania, Faculty of Industrial Design and Business Management, Blvd. Mangeron, No. 29, 700050, Iasi, Romania

[2]Centre for Research and Innovation in Textiles and Fashion Industry – SMART-Tex-IS, Prof. Dr. Doc. Dimitrie Mangeron, 29, 700050, corp TEX 4, Iasi, Romania

[3]University Of Medicine and Pharmacy "Gr. T. Popa" of Iasi-Romania, Faculty of Medicine, University Street, No 16, 700115, Iasi, Romania

Corresponding author:

MIRELA BLAGA
e-mail: mirela.blaga@academic.tuiasi.ro

Equity structure, incentive and constraint mechanisms, and corporate agency costs: An empirical study of listed companies in China's textile industry

DOI: 10.35530/IT.077.03.202540

GUANG CHEN
C.S NAJIB DAFIA
SONG KANG

ABSTRACT – REZUMAT

Equity structure, incentive and constraint mechanisms, and corporate agency costs: An empirical study of listed companies in China's textile industry

Equity structure forms the basis of governance, while incentive and constraint mechanisms represent its core. Together, they constitute a comprehensive corporate governance system. This study uses data from listed textile firms in China's Shanghai and Shenzhen A-share markets (2013–2024) to construct incentive and constraint mechanism indices via principal component analysis. It explores how equity structure and these mechanisms affect agency costs and examines their interrelationships. Results show that equity structure, incentive mechanisms, and constraint mechanisms all significantly reduce agency costs, with incentives being the most effective. There are complementary effects between equity structure and incentive mechanisms, and substitutability between equity structure and constraint mechanisms, as well as between incentive and constraint mechanisms. Robustness checks confirm the reliability of these findings. Based on these results, we recommend deepening equity-based incentive reforms, improving diversified monitoring systems, and integrating governance mechanisms to maximise marginal governance efficiency. This study not only provides a systematic theoretical foundation and actionable practical solutions for optimising corporate governance in textile enterprises, but also offers a transferable analytical framework to inform governance practices in other sectors.

***Keywords**: corporate agency costs, equity structure, constraint mechanism, incentive mechanism, China's textile industry*

Structura capitalului propriu, mecanismele de stimulare și de constrângere, precum și costurile de agenție corporativă: un studiu empiric privind societățile cotate la bursă din industria textilă din China

Structura capitalului propriu stă la baza guvernanței, în timp ce mecanismele de stimulare și de constrângere reprezintă nucleul acesteia. Împreună, constituie un sistem cuprinzător de guvernanță corporativă. Prezentul studiu utilizează date provenite de la întreprinderile textile cotate pe piețele de acțiuni de tip A din Shanghai și Shenzhen, China (2013–2024), pentru a construi indici ai mecanismelor de stimulare și de constrângere prin intermediul analizei componentelor principale. Studiul explorează modul în care structura capitalului propriu și aceste mecanisme influențează costurile de agenție și examinează interrelațiile dintre acestea. Rezultatele arată că structura capitalului propriu, mecanismele de stimulare și mecanismele de constrângere reduc semnificativ costurile de agenție, stimulentele fiind cele mai eficiente. Există efecte complementare între structura capitalului propriu și mecanismele de stimulare, precum și substituibilitate între structura capitalului propriu și mecanismele de constrângere, precum și între mecanismele de stimulare și cele de constrângere. Verificările de robustețe confirmă fiabilitatea acestor constatări. Pe baza acestor rezultate, recomandăm aprofundarea reformelor privind stimulentele bazate pe capitalul propriu, îmbunătățirea sistemelor de monitorizare diversificate și integrarea mecanismelor de guvernanță pentru a maximiza eficiența guvernanței marginale. Acest studiu nu numai că oferă o bază teoretică sistematică și soluții practice aplicabile pentru optimizarea guvernanței corporative în întreprinderile textile, ci oferă și un cadru analitic transferabil pentru a informa practicile de guvernanță din alte sectoare.

***Cuvinte-cheie**: costurile de agenție ale întreprinderilor, structura capitalului propriu, mecanism de constrângere, mecanism de stimulare, industria textilă din China*

INTRODUCTION

The separation of equity and control is a significant characteristic of modern corporate management. This division maximises the professional advantages of managerial executives but also leads to conflicts between management and shareholders. The agency problem has gradually garnered attention and has become one of the most critical aspects of modern corporate governance theory. The contractual relationship between owners and managers is primarily established through incentives and constraints imposed on management. The relationship between owners and managers regarding incentives and constraints affects the decision costs and benefits for managers, which in turn directly influences their decision-making motivations and effort levels. These factors ultimately impact the performance of the firm.

As a traditional manufacturing sector in China, the textile industry not only directly influences the level of national economic development but also plays a vital role in employment, trade exports, and technological innovation. Accordingly, the "14th Five-Year Plan" and the 2035 Vision Outline have repositioned the textile industry in China: it is described as "a pillar industry for national economic and social development, a foundational industry for improving livelihoods and enhancing quality of life, and a competitive industry for international cooperation and integration". The agency costs of management in textile enterprises have diminished operational efficiency and performance, becoming a primary issue that needs to be addressed in corporate governance. According to results from the Choice database, over the past decade, the proportion of management expenses in listed textile companies has increased by 26.6%, significantly higher than the 15.72% growth rate for the entire manufacturing sector. This indicates that the agency problem in listed companies within the textile industry is quite severe.

Equity structure serves as the cornerstone of corporate governance, encompassing the nature of shareholders and the degree of equity concentration. In this study, it is measured by the proportion of state-owned capital shareholding. Shareholders, as capital investors, hold ownership rights, which in turn grant them claims on residual profits and control. The contractual relationship between shareholders and management is primarily realised through incentive and constraint mechanisms. For shareholders seeking wealth maximisation, designing effective incentive and constraint mechanisms to optimise managerial behaviour and minimise agency costs is a critical issue faced by every company. Using listed textile firms in China as a sample, this study explores how equity structure and incentive-constraint mechanisms influence agency costs and examines their underlying mechanisms.

LITERATURE REVIEW

Under the modern enterprise system, the separation of ownership and management rights leads to the emergence of agency problems, consequently eroding firm value. As a significant component of the corporate landscape, listed textile companies also grapple substantially with the issue of agency costs. Numerous scholars have conducted in-depth research on this topic. Early literature primarily focused on the root causes and manifestations of agency costs. For instance, Jensen and Meckling proposed that the misuse of free cash flow and managerial defensive behaviours are key manifestations of agency problems, which can severely undermine firm value [1]. Subsequent research has progressively delved into the impact of various corporate governance elements on agency costs, providing a rich theoretical foundation for this study. However, there remains scope for improvement in the comprehensiveness, depth, and industry-specific applicability of these analyses.

Ownership structure and agency costs

Ownership structure, as one of the core elements of corporate governance, has attracted significant attention regarding its influence on agency costs. Nevertheless, academic consensus on this issue has yet to be reached. On the one hand, government shareholding has been empirically shown to have a U-shaped relationship with firm value [2]. Within the textile industry, when government ownership is low, insufficient government oversight may provide opportunities for managerial self-serving behaviour, leading to higher agency costs. Conversely, once government ownership exceeds a certain threshold, excessive government intervention in business operations may also impede value enhancement. On the other hand, direct shareholding by the actual controller can effectively mitigate conflicts among shareholders [3]. In listed textile companies, such direct holdings can strengthen the actual controller's motivation and capacity to supervise management, reducing moral hazard and adverse selection problems, thereby lowering agency costs.

Regarding the impact of ownership checks and balances (ownership concentration), existing research conclusions diverge significantly. Some scholars argue that moderate ownership concentration can enhance monitoring effectiveness [4]. In the textile sector, large shareholders possess greater incentives and resources to oversee management, curbing self-serving behaviours. Conversely, other scholars emphasise the role of ownership checks and balances in restraining self-serving actions by large shareholders [5]. The proportion of state-owned shares, a critical dimension of mixed-ownership reforms, exerts a significant influence on governance effectiveness within listed textile companies. Empirical studies confirm that the rational allocation of state-owned shares can improve social security contribution compliance [6], promote green innovation [7], and optimise human capital allocation [8]. This suggests that state-owned shares possess potential advantages in refining corporate governance structures and reducing agency costs. Based on this analysis, this paper proposes Hypothesis H1: The proportion of state-owned shares can effectively reduce agency costs in listed textile companies.

Incentive mechanisms and agency costs

Incentive mechanisms are crucial instruments for alleviating principal-agent problems. Theoretically, principal-agent theory emphasises designing rational incentive mechanisms to align the goals of management and employees with shareholder interests, thereby reducing agency conflicts. Human capital theory posits that effective incentive mechanisms can fully realise the value of human capital and enhance operational efficiency. Empirically, existing literature has yielded numerous findings. Research indicates

that the relationship between managerial ownership ratio and agency efficiency exhibits an inverted U-shape [9]. This suggests that increasing managerial ownership within a certain range can enhance responsibility and monitoring awareness, but excessively high ownership may trigger managerial shortsightedness, detrimental to long-term development. Performance-linked equity incentives can effectively weaken agency conflicts [10]. In listed textile companies, tying management's equity incentives closely to firm performance can motivate them to focus more on operational efficiency, reducing self-serving behaviour. Furthermore, employee stock ownership plans (ESOPs) demonstrate more pronounced effects in technology-intensive textile enterprises [11]. This is likely because, in such firms, employee knowledge and skills are vital to development; ESOPs can actively mobilise employee initiative and creativity, enhancing core competitiveness.

However, existing research still exhibits shortcomings concerning internal variations within incentive mechanisms and industry-specific applicability. In terms of compensation structure design, efficiency and fairness need to be balanced. Excessive pay disparity can easily trigger negative employee sentiment [12]. In the labour-intensive textile industry, stable employee morale is particularly crucial for maintaining production efficiency. Conversely, moderate pay disparity can enhance competitive efficiency [13]. Based on the above analysis, this paper proposes Hypothesis H2: Effective incentive mechanisms can reduce agency costs in listed textile companies.

Constraint mechanisms and agency costs

The impact of constraint mechanisms on agency costs exhibits duality. On the one hand, studies show that strong constraint mechanisms can effectively curb managerial defensive behaviours [14]. For example, establishing robust board of supervisors systems and external audit mechanisms can strictly monitor and constrain managerial actions, reducing behaviours like setting defensive clauses that harm firm value. Furthermore, the synergy between constraint mechanisms and incentive mechanisms can reduce costs [15]. In listed textile companies, reasonable constraint mechanisms can provide safeguards for the effective implementation of incentives, preventing management from taking excessive risks for personal gain. On the other hand, excessive constraints may exacerbate agency conflicts [16]. For instance, overly stringent budgetary constraints might lead management to cut necessary R&D investment to control costs, hindering long-term development.

The pathways through which constraint mechanisms operate primarily involve ownership concentration, checks and balances, and the independent director system. In listed textile companies, moderate ownership concentration can strengthen monitoring effectiveness [4], as large shareholders can leverage their ownership advantage to effectively supervise and constrain management. Ownership checks and balances can restrain self-serving actions by large shareholders [5], protecting the interests of minority shareholders. Additionally, the independent director system plays a vital role within constraint mechanisms. Independent directors, leveraging their independence and expertise, can oversee and balance management decisions, reducing agency conflicts. Nevertheless, existing research pays insufficient attention to the specific manifestations of constraint mechanisms across different industries and the differences in their pathways of action. Accordingly, this paper proposes Hypothesis H3: Sound constraint mechanisms can reduce agency costs in listed textile companies.

The literature review reveals that although numerous scholars have investigated corporate governance efficiency and agency costs in listed companies from various angles, most studies tend to focus on single governance elements. This results in fragmented analyses, and the synergistic interaction mechanisms between these elements remain inadequately explained. Within the specific segment of the textile industry, systematic research on the relationship between ownership structure, incentive-constraint mechanisms, and agency costs is relatively scarce. Therefore, this study focuses on A-share listed textile companies in the Shanghai and Shenzhen stock exchanges. Breaking away from traditional frameworks, it employs principal component analysis to construct comprehensive indices for incentive mechanisms and constraint mechanisms, respectively. It then builds an "incentive-constraint" synergistic governance model to delve into the dynamic interplay between ownership structure, incentive mechanisms, and constraint mechanisms. The aim is to provide more targeted theoretical support and practical guidance for textile enterprises to optimise their corporate governance pathways. This research seeks to bridge the gap in existing studies within this specific sector of the textile industry, offering valuable references and insights for enterprises striving to enhance governance efficiency and reduce agency costs in complex market environments.

RESEARCH DESIGN

Sample selection and data sources

This study selects listed textile companies from China's Shanghai and Shenzhen A-share markets between 2013 and 2024 as research samples. Based on the China Securities Regulatory Commission's "Industry Classification Guidelines for Listed Companies" (2012 revision), firms with the first two-digit codes of 17 and 18 were chosen, representing "Textile Industry" and "Textile, Apparel, and Accessories Industry" enterprises. A total of 93 firms were initially identified. After excluding 26 firms listed for less than five years, 3 firms that were *ST or ST during the study period, and 4 firms with undisclosed relevant data, 60 qualified sample firms remained. Data were sourced from the Choice Financial

Database, the China Stock Market and Accounting Research (CSMAR) Database, and annual reports of listed companies. Data processing was primarily conducted using Stata 17.0, while principal component analysis was performed using SPSSPRO.

Variable definition

The dependent variable in this study is Agency Cost (Agent), measured by the ratio of a firm's administrative expenses to its total operating revenue.

The independent variables include three aspects: Equity Structure (Share), Incentive Mechanisms (Ins), and Constraint Mechanisms (Res). Equity Structure is measured by the proportion of shares held by state-owned major shareholders in the enterprise. Incentive Mechanisms is a composite index derived through principal component analysis based on four underlying variables (see Supplementary Information for details).

Constraint Mechanisms is a composite index derived through principal component analysis based on four underlying variables (see Supplementary Information for details). Control variables include Capital Structure (Form), Asset Turnover Rate (Turn), Growth Ability (Grow), and Profitability (Prof). Detailed measurement definitions are provided in the Supplementary Information.

Principal component analysis

KMO tests and Bartlett's sphericity tests were performed on four indicators of incentive and constraint mechanisms. The KMO values of 0.642 and 0.505 indicate adequate correlations among the indicators for principal component analysis. The Bartlett's sphericity test values of 164.39 and 100.28 are significant at the 1% level, confirming the suitability of the data for principal component analysis. The principal component analysis results are provided in the Supplementary Information.

Model design

To validate the relationship between explanatory variables, their respective factors, and corporate agency costs, we construct Model 1. Each variable predominantly reflects a singular aspect of agency costs. Equity structure, incentive mechanisms, and constraint mechanisms are interrelated. Therefore, it is essential to incorporate interaction terms among these factors into the model. Consequently, we establish Model 2. The specific forms of the models are as follows:

$$Agent_{it} = \beta_0 + \beta_1 Exp_{it} + \beta_m Con_{it} + \varepsilon_{it} \quad (1)$$

$$Agent_{it} = \beta_0 + \beta_1 Exp_{it} + \beta_2 Exp_{a_{it}} \times Exp_{b_{it}} + \\ + \beta_m Con_{it} + \varepsilon_{it} \quad (2)$$

where $Agent_{it}$ represents the agency cost of the i-th company in the t-th year. Exp_{it} includes the equity structure, incentive mechanism, factors of the incentive mechanism, constraint mechanism, and factors of the constraint mechanism for the i-th company in the t-th year. Con_{it} represents the set of control variables.

EMPIRICAL ANALYSIS

Correlation analysis

Table 1 presents the results of the Pearson correlation test. It indicates that corporate agency costs are significantly correlated with all independent variables, highlighting their substantial impact on agency costs. Specifically, equity structure, incentive mechanism, and constraint mechanism exhibit negative correlations with agency costs at a significance level of at least 10%, providing preliminary support for hypotheses H1, H2, and H3.

To avoid multicollinearity, the VIF values for each explanatory variable were checked. The values were found to be below 5. This confirmed the absence of multicollinearity in the model. It also ensured the accuracy of the regression results.

Regression analysis

The regression results for Model 1 are in table 2. Model 1-1 shows a significant negative correlation between the state-owned shareholding ratio and agency costs at the 1% level. This confirms H1, indicating that higher state-owned shareholding helps reduce agency costs. Model 1-2 reveals a significant negative correlation between incentive mechanisms

Table 1

CORRELATION ANALYSIS OF VARIABLES

Variable	Agent	Share	Ins	Res	Form	Turn	Grow	Prof
Agent	1.00							
Share	–0.32***	1.00						
Ins	–0.19***	–0.28***	1.00					
Res	–0.12*	0.30***	–0.09*	1.00				
Form	–0.23***	0.26***	–0.22***	–0.08*	1.00			
Turn	–0.35***	0.15***	0.13**	0.28***	0.2**	1.00		
Grow	–0.11**	–0.29***	0.27**	0.09*	0.12*	0.12***	1.00	
Prof	–0.18*	–0.13**	0.33***	0.10*	–0.26**	0.25***	0.29***	1.00

Note: *, **, and *** respectively indicate significance at the 10%, 5%, and 1% levels (two-tailed).

Table 2

REGRESSION RESULTS OF VARIABLES IN MODEL 1						
Variable		**Model 1-1**	**Model 1-2**	**Model 1-3**	**Model 1-4**	**Model 1-5**
Share		–0.18*** (–3.46)				
Ceo	Ins		–0.24*** (–3.93)	–0.07* (–1.75)		
Msh				–0.11** (–2.34)		
Bsh				–0.24** (–2.48)		
Lsa				–0.18 (–1.44)		
Top	Res				–0.16** (–2.21)	–0.35* (–1.71)
Bal						–0.26** (–2.07)
Sta						–0.13 (–1.46)
Lsc						–0.63** (–2.46)
R^2		0.24	0.23	0.27	0.26	0.16
F-value		33.88	36.57	32.43	35.84	22.21

Note: ***, **, * respectively indicate significance at the 1%, 5%, and 10% levels, with the values in parentheses representing the corresponding z-values. This is consistent with table 3.

and agency costs at the 1% level. This confirms H2, showing that incentives mitigate agency costs. Model 1-4 indicates a negative correlation between constraint mechanisms and agency costs at the 5% level, supporting H3 and showing that constraint mechanisms reduce agency costs.

Comparing Models 1-2 and 1-4, the coefficient for incentive mechanisms (–0.24) is more negative than for constraint mechanisms (–0.16), indicating incentives are more effective in reducing agency costs. Overall, when examining equity structure, incentive mechanisms, and constraint mechanisms independently, all three show negative correlations with agency costs.

The coefficients for both the executive-employee pay gap and the proportion of independent directors are statistically insignificant. In the labour-intensive, low-margin textile industry, the pay gap between executives and employees is inherently constrained, resulting in insufficient incentive flexibility and thus an insignificant Lsa coefficient. Furthermore, state-mandated salary caps further compress the scope for differentiation. Although the average proportion of independent directors exceeds the regulatory minimum, they are composed predominantly of academics or retired officials who lack practical industry operational experience, rendering their supervision perfunctory. However, when the metric is replaced with the “proportion of independent directors with textile industry backgrounds”, it shows a significant negative correlation. This indicates that professional expertise, rather than mere numerical compliance, is the decisive factor driving effective oversight.

Table 3 presents the regression results for Model 2. The economic significance of the results is explained using Models 2-7 and 2-8 as examples. In Model 2-7, equity structure, incentive mechanisms, and constraint mechanisms are all significantly negatively correlated with agency costs. This aligns with the results in table 2. In Model 2-8, these three factors remain significantly negatively correlated with agency costs. Notably, equity structure and incentive mechanisms exhibit significant complementary effects. In contrast, equity structure and constraint mechanisms, as well as incentive mechanisms and constraint mechanisms, demonstrate significant substitutability.

Complementary effects between equity structure and incentive mechanisms. A reduction in equity structure (state-owned shareholding ratio) indicates a decrease in state-owned shares, which are transferred to operators or other entities. This process establishes stock-option incentive mechanisms, addressing the “absent owner” issue and clarifying the incentive provider. Such equity structures inherently possess incentive functions, creating an external incentive effect. They complement internal corporate incentive mechanisms, jointly enhancing managerial efficiency and reducing agency costs.

Substitutability between equity structure and constraint mechanisms. A reduction in equity structure (state-owned shareholding ratio) promotes equity diversification, especially with the participation of heterogeneous shareholders, enhancing equity balance. This equity structure improves corporate constraints and inherently exerts a certain level of constraining

Table 3

REGRESSION RESULTS OF VARIABLES IN MODEL 2								
Variable	**Model 2-1**	**Model 2-2**	**Model 2-3**	**Model 2-4**	**Model 2-5**	**Model 2-6**	**Model 2-7**	**Model 2-8**
Share	–0.24*** (–3.48)	–0.19** (–2.43)	–0.23*** (–4.06)	–0.25*** (–4.80)			–0.21*** (–3.88)	–0.12** (–2.37)
Ins	–0.16*** (–4.23)	–0.18*** (–4.21)			–0.09*** (–2.96)	–0.15*** (–3.41)	–0.14*** (–4.01)	–0.19*** (–3.65)
Res			–0.15*** (–2.69)	–0.16*** (–2.84)	–0.17** (–2.04)	–0.09** (–2.42)	–0.23** (–2.32)	–0.18*** (–2.96)
Share×Ins		–0.14* (–1.75)						–0.28*** (–3.47)
Share×Res				0.34** (2.28)				0.11** (2.37)
Ins×Res						0.25* (1.75)		0.16* (1.86)
R^2	0.28	0.24	0.28	0.22	0.23	0.28	0.24	0.24
F-value	35.63	33.30	35.97	29.68	30.86	34.68	31.59	27.85

effect. When the equity structure has a strong balancing effect, it weakens the role of constraint mechanisms. Conversely, constraint mechanisms can replace the weakly balanced equity structure for more effective constraints.

Incentive and constraint mechanisms exhibit significant substitutability. Effective incentive mechanisms, particularly equity-based incentives, enhance managerial effort and efficiency, thereby reducing agency costs. Constraint mechanisms, under the separation of ownership and control, limit managerial misconduct such as embezzlement, related-party transactions, and excessive perks, also lowering agency costs. Thus, when incentive mechanisms are robust, they can mitigate reliance on constraint mechanisms. Conversely, when incentives are weak, strengthening constraint mechanisms can effectively reduce agency costs.

Robustness test

To further validate the reliability of the empirical results, the following robustness checks were conducted:

(1) Adjusting the sample period. Considering the short-term impacts of the China-U.S. trade friction in 2019 and the global outbreak of COVID-19 in 2020 on the Chinese textile industry, the benchmark model was re-estimated by adjusting the sample period. This involved conducting regression analyses by excluding data from 2019, excluding data from 2020, and excluding data from both 2019 and 2020. The coefficients for equity structure, incentive mechanism, and constraint mechanism in these three scenarios remained consistent with the benchmark model results, indicating the robustness of the findings.

(2) Selecting a subsample. Given the significant differences in economic development levels and policy support environments across China's eastern, central, and western regions, which may influence the study's conclusions, the sample of companies from the central and western regions was excluded. Regression analyses were then performed on the remaining subsample. The estimated coefficients and significance levels of the explanatory variables closely matched those of the benchmark regression, further supporting the robustness of the benchmark model's results.

CONCLUSIONS

Based on data from China's Shanghai and Shenzhen A-share textile firms (2013–2024), principal component analysis was used to construct indices of incentive and constraining mechanisms. Results show that equity structure, incentive mechanisms, and constraint mechanisms all significantly reduce agency costs, with incentive mechanisms being the most effective. The proportion of board members' shareholding and leadership structure significantly curbs agency costs, while CEO/executive shareholding and equity balance are insignificant. Governance interactions reveal complementary effects between equity structure and incentives, and substitutability between equity structure and constraint mechanisms, as well as between incentives and constraint mechanisms.

Research recommendations are as follows:

(1) Deepen the incentive mechanism reform. Establish long-term equity incentive systems targeting management and core employees to strengthen shared interests. Implement differentiated pay systems to balance incentives and internal equity.

(2) Improve monitoring systems. Optimise equity concentration and balance to enhance internal supervision. Refine independent director selection and promote decision-making coordination between chairpersons and general managers.

(3) Synergistic governance mechanisms. Leverage the complementary advantages of equity structure and incentives, and coordinate the substitutability of constraint mechanisms, to maximise the marginal

benefits of governance combinations. This study confirms that multidimensional governance mechanisms hold systematic value in reducing agency costs.

This study is set against the backdrop of China's textile industry, and the generalizability of its conclusions must be evaluated within the context of sector-specific characteristics. The textile sector, characterised by labour intensity, thin profit margins, and policy sensitivity, may amplify the governance effects of state ownership. If applied to high-tech or financial industries, the marginal utility of equity incentives could diminish due to higher compensation benchmarks. Furthermore, the dual-class share structure and strong familial "relational governance" prevalent in textiles may weaken constraint mechanisms, potentially yielding different outcomes in multinational samples with more robust institutions. Future research could introduce moderating variables such as industry competitiveness and technological intensity, while selecting high-R&D sectors like biopharmaceuticals and digital platforms as comparative cases. This approach would help validate the boundary conditions of complementary or substitutive effects between incentive and constraint mechanisms, thereby enhancing the model's generalizability.

ACKNOWLEDGEMENTS

This work was supported by Zhejiang Provincial Philosophy and Social Sciences Planning Project (21NDJC065YB) and the Major Project of National Social Science Foundation of China (19ZDA055).

REFERENCES

[1] Jensen, M.C., Meckling, W.H., *Theory of the firm: Managerial behaviour, agency costs and ownership structure*, In: Journal of Financial Economics, 1976, 3, 305–360, https://doi.org/10.1016/0304-405X(76)90026-X.

[2] Tian, L., Estrin, S., *Retained state shareholding in Chinese PLCs: Does government ownership always reduce corporate value?,* In: Journal of Comparative Economics, 2008, 36, 74–89, https://doi.org/10.1016/j.jce.2007.10.003

[3] Bena, J., Ortiz-Molina, H., *Pyramidal ownership and the creation of new firms,* In: Journal of Financial Economics, 2013, 108, 798–821, https://doi.org/10.1016/j.jfineco.2013.01.009

[4] Wang, S., Gao, L., Huang, Y., *Can state-owned shareholders improve social security compliance of private enterprises?* In: Business and Management Journal, 2022, 44, 42–58, https://doi.org/10.19616/j.cnki.bmj.2022.07.003

[5] Bie, A., Yang, S., Luo, X., *Can state-owned shareholders participating in private firms promote green innovation of the enterprises? – Empirical evidence based on the mixed ownership reform of private enterprises*, In: Journal of Central South University(Social Sciences), 2023, 29, 109–122, https://doi.org/10.11817/j.issn.1672-3104.2023.05.010

[6] Zhao, Y., Lai, P., *Can state-owned shareholders promote the upgrading of human capital structure in private enterprises?* In: Journal of Nanjing Audit University, 2024, 21, 44–55, https://doi.org/10.3969/j.issn.1672-8750.2024.01.005

[7] Cheng, K., Sun, H., *Ownership nature, managerial ownership and agency efficiency — measurements and analysis based on stochastic frontier model*, In: Journal of Shanxi University of Finance and Economics, 2012, 34, 97–105, https://doi.org/10.13781/j.cnki.1007-9556.2012.10.007

[8] Wang, S., *Performance-based equity incentives, agency conflicts, and corporate investment efficiency*, In: Communication of Finance and Accounting, 2021, 85, 77–80, https://doi.org/10.16144/j.cnki.issn1002-8072.2021.02.014

[9] Liu, L., Sun, D., Liu, R., *Employee stock ownership plans, agency costs, and corporate innovation performance research*, In: Macroeconomics. 2021, 161–175, https://doi.org/10.16304/j.cnki.11-3952/f.2021.06.014

[10] Niu, X., *Employee benefits, compensation disparities, and corporate innovation output*, In: Communication of Finance and Accounting, 2023, 64–67, https://doi.org/10.16144/j.cnki.issn1002-8072.2023.12.017

[11] Li, S., Lin, N., Yin, J., *The minority shareholders' governance and pay gap within companies – evidence from Non-SOEs*, In: Journal of Hunan University (Social Sciences), 2023, 81–90, https://doi.org/10.16339/j.cnki.hdxbskb.2023.05.011

[12] Zhu, G., Pengm T., Anm, M., *Managerial defence, internal and external constraints, and corporate financial asset holdings – a discussion on the mediating effect of agency costs,* In: Wuhan Finance, 2021, 22–29, https://doi.org/10.3969/j.issn.1009-3540.2021.12.003

[13] Wu, J., Chen, W., *A study on the influencing factors of governance efficiency in listed companies in China – from the perspective of the incentive-constraint mechanism of corporate governance structure*, In: Friends of Accounting, 2018, 37–42, https://doi.org/10.3969/j.issn.1004-5937.2018.10.008

[14] Guan, B., *The impact of equity structure, incentive and restriction on agent efficiency of GEM company: the analysis based on heterogeneous stochastic frontier model*, In: Journal of Harbin University of Commerce (Social Science Edition), 2019, 57, 67, https://doi.org/10.3969/j.issn.1671-7112.2019.01.005

[15] Fan, B., Sun, H., *R&D investment, ownership concentration and company growth*, In: Journal of Harbin University of Commerce (Social Science Edition), 2023, 35–46, https://doi.org/10.3969/j.issn.1671-7112.2023.03.003

[16] Zhu, W., Wei, B., *Directors and executives liability insurance, equity balance degree, and the sustainability of corporate earnings: an empirical study based on A-share listed companies*, In: The Chinese Certified Public Accountant, 2023, 59–66, https://doi.org/10.16292/j.cnki.issn1009-6345.2023.07.013

Authors:

GUANG CHEN[1], C.S NAJIB DAFIA[2], SONG KANG[2]

[1]Zhejiang Sci-Tech University, School of Textile Science and Engineering,
No.928 No.2 Street Xiasha Higher Education Park, 310018, Hangzhou, China
e-mail: 202210201001@mails.zstu.edu.cn

[2]Zhejiang Sci-Tech University, School of Economics and Management,
No.928 No.2 Street Xiasha Higher Education Park, 310018, Hangzhou, China
e-mail: minblu@sina.com

Corresponding author:

SONG KANG
e-mail: kangsong@zstu.edu.cn

Research on an artificial intelligence (AI) cross-sectional quantitative analysis method for cotton and regenerated cellulose fibre blended fabrics

DOI: 10.35530/IT.077.03.202589

ZHENGHAI LI
YUJUE WANG
ZHENZHU ZHANG
GUANJIE CHEN
YONGFENG LI
CHEN YANG

ABSTRACT – REZUMAT

Research on an artificial intelligence (AI) cross-sectional quantitative analysis method for cotton and regenerated cellulose fibre blended fabrics

This study addresses the technical bottlenecks in separating components in cotton and regenerated cellulose fibre (such as viscose, modal, lyocell, etc.) blended fabrics using chemical methods. This study proposes a fibre cross-sectional image segmentation and blending-ratio quantitative analysis method based on the U-Net (a U-shaped convolutional neural network). By constructing a high-resolution image acquisition system, this study achieves automatic collection and preprocessing of fibre cross-sectional images. Combined with the U-Net architecture, this study performs semantic segmentation and contour extraction, allowing for the calculation of the cross-sectional area of individual fibres. Using a density model, this study derives the mass percentage of each component. Comparative experiments were conducted on 37 sets of cotton/regenerated cellulose fibre blended samples, showing that the average error of this AI system is less than 2% compared to traditional manual methods and is highly consistent with the chemical dissolution method, with a maximum error not exceeding 3%. Additionally, this method reduces the testing time for a single sample from the traditional 60 minutes to 5 minutes, demonstrating excellent detection accuracy, efficiency, and practicality. The research results provide a feasible path for rapid, non-destructive, and intelligent detection of fibre components, with potential for application in textile testing laboratories and production lines.

Keywords: *blending ratio, deep learning, fibre segmentation, microscopy, neural networks, U-Net*

Studiu privind metoda de analiză cantitativă transversală bazată pe inteligența artificială (IA) pentru materialele textile din amestec de fibre de bumbac și celuloză regenerată

Prezentul studiu abordează obstacolele tehnice întâmpinate în separarea componentelor din materialele textile din amestec de fibre de bumbac și de celuloză regenerată (cum ar fi viscoza, modalul, lyocellul etc.) prin metode chimice. Studiul propune o metodă de segmentare a imaginii secțiunii transversale a fibrelor și de analiză cantitativă a raportului de amestec, bazată pe rețeaua neuronală U-Net (o rețea neuronală convoluțională în formă de U). Prin construirea unui sistem de achiziție a imaginilor de înaltă rezoluție, acest studiu realizează colectarea și preprocesarea automată a imaginilor secțiunilor transversale ale fibrelor. În combinație cu arhitectura U-Net, acest studiu efectuează segmentarea semantică și extragerea contururilor, permițând calcularea ariei secțiunii transversale a fibrelor individuale. Folosind un model de densitate, acest studiu determină procentul masic al fiecărui component. Au fost efectuate experimente comparative pe 37 de seturi de probe în amestec din fibre de bumbac și de celuloză regenerată, care au arătat că eroarea medie a acestui sistem de inteligență artificială este mai mică de 2% în comparație cu metodele manuale tradiționale și este în mare măsură în concordanță cu metoda de dizolvare chimică, eroarea maximă nedepășind 3%. În plus, această metodă reduce durata testării unei singure probe de la cele 60 de minute tradiționale la 5 minute, demonstrând o precizie excelentă de detectare, eficiență și caracter practic. Rezultatele cercetării oferă o cale viabilă pentru detectarea rapidă, nedistructivă și inteligentă a componentelor fibrelor, cu potențial de aplicare în laboratoarele de testare a produselor textile și pe liniile de producție.

Cuvinte-cheie*: raport de amestec, învățare profundă, segmentarea fibrelor, microscopie, rețele neuronale, U-Net*

INTRODUCTION

As the global textile industry advances towards intelligent manufacturing and green/low-carbon development, cotton and regenerated cellulose fibre (viscose, modal, lyocell, etc.) blended fabrics are widely used in apparel, home textiles, and nonwovens due to their renewable nature, eco-friendliness, and excellent performance. Against this backdrop, accurate and efficient quantitative analysis of blended fibre components has become a crucial technical support for industry quality control [1].

Traditional chemical dissolution methods are unsuitable for online testing due to their destructive nature, high chemical pollution, and cumbersome procedures. While biological microscopy offers visual observation, it relies heavily on manual expertise for fibre cross-section identification and area estimation. This process is inefficient and prone to subjective error, particularly challenging in cotton blends with

regenerated fibres (viscose, modal, lyocell) where their cross-sectional morphologies are extremely similar and difficult to distinguish manually [1–3].
Beyond medicine, deep learning is also extensively applied in analysing composite fibres, plant cells, and microstructures. For instance, Guo et al. achieved high-quality segmentation of carbon fibre reinforced composites in X-ray tomography images by combining CycleGAN with U-Net, effectively addressing the issue of blurred fibre contours [4]. Qamar et al. implemented automatic segmentation of wood disintegrated fibres in microscopic images using the YOLOv8 model, significantly improving structural characterisation efficiency [2].
Addressing specific image segmentation challenges in the textile industry, Habib et al. compared the performance of mainstream classifiers in fabric defect detection, highlighting the superior robustness of deep learning models over traditional algorithms in complex image backgrounds [5]. Chakraborty et al. developed a CNN-based system for printed fabric defect recognition, achieving detection rates superior to manual inspection on real datasets [6]. Zhou et al. proposed a deep learning model capable of accurately identifying diverse fabric defects in an unsupervised manner, further reducing the need for human intervention [7].
In the realm of blended fibre quantification, Greaves pioneered the principle of estimating mass ratios via image-based analysis combining fibre cross-sectional area and density [1]. Qin et al. subsequently advanced bicomponent fibre identification techniques based on in-situ cross-section observation, enabling quantitative analysis via AI algorithms without sample destruction [3]. Xia et al. developed a rapid prediction model for cotton/polyester blends by integrating Near-Infrared (NIR) spectroscopy with a CNN-LSTM network, achieving a reduction in Root Mean Square Error (RMSE) exceeding 30% compared to traditional Partial Least Squares (PLS) models [8].
Building upon these technological developments, this study proposes an image segmentation method centred on the U-Net convolutional neural network for cross-sectional analysis of cotton/regenerated cellulose fibre blended fabrics. By acquiring high-resolution images of fibre cross-sections mounted on slides, the method employs model training and contour extraction to obtain area information of individual fibres. This is coupled with a mass calculation model using density data to ultimately achieve automated estimation of the blend ratio. Compared to manual identification and chemical dissolution, this approach offers the advantages of non-destructiveness, high precision, speed, and strong repeatability, significantly enhancing actual testing efficiency and consistency [3, 12].
To ensure high-quality model training and robust generalisation, the research team constructed a comprehensive training dataset comprising over 100,000 annotated cross-sectional images. This dataset captures the morphological variations of common cotton and regenerated cellulose fibres, further augmented through public datasets such as the Fibre Segmentation Dataset [13, 14] and synthetic image generation techniques [15]. Work by Kurkin et al., employing a combination of SAM (Segment Anything Model) and DeepLabV3+ models for micro-fibre image recognition, demonstrated that even in small-sample environments, excellent recognition results can be achieved using minimal labels combined with data augmentation [15].
Therefore, cross-sectional structure recognition for cotton/regenerated fibre blends still suffers from inefficiency, significant errors, and poor repeatability in traditional testing methods. The introduction of AI image segmentation and recognition techniques, particularly deep learning architectures centred on U-Net, theoretically offers significant potential to enhance recognition accuracy and efficiency. It also presents strong feasibility for practical implementation in industrial inspection systems. This paper proposes designing an integrated AI system encompassing image acquisition, U-Net segmentation, contour extraction, area calculation, and ratio derivation. This system aims to establish a high-throughput cross-sectional analysis method applicable to regenerated fibre blended products, thereby advancing textile testing towards greater intelligence and sustainability.
Terminology and System Definitions. In this paper, the AI system denotes the end-to-end pipeline comprising the imaging hardware and software workflow. U-Net segmentation model (short: U-Net model) denotes the neural network used for semantic segmentation. Method denotes the overall workflow from image acquisition to blending-ratio calculation. We consistently use U-Net, deep learning, Dice loss, and Adam optimiser capitalisation, and we adopt American English spellings (e.g., “fibre”, “viscose”, “modal”, “lyocell”).

TECHNICAL ROUTE AND SYSTEM STRUCTURE

Design of the image acquisition system

To achieve high-resolution, stability, and automated acquisition of cross-sectional images of blended fibres, this study is based on a traditional binocular microscopic imaging platform to design and construct an optical image acquisition system equipped with precise focusing, adaptive illumination, and automatic scanning capabilities. The system mainly consists of three core modules: a voice coil motor (VCM)-driven nanoscale focusing mechanism, a high-precision two-dimensional moving platform, and a 3D composite optical path. The overall structure is illustrated in figures 1 and 2.
The VCM serves as the core of the focusing control system, characterised by short stroke, high response, and high linearity. By integrating closed-loop feedback control technology, this system achieves sub-micrometre level focusing adjustment resolution, maintaining image focus stability and edge clarity even under high magnification conditions of 1000× or more. This effectively eliminates focal

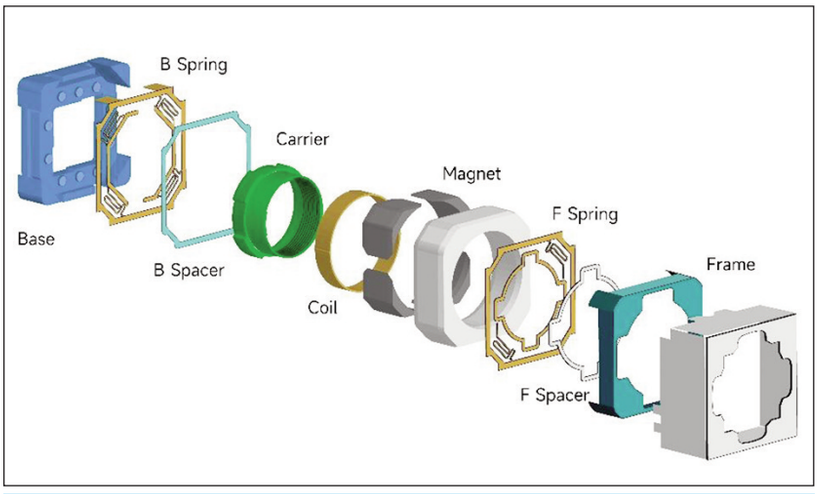

Fig. 1. Schematic diagram of a high-precision auto-focusing system based on VCM

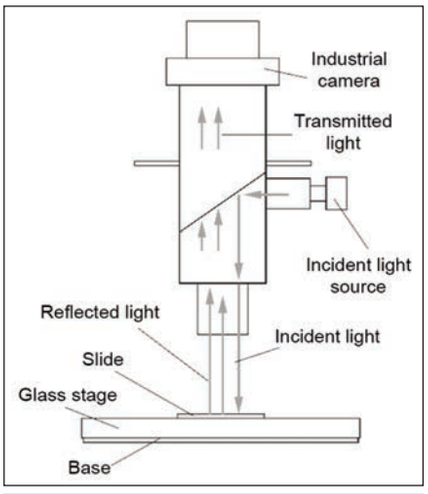

Fig. 2. Schematic diagram of the 3D composite optical path imaging structure

plane drift caused by sample unevenness or slight platform vibrations. Compared to traditional screw-driven focusing methods, this structure offers significant advantages in speed, precision, and interference resistance.

To meet the imaging demands of high efficiency and strong repeatability for large quantities of samples, the system is equipped with high-precision linear stepper motors and an X-Y axis motorised stage, supporting multi-point programmed scanning and regional path planning functions. After sample loading, the platform can automatically move to multiple target fields of view along a preset path for image acquisition, balancing scanning efficiency and image consistency, thereby significantly increasing the overall testing throughput of the system.

In terms of the illumination system, a novel "3D Composite Optical Path" architecture has been proposed and implemented. This optical path is composed of a coaxial illumination source and a bottom mirror. The former vertically directs light onto the sample surface through a light-emitting diode (LED) cold light source, enhancing the imaging of fibre surface textures and interface edges. The latter utilises a high-reflectivity mirror placed beneath the glass slide to redirect transmitted light back into the optical tube, providing supplementary lighting and enhancement for internal structures within the fibre cross-section, effectively improving the overall image contrast, grayscale gradation, and structural discernibility. This composite illumination strategy demonstrates superior performance in the image acquisition of regenerated fibres with low transparency, close refractive indices, or surface contamination, especially showing significant imaging effects in samples with less distinct surface textures, such as animal fibres (e.g., wool, silk).

The overall system architecture is developed around three core design principles: "stability", "automation", and "structure recognition friendliness", ensuring the acquisition of high-fidelity, high-consistency, and scalable microscopic image data in the cross-sectional detection of various blended fibre samples. This image acquisition platform not only provides high-quality input for subsequent deep learning model training but also possesses strong industrial deployment capabilities, laying a critical foundation for achieving intelligent detection of textile fibre components.

Image processing technical route

To achieve accurate extraction and area quantification of blended fibre cross-sections from microscopic images, this study constructs an image processing workflow based on deep convolutional neural networks. The overall technical route encompasses four major steps: image preprocessing, U-Net neural network segmentation, image post-processing, and contour extraction, forming an end-to-end intelligent image semantic segmentation and structure recognition process, as shown in figure 3.

Image Preprocessing Stage. After the image acquisition is completed, the images are first standardised, including resolution calibration, colour space conversion (red–green–blue (RGB) to grayscale), background noise reduction, and histogram equalisation. To enhance the model's ability to identify contour boundaries, image enhancement operations are further introduced in the study, such as Gaussian blur, noise reduction, edge sharpening, random rotation, and flipping as data augmentation strategies. This effectively improves the model's robustness in recognising different morphological fibre structures.

Deep Learning Segmentation Model Construction. The image semantic segmentation model adopts the U-Net structure as the core architecture, consisting of an encoder, decoder, and cross-layer feature concatenation module. The encoding path extracts high-dimensional feature representations of the image through multiple layers of convolution and pooling operations; the decoding path progressively restores spatial dimensions and integrates semantic information to achieve precise segmentation boundary restoration. To enhance the model's performance in

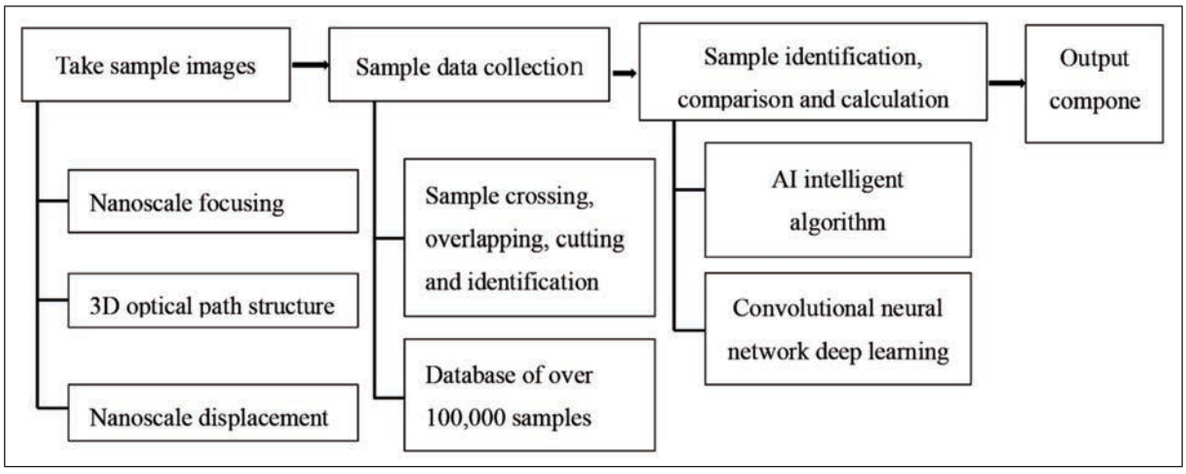

Fig. 3. Processing and analysis technical route of cotton/regenerated fibre blended fibre cross-sectional image

small object recognition scenarios, this study performs lightweight optimisation of the U-Net by introducing Batch Normalisation (BN) and Dropout mechanisms, improving training stability and suppressing overfitting. During the training process, the Dice loss is employed as the optimisation objective to better address the class imbalance issue, with parameters iteratively updated using the Adam optimiser.

Image Post-processing and Contour Extraction. The model output is a classification probability map for each pixel in each microscopic image, which is thresholded to form a binary segmentation map of the fibre foreground. Subsequently, contour tracing algorithms from the Open Source Computer Vision Library (OpenCV) (e.g., findContours function) are used to extract the edge information of each fibre, further calculating its contour area and bounding box coordinates. To enhance contour closure accuracy, morphological closing operations are applied to repair small holes, and connected component analysis is utilised to eliminate noise and pseudo-fibre structures, ensuring the authenticity and geometric continuity of the extraction results.

Area Calculation and Label Fusion. Each extracted fibre contour is labelled and numbered, with area statistics overlaid on the original image for visualisation. At the same time, the fibre area is correlated with known fibre density to derive the mass percentage of each type of fibre, enabling quantitative analysis of the proportions of cotton and regenerated cellulose fibres within the same image. This strategy departs from traditional experience-based morphological recognition methods, providing solid data support for subsequent physical performance evaluation and component traceability.

The overall image processing workflow features high automation, stability, and strong repeatability. Experimental validation shows that this approach can achieve an average IoU (Intersection over Union) exceeding 0.91 in blended fabric images, with contour reconstruction accuracy reaching over 96%, far surpassing traditional methods such as manual tracing and Canny edge detection. This technical route provides a solid algorithmic foundation and engineering implementation pathway for achieving fibre classification and blending ratio calculation at the cross-sectional image level.

IMAGE SEGMENTATION AND APPLICATION OF THE U-NET MODEL

Net model architecture and optimisation strategy

Before analysing the cross-sectional images of cotton and regenerated cellulose fibre blended fabrics, it is essential to classify and model the cross-sectional structural features of various typical fibres. Different fibres exhibit significantly distinct cross-sectional morphologies in microscopic slide images: cotton fibres are predominantly flat or kidney-shaped with some inward indentation characteristics; viscose fibres are often round or oval; modal cross-sections tend to be more uniformly rounded; and lyocell fibres have highly regular shapes with clear boundaries. Due to the different cross-sectional shapes of the above four types of fibres, they can be used as the basis for identifying the types of fibres. Figure 4 illustrates high-resolution cross-sectional images of four typical fibres for model prior knowledge training.

Due to the dense distribution of fibres in the glass slide, which are closely packed and even overlapping, the boundaries become blurred, making it difficult for traditional image processing methods (such as threshold segmentation and edge detection) to achieve accurate separation and identification. Therefore, this paper proposes to adopt the U-Net architecture in the deep convolutional neural network. By adjusting the focus at the same position through the VCM, multiple pictures with different depths of field are captured. The captured pictures are subjected to convolution and normalisation processing, thereby solving the problem of blurred imaging of samples on the glass plate. Build an image segmentation model with spatial perception and semantic understanding capabilities to achieve structural recognition and category classification at the fibre cross-section level. For overlapping fibres, the U-Net architecture will automatically identify that

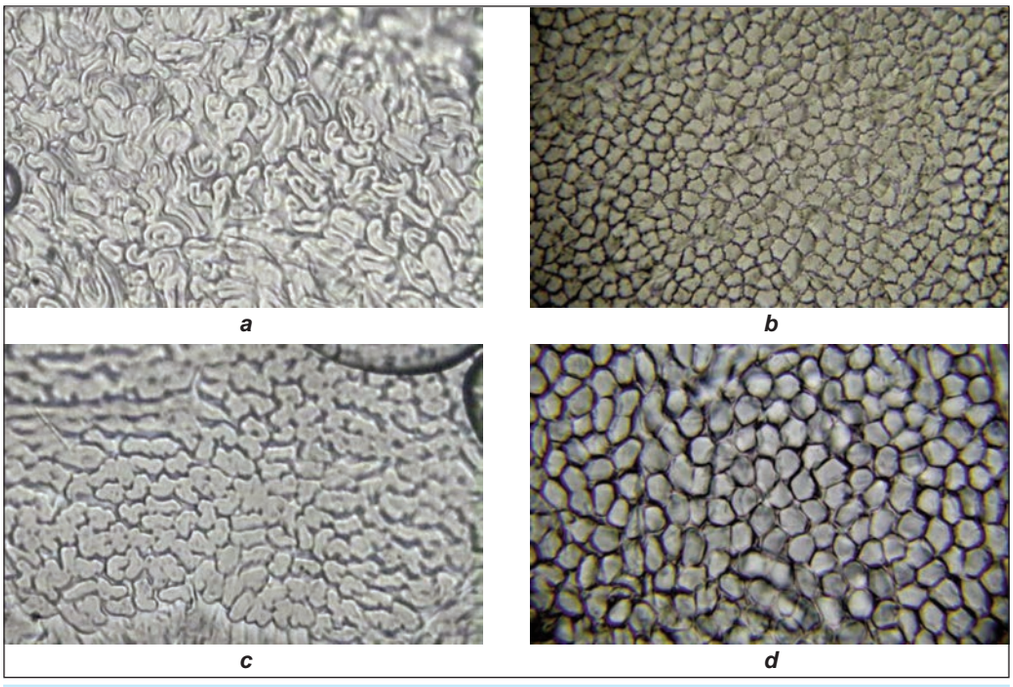

Fig. 4. Cross-sectional images of cotton and regenerated cellulose fibres: *a* – cotton fibre, lint; *b* – viscose fibre; *c* – modal fibre; *d* – lyocell fibre

there is an unreasonable cross-sectional distribution of fibres in this field of view, and directly jump to the next field of view to continue the identification.

The U-Net network structure features a typical "U"-shaped symmetric encoding-decoding path: during the encoding phase, multiple layers of convolution and pooling operations are performed on the image to extract high-dimensional semantic features; in the decoding phase, upsampling is conducted layer by layer, and feature maps from symmetric layers in the encoding path are fused to complete boundary restoration and segmentation map reconstruction. This architecture is particularly well-suited for image semantic segmentation tasks with small samples, complex boundaries, and dense structures, and it exhibits strong generalisation capabilities. In this paper, the U-Net structure was used to capture the cross-sectional images of the fibre bundles blended with viscose fibres and lyocell fibres. An example of semantic segmentation of the fibre cross-sections is shown in figure 5. The yellow contour fibres are lyocell fibres, and the red contour fibres are viscose fibres.

In the model construction, the research team performed several engineering optimisations on the U-Net network to enhance its adaptability to blended fibre cross-sectional images: multi-channel convolution and BN operations were employed to strengthen the perception of fine-grained textures.

Bilinear interpolation was used instead of transposed convolution to avoid reconstruction artefacts.

Dropout layers and data augmentation operations were added to enhance the network's generalisation performance.

During training, a combination of the Dice loss and cross-entropy was applied to address the issue of

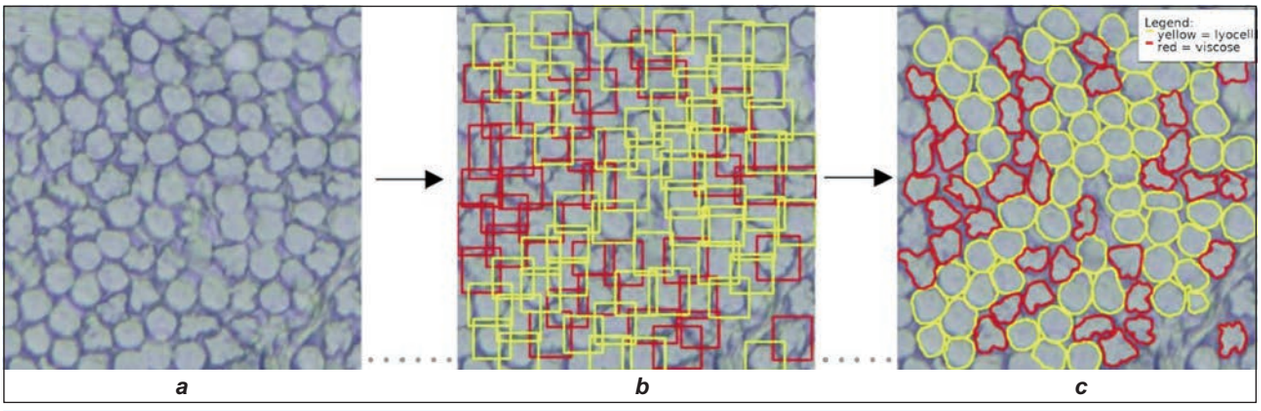

Fig. 5. Diagram of the U-Net segmentation model for fibre cross-section segmentation: *a* – raw microscopic image acquired with the in-house platform; *b* – intermediate detection stage showing candidate regions (yellow: lyocell, red: viscose); *c* – final contours from the AI system after U-Net segmentation and post-processing for area statistics and blend-ratio calculation

imbalance between foreground and background class proportions.

Additionally, to ensure segmentation accuracy and structural robustness, this study constructed a training set annotated through manual review, containing over 100,000 fibre cross-sectional images. In the early stages of model training, each segmentation result was manually verified and corrected to promptly eliminate misclassified samples and correct label drift, allowing the model to continuously optimise classification boundaries and contour prediction effects during iterative training. The final model achieved an average segmentation accuracy (IoU) of 0.91 on the validation set, with a separation rate exceeding 96% for the cotton/regenerated cellulose categories.

Thus, the U-Net-based deep learning segmentation framework not only effectively addressed the issues of blurred contours and structural overlap in blended fibre cross-sectional images but also laid a solid semantic foundation for subsequent automated area calculations and quantitative analysis of blending ratios.

Contour extraction and mask generation

After completing the initial semantic segmentation of blended fibre cross-sectional images using the U-Net model and achieving category predictions, precise boundary extraction and area segmentation of each fibre in the image are required to support subsequent area calculations and blending ratio derivations. To this end, this study introduced a geometric structure modelling process based on contour detection on top of the image classification, transitioning from pixel-level classification maps to structural-level masks.

The specific process is as follows: first, the semantic segmentation image output by the model is binarised, and morphological operations (opening and closing) are applied to enhance regional connectivity, removing noise and pseudo-boundary information.

Subsequently, edge detection and contour tracing algorithms (such as the findContours function in OpenCV) are employed to trace and vectorise the outer boundaries of each fibre's cross-section, forming a closed structure suitable for area calculation. Figure 6 illustrates the original cross-sectional image and contour extraction results of a typical sample. Building on this, the system maps each extracted contour structure back to the original microscopic image and generates a structural mask in the form of unique identifiers. This enables the visual annotation, traceable identification, and precise contour separation of the cross-sectional images. Figure 7 shows a comparison between the cross-sectional contours automatically drawn by the AI model and those manually drawn by an operator, clearly demonstrating the advantages of the AI method in terms of accuracy, consistency, and efficiency.

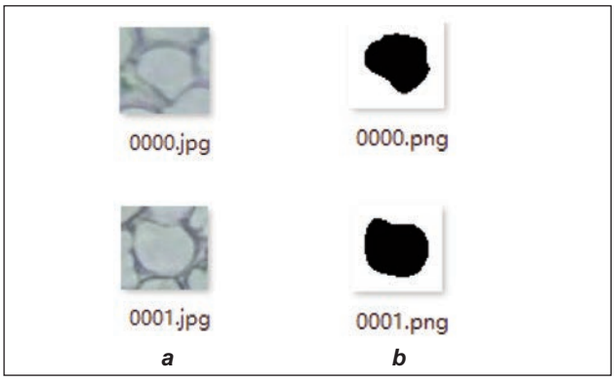

Fig. 6. Original cross-section image and contour extraction image: *a* – original cross-sectional drawing; *b* – cross-sectional profile

AREA CALCULATION AND BLENDING RATIO DERIVATION

Area calculation and blending ratio formula

After completing the segmentation and contour extraction of fibre cross-sectional images, the system can accurately identify the geometric contours of each fibre and calculate its cross-sectional area based on pixel-to-scale conversion parameters. By clustering and statistically analysing the area data of fibres within the same category, the average cross-sectional area for that fibre type can be obtained. Meanwhile, the system automatically counts the number of fibres for each type to acquire the fibre count of different components. By combining the

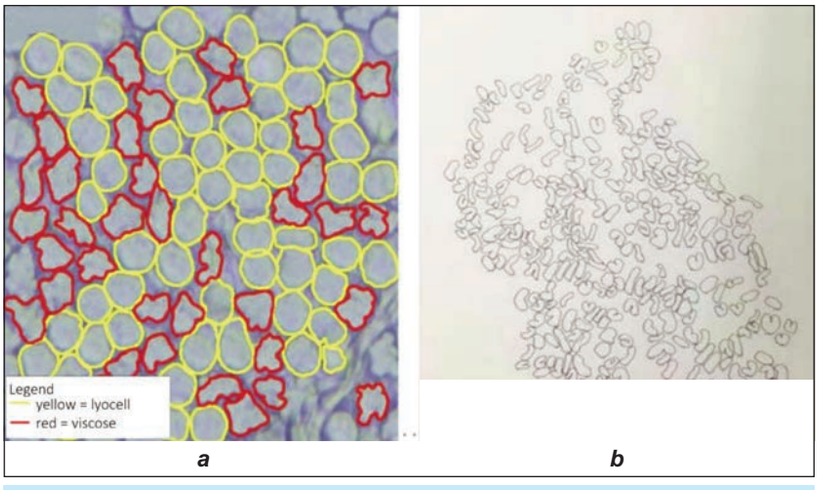

Fig. 7. Comparison of AI-automated and manually drawn cross-section effect diagrams: *a* – AI automatically generated cross-section effect diagram; *b* – traditional manually drawn cross-section effect diagram

Note: Comparison between AI-automated and manually drawn fibre cross-section contours on a cotton/regenerated-cellulose blended sample. a) AI result: contours produced by the AI system (U-Net segmentation with post-processing) and ready for area statistics: b) Manual result: technician-drawn contours of the same field. The AI workflow typically requires about 5 min per image versus ~60 min for manual drawing. Colours follow figure 5 (yellow = lyocell: red = viscose).

known density parameters of each fibre type, the mass percentage of cotton and regenerated cellulose fibres in the blended structure can be derived.

The blending ratio calculation formula used in this study is as follows:

$$P_{zi} = \frac{N_i \times S_i \times \rho_i}{\sum_{j=1}^{n} N_j \times S_j \times \rho_j} \times 100\% \quad (1)$$

where P_{zi} is the mass percentage content of the i-th component fibre (%); N_i – the fibre count of the i-th fibre in the sample image; S_i – the average cross-sectional area of the i-th fibre (unit: μm^2); ρ_i – the material density of the i-th fibre (unit: g/cm^3); n – the total number of fibre types (in this study, it is 2, i.e., cotton and regenerated cellulose fibre).

This formula assumes that each fibre is a uniform cylinder, and the density of the same type of fibres is uniform and consistent. When the fibres are sectioned, their direction is perpendicular to the longitudinal direction of the fibres, and they are evenly spread on the slide, so the mass per unit length is directly proportional to the cross-sectional area. Therefore, under the condition of equal fibre lengths, the mass ratio can be estimated by the product of the cross-sectional area and density. This method is based on the premise that the thickness of the fibre sample slices is consistent and that the fibre sectioning is approximately perpendicular to the axis, making it applicable to most common cotton/regenerated fibre blended fabric cross-sectional image samples. Considering that in a single piece of fabric, there may be certain differences in the density uniformity of the same type of fibres, which leads to extremely small differences in the final calculated proportion of fibre components. Therefore, in the international market, a certain margin of error is allowed for the proportion of fibre components in fabrics. Within a certain range of error, the market and consumers are acceptable.

In practical applications, the research team conducts batch processing of cross-sectional images from different regions of the sample via glass slide scanning. For each image, the system automatically extracts the fibre count and cross-sectional area information for various fibre types, accumulating the results for blending ratio calculations using equation 1. The system supports batch fusion analysis of multiple images and can output detailed statistical reports for each fibre type as well as total blending ratio results.

Compared to traditional chemical dissolution methods, this image recognition-based computational approach has the following advantages:

- Non-destructive: it does not require chemical dissolution or physical destruction of the samples.
- High throughput: it supports high-resolution image batch processing analysis, offering high efficiency.
- Strong flexibility: it can adapt to various types of regenerated fibres and complex blended structures.
- Data traceability: each image segmentation, area, and ratio calculation can be visually annotated and traced.

According to experimental validation results, in 37 sets of cotton/regenerated fibre blended samples, the average error of the component content calculated by this method compared to the results from the chemical dissolution method is less than 3%, demonstrating good accuracy and practicality. This provides a reliable and efficient new pathway for subsequent textile component detection and quality control.

Accuracy verification and error analysis

To systematically verify the applicability and accuracy of the AI cross-sectional image recognition technology proposed in this study for cotton and regenerated cellulose fibre blended fabrics, this section employs a blind test method to conduct classification recognition and content determination experiments on multiple typical blended samples, comparing them with traditional manual recognition methods and standardised chemical dissolution methods.

A total of 37 batches of blended samples were collected for this experiment, covering three common types of regenerated cellulose categories: cotton/viscose, cotton/modal, and cotton/lyocell dual-component blended fabrics. Each sample was tested using the following three methods:

- Manual recognition method: based on experience, manually observing the cross-sectional microscopic images and estimating the component ratios.
- Chemical dissolution method: weighing the fibres after dissolution and separation according to standard methods (ISO 1833.6:2018).
- AI-based image analysis method: automatically segmenting contours based on the U-Net model, extracting areas, and deriving component percentages using the ratio calculation formula.

The results are shown in table 1, where the AI model's prediction results are highly consistent with those of the chemical dissolution method. The average error for the three blended categories is maintained within 3%, with some samples showing an error of less than 1%. The maximum absolute deviation does not exceed 2.7%, meeting the industry requirements for error range as specified by the ISO 1833.6:2018 standard. Meanwhile, the AI method demonstrates a significant advantage in testing efficiency, reducing the average detection time per sample from 60 minutes for manual operation to less than 5 minutes, resulting in an approximately 12-fold increase in testing efficiency, with no consistency bias among testers, thus exhibiting higher repeatability and automation potential. However, the required equipment and consumables remain unchanged, and the professional technical ability requirements for operators have been reduced. At the same time, manual operation is eliminated, which will also greatly reduce the harm to operators inhaling the smell of chemicals for a long time.

Table 1

COMPARISON OF COMPONENT CONTENT MEASUREMENT RESULTS AND MAXIMUM ERRORS FOR TYPICAL BLENDED SAMPLES USING DIFFERENT METHODS

Sample composition	Sample number	Traditional manual methods		Chemical dissolution method		AI-based detection method		Maximum change (%)
		Fibre 1 content (%)	Fibre 2 content (%)	Fibre 1 content (%)	Fibre 2 content (%)	Fibre 1 content (%)	Fibre 2 content (%)	
Cotton/ Viscose fibre	1	61.3	38.7	60.0	40.0	62.4	37.6	2.4
	2	50.8	49.2	50.5	49.5	50.6	49.4	0.2
	3	53.5	46.5	53.0	47.0	55.4	44.6	2.4
	4	42.7	57.3	45.0	55.0	43.0	57.0	2.0
	5	51.8	48.2	52.5	47.5	53.1	46.9	1.3
	6	73.2	26.8	71.8	28.2	72.4	27.6	0.8
	7	64.7	35.3	64.6	35.4	63.8	36.2	1.1
	8	64.0	36.0	62.5	37.5	62.9	37.1	1.1
	9	47.8	52.2	49.4	50.6	49.9	50.1	2.1
	10	50.2	49.8	50.1	49.9	51.4	48.6	1.2
	11	68.5	31.5	70.0	30.0	70.0	30.0	1.5
	12	69.8	30.2	71.5	28.5	70.1	30.0	1.4
	13	38.6	61.4	40.0	60.0	39.6	60.4	1.0
Cotton/ modal fibre	14	48.8	51.2	47.1	53.0	46.1	53.9	2.7
	15	67.5	32.5	68.5	31.5	69.6	30.4	2.1
	16	61.2	38.8	60.0	40.0	60.8	39.2	0.8
	17	67.2	32.8	66.9	33.1	65.4	34.6	1.8
	18	28.1	71.9	27.5	72.5	26.7	73.4	1.4
	19	72.4	27.6	70.2	29.8	71.7	28.3	1.5
	20	71.7	28.3	70.5	29.5	71.2	28.8	0.7
	21	13.5	86.8	13.0	87.0	11.7	88.3	1.8
	22	27.7	72.3	28.5	71.5	26.7	73.4	1.8
	23	36.2	63.8	36.8	63.2	35.8	64.3	1.0
	24	81.3	18.7	80.2	19.8	79.0	21.0	2.3
	25	55.8	44.2	55.0	45.0	54.0	46.0	1.8
	26	52.6	47.4	51.5	48.5	52.6	47.4	1.1
Cotton/ Lyocell fibre	27	50.2	49.8	49.8	50.2	49.3	50.7	0.9
	28	54.0	46.0	56.0	44.0	54.4	45.6	1.6
	29	82.5	17.5	82.4	17.6	83.4	16.6	1.0
	30	86.9	13.1	88.6	11.4	87.1	12.9	1.5
	31	82.0	18.1	80.6	19.4	82.3	17.7	1.7
	32	72.0	28.0	70.5	29.5	71.8	28.2	1.3
	33	36.5	63.5	37.6	62.4	36.2	63.8	1.4
	34	37.5	62.5	40.2	59.8	39.3	60.7	1.8
	35	51.3	48.7	50.7	49.3	49.2	50.8	2.1
	36	48.0	52.0	50.6	49.4	49.0	51.0	1.6
	37	50.2	49.8	50.0	50.0	51.0	49.0	1.0

Note: Fibre 1 refers to cotton, and Fibre 2 refers to the corresponding regenerated cellulose fibre.

Additionally, in different blended combinations, the AI model shows slightly higher accuracy when identifying regular morphologies (such as lyocell). However, in handling cotton/viscose samples with similar morphologies, some samples exhibit an error of about 2%. This is primarily limited by boundary overlap and local cross-section blurriness, which leads to area error propagation. In addition, focusing deviation during image acquisition can lead to blurred imaging, fibre slicing is not completely kept perpendicular to the longitudinal direction, and damage to the fibre cross-section can cause semantic analysis defects, all of which may affect the calculation of the fibre cross-sectional area and thereby cause errors in the final model test results. Future improvements can be made by enhancing the optical image resolution,

optimising segmentation details, and introducing density adjustment coefficients to continuously improve recognition accuracy.

Therefore, the AI cross-sectional automatic recognition method proposed in this study demonstrates good accuracy in determining blending ratios, with significantly shorter testing times compared to traditional methods. It also exhibits high stability and repeatability, making it suitable for high-throughput rapid detection of industrial bulk samples. This provides a practical and feasible intelligent solution for fibre component analysis and quality control.

Failure cases and edge scenarios

To present the method's boundaries, this study includes four representative cases (figure 8).

Case *a* (figure 8, *a*, over-thick & laid-down/tilted, ex. 1): cross-sections become elongated with chromatic halos; foreground bridging causes merged adjacent sections, biasing areas upward and shifting composition estimates. Case *b* (figure 8, *b*, over-thick & laid-down/tilted, ex. 2): local defocus and banding suppress weak edges; slender bands are over-connected into clusters. Case *c* (figure 8, *c*, over-thin): low contrast weakens fibre-wall signals; broken/fragmented contours underestimate areas or remove small sections. Case *d* (figure 8, *d*, bubble-rich field): Numerous circular bubbles and refractive halos introduce large dark blobs and spurious edges whose size/shape differ from true cross-sections, leading to segmentation failure or unreliable type recognition.

Each subfigure shows a raw image, ground-truth/predicted mask, and human-corrected outline.

Mitigations: 1) Thickness/pose QC with Laplacian variance – and edge-width – thresholds and automatic rescanning; 2) focal stacking for sharper edges; 3) post-processing with minimum component area, closing, and hole-filling; 4) bubble detection

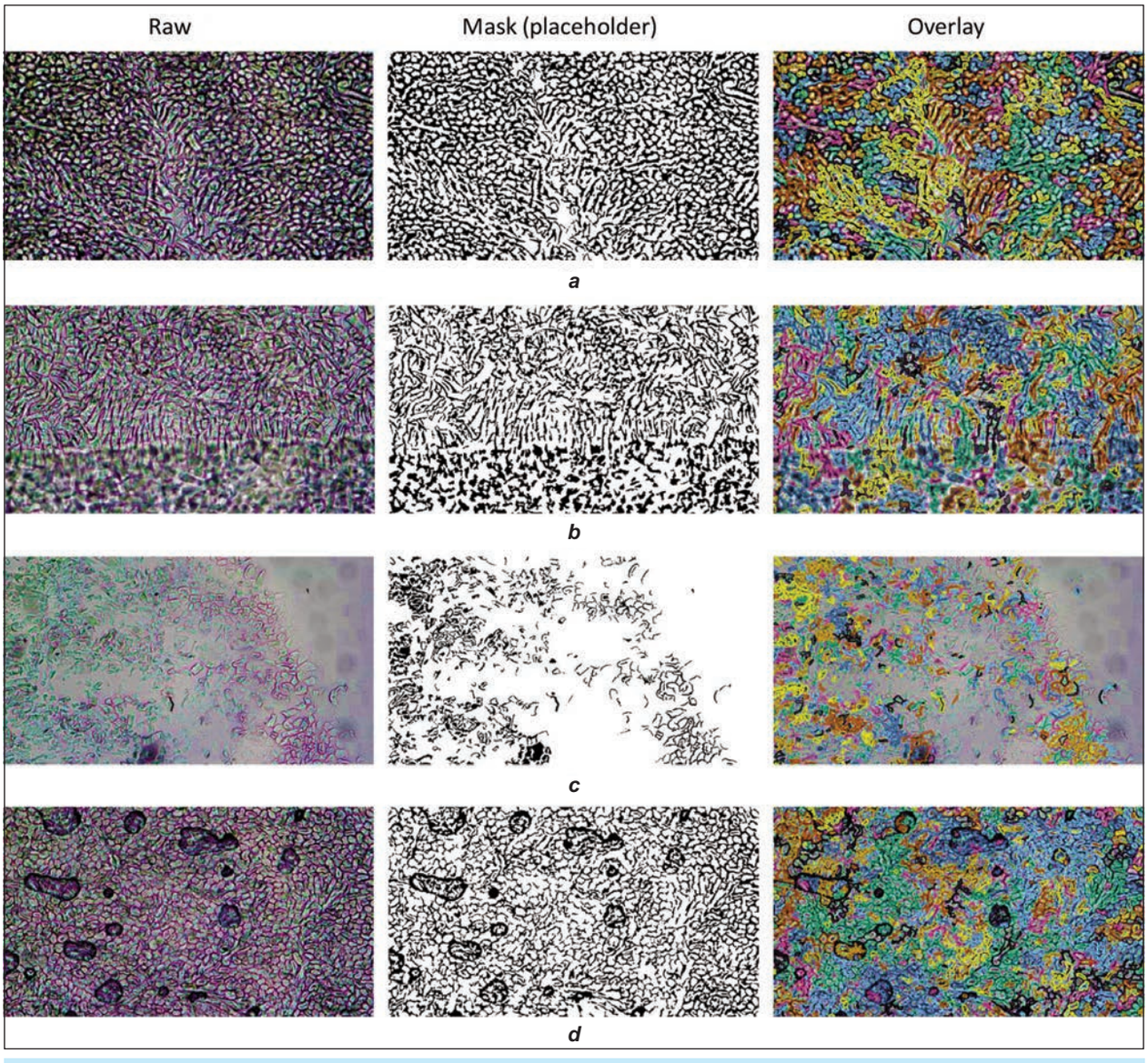

Fig. 8. Representative failure/edge scenarios: *a* and *b* – over-thick, laid-down/tilted slices (two examples): strong halos and banding lead to bridging/merging of adjacent sections; *c* – over-thin slice: low contrast breaks contours, causing fragmentation and area under-estimation; *d* – bubble-rich field: numerous bubbles and refractive halos create spurious edges and large connected components, breaking segmentation and fibre-type recognition

and masking using circularity/diameter/gradient cues; 5) ±Δ sensitivity analysis on density and threshold parameters with confidence intervals. These measures substantially reduce errors in problematic fields.

EXPERIMENTAL DESIGN AND DATA ANALYSIS

Experimental samples and operating procedures

To verify the applicability and accuracy of the AI image segmentation method for cotton and regenerated cellulose blended fibres, this study established a standardised experimental process, including sample selection, section preparation, image acquisition, model recognition, and ratio calculation. The specific operational steps are presented in the following subsections.

Source and categories of experimental samples

This study tested a total of 37 batches of blended samples, covering three typical dual-component combinations, as detailed below:

- Cotton/Viscose fibres: 13 batches;
- Cotton/Modal fibres: 13 batches;
- Cotton/Lyocell fibres: 11 bat0ches.

A cooperating laboratory provided all samples with testing qualifications, and the original blending ratios are known, covering a range of component ratios from 30% to 80%, making them highly representative and generalizable. Some physical samples are displayed in figure 9.

Preparation of cross-sectional slices

The following standardised slicing steps were used to prepare fibre cross-section observation slides:

- use resin embedding material for vacuum impregnation and shaping of the samples;
- employ a precision microtome to cut along the vertical direction with a thickness controlled between 10–15 μm;
- after pre-drying, impurity removal, and drying treatment, standard slices suitable for microscopic observation are obtained.

All samples are processed under the same batch conditions to ensure thickness consistency and microscopic imaging contrast.

Microscopic image acquisition and calibration

Using a self-developed image acquisition platform (as detailed in the 2nd section), high-definition cross-sectional images are captured at a magnification of 200× – 400×. For each sample area, at least 10 images are collected, and, through pixel-size calibration, the images are converted to a μm^2 scale. The collected images undergo preliminary quality screening before being used for AI model analysis.

For each field, this study computes Laplacian variance S and an edge-width metric W as proxies for imaging/thickness; frames with $S < S_{min}$ or $W > W_{max}$ are flagged as over-thin/over-thick or defocused and rescanned. This study also detects bubble-rich fields using circularity/diameter and local-contrast heuristics and either masks the affected regions or triggers rescanning. This study performs ±Δ sensitivity analysis on the binarisation threshold and density parameters and reports confidence intervals of composition changes.

An AI model for automatic recognition and segmentation

The collected images are input into the fully trained U-Net deep learning model, which automatically performs the following operations:

- conduct pixel-level semantic segmentation of all cross-sectional fibres in the image;
- output category label mask images and individual contour data;
- automatically identify fibre types (Cotton/Regenerated Cellulose) and perform quantity statistics.

After the segmentation results are exported, they enter the post-processing module for area calculation and contour visualisation.

Blending ratio calculation and output

The system calculates the blending ratio based on the mass percentage formula provided in equation 1. The parameters for each fibre type are derived from the area, fibre count, and standard density data extracted from the images.

Verification and error validation

To ensure model stability and result reliability:

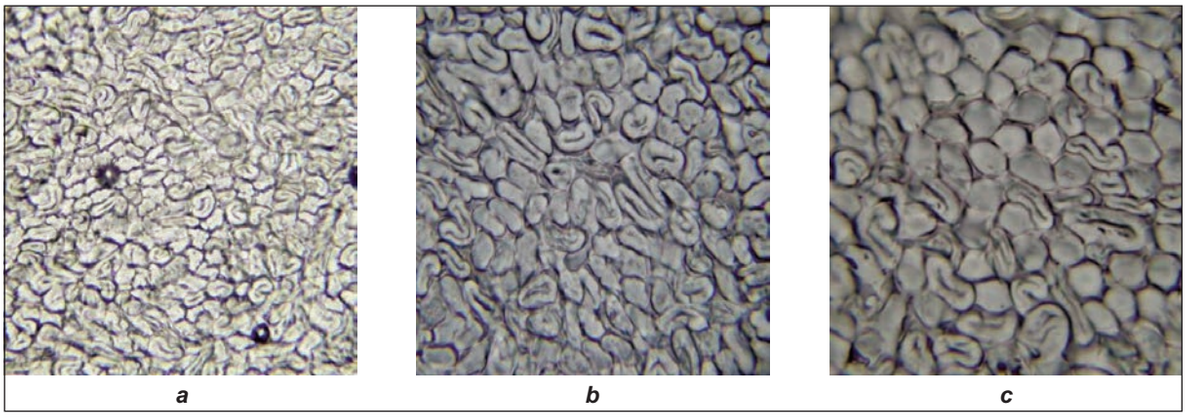

Fig. 9. Physical image of cotton and regenerated cellulose blended fibre samples for experiment: *a* – Cotton/viscose fibre; *b* – Cotton/modal fibre; *c* – Cotton/lyocell fibre

- randomly sample 10% of the image results for each type of sample, and have an expert manually review the contour and classification accuracy;
- compare the AI results with the chemical dissolution method, calculating the absolute error as a standard for system performance evaluation.

Use statistical indicators such as standard deviation and maximum deviation to analyse the robustness of the methods.

Summary and discussion of experimental data

To comprehensively assess the practical performance of the AI cross-sectional analysis method based on the U-Net model in identifying blended fabric components, the research team conducted experimental determinations and comparative analyses on 37 batches of cotton/regenerated cellulose blended samples. The samples covered three typical blended combinations: cotton/viscose, cotton/modal, and cotton/lyocell. The measured results were obtained using manual interpretation, standardised chemical dissolution methods, and AI recognition methods, with a systematic comparison focusing on accuracy, efficiency, and stability.

From an overall accuracy perspective, the performance of the AI method is highly consistent with the chemical dissolution method. The average absolute error for the detection results of the three types of blended samples is 1.42%, with a maximum deviation not exceeding 2.7%. Among them, the recognition accuracy for the cotton/lyocell group is the highest, with an average error of only 1.31%. This trend is closely related to the geometric morphology of the fibre cross-sections: Lyocell fibres have regular cross-sections and clear boundaries, which facilitate accurate segmentation by the model; whereas cotton and viscose have more similar cross-sectional morphologies and grayscale distributions, which can lead to some misidentifications, resulting in slightly higher errors. Overall, the AI model demonstrates strong adaptability and robustness across all three combinations.

To visually represent the error differences among the three typical blended combinations, figure 10 illustrates the maximum error bar chart for six representative samples between the AI detection method and the chemical dissolution method. The results indicate that the AI method exhibits higher consistency in the cotton/lyocell samples, while some samples in the cotton/viscose combination show slightly higher errors but remain within an acceptable range. This reflects the AI model's stronger segmentation adaptability for fibre morphologies with clearer cross-sections.

Further analysis reveals that the errors in some samples primarily stem from fluctuations in image quality, deviations in fibre cutting angles, and assumptions regarding the use of standard density parameters. For instance, issues such as fibre stacking, uneven dyeing, and local blurriness in certain areas may lead to slight deviations in the segmentation model's judgment of boundaries, thereby affecting the accuracy of area extraction. Additionally, in the experiments, all fibre components were calculated using a uniform density value, neglecting microscopic density fluctuations caused by different sources of raw materials, which may result in slight deviations in the calculations for edge samples. Nevertheless, these errors are controlled within 2%, sufficiently meeting the accuracy requirements of current industry standards.

To verify the stability of the AI detection method, 10 samples were randomly selected from 37 samples, and each sample was tested 10 times. The experimental results showed that the maximum standard deviation of the 10 samples was 0.028 and the minimum was 0.011, indicating that this method has good reliability and repeatability. Apart from accuracy performance, the advantages of the AI detection method in testing efficiency are particularly significant. Traditional manual methods typically require 60 minutes to complete the identification and mapping of a single sample, while the AI method can output component ratios and statistical results in just about 5 minutes under standard image input conditions, achieving an efficiency increase of over 10 times. More importantly, this method does not require any chemical dissolution processes, making it non-destructive and environmentally friendly, particularly suitable for large-scale testing scenarios and subsequent quality traceability needs.

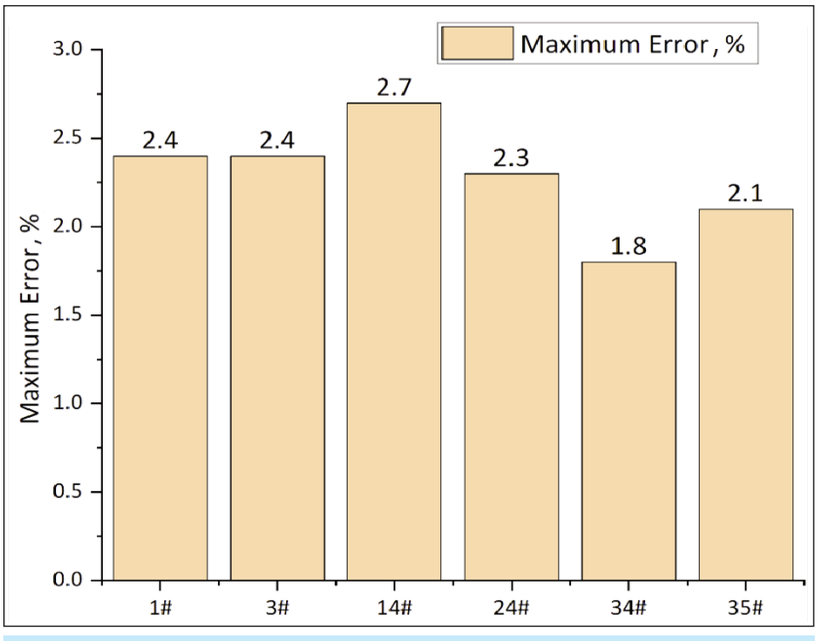

Fig. 10. Comparison bar chart of maximum errors between the AI detection method and the chemical method for different typical blended samples

Combining experimental results with system performance, it is evident

that the U-Net model-based cross-sectional image recognition method not only possesses good quantitative analysis capabilities but also maintains stable output under different fibre types, blending ratios, and imaging conditions. Compared to traditional methods, it exhibits significant advantages in accuracy, efficiency, and operational safety. In the future, this method is expected to be extended to more complex three-component or functional fibre blended systems, while optimising model parameters through big data training to further enhance classification accuracy and application breadth.

CONCLUSION AND OUTLOOK

This study addresses the challenge of detecting fibre components in cotton and regenerated cellulose blended fabrics that are difficult to separate chemically, proposing an AI cross-sectional quantitative recognition method that integrates high-resolution microscopic image acquisition, deep learning segmentation models, and structural contour analysis. This method centres on the U-Net architecture and combines multi-image fusion strategies and contour vector reconstruction techniques to achieve automatic recognition of fibre cross-section structures, area extraction, and blending ratio derivation, establishing an intelligent pathway from “image perception” to “quantitative analysis”.

In terms of the image acquisition system, this paper constructs a multi-modal microscopic imaging platform that integrates VCM focusing, high-precision moving platforms, and 3D composite optical paths, significantly enhancing the stability, depth, and contrast of high-magnification images, ensuring the quality and stability of the input data for the AI model. In the image analysis phase, the U-Net model was trained on over 100,000 sample images and optimised through expert review, ultimately achieving high-precision segmentation and recognition in typical cotton/regenerated cellulose blended fabrics. Experimental results indicate that this method achieves an average absolute error of 1.42% across 37 test samples, with a maximum deviation not exceeding 2.7%. This performance surpasses the consistency of manual methods and maintains high agreement with standardised chemical dissolution methods. Meanwhile, detection efficiency has improved to one-tenth of the original, demonstrating strong potential for engineering applications.

The AI cross-sectional analysis method proposed in this paper retains core advantages of being non-destructive, rapid, and automated while fully adapting to the differences in fibre microstructures. It provides a new pathway for addressing the issues of traditional methods in handling complex fibre systems, such as poor timeliness, high environmental burden, and strong subjectivity. It has good expansion value in standardising detection, smart production, textile quality control, and traceability system construction.

This study additionally reports four failure/edge cases (two over-thick laid-down/tilted, one over-thin, and one bubble-rich field) with targeted QC and post-processing strategies, delineating the method’s applicability under non-ideal slicing.

Future research can further optimize and expand in the following directions: (1) constructing a multi-channel segmentation network with stronger generalization capabilities for three-component and functional fibre blended structures; (2) introducing spatial attention mechanisms or Transformer architectures to enhance the model’s sensitivity to low-contrast areas; (3) establishing a dynamic weighting system in conjunction with a density database to further improve the true accuracy of ratio calculations; (4) integrating this system into a real-time detection platform on production lines to achieve closed-loop control of fibre component analysis throughout the entire process. Through bidirectional iteration of technology and application, this method is expected to become a core foundational tool for fibre identification and blending analysis in the future textile industry.

ACKNOLEDGEMENTS

The authors would like to thank the technical teams from United Testing Services (Foshan) Co., Ltd. and United Testing Services (Jiangxi) Co., Ltd. for their valuable support in sample preparation and image acquisition. Special appreciation is extended to the Jiangxi Centre for Modern Apparel Engineering and Technology for their assistance in data annotation and model validation. This paper was financially supported by the Science and Technology Research Project of the Jiangxi Provincial Department of Education, titled “R&D and Innovation in Textile Product Testing Technologies” (CN) (GJJ250XXXX). This paper was financially supported by the United Testing Services (Jiangxi) Co., Ltd. project titled “R&D and Innovation Support for Textile Product Testing” (CN) (JFHX202521). This paper was financially supported by the China National Textile and Apparel Council Scientific Guidance Project (CN) (2019111). This paper was financially supported by the Research Project of United Testing Services (Foshan) Co., Ltd. (CN) (RD2518).

REFERENCES

[1] Greaves, P.H., *Fibre identification and the quantitative analysis of fibre blends*, In: Review of Progress in Coloration and Related Topics, 1990, 20, 1, 32–39, https://doi.org/10.1111/j.1478-4408.1990.tb00072.x

[2] Qamar, S., Baba, A.I., Verger, S., Andersson, M., *Segmentation and characterisation of macerated fibres and vessels using deep learning*, In: Plant Methods, 2024, 20, 1, 126, https://doi.org/10.1186/s13007-024-01244-w

[3] Qin, J., Lu, M., Li, B., Li, X., You, G., Tan, L., Zhai, Y., Huang, M., Wu, Y., *A rapid quantitative analysis of bicomponent fibres based on cross-sectional in-situ observation*, In: Polymers, 2023, 15, 4, 842, https://doi.org/10.3390/polym15040842

[4] Guo, R., Stubbe, J., Zhang, Y., Schlepütz, C.M., Gomez, C.R., Mehdikhani, M., Breite, C., Swolfs, Y., Villanueva-Perez, P., *Deep-learning image enhancement and fibre segmentation from time-resolved computed tomography of fibre-reinforced composites*, In: Composites Science and Technology, 2023, 244, 110278, https://doi.org/10.1016/j.compscitech.2023.110278

[5] Habib, M.T., Faisal, R.H., Rokonuzzaman, M., Ahmed, F., *Automated fabric defect inspection: a survey of classifiers*, In: arXiv preprint, arXiv:1405.6177, 2014, https://doi.org/10.48550/arXiv.1405.6177

[6] Chakraborty, S., Moore, M., Parrillo-Chapman, L., *Automatic defect detection of print fabric using a convolutional neural network*, In: arXiv preprint, arXiv:2101.00703, 2021, https://doi.org/10.48550/arXiv.2101.00703

[7] Zhou, H., Chen, Y., Troendle, D., Jang, B., *One-class model for fabric defect detection*, In: arXiv preprint, arXiv:2204.09648, 2022, https://doi.org/10.48550/arXiv.2204.09648

[8] Xia, H., Zhu, R., Yuan, H., Song, C., *Rapid quantitative analysis of cotton-polyester blended fabrics using near-infrared spectroscopy combined with CNN-LSTM*, In: Microchemical Journal, 2024, 200, 110391, https://doi.org/10.1016/j.microc.2024.110391

[9] Kumar, S., *Microscopic View – Fibre Identification*, Tiruppur: Style2Designer, c.2013, Available at: https://style2designer.com/apparel/fibre-yarn/microscopic-view-fibre-identification/ [Accessed on June 16, 2025]

[10] Ronneberger, O., Fischer, P., Brox, T., *U-net: Convolutional networks for biomedical image segmentation*, In: Medical Image Computing and Computer-Assisted Intervention – MICCAI 2015, 18th International Conference, Munich, Germany, October 5–9, 2015, Proceedings, Part III, Springer, 2015, 234–241, https://doi.org/10.1007/978-3-319-24574-4_28

[11] Pereira, G.H.d.A., Fusioka, A., Nassu, B.T., Minetto, R., Jung, C.R., *Active fire detection in Landsat-8 imagery: a large-scale dataset and a deep-learning study*, 2021, Available at: https://www.researchgate.net/Fig./U-Net-architecture-for-image-segmentation_fig6_352994766 [Accessed on June 16, 2025]

[12] Jha, D., Smedsrud, P.H., Riegler, M.A., Johansen, D., De Lange, T., Halvorsen, P., Johansen, H.D., Resunet++: *An advanced architecture for medical image segmentation*, In: 2019 IEEE International Symposium on Multimedia (ISM), IEEE, 2019, 225–2255, https://doi.org/10.1109/ISM46123.2019.00049

[13] Dataset Ninja, *Fibre Segmentation Dataset*, 2025, Available at: https://datasetninja.com/fibre-segmentation [Accessed on June 17, 2025]

[14] Wagner, F., Maas, H.-G., *Fibre Segmentation Dataset*, Kaggle, 2023, Available at: https://www.kaggle.com/datasets/franzwagner/pe-fibres [Accessed on June 17, 2025]

[15] Kurkin, E., Minaev, E., Sedelnikov, A., Pioquinto, J.G., Chertykovtseva, V., Gavrilov, A., *Computer vision technology for short fibre segmentation and measurement in scanning electron microscopy images*, In: Technologies, 2024, 12, 12, 249, https://doi.org/10.3390/technologies12120249

Authors:

ZHENGHAI LI[1], YUJUE WANG[2], ZHENZHU ZHANG[1], GUANJIE CHEN[3], YONGFENG LI[1], CHEN YANG[2,4]

[1]United Testing Services (Foshan) Co., Ltd, Nanfang Technology Innovation Centre, Textile and Accessory City, Xiqiao, 528211, Foshan City, China
e-mail: knightlzh@126.com, 195466058@qq.com, 1361906678@qq.com
ORCID: 0000-0002-0665-3462, 0009-0007-2720-3923, 0009-0002-7677-5024

[2]Jiangxi Institute of Fashion Technology, No. 108, Lihu Middle Avenue, Xiangtang Economic Development Zone, 330201, Nanchang City, China
e-mail: wwmm.4jr@qq.com
ORCID: 0009-0009-1359-6732

[3]United Testing Services(Jiangxi) Co., Ltd., Floor 4-5, Building 14, Nanchang Light Textile City, No. 666, Changdong Avenue, Qingshan Lake District Hi-tech Industrial Park, 330012, Nanchang City, China
e-mail: 04guanjie@163.com
ORCID: 0009-0008-3234-9916

[4]Wuhan Textile University Gongqingcheng Textile and Garment Industry Research Institute, 2nd Floor, Down Museum, Yaya Industrial Park, Gongqingcheng Industrial New Area, 332020, Jiujiang City, China

Corresponding author:

CHEN YANG
e-mail: comradeyang@qq.com
ORCID: 0000-0003-1593-7739

Optimisation method for the quality of combed sliver

DOI: 10.35530/IT.077.03.202534

LI XINRONG
LIU RONGFANG
SHI SHUAIXING

WANG BIAO
LI LI

ABSTRACT – REZUMAT

Optimisation method for the quality of combed sliver

The quality of the sliver is a key parameter for assessing the technical level of spinning equipment. As a critical machine in the spinning process, the sliver-quality optimisation system of the cotton comber is crucial for enhancing cotton sliver quality. Based on the process characteristics of cotton combers, this paper proposes a new non-real-time optimisation method for improving the evenness of combed slivers and verifies the feasibility of this method through experiments on combed slivers. Firstly, the paper introduces a new method for optimizing sliver quality. Secondly, online sliver quality data are collected and then processed through smoothing and correlation analysis to determine the periodic variations in sliver quality. Next, according to the principle of sliver evenness and the open-loop control system, a model is established between sliver quality variation and the middle roller speed. The periodic motion law of the middle roller is then determined. Experimental results show that the method, after non-real-time processing of sliver data, reduces the coefficient of variation (CV) of the sliver by 0.5%. Furthermore, a multi-stage speed control for the middle roller is proposed to replace the continuously variable speed control. This reduces the requirements and cost of the control system and still lowers the sliver CV by 0.38%. This proves that the method meets the combed sliver quality optimisation requirements. Finally, the impact of open-loop system delay time on non-real-time processing time during actual operation is analysed to further ensure the optimisation of roller speed regulation. This study provides a practical technical solution and a theoretical basis for online sliver leveling in the combing process.

Keywords: *non-real-time processing, open loop, comber, sliver, quality optimisation*

Metodă de optimizare a calității benzii pieptănate

Calitatea benzii fibrelor de bumbac reprezintă un parametru cheie pentru evaluarea nivelului tehnic al echipamentelor de filare. Fiind o mașină esențială în procesul de filare, sistemul de optimizare a calității benzii de fibre al mașinii de pieptănat bumbac este deosebit de important pentru îmbunătățirea calității benzii fibrelor de bumbac. Pe baza caracteristicilor procesului de pieptănare a bumbacului, lucrarea de față propune o nouă metodă de optimizare în timp real pentru îmbunătățirea uniformității benzilor pieptănate și verifică fezabilitatea acestei metode prin experimente efectuate pe benzi de bumbac pieptănat. În primul rând, lucrarea prezintă o nouă metodă de optimizare a calității benzii de fibre. În al doilea rând, datele privind calitatea benzii de fibre sunt colectate în timp real și apoi prelucrate prin metode de netezire și analiză de corelație pentru a determina variațiile periodice ale calității benzii de fibre. În continuare, pe baza principiului uniformității benzii de fibre și a sistemului de control în buclă deschisă, se elaborează un model care leagă variația calității benzii de fibre de viteza cilindrului central. Se determină apoi legea mișcării periodice a cilindrului central. Rezultatele experimentale arată că această metodă, după prelucrarea în regim non-real-time a datelor privind banda de fibre, reduce coeficientul de variație (CV) al benzii cu 0,5%. În plus, se propune un control al vitezei în mai multe trepte pentru cilindrul central, în locul controlului continuu al vitezei. Acest lucru reduce cerințele și costurile sistemului de control și scade în continuare coeficientul de variație al benzii cu 0,38%. Acest lucru demonstrează că metoda îndeplinește cerințele de optimizare a calității benzii pieptănate. În final, se analizează impactul timpului de întârziere al sistemului în buclă deschisă asupra duratei de procesare în regim non-real-time în timpul funcționării efective, pentru a asigura și mai mult optimizarea reglării vitezei cilindrilor. Acest studiu oferă o soluție tehnică practică și o bază teoretică pentru optimizarea online a benzii în procesul de pieptănare.

Cuvinte-cheie*: prelucrare în regim non-real-time, buclă deschisă, mașină de pieptănat, banda de fibre, optimizarea calității*

INTRODUCTION

The textile industry, as a pillar industry of the global manufacturing system, has a continuous demand for improving quality and standards [1]. The quality of the spinning process directly determines the quality of subsequent textiles [2], and sliver quality is the basis of yarn quality, which largely determines the development of the textile industry. Current sliver quality optimisation generally refers to self-leveling control on carding and drawing machines. In actual production, however, the impact of the combing process on sliver quality cannot be ignored [3]. However, the open-loop, closed-loop, and mixed-loop self-levelling control methods used on carding and drawing machines

are not suitable for cotton combers, which have complex structures, limited sensor installation positions, and a long distance from the drafting zone. In recent years, with the rapid development of technologies such as digital twins [4] and artificial intelligence [5], new technological support has been provided to solve this problem. Therefore, further strengthening research on quality optimisation methods for combed cotton sliver and integrating the latest intelligent and digital technologies is of great practical significance for improving overall spinning quality and promoting industry development.

Current optimisation methods for sliver quality mainly focus on the self-leveling control methods on carding and drawing machines [6]. Wang et al. [7] set short closed-loop control at the feeding roller and the doffer to optimise sliver quality through speed regulation. Li et al. [8] conducted a detailed analysis of the delay time to enhance yarn optimisation. Wang et al. [9] researched the closed-loop control of carding machines and improved the system's anti-interference ability by changing the self-levelling controller. Domestic and foreign experts have also researched and analysed the control of the loading mixing ring on the carding machine [10]. Although optimisation has advanced, shortcomings in control and cost remain challenging to resolve. At present, concave-convex rollers are generally used on drawing frames to detect sliver quality, after which the speed of the drafting roller on the drawing frame is adjusted to achieve sliver evenness. Jie et al. [11] used concave-convex rollers to detect the sliver quality earlier and then optimised the sliver quality by controlling the speeds of the rear and middle rollers. Hongliang et al. [12] set up two detection devices between the drafting components and behind the drafting area, adjusting the speeds of the front and rear rollers to achieve uniform yarn quality. Some experts have also applied the mixed-loop control method on the drawing frame [13], which can ensure optimisation, but the economic cost is still high. Based on the research on drawing machines by these experts, the above methods are all real-time feedback optimisation, in which detection and adjustment are carried out simultaneously. By detecting and adjusting the drafting roller at the same time, the optimisation of sliver quality can be achieved. Although open-loop control has been well optimised, delay still significantly affects the real-time optimisation of yarn. Unlike the aforementioned self-levelling control method, this paper introduces a novel non-real-time optimisation approach that enhances cotton sliver quality by acquiring and processing quality data, analysing its inherent patterns, and subsequently optimising the roller speed.

This paper proposes a novel method for optimizing sliver quality in combing machines. First, cotton sliver quality data are smoothed and correlation-analysed to eliminate interference, then the DS-MMFI algorithm is used for cyclic data collection and error analysis. Based on momentum conservation and the relationship between sliver weight and count, a mathematical model linking middle roller speed to sliver quality is established. This model reveals periodic behaviour and is validated experimentally.

Furthermore, by analysing delayed data and the relationship between roller speed and sliver weight variations, the motion cycle is deduced, and sliver quality is optimised, reducing non-uniformity by 0.5%. Considering the complexity and cost of servo control, a multi-stage speed adjustment method is proposed as an alternative to continuous variable speed control, with experiments showing a 0.38% reduction in non-uniformity. Finally, analysis of control delay indicates that, with an optimal delay, the middle roller's periodic motion can be more precisely synchronised with the drafting cycle, further refining the process. Non-real-time processing provides ample time for data analysis and delay evaluation, reducing real-time errors, while the periodic multi-stage speed control lowers system demands and offers theoretical support for future cotton sliver quality optimisation.

OPTIMISATION METHOD FOR SLIVER QUALITY

Sliver quality optimisation is achieved by adjusting the speed of the middle roller in the drafting zone of the comber. Due to the complex mechanical transmission of the comber, the front roller is tightly integrated with the feeding system, while the rear roller cooperates with the output system. In contrast, the operation of the middle roller is relatively independent, exerting minimal influence on the preceding and succeeding processes. Moreover, as the front and rear rollers determine the overall drafting ratio, and with the rear roller imposing higher motor requirements, the optimisation range and fluctuation of the middle roller speed are relatively limited. Therefore, adjusting the middle roller speed can reduce interference with the operation of other components. The sliver quality optimisation method is shown in figure 1 and is different from traditional self-leveling control. This method adopts a non-real-time open-loop control method. The sliver quality data is processed over time after being detected by the sensor. After obtaining the sliver quality cycle law, the corresponding motion law of the middle roller is obtained, and the sliver quality is adjusted by adjusting the middle roller's speed.

Based on the specific analysis shown in figure 1, the drafting components are operated according to the original draft ratio, and the detection device is installed at the sliver outlet during the sensor detection stage, and before quality optimisation adjustments, to reduce the impact on the original structure of the comber. After obtaining the sliver quality cycle through data processing, the model relating the sliver quality and the middle roller speed is combined to obtain the periodic motion law of the middle roller. At the same time, the motion law of the middle roller is approximated in multiple stages to reduce control system requirements and ultimately achieve sliver quality optimisation.

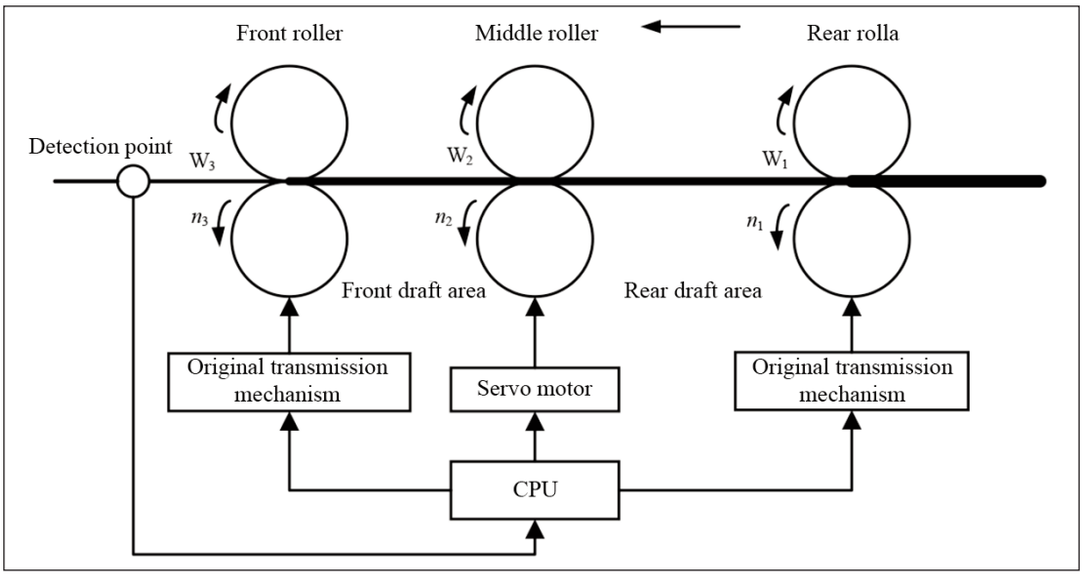

Fig. 1. Diagram of the evenness quality optimisation method: W_1 – input sliver quantity; W_2 – quantification of cotton sliver after rear zone stretching; W_3 – output sliver quantity; n_1 – front roller speed; n_2 – middle roller speed; n_3 – rear roller speed

DATA PROCESSING

Due to the complexity of the online detection environment, firstly, smoothing and correlation preprocessing are performed on the sliver quality data. Subsequently, a period extraction algorithm is used to determine the period of sliver quality data, and error analysis is conducted to ensure the accuracy of the extracted period, laying the foundation for subsequent sliver quality optimisation.

Data preprocessing

Data preprocessing mainly ensures quality by eliminating interference such as noise. Before adjusting the speed of the middle roller, it is necessary to predict the sliver data pattern and determine the middle roller speed pattern. Given the actual drafting speed and machine structure, it takes about 1–3 seconds for the sliver to travel from the drafting zone to the detection position. Therefore, a 10-second sampling time is set to collect sliver quality data, as shown in figure 2.

The sliding average method [14] is used to complete the smoothing process. The data obtained after processing is recorded as follows, based on the moving average analysis:

$$\begin{cases} m(1) = \dfrac{[4u(1) + u(2)]}{5} \\ m(t) = \dfrac{[u(t-1) + 3u(t)u(t+1)]}{5}, \ 1 < t < n \\ m(n) = \dfrac{[u(n-1) + 4u(n)]}{5} \end{cases} \quad (1)$$

Where $\{u(t)\}$ is the dataset, $t \in Q$, Q is a positive integer.

After completing the data smoothing process, the data shown in figure 3 shows a clear trend with significantly reduced random interference. Next, the correlation of the data is analysed to remove small fluctuations and improve the accuracy in obtaining cycles. The autocorrelation function of the discrete sequence mentioned above is

$$R_{(k)} = \lim_{N\to\infty} \frac{1}{2N+1} \sum_{h=-N}^{N} u(h)u(h-k) \quad (2)$$

where k are the delay points. The sample size N of the time series is 1000.

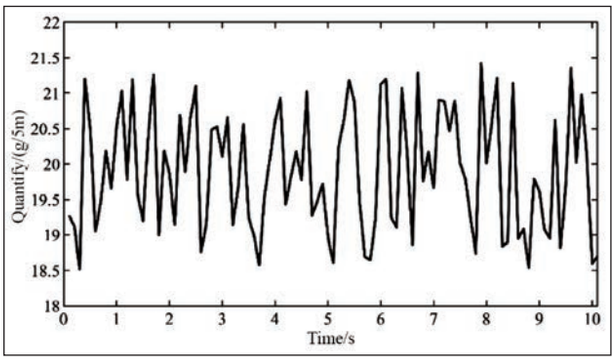

Fig. 2. Evenness quality data

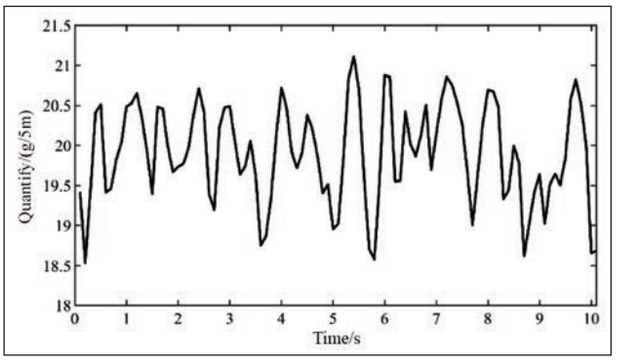

Fig. 3. Smoothed data

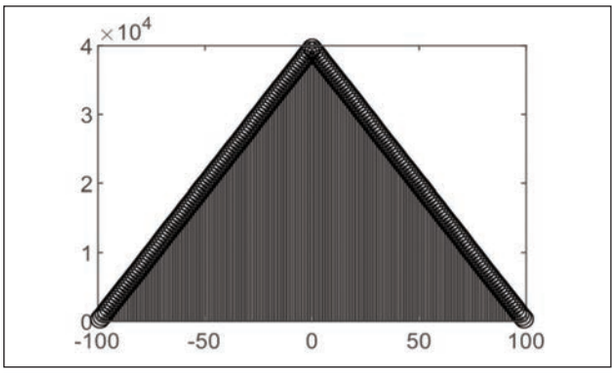

Fig. 4. Data autocorrelation analysis results

Autocorrelation reflects the similarity between the data and itself after a specified delay [15]. Figure 4 shows the sequence autocorrelation results, and the data can then be autocorrelated to further extract the data period.

Cycle extraction

Currently, the most frequently used periodic sequence data mining algorithms include the Max Miner, MAFIA, FP Max, and MMFI algorithms. The MMFI algorithm has the highest extraction efficiency and mining frequency, while analysis of sliver quality data focuses on its variation trend [16]. Therefore, the DS-MMFI algorithm based on variable periods is most suitable. This method avoids sequence loss due to strict cycle start and end restrictions. The most representative part of the mined sliver quality data, determined through frequent mining, is the periodic component, which is approximately 1.6 seconds long. Finally, to minimise the error in extracting periodic data, it is necessary to average the data from the first cycle with other cycles. The resulting data cycle is shown in figure 6, and the error for the corresponding period is shown in figure 7. According to the error analysis, the accuracy and precision of the extracted data cycle are relatively high, demonstrating that the sliver quality data exhibit distinct periodic patterns and high cycle similarity.

Optimisation of the middle roller motion law

After obtaining the periodic characteristics of the sliver data, it is necessary to establish a functional model between the rotational speed of the middle roller and the sliver quality. From this model, the corresponding periodic motion pattern of the middle roller can be derived to optimize sliver quality.

According to the law of conservation of momentum in the actual drafting process:

$$v_1 \times W_1 = v_2 \times W_2 = v_3 \times W_3 \quad (3)$$

where v_1 is the speed of the sliver at the rear roller, v_2 – the speed of the sliver at the middle roller, and v_3 – the speed of the front roller at the sliver.

Based on the quality optimisation method diagram in figure 1, the detection point is set behind the drafting component, and the middle roller speed is adjusted by detecting the weight change of the drafted sliver. The control principle diagram is shown in figure 7. First, the sliver dry weight is set according to the process requirements. At this point, the dry weight should reach the standard value h_0, but there may be a deviation Δh between the actual dry weight and the standard value. After processing the delay time, the controller determines the roller speed change based on the dry weight change, and the speed change is set to Δn. Under this condition, the sliver quality is optimised.

A mathematical model must be established before verifying the above control method. The evenness model of the comber is established by ensuring that the input fibre amount per unit time equals the sum of the output fibre amount and the fibre amount inside the comber [17]:

$$Q_{in}(t) \times (1 - \eta) = Q_{out}(t) + Q(t) \quad (4)$$

where $Q_{out}(t)$ is the amount of fibre output per unit time, g/min; $Q_{in}(t)$ – the amount of fibre input per unit time, g/min; $Q(t)$ – the fibre quantity inside the comber, g/min; η – the cotton drop rate.

Equation 4 represents the basic principle of evenness. For analytical convenience, the cotton drop rate η is set to zero, and the fibre quantity $Q(t)$ inside the drafting zone remains unchanged:

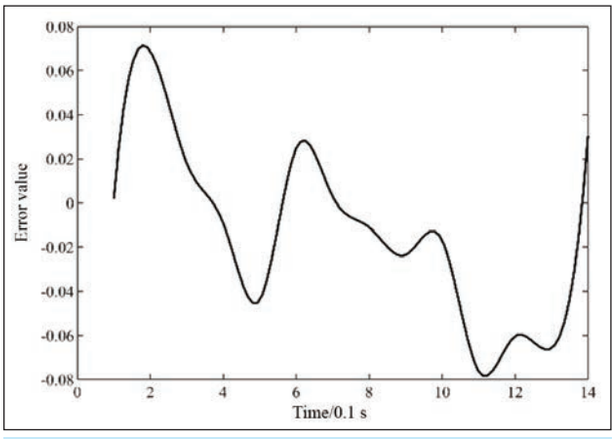

Fig. 5. Periodic data

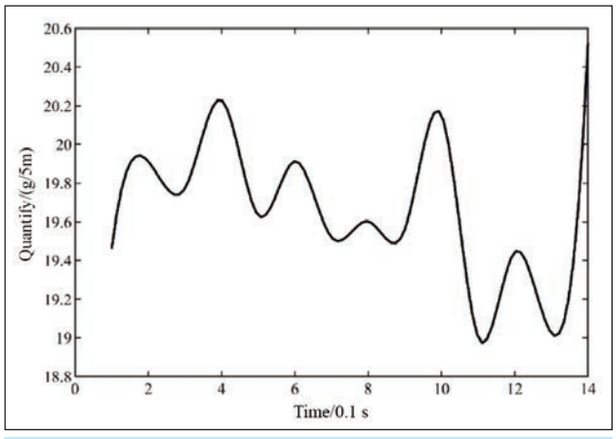

Fig. 6. Data error

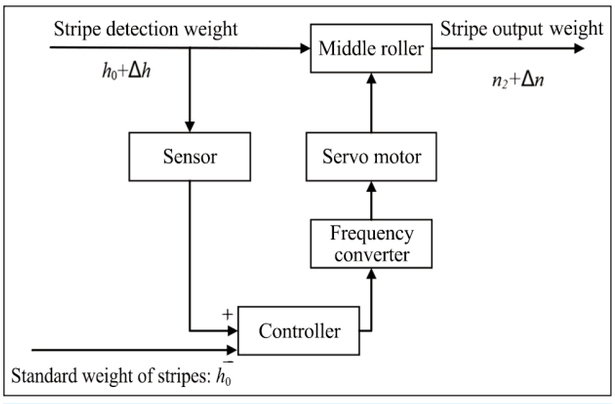

Fig. 7. Control schematic diagram of the quality optimisation method

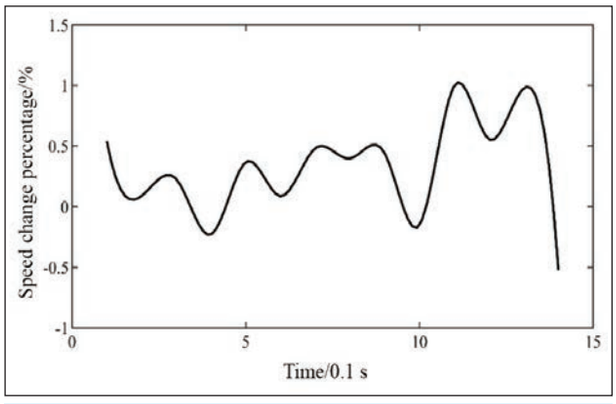

Fig. 8. Periodic variation of middle roller rotational speed

$$Q_{in}(t) = Q_{out}(t) + Q(t) \quad (5)$$

Selecting sliver density as the detection target and adjusting the middle roller speed have little impact on rear drafting, which can be ignored. Therefore, only the section from the middle roller's input to the front roller's output is considered. Accordingly, the amount of fibre input per unit time can be expressed as:

$$Q_{in}(t) = h_0 = \rho_1 V_1 \quad (6)$$

where ρ_1 is the density of the input sliver of the middle roller, g/cm^3; h_0 – the input sliver weight; V_1 – the corresponding unit volume of the input sliver, m^3.

The linear speed at each roller refers to the magnitude of the surface speed at that point. The conversion relationship between it and the middle roller speed is:

$$v_{in} = \pi D n_2 \quad (6)$$

where v_{in} is the original input speed of the middle roller, m/min; n_2 – the middle roller speed, m/min; D – the diameter of the middle roller, mm.

The purpose of drafting is to ensure that the weight of the output sliver remains unchanged. Therefore, $Q_{out}(t)$ can be considered a constant value under ideal conditions. If the output sliver weight is equal to the original $Q_{out}(t)$ before and after changing the middle roller speed and satisfies the momentum conservation theorem in equation 3, then

$$v_{out} \cdot Q_{out}(t) = v_{in} \cdot Q_{in}(t) = h_0 \cdot v_{in} = (h_0 + \Delta h) \cdot (v_{in} + \Delta v) \quad (7)$$

where $v_{in}(t)$ is the speed of the input bar, m/min; $v_{out}(t)$ – the speed of the output bar, m/min.

By substituting the relationship between rotational speed and linear speed in equation 7 into equation 8 for simplification:

$$\Delta n = -\frac{n_2}{1 + \frac{h_0}{\Delta h}} \quad (9)$$

Equation 9 is the quality optimisation model for the middle roller speed, and the drafting quality optimisation can be completed based on this. By combining the extracted sliver data period with the relationship in equation 9, the change in the middle roller speed can be determined, as shown in figure 9. Based on this, the middle roller only needs to adjust its speed according to the percentage change shown in figure 8 to optimise the sliver quality.

EXPERIMENTATION

To verify the effectiveness of the non-real-time open-loop control method in regulating sliver quality, the modification experiment was conducted on the AHC601 combing machine produced by Henan Haochang Combing Machine Joint-Stock Co., Ltd. The drafting device used in this comber is a 3-over-3 roller drafting system, with an experimental speed of 350 nips per minute. The control system uses Delta's ECMA-C20604RS servo motor, ASDA-B2-0421-B driver, and Omron's CP1H controller. The raw materials used in the experiment were from the same batch of cotton, and their main fibre characteristic parameters are as follows: fibre length of 26.5–27.3 mm, fineness of 148–153 mtex, and maturity of 0.80–0.83.

Figure 9 shows the schematic control diagram for the quality optimisation method. First, the detected sliver data is input into the system for time-series processing. The delay time is initially set to 3 seconds, which is combined with the travel time of the sliver from the drafting position to the detection point. After obtaining the sliver quality data cycle, the model describing the relationship between sliver weight and middle roller speed is used to derive the periodic motion law of the middle roller speed, thereby optimising the sliver quality. The first "Fcn" module in the figure corresponds to the functional relationship of equation 9. Because this relationship links the variation in sliver length to the variation in middle roller speed, it is necessary to subtract the rated quantitative value h from the data, with a size of 20 g/5 m. Within the set 3-second period, the analysis of the proportion of changes in the middle roller speed in equation 9 is completed, and the variation law of the middle roller motion is obtained. This computed variation is then added to the original constant roller speed n to obtain the optimised roller speed law. After the unit conversion of the second "Fcn" module, the final sliver weight data is obtained from the output module.

After 10 sets of repeated experiments, the optimisation scheme reduced the sliver CV% by approximately 0.5%. However, frequent high-speed changes in roller speed are undesirable in the actual production process. Therefore, a multi-stage motion method is adopted here instead of frequent variable speed motion. From the actual impact data trend in figure 9, it can be set as a three-stage speed change, and then the intermediate value of the three-stage speed change can be obtained. At this point, the three-stage speed change can be identified as a proportional change in the speed magnitude centred on the original roller speed, as illustrated in figure 10.

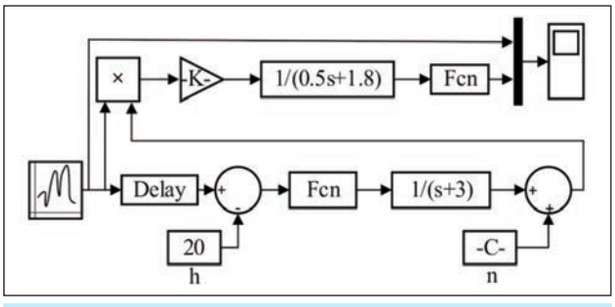

Fig. 9. Principle of quality optimisation method

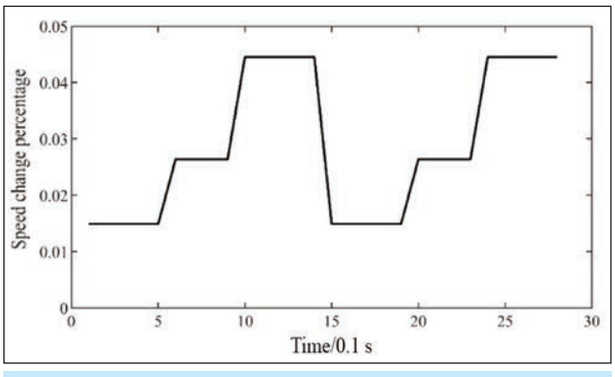

Fig. 10. Three-stage periodic change in speed

To verify the uniformity improvement effect of the multi-level motion method, experiments were conducted using the same equipment and identical production conditions as those of the aforementioned optimisation method. The motion law was directly applied to the middle roller through a servo motor, and then the sliver data obtained after the quality optimisation method was collected online. Figure 11 shows the comparison of effects before and after the application. After 10 sets of repeated experimental analyses, it was found that the sliver CV% was reduced by about 0.38%. Although this method is not as effective as the frequent variable speed method, it significantly reduces costs and implementation difficulties.

ANALYSIS AND DISCUSSION

There is a delay in the open-loop adjustment method behind the machine. If the delay time could be better determined and set in the control system, it would inevitably improve the cotton sliver quality. The following is an analysis of the delay time.

After a processing period, the total hysteresis τ_0 of the rear open loop can be expressed as:

$$\tau_0 = \tau_1 - \tau_1' \quad (10)$$

where τ_1 is the time from the rear detection point to the variable speed draft point, and τ_1' – the time taken for the detection point to change speed from the open-loop system to the central roller.

One key aspect of an open-loop system is to determine the delay time τ_0. The first step is to establish a mathematical model of the control system, as shown in figure 12.

Under ideal conditions, the sliver satisfies the momentum conservation principle before and after drafting, so:

$$v_2(t)W_2(t) = v_1(t)W_1(t) \quad (11)$$

where v_1 is the sliver speed at the front roller, m/min; v_2 – the sliver speed at the middle roller, m/min; $W_2(t)$ is the quantitative value of the sliver before this period.

After a time interval τ_2, the sliver reaches a speed change point and begins drafting. At this point, $W_2(t)$ can be regarded as the quantitative value of the sliver before this period, so $W_2(t) = W_3(t - \tau_2)$. However, the actual t is unknown, and its value is set to τ_2'. Then, from equation 11:

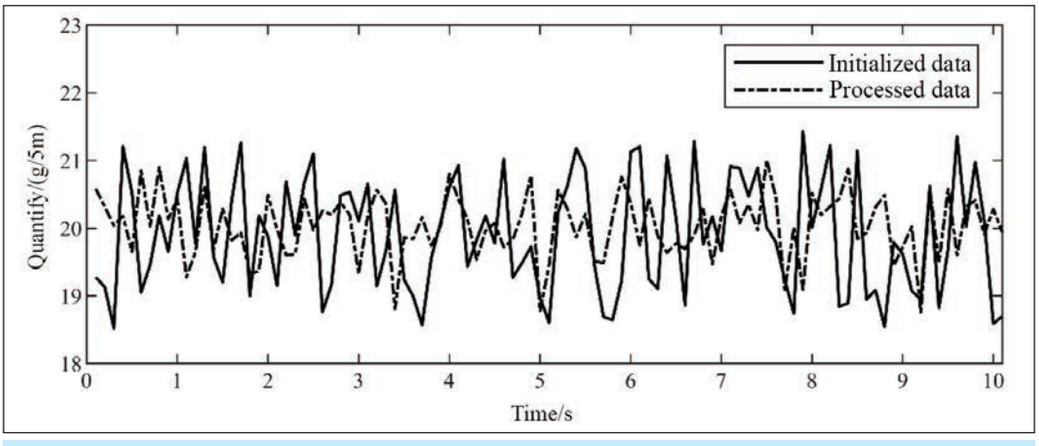

Fig. 11. Comparison of sliver quality before and after optimisation

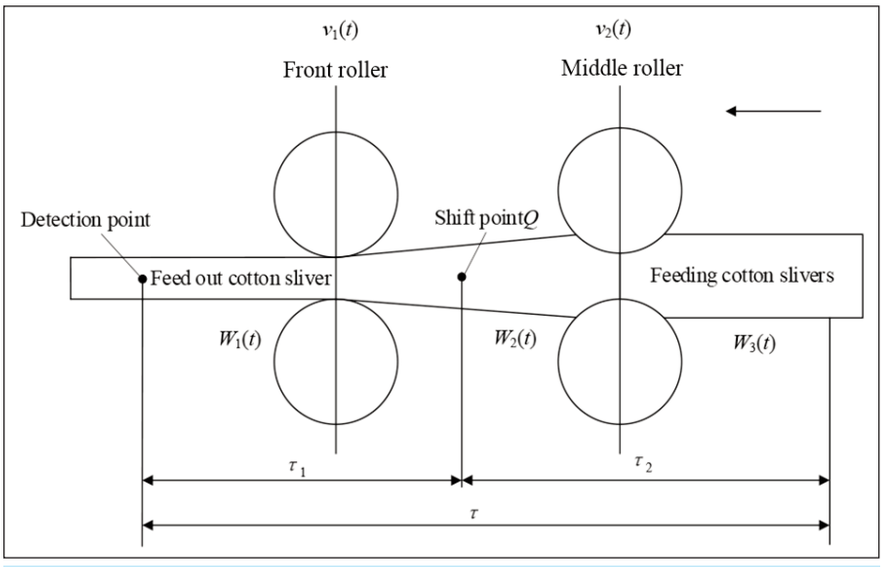

Fig. 12. Control system mathematical model

$$W_1(t) = \frac{v_2(t)W_2(t)}{v_1(t)} = \frac{v_2(t)W_2(t)}{v_2(t)W_3(t-\tau_2')} = \\ = W_1(t)\frac{W_3(t-\tau_2)}{W_3(t-\tau_2')} \quad (12)$$

If the sliver quantity of the detection point is $W_0(t)$, which can also be regarded as $W_1(t)$ after a time interval τ_2, then:

$$W_0(t) = W_1[t-(\tau-\tau_2)] = W_1(t+\tau_2-\tau) = \\ = W_1(t)\frac{W_3(t-\tau)}{W_3(t-\tau+\tau_2-\tau_2')} \quad (13)$$

When the delay time given by the system is equal to the actual delay time, the sliver quantity is output at the ideal set value. According to figure 12, the delay distance L in the actual drafting process refers to the distance between the detection point and the middle roller group. While the sliver passes through L, the draft ratio of the drafting zone remains unchanged, and the delay time can be determined as a fixed value under ideal conditions based on the correlation between the data.

The output cotton sliver quantity $W_1(t)$ and the input cotton sliver quantity $W_3(t)$ are two random processes with different time states. Since they belong to a unified system and are governed by certain deterministic factors, an internal connection exists between them, which meets the basic conditions for autocorrelation analysis. If its autocorrelation function is $R_W(\tau_3)$, then

$$R_W(\tau_3) = E[W_3(t)\,W_0(t+\tau_3)] = \\ = E\left[W_3(t)\,W_1(t)\frac{W_3(t+\tau_3-\tau)}{W_3(t+\tau_3-\tau+\tau_2-\tau_2')}\right] \quad (14)$$

where τ_3 is the random correlation time between the input and output cotton sliver quantification.

From equation 14, it can be seen that there is $\tau_3' = \tau$, and at this point, the autocorrelation function $R_W(\tau_3)$ reaches a maximum value. Because the combed sliver is the research object of this article, the distance of the sliver from the input point to the speed change point is small and can be approximately ignored during the actual drafting process.

Therefore, the calculation of the delay time is transformed into a calculation of the time-dependent variable in the autocorrelation function between the input and output sliver quantities. The delay time of the open-loop control method can be obtained by analysing the correlation between input and output cotton sliver quality and combining it with its autocorrelation function.

CONCLUSIONS

This paper proposes a non-real-time open-loop control method for optimising the evenness of slivers in a cotton comber. Online quality data are collected, smoothed, and analysed for correlation, and error analysis is conducted using the DS-MMFI algorithm. A mathematical model linking roller speed and sliver weight is established, and a multi-stage speed regulation strategy is employed to adjust the drafting ratio, thereby achieving effective sliver quality optimisation. Experimental results show that when frequent speed adjustments were applied via a servo motor, the CV value of the sliver decreased by 0.5%, whereas under multi-stage speed control, the CV value decreased by 0.38%. These findings demonstrate that the periodic motion of the middle roller under multi-stage speed-control can not only effectively improve sliver evenness but also provide cost advantages, thereby confirming the feasibility of achieving online quality optimisation in cotton combers. Moreover, correlation analysis between sliver quality input and output data further reveals the motion law of the middle roller, enabling a more accurate correspondence to the drafting cycle of sliver quality and thus enhancing the optimisation effect.

However, the control strategy proposed in this study primarily targets short-term sliver evenness by modulating the middle-roller speed in the rear drafting zone. Because short fibre content, neps, and sliver weight per meter are only weakly affected by adjustments in the rear drafting zone, they were not considered in this study. Nevertheless, these metrics are critical for evaluating overall yarn quality and subsequent spinning performance. Future work will systematically investigate these key quality parameters to establish a more comprehensive quality optimisation framework.

ACKNOWLEDGEMENTS

2021 Industrial Technology Basic Public Service Platform Project of the Ministry of Industry and Information Technology of the People's Republic of China – Building a Public Service Platform for Testing and Verification of Intelligent Manufacturing Standards "Building a Public Service Platform for Testing and Verification of Intelligent Manufacturing Standards Around the Textile Industry" (2021-0173-2-1). Key Project of the Natural Science Foundation of Tianjin City (24JCZDJC00670). This work was supported by the Key Project of Tianjin Natural Science Foundation (Grant No. 24JCZDJC00670).

REFERENCES

[1] Yin, Q., Wang, Z., Wu, X., Chen, S., *Exploration and Practice of Standardization in Digital Transformation of Spinning Industry*, In: Information Technology & Standardization, 2023, 05, 28–33

[2] Tao, J., Zhang, H., Cheng, X., Liu, N., Zhang, X., *Evenness quality control for worsted pure wool yarn based on quality index number*, In: Journal of Textile Research, 2014, 35, 28–34

[3] Han, P.H., Li, X. R., Liu, R.F., Zhang, S., Yuan, C., *Prediction method of carding process production quality based on digital twin technology*, In: Textile Research Journal, 2024, 94, 5–6, 713–724

[4] Tuser Tirtha, B., Will, M., Kadi, N., *Predicting Fiber Length Characteristics of Recycled Cotton and Cellulose Fiber Blends Using Machine Learning Models*, In: Advanced Theory and Simulations, 2025, 2500086

[5] Ren, J., *Innovative development and prospect of domestic cotton comber*, In: Cotton Textile Technology, 2023, 51, 10, 25–32

[6] Zhang, S., Zhao, J., Liu, B., Li, D., Zhang, F., *Application of carding self-leveling device in spinning quality control*, In: Cotton Textile Technology, 2017, 45, 8–12

[7] Cai, W., Li, J., Gu, X., Li, C., *Design and development of a new self-leveling device for a carding machine*, In: Cotton Textile Technology, 2006, 04, 206–209

[8] Li, X., Ma, C., Zhou, B., *Self-leveling control of digital carding machine*, In: Journal of Textile Research, 2015, 36, 139–143

[9] Wang, C., Li, J., Zhang, G., Li, C., *Weighted adaptive generalized predictive control for carding autoleveler*, In: Journal of Shanghai Jiaotong University (Science), 2006, E-11, 436–439

[10] Zhao, Q., Meng, X., *Enhance the control stability of self-leveling mixing loop*, In: Journal of Textile Research, 2004, 06, 7–9

[11] Yao, J., Ye, G., *Analysis of a new open-loop self-leveling device,* In: Journal of Textile Research, 2005, 03, 44–45

[12] Li, H., Zhou, W., Wang, X., *Self-leveling double open ring of drawing frame*, In: Journal of Textile Research, 2010, 31, 106–109

[13] Mahmood, N., Jamil, N., Shoaib Ahmad, S., *Technological study of auto-leveller at draw frame on cotton yarn quality,* In: Journal of Applied Sciences, 2006, 2, 287–291

[14] Song, S., Yang, Y., Wang, Y., *Weighted temporal association rules based on periodic law*, In: Computer Engineering, 2013, 39, 03, 41–45

[15] Sienkowski, S., Krajewski, M., *On the statistical analysis of the harmonic signal autocorrelation function*, In: International Journal of Applied Mathematics and Computer Science, 2021, 4, 31

[16] Zhang, L., Chen, S., Zhang, Y., *Time series based on autocorrelation acquisition period*, In: J Inf Eng Univ, 2015, 16, 209–213

[17] Chen, H., Feng, Y., Cui, H., *Theory and practice of self-leveling control for drawing frame,* In: Cotton Textile Technology 2020, 12, 21–25

Authors:

LI XINRONG[1,2,3], LIU RONGFANG[1,2,3], SHI SHUAIXING[1,2,3], WANG BIAO[1,2,3], LI LI[1,2,3]

[1]School of Mechanical Engineering, Tiangong University, Tianjin 300387, China

[2]Tianjin Key Laboratory of Advanced Mechatronics Equipment Technology, Tianjin 300387, China

[3]Shaoxing Keqiao Institute of Tiangong University, Shaoxing, Zhejiang 312030, China

Corresponding author:

LI XINRONG

e-mail: lixinrong7507@hotmail.com

Influence of wet thermal treatment on the performance of three-dimensional weft-knitted fabrics intended for personal protective equipment applications

DOI: 10.35530/IT.077.03.2025154

CRISTINA GROSU
MIRELA BLAGA
RODICA HARPA
DANIELA FĂRÎMĂ
MIHAI PENCIUC
ANA RAMONA CIOBANU
MIHAELA PERDEVARĂ

ABSTRACT – REZUMAT

Influence of wet thermal treatment on the performance of three-dimensional weft-knitted fabrics intended for personal protective equipment applications

This study evaluates the influence of wet thermal treatments (washing and steaming) on the structural, comfort, and functional properties of a set of twelve three-dimensional weft-knitted fabrics, all based on a sandwich configuration with identical cotton outer layers and a polyester monofilament binding yarn. The experimental design considered three machine set-up stitch cam divisions NP (13, 12, 11) corresponding to loose, medium and highly compact fabric structures and four binding ratios of the monofilament yarn (1:1; 1:3; 1:7; 1:15). Mass, thickness, and stitch density were measured before and after the wet thermal treatment, while air and water-vapour permeability, bursting strength, abrasion resistance, and dimensional behaviour were determined on the finished fabrics, according to relevant standards. Results showed that mass and stitch density increased, while thickness generally decreased after wet thermal stabilisation. For the finished fabrics, abrasion resistance and bursting strength increased with the monofilament binding ratio, reaching up to 15,000 cycles and 590 kPa, respectively, while air permeability showed an inverse trend, decreasing to approximately 1,000 L/m^2/s for the most compact variants. These findings highlight the role of the binding ratio and stitch cam division of the knitting machine in defining the trade-off between comfort and protective performance. Overall, the investigated fabrics exhibit a balanced structural and functional behaviour, indicating their suitability as constituent layers for Category II PPE, such as gloves, workwear, jackets and vests, where mechanical durability and breathability are required.

Keywords: *sandwich knitted fabrics, wet thermal treatment, structural parameters, comfort, dimensional stability, workwear, PPE applications*

Influența tratamentului de finisare umido-termic asupra performanțelor tricoturilor 3D destinate echipamentelor individuale de protecție

Acest studiu evaluează influența tratamentului de finisare umido-termic (spălare și aburire) asupra proprietăților structurale, de confort și funcționale ale unui set compus din 12 tricoturi tridimensionale (3D) din bătătură, având o configurație tip sandwich, cu straturile exterioare din bumbac, conectate între ele cu ajutorul unui fir monofilamentar din poliester. Tricoturile au fost realizate prin varierea a doi parametri tehnologici și structurali: adâncimea de buclare (NP = 13, 12, 11), corespunzătoare structurilor cu compactitate scăzută, medie, ridicată și raportul de legare al firului monofilamentar (1:1; 1:3; 1:7; 1:15). Masa, grosimea și desimea tricotului au fost măsurate înainte și după tratamentul umido-termic, în timp ce permeabilitatea la aer și la vapori de apă, rezistența la plesnire, rezistența la abraziune și stabilitatea dimensională, au fost evaluate pentru tricoturile în stare finisată. Rezultatele au evidențiat o creștere a masei și a desimii tricotului, în timp ce grosimea a prezentat o tendință generală de scădere ca urmare a aplicării tratamentului umido-termic. Rezistența la abraziune și rezistența la plesnire au crescut odată cu raportul de legare al monofilamentului, ajungând până la 15.000 de cicluri și, respectiv, 590 kPa, în timp ce permeabilitatea la aer a prezentat o tendință inversă, scăzând la aproximativ 1.000 L/m^2/s pentru structurile cele mai compacte. Aceste rezultate evidențiază rolul raportului de legare și al adâncimii de buclare în armonizarea performanțelor de protecție cu cerințele de confort. În ansamblu, tricoturile 3D investigate prezintă un comportament structural și funcțional echilibrat, confirmând aplicabilitatea lor ca materiale cu rol activ de protecție în configurația EIP de Categoria II, cum ar fi mănuși, îmbrăcăminte de lucru, jachete și veste, unde sunt necesare atât durabilitatea mecanică, cât și respirabilitatea.

Cuvinte-cheie: *tricoturi stratificate, tratament umido-termic, parametri de structură, confort, stabilitate dimensională, echipamente de lucru, echipamente individuale de protecție*

INTRODUCTION

Personal protective equipment (PPE) represents a crucial component in ensuring safety and occupational health in industrial environments. The design of PPE materials has progressively evolved from rigid, heavy, and low-comfort structures to advanced textile systems capable of providing both mechanical protection and physiological comfort. Among such textile systems, three-dimensional knitted fabrics are playing an increasingly important role due to their structural

versatility, conformability, and the possibility of engineering multilayer configurations that meet diverse protection requirements. Previous studies of the authors have also explored the use of these fabrics for vibration damping and protective applications, highlighting the relationship between their structural design and functional performance [1, 2].

In recent years, sandwich or spacer knitted fabrics have been widely studied for use in PPE applications, particularly in gloves, protective garments and cushioning layers. Their three-dimensional architecture, composed of two outer knitted layers connected by monofilament or multifilament binding yarns, enables the creation of lightweight, breathable, and mechanically resilient materials [3, 4]. The ability to tune their structural parameters, such as the binding ratio and stitch cam depth setting, offers a significant advantage in controlling mass, thickness, porosity and consequently the comfort and protection levels.

While numerous studies have investigated the mechanical and comfort-related performance of technical knitted fabrics in their finished state, comparative analyses assessing fabric properties before and after wet thermal stabilisation treatments remain limited [5]; a systematic correlation between wet thermal stabilisation and structural rearrangements in three-dimensional knitted structures intended for PPE applications has not been extensively reported. Unlike conventional finishing processes, these treatments are not designed to enhance surface appearance or handle, but to stabilise the knitted structure by releasing the residual stresses generated during knitting. Understanding how technological parameters such as the binding ratio and stitch cam depth setting affect the properties of stabilised fabrics is essential for designing reliable, high-performance materials.

The present study aims to investigate the effect of wet thermal stabilisation on the structural, comfort, and functional properties of three-dimensional weft-knitted fabrics designed for PPE applications. These materials are evaluated in accordance with the general framework established by Regulation (EU) 2016/425 [6] on PPE and the essential performance requirements specified in EN ISO 13688:2013+A1: 2021 [7], which define criteria for ergonomics, comfort, innocuousness, and mechanical robustness of protective textiles. By analysing twelve variants differing in binding ratio and stitch cam depth setting, this work seeks to identify how these technological parameters influence the balance between mechanical resistance, permeability, and dimensional behaviour. The results provide a framework for selecting and engineering knitted fabrics suitable for inclusion as constituent layers in Category II PPE, such as gloves, workwear, jackets, and vests.

MATERIALS AND METHODS

Knitted fabrics

Twelve three-dimensional weft knitted fabrics were produced on a flat knitting machine, each consisting of two identical cotton outer layers (100% cotton, Nm 50/1×2) interconnected by an inner high-tenacity polyester monofilament binding yarn (5.5 cN/dtex) with a diameter of 0.10 mm.

The binding yarn (E-SPACE®) was especially developed by the Monosuisse company as an alternative to conventional polyurethane foam fillings in three-dimensional textile structures, providing high elastic recovery, reduced weight, enhanced breathability and effective structural reinforcement of the new architecture [8]. Two technological variables were controlled: (i) the monofilament binding ratio (four levels, coded A–D) and (ii) the stitch cam depth setting (three levels: 13, 12 and 11, corresponding to loose, medium and highly compact structures, coded 1–3). The binding yarn setting was kept constant across all variants (table 1). For clarity, codes A1-D3 refer to the unfinished fabrics, while the suffix (F) denotes the corresponding fabrics after wet thermal treatment (washing and steaming), applied as a structural stabilisation stage.

Table 1

KNITTED FABRICS CODING

Binding ratio	Stitch cam division (N.P.)	Knitted fabric code	
		Untreated fabric	Treated fabric
1:1	13	A1	A1 (F)
	12	A2	A2 (F)
	11	A3	A3 (F)
1:3	13	B1	B1 (F)
	12	B2	B2 (F)
	11	B3	B3 (F)
1:7	13	C1	C1 (F)
	12	C2	C2 (F)
	11	C3	C3 (F)
1:15	13	D1	D1 (F)
	12	D2	D2 (F)
	11	D3	D3 (F)

Wet thermal treatment

The wet thermal treatment was applied as a structural stabilisation stage after knitting, using a domestic-type manual procedure [9], in accordance with the general principles described in EN ISO 3759:2008 [10] and EN ISO 6330:2022 [11]. The washing sequence consisted of the following steps: ***soaking*** in a warm water bath at (30–40)°C for 60 min, with a liquor ratio of 1:30 and a detergent concentration of 3 g/L, followed by ***washing*** under gentle manual agitation, at 40±2°C for 15 min. A commercially available manual laundry detergent intended for delicate white and coloured textiles (Savex®) was used, selected for its mild formulation based on anionic surfactants and the absence of bleaching agents or aggressive finishing additives, to minimise any chemical influence on the structural behaviour of the knitted fabrics. After draining the washing bath, the specimens were

subjected to five consecutive ***rinsing*** cycles in clean water, using a liquor ratio of 1:50. Rinsing was carried out at an initial water temperature of 40°C for 3 min per cycle, followed by repeated rinsing with gradual cooling of the water. Excess water was removed by gentle manual pressing without wringing. The samples were then ***dried*** flat on a horizontal surface until constant mass was achieved. After drying, the fabrics were first subjected to a steaming step to ensure controlled ***re-moistening*** of the structure, followed by ***ironing*** using a steam iron at approximately 200°C, corresponding to the recommended temperature for cotton fabrics. The treated panels were subsequently relaxed under standard atmospheric conditions for 24 hours before dimensional measurements. This treatment sequence ensured the effective release of residual stresses and the structural stabilisation of the knitted fabrics before further testing.

RESULTS AND DISCUSSIONS

The experimental design primarily focused on identifying the influence of the wet thermal treatment on the defining structural parameters of the three-dimensional weft knitted fabrics (i.e. fabric mass, fabric thickness and stitch density). Comfort and function-related properties (i.e. air permeability, dimensional behaviour, abrasion resistance, bursting strength and deformation) were subsequently assessed on the wet thermal-stabilised fabrics, as this condition represents the intended and relevant state for PPE-oriented performance assessment.

The influence of wet thermal treatment on structural parameters

Influence on fabric mass

The mass per unit area of the knitted fabrics [12] generally increased after wet thermal treatment, indicating a densification of the loop structure associated with the release of internal stresses generated during knitting. For the treated fabrics, mass values ranged from approximately 270 to 640 g/m^2, depending on the stitch cam division and the monofilament binding ratio. This increase followed a consistent trend across all fabric groups, with higher mass values recorded for lower stitch cam divisions (NP 11) and higher binding ratios (groups C and D). For instance, variants knitted at NP = 11 showed post-treatment masses above 440 g/m^2, reaching up to 642 g/m^2 for D3 (F), whereas looser structures (NP=13) generally remained below 430 g/m^2. The mass growth is mainly attributed to structural compaction occurring during the combined washing and steaming process, which resulted in shorter loop lengths and a more cohesive fabric surface. Only two exceptions were recorded, variants A1 and B1, where the mass decreased slightly after treatment (from 294 to 273 g/m^2 and from 278 to 268 g/m^2, respectively). These variants also exhibited among the highest extension values in the wale direction after stabilisation, leading to a looser configuration and consequently, to a reduction in surface mass (figure 1). From an application perspective, the resulting mass range remains compatible with flexible PPE components, where sufficient surface mass is required to ensure mechanical robustness, while maintaining conformability and ergonomic comfort.

Influence on fabric thickness

As shown in figure 2, the thickness response to wet thermal treatment [13] depended strongly on the structural parameters. Most fabric variants exhibited a moderate decrease in thickness, from initial values ranging between 2.75 and 5.67 mm for untreated fabrics to a narrower range of 2.04 to 4.00 mm after wet thermal treatment, indicating a consolidation of the sandwich architecture. This behaviour is attributed to a partial collapse of the sandwich structure, which promoted closer contact between the outer layers and the monofilament binding yarn, resulting in a reduction of the overall fabric height. For variants produced with a higher stitch cam division (NP 13), a pronounced thickness reduction was observed after treatment, reflecting the relaxation and rearrangement of initially looser loop structures. In contrast, fabrics with higher monofilament binding ratios (groups C and D) retained comparatively greater thickness due to stronger internal reinforcement, confirming the stabilising effect of an increased number of monofilament connections. From an application perspective, the resulting thickness interval of the stabilised fabrics remains suitable for flexible PPE components, where moderate thickness is required

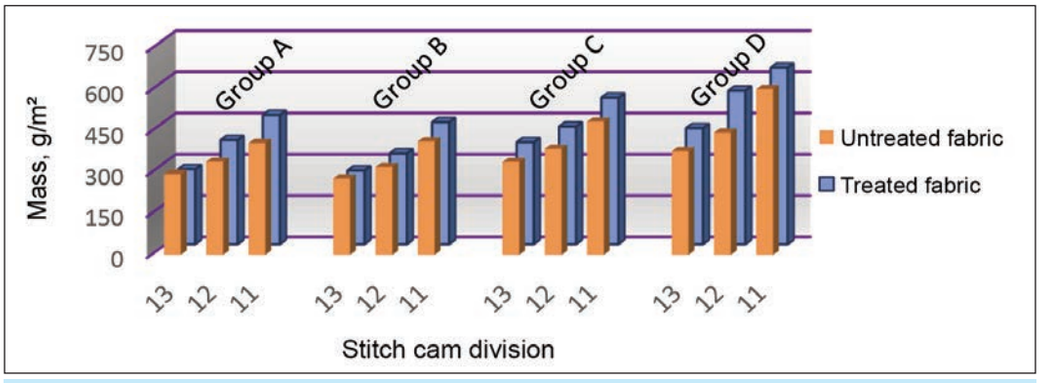

Fig. 1. Fabric mass per unit area (g/m^2) before and after wet thermal treatment

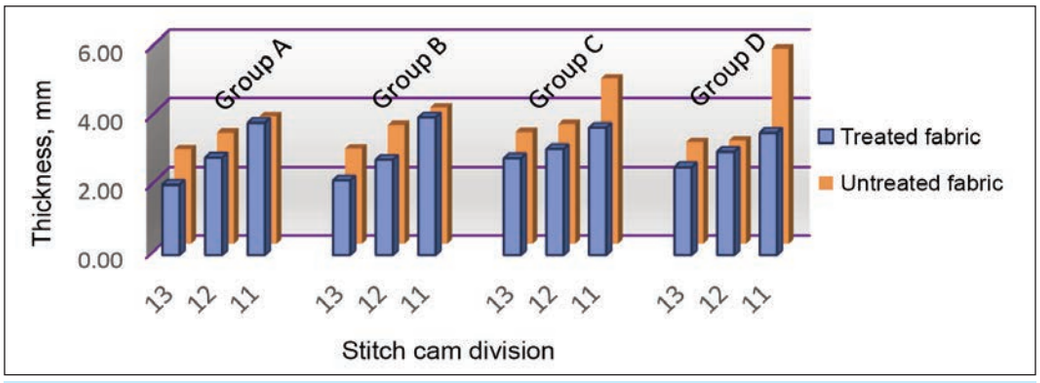

Fig. 2. Fabric thickness (mm) before and after wet thermal treatment

to provide mechanical support and durability while preserving conformability and ergonomic comfort.

Influence on fabric stitch density

Stitch density was determined according to EN 14971 [14], both before and after wet thermal treatment, in order to quantify the degree of structural compactness and the dimensional rearrangement of the knitted fabrics. After wet thermal treatment, stitch density increased in both wale and course directions, reflecting the contraction of the knitted structure during stabilisation. For the treated fabrics, stitch density values ranged approximately from 970 to over 2100 stitches/5 cm^2, depending on the stitch cam division and the monofilament binding ratio. This increase followed a consistent pattern and was more pronounced in fabrics knitted with the smallest stitch cam division (NP = 11), compared to those knitted at NP = 12 or NP = 13. The reduced cam depth results in shorter loop lengths and inherently higher compactness, which amplifies the dimensional contraction occurring during wet thermal stabilisation. The combined increase in mass per unit area and stitch density confirms the effective structural stabilisation of the knitted fabrics after wet thermal treatment, which is essential for ensuring uniformity and reproducibility in technical and protective textile applications, where dimensional stability and mechanical integrity are required without excessively compromising flexibility (figure 3).

Comfort properties of wet thermal-treated fabrics

Air permeability after wet thermal treatment

The air permeability of the wet thermal-treated fabrics exhibited a systematic decrease in air flow rate with increasing structural compactness, primarily governed by the stitch cam division and the monofilament binding ratio. Fabrics knitted at NP = 13 (loose setting) recorded the highest air flow rates, exceeding 2000 L/m^2/s, whereas those produced at NP = 11 (compact setting) showed values close to 1000 L/m^2/s. Within each stitch cam division, air permeability decreased progressively from group A (binding ratio 1:1) to group D (binding ratio 1:15), as higher binding ratios involve an increased number of monofilament connections and a denser inner layer (figure 4). The reduced permeability observed in the stabilised fabrics indicates that the increased number and length of monofilament connections between the outer layers lead to a reduction in effective pore size, thereby restricting air passage through the three-dimensional structure. This behaviour is consistent with previously reported trends in multilayer knitted structures, where increased loop compactness and reduced inter-yarn spacing result in lower air permeability [3, 15, 16]. Despite this reduction, the measured permeability values remain within ranges compatible with PPE applications requiring a balance between

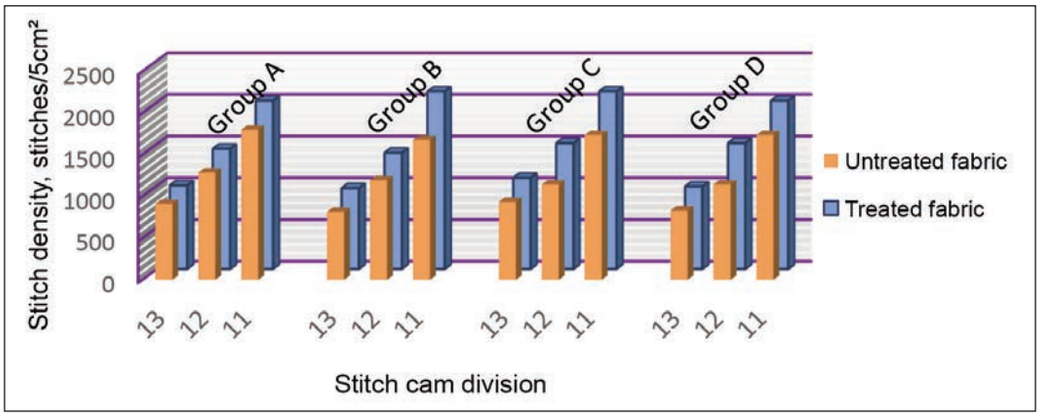

Fig. 3. Stitch density of the fabric (stitches/5 cm^2) before and after wet thermal treatment

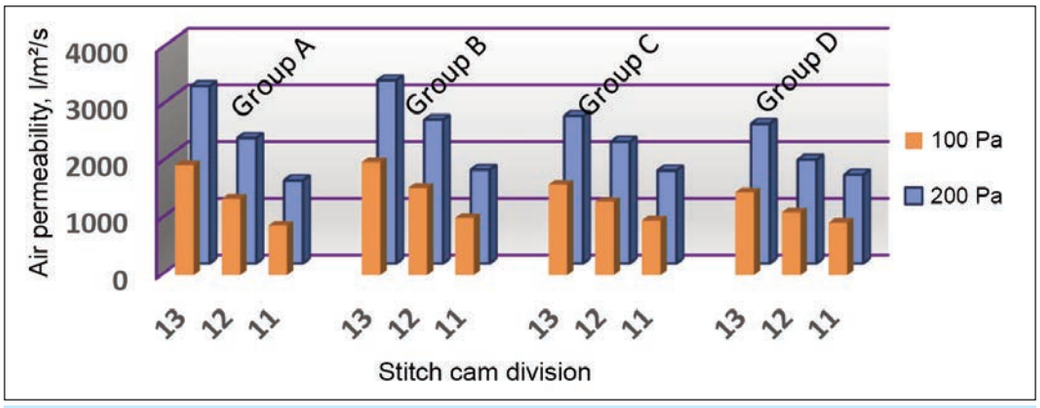

Fig. 4. Air permeability (L/m^2/s) of the wet thermal-treated fabrics

breathability and mechanical integrity, such as gloves and workwear components.

Dimensional behaviour after wet thermal treatment

The dimensional behaviour of the knitted fabrics was evaluated after the complete wet thermal treatment sequence- consisting of washing, drying, steaming and relaxation- according to EN ISO 5077:2008 [17]. Dimensional changes were expressed as a percentage, in both the course and wale directions, using the following relation:

$$\lambda = \frac{l_1 - l_0}{l_0} \cdot 100, \ \% \qquad (1)$$

where l_0 is the distance between reference marks, before the treatment (mm), and l_1 – the corresponding distance, after the treatment (mm).

A positive value of λ indicates elongation, while a negative value denotes shrinkage [18].

As illustrated in figure 5, the dimensional changes were more pronounced in the wale direction, reaching a contraction of up to –27%, whereas the course direction exhibited moderate extension values, up to +28%. This anisotropic behaviour reflects the structural rearrangement of the knitted loops during the wet thermal stabilisation process. Fabrics with looser structures (NP 13, binding ratio 1:1) showed higher dimensional deformation, while more compact variants (NP 11, binding ratio 1:15) exhibited superior dimensional stability. These results confirm that the applied wet thermal treatment effectively released the internal stresses accumulated during knitting, leading to a stable structural configuration suitable for subsequent functional testing.

Functional properties of wet thermal-treated fabrics

Bursting strength and deformation of wet thermal-treated fabrics

The bursting strength [19] of the stabilised knitted fabrics increased markedly with both structural compactness and the monofilament binding ratio. Values ranged from approximately 227 kPa for the A1 (F) variant to about 590 kPa for D3 (F), indicating that tighter interconnections between the outer layers

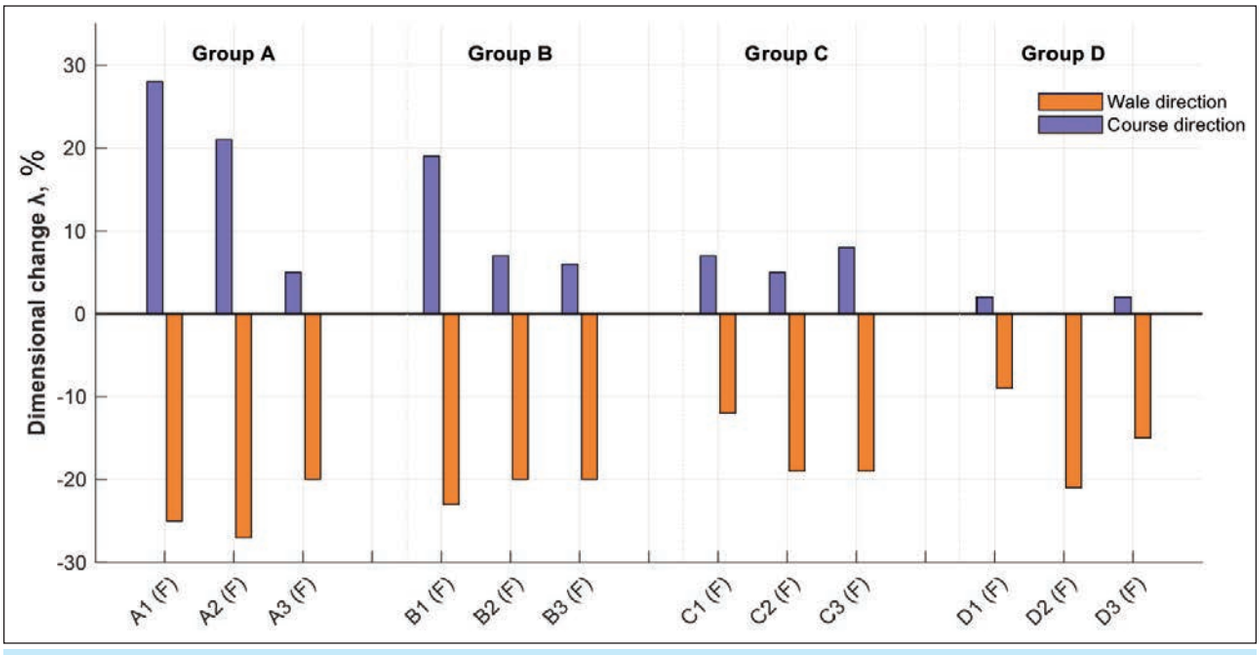

Fig. 5. Dimensional changes (%) in wale and course directions after wet thermal treatment

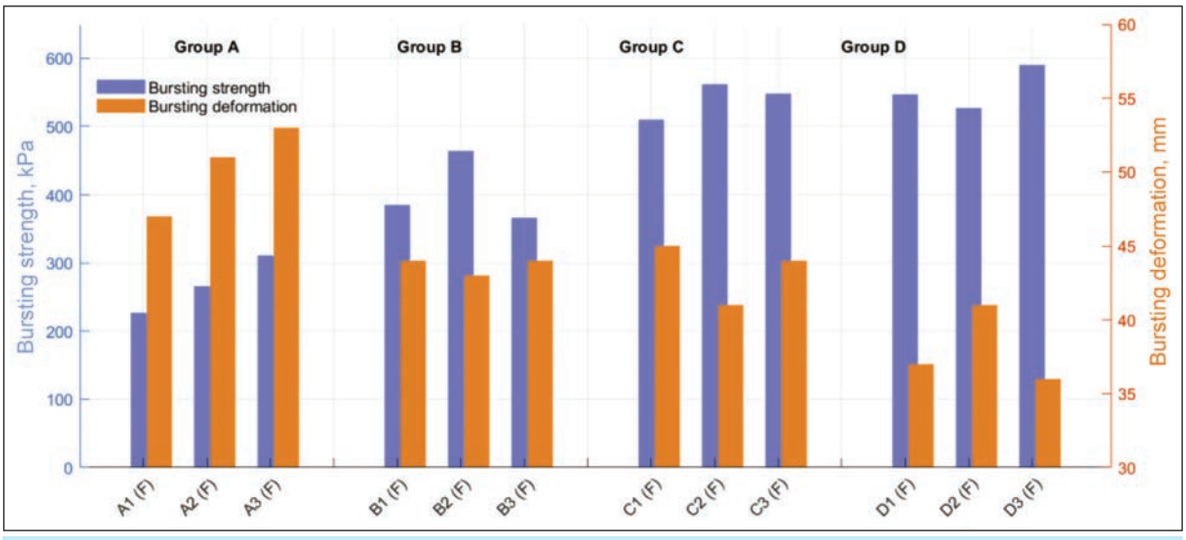

Fig. 6. Bursting strength (kPa) and deformation (mm) of the wet thermal-treated fabrics

significantly enhance resistance to multidirectional stress. This improvement can be attributed to the increased number of binding points, which promote a more uniform distribution of the applied load across the three-dimensional network, thereby reducing localised strain concentration. Conversely, bursting deformation (expressed in mm) exhibited an inverse trend, slightly decreasing with increasing fabric density. This behaviour suggests that looser fabrics (groups A and B) were more extensible and capable of sustaining greater elastic deformation before rupture, whereas more compact fabrics (groups C and D) provided superior strength at the expense of reduced deformability (figure 6). The observed balance between strength and deformation confirms that the monofilament binding ratio is a key parameter governing the mechanical response of spacer knitted fabrics, in agreement with previous studies on knitted structures for protective and technical applications [12, 20].

Abrasion resistance of wet thermal-treated fabrics

The abrasion resistance [21] results showed a pronounced dependence on the internal architecture of the knitted sandwich structure, particularly on the monofilament binding ratio and stitch cam division. Fabrics from groups A and B, characterised by a lower binding ratio (1:1 and 1:3), exhibited moderate abrasion resistance, with failure occurring between 3300 and 10,000 abrasion cycles. In contrast, samples from groups C and D (binding ratios 1:7 and 1:15) withstood up to 15,000 abrasion cycles without significant surface damage, highlighting the mechanical reinforcement provided by the increased number of monofilament connections. This reinforcement effectively restricted yarn mobility and reduced frictional wear, thereby enhancing endurance under repeated contact. However, the increased internal reinforcement was also associated with reduced elasticity and breathability, consistent with the trade-off previously observed between abrasion resistance, bursting strength and air permeability (figure 7).

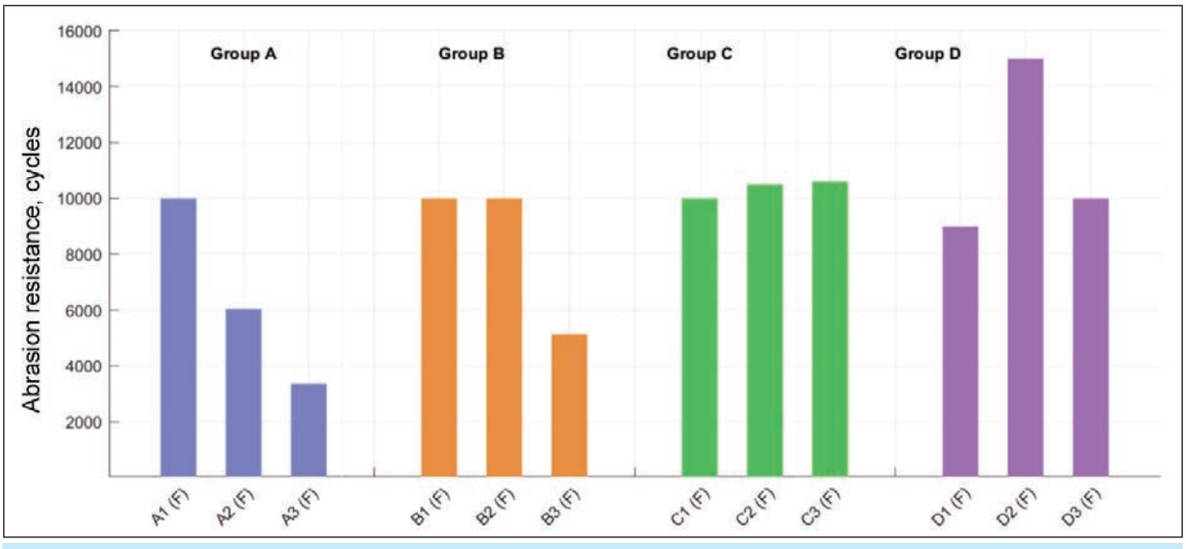

Fig. 7. Abrasion resistance (cycles) of the wet thermal-treated fabrics

These findings confirm that an optimal balance between flexibility and abrasion durability can be achieved by tailoring the monofilament binding ratio, in agreement with prior studies on technical and protective knitted fabrics [22, 23].

The mechanical performance results demonstrate that the three-dimensional weft-knitted fabrics stabilised through the wet thermal treatment process exhibit property levels corresponding to Category II personal protective equipment, as defined by Regulation (EU) 2016/425. According to this regulation, Category II PPE covers protective equipment intended for intermediate risks, which are neither classified as minimal risks under Category I nor as risks that may cause very serious consequences or irreversible harm under Category III. In accordance with the general framework of EN ISO 13688, which establishes requirements related to material robustness, dimensional stability and ergonomic comfort, the investigated fabrics exhibited a balanced combination of mechanical resistance and comfort-related properties. In particular, the experimentally determined abrasion resistance values of up to 15,000 cycles correspond to performance level 4, while the bursting strength values ranging between 227 and 590 kPa correspond to levels 1–3, according to the classification system defined in EN 388:2016+A1: 2018 [24] for protection against mechanical risks. These performance levels are representative of PPE intended for intermediate mechanical and physical risks, confirming that the stabilised knitted fabrics are suitable as constituent layers for Category II PPE applications, such as gloves, workwear, jackets and vests, where mechanical robustness must be ensured without compromising comfort and conformability [25–27].

CONCLUSIONS

The present study investigated the influence of wet thermal treatment, applied as a structural stabilisation stage immediately after knitting, on the structural, comfort-related and functional properties of weft-knitted sandwich fabrics intended for personal protective equipment applications. By systematically varying the monofilament binding ratio and the stitch cam division, clear relationships were identified between manufacturing parameters and the resulting fabric performance.

The results showed that the wet thermal treatment induced a structural rearrangement of the knitted architecture, reflected by changes in mass, thickness and stitch density, confirming the effective release of residual stresses generated during the knitting process. An increase in structural compactness was generally observed after stabilisation, with its magnitude strongly dependent on both the stitch cam division and the monofilament binding ratio.

From a structural perspective, mass per unit area and stitch density generally increased, whereas thickness slightly decreased due to the closer contact between the outer layers and the monofilament binding yarn. Dimensional analysis revealed anisotropic behaviour, characterised by contraction in the wale direction and moderate extension in the course direction, depending on fabric looseness and binding configuration.

In terms of comfort-related properties, air permeability decreased systematically with increasing structural compactness and binding ratio, indicating that reduced inter-yarn spacing and tighter loop configurations limited airflow through the fabric structure.

With respect to functional properties, both bursting strength and abrasion resistance improved substantially with higher binding ratios and tighter stitch cam settings, reaching maximum values of 590 kPa and 15,000 abrasion cycles, respectively. This mechanical reinforcement was associated with a reduced deformation capacity at rupture and lower air permeability, highlighting the inherent trade-off between mechanical protection and comfort-related performance.

Overall, the findings demonstrate that the structural parameters, namely the monofilament binding ratio and stitch cam division, are key factors governing the balance between structural stability, mechanical resistance and comfort-related properties. Within the scope of the investigated characteristics, the stabilised knitted fabrics exhibit a balanced structural and functional behaviour, supporting their suitability as constituent layers for Category II personal protective equipment, such as gloves and workwear garments, jackets, and vests.

ACKNOWLEDGEMENT

This paper is published within the framework of the project Centre for Research and Innovation in Textiles and Fashion Industry – SMART-Tex-IS, MySmis code 334492.

REFERENCES

[1] Grosu, C., Scarlat, V.R., Stefan, E.I., Blaga, M., *Interactive Guide for Study the Vibrations Protection Textile Materials*, The 17th International Scientific Conference eLearning and Software for Education, 2021

[2] Blaga, M., Seghedin, N.E., Horodinca, M., Grosu, C, Gaaloul, H., Babay, A., Dhouib, S., Azouz, B., *Behaviour of Knitted Materials in a Vibrating Environment*, In: Materials, 2025, 18, 3, 1–22

[3] Asayesh, A., Shahangian, Z.S., *The influence of stress relaxation on the compressional properties of weft-knitted spacer fabrics compared to PU foam*, In: Rapid Prototyping Journal, 2025, 31, 9, 1977–1989

[4] Dejene, B.K., Gudayu, A.D., *Exploring the potential of 3D woven and knitted spacer fabrics in technical textiles: A critical review*, In: Journal of Industrial Textiles, 2024, 54

[5] Bukhonka, N.P., *Experimental study of structural characteristics, dimensional change in washing, non-creasing properties and air permeability of Swiss double piqué flax knit fabrics*, In: Journal of Engineered Fibers and Fabrics, 2023, 18, 1–20
[6] European Parliament and of the Council, *Regulation (EU) 2016/425 on personal protective equipment*, 2016
[7] EN ISO 13688:2013+A1:2021. Protective clothing – General requirements, 2013
[8] Monosuisse, *Spacer Fabrics*, Available at: https://monosuisse.com/ [Accessed on August 2025]
[9] Harpa, R., *Metrologie in Textile – Pielarie. Aplicatii ale proceselor de măsurare*, Performantica, 2008
[10] EN ISO 3759. Textiles – Preparation, marking and measuring of fabric specimens and garments in tests for determination of dimensional change, 2008
[11] EN ISO 6330. Textiles – Domestic washing and drying procedures for textile testing, 2022
[12] EN 12127. Textiles – Fabrics – Determination of mass per unit area using small samples, 2003
[13] EN ISO 5084. Textiles – Determination of thickness of textiles and textile products, 2001
[14] EN 14971. Textiles – Knitted fabrics – Determination of number of stitches per unit length and per unit area, 2006
[15] Akkas, M., Erdumlu, N., Candan, C., *Effects of structural parameters on the bursting strength and air permeability of knitted fabrics*, In: Fibres & Textiles in Eastern Europe, 2017, 25, 1, 59–64
[16] EN ISO 9237. Textiles – Determination of permeability of fabrics to air, 1995
[17] ISO 5077. Textiles – Determination of dimensional change in washing and drying, 2007
[18] Acar, E., Tama D. B., Özdemir, G., *Impact of repetitive washing on recycled cotton knitted fabrics: a comprehensive physical property analysis*, In: Industria Textila, 2025, 76, 1, 98–106
[19] EN ISO 13938-2. Textiles – Bursting properties of fabrics. Part 2: Pneumatic method, 2019
[20] Zhang Y., Hu, H., *Compression and mechanical performance of warp-knitted spacer fabrics for protective applications*, In: Textile Research Journal, 2014, 84, 6, 659–670
[21] EN ISO 12947-2. Textiles – Determination of abrasion resistance of fabrics by the Martindale method. Part 2: Determination of specimen breakdown, 2016
[22] Matusiak M., Skowrońska, A., *Influence of structural parameters of knitted fabrics on abrasion resistance and pilling tendency*, In: Textile Research Journal, 2019, 89, 3, 467–478
[23] Özdil, N., Kanat, Z.E., Topuz, B.E., Özçelik, G., Mengüç, G.S., *Properties of the fabrics knitted from yarns with different slub parameters*, In: Industria Textila, 2025, 76, 1, 89–97
[24] EN 388:2016 + A1:2018. Protective gloves against mechanical risks, 2018
[25] Grosu, C., Blaga, M., Seghedin, N.-E., Avădanei, M.-L., Perdevară, M., Marmarali, A., *Knitted linings for protective equipment against vibrations*, In: Industria Textila, 2025, 76, 1, 44–51, https://doi.org/10.35530/IT.076.01.2023142
[26] Loghin, E.C., Dulgheriu, I., Hristian, L., Buhu, L., Avădanei, M., Ionesi, S.D., *Assessing the quality level of the technical fabrics intended for protective equipment for firefighters by determining synthetic indicators*, In: Industria Textila, 2024, 75, 6, 710–721, http://doi.org/10.35530/IT.075.06.202465
[27] Lexi, T., Fumei, W., Tong, P., Yi, S., Zimin, J., Xinghua, H., Hua, S., *Investigation of thermal insulation of cold protective clothing under different underwear and ambient conditions*, In: Industria Textila, 2025, 76, 1, 31–37, https://doi.org/10.35530/IT.076.01.2023131

Authors:

CRISTINA GROSU[1,2], MIRELA BLAGA[2,3], RODICA HARPA[2], DANIELA FĂRÎMĂ[2], MIHAI PENCIUC[2], ANA RAMONA CIOBANU[2], MIHAELA PERDEVARĂ[2]

[1]National Research and Development Institute for Textiles and Leather,
16 Lucretiu Patrascanu Street, 030508, Sector 3, Bucharest, Romania
e-mail: cristina.grosu@incdtp.ro

[2]''Gheorghe Asachi'' Technical University of Iasi, Romania, Faculty of Industrial Design and Business Management,
Blvd. Mangeron, No. 29, 700050, Iasi, Romania
e-mail: rodica.harpa@academic.tuiasi.ro; daniela.farima@academic.tuiasi.ro; mihai.penciuc@academic.tuiasi.ro; ana-ramona.ciobanu@academic.tuiasi.ro; mihaela.perdevara@student.tuiasi.ro

[3]Centre for Research and Innovation in Textiles and Fashion Industry – SMART-Tex-IS,
Prof. Dr. Doc. Dimitrie Mangeron, 29, 700050, corp TEX 4, Iasi, Romania

Corresponding author:

MIRELA BLAGA
e-mail: mirela.blaga@academic.tuiasi.ro

Advancing the future of fashion: a bibliometric analysis of 3D technology in the apparel industry (2011–2024)

DOI: 10.35530/IT.077.03.202544

XIZHUO CHEN
ANDING LIU
YU HOU
BIN LI

ABSTRACT – REZUMAT

Advancing the future of fashion: a bibliometric analysis of 3D technology in the apparel industry (2011–2024)

The application of 3D technology in the apparel industry has accelerated significantly over the past decade, catalysing innovations in digital design, virtual simulation, and sustainable manufacturing. This study conducts a comprehensive bibliometric analysis of 1,079 publications (2011–2024) from the Web of Science using CiteSpace, mapping the field's temporal, spatial, and thematic evolution. To move beyond descriptive mapping and provide a critical interpretive lens, we introduce a three-tier conceptual framework that structures the analysis around the Technical core layer (e.g., 3D body scanning, virtual simulation, additive manufacturing), the Application and Integration layer (e.g., virtual try-on, digital showrooms, Metaverse fashion), and the Macro-impact layer (e.g., sustainability, consumer behaviour, ethical implications). Findings reveal China's dominant role in both research output and influence, driven by its robust apparel industry and national digitalisation policies. While significant progress has been made, persistent challenges remain, including the fidelity-realizability gap in fabric simulation, algorithmic biases in AI-driven sizing, and interoperability across digital platforms. Future research should prioritise enhancing simulation realism, developing standardised digital formats, integrating multi-sensory feedback, and establishing ethical frameworks to support a more inclusive and sustainable digital fashion ecosystem. This study offers a structured roadmap for scholars and practitioners aiming to leverage 3D technologies for transformative impact in the global apparel industry.

Keywords: *3D technology, virtual simulation, body scanning, digital fashion, sustainability, bibliometric analysis, conceptual framework*

Construind viitorul modei: o analiză bibliometrică a tehnologiei 3D în industria de îmbrăcăminte (2011–2024)

Aplicarea tehnologiei 3D în industria de îmbrăcăminte a cunoscut o accelerare semnificativă în ultimul deceniu, catalizând inovații în domeniul proiectării digitale, al simulării virtuale și al producției durabile. Prezentul studiu realizează o analiză bibliometrică cuprinzătoare a 1.079 de publicații (2011–2024) din Web of Science, utilizând CiteSpace, și cartografiază evoluția temporală, spațială și tematică a domeniului. Pentru a depăși cartografierea descriptivă și a oferi o perspectivă interpretativă critică, introducem un cadru conceptual pe trei niveluri care structurează analiza în jurul nivelului Tehnic de bază (de exemplu, scanarea 3D a corpului, simularea virtuală, fabricația aditivă), nivelului de Aplicare și integrare (de exemplu, probarea virtuală, showroom-urile digitale, moda Metaverse) și nivelului de Impact macro (de exemplu, sustenabilitatea, comportamentul consumatorilor, implicațiile etice). Rezultatele relevă rolul dominant al Chinei atât în ceea ce privește cercetarea, cât și în ceea ce privește influența, datorită industriei sale solide de articole de îmbrăcăminte și politicilor naționale de digitalizare. Deși s-au înregistrat progrese semnificative, persistă încă o serie de provocări, printre care decalajul dintre fidelitate și fezabilitate în simularea materialelor textile, prejudecățile algoritmice în stabilirea mărimilor bazată pe IA și interoperabilitatea între platformele digitale. Cercetările viitoare ar trebui să acorde prioritate îmbunătățirii realismului simulării, dezvoltării de formate digitale standardizate, integrării feedback-ului multisenzorial și stabilirii unor cadre etice pentru a sprijini un ecosistem digital al modei mai incluziv și mai durabil. Acest studiu oferă un parcurs structurat pentru cercetători și practicieni care doresc să utilizeze tehnologiile 3D pentru a genera un impact transformator în industria globală a articolelor de îmbrăcăminte.

Cuvinte-cheie*: tehnologie 3D, simulare virtuală, scanare corporală, modă digitală, sustenabilitate, analiză bibliometrică, cadru conceptual*

INTRODUCTION

In recent years, the apparel industry has been progressively transforming through digitalisation and intelligentization. Traditional fashion design faces challenges such as low efficiency, limited variety, long sample-making cycles, and high development costs, prompting the market to demand higher standards for design. As a three-dimensional digital technology supported by computers and the Internet, 3D technology has evolved to construct virtual environments and simulate the real world with high realism and interactivity. Its application in fashion design significantly expands designers' creative possibilities and serves as a key to overcoming the limitations of traditional design. With 3D technology, designers and users can achieve highly realistic silk garment effects and transcend the constraints of traditional flat

designs through 360-degree simulation displays. Integrating 3D digital technology into the fashion industry is gradually transforming traditional design and manufacturing processes. It plays a crucial role in achieving zero-waste designs, reducing inventory, streamlining production, and promoting environmental sustainability. This not only enhances the efficiency and quality of the fashion manufacturing sector but also captures shifts in consumer demand, fostering healthy development on both the supply and demand sides. Despite the growing body of research and technological advancements in the field of 3D apparel, existing studies lack systematic reviews of research hotspots and development trends.

Therefore, this study selects relevant literature from the Web of Science database as the research object and employs CiteSpace for visualisation analysis to map the knowledge landscape. The aim is to review the global research progress in the 3D apparel domain over the past two decades and identify research hotspots, evolution trends, and future directions.

While bibliometric analysis is powerful for mapping the intellectual structure of a field, identifying key contributors, popular topics, and temporal trends, a purely descriptive approach offers limited insight into the *interconnections* between technological developments, their practical applications, and their broader implications. To address this gap and provide a more critical and interpretative lens, this study introduces a three-tier conceptual framework (figure 1) to analyse the findings. This framework posits that research in 3D apparel technology evolves through the dynamic interplay of three layers:

1. The Technical core layer, which encompasses foundational technologies such as 3D body scanning, virtual garment simulation, and additive manufacturing.
2. The Application and Integration layer, where core technologies are synthesised into practical solutions like virtual try-on systems and digital showrooms.
3. The Macro-impact layer, which addresses the broader consequences of these technologies on sustainability, consumer behaviour, and ethical norms.

This framework will not only serve to organise the bibliometric results but also to critically interpret them. It guides our analysis beyond describing *what* the research hotspots are, to exploring *why* they have emerged and *how* they influence and are influenced by broader industry and societal trends. Consequently, this paper seeks to not only map the landscape of 3D apparel technology research but also to provide a structured understanding of its drivers, dynamics, and future trajectory.

DATA SOURCES AND RESEARCH METHODS

Data sources

This study focuses on Web of Science (WOS), one of the most comprehensive and authoritative academic databases, covering high-impact journals across disciplines, including natural sciences, engineering, and biomedical sciences. Its robust indexing capabilities and multidisciplinary scope make it particularly suitable for bibliometric analysis [1]. The keywords “cloth”, “clothes”, “garment”, or “clothing” were used for retrieval, with an additional requirement that the

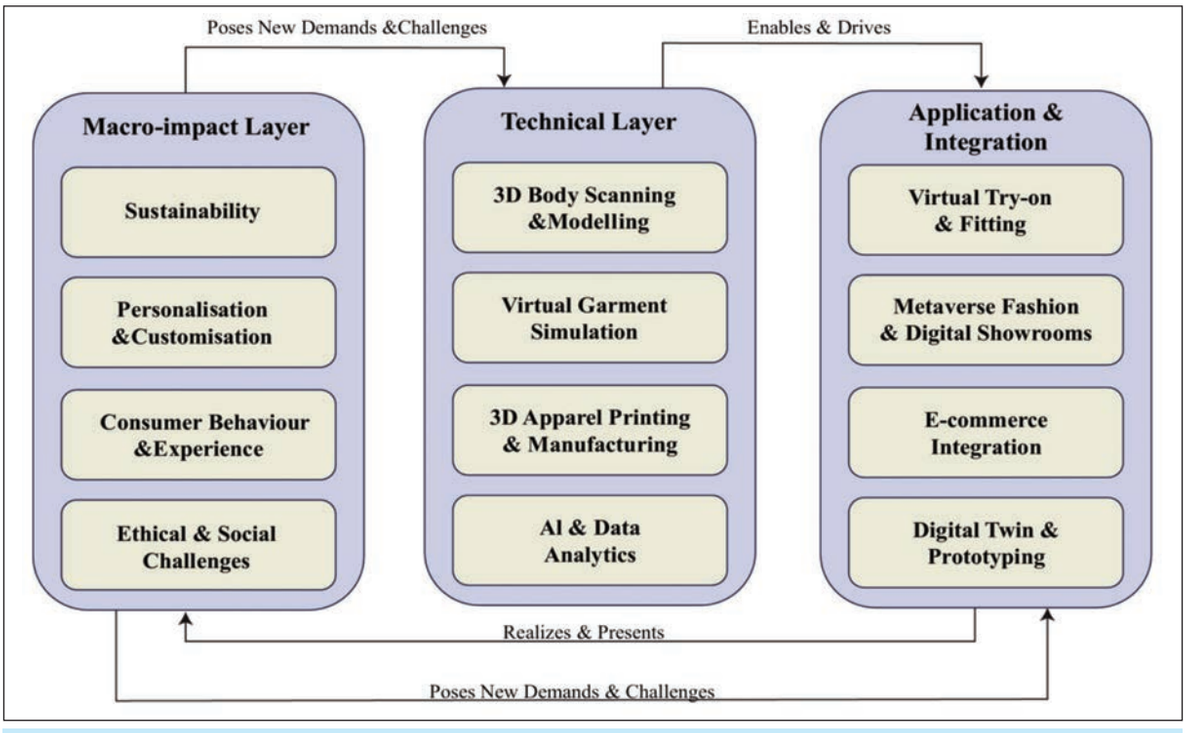

Fig. 1. A conceptual framework for analysing 3D apparel technology research, showing the interplay between the Technical core, Application & Integration, and Macro-impact layers

search results must include “3D” (include 3D). The time range for retrieval was not restricted. After deduplication using CiteSpace, all records were manually reviewed and validated. A total of 1,079 valid documents were identified, covering 387 journals, 4,095 authors, 2,525 institutions, and 221 countries and regions. The data retrieval was completed on December 28, 2024.

Research methods

The concept of information visualisation refers to the process of converting large-scale, complex, and often unstructured information into visual formats to enhance cognitive understanding and analytical decision-making. It plays a vital role in domains such as literature analysis, where traditional manual methods often fall short in capturing research hotspots and intellectual structures over time [2]. Given the extensive volume of literature involved in this study, traditional literature analysis methods may result in omissions and fail to comprehensively and objectively reflect the research hotspots and frontiers in this field over the past two decades. Moreover, traditional manual literature review methods are prone to subjective biases. In contrast, bibliometric-based visual analysis and knowledge mapping, particularly through tools such as CiteSpace, enable a structured and objective synthesis of key literature, uncovering emerging research trends, intellectual structures, and thematic clusters within a field [3]. Specifically, techniques such as burst detection and timeline mapping, central to the CiteSpace toolkit, are powerful for identifying the evolution of research foci over time [3–15, 16].

This study primarily employs CiteSpace 6.4.R1 (64-bit), a software developed by Professor Chaomei Chen and his team at Drexel University in the United States, to conduct a multidimensional, temporal, and dynamic visualisation analysis of research literature in the 3D apparel field [3]. The analysis explores the academic pathways and development trends of 3D digital technology in the apparel sector through various dimensions, including the spatial and temporal distribution of literature, high-frequency keywords, highly cited papers, keyword clustering, and temporal evolution.

During the process of conducting a visual analysis of literature using CiteSpace, the following parameters were configured: first, the time slicing parameter was set from 2011 to 2024 to analyse the characteristics of literature on the application of 3D digital technology in the apparel field over the past decade. The granularity of time slicing (Years Per Slice) was set to one year, resulting in a total of 14 time slices. Second, the node types included various dimensions such as authors, countries, institutions, and citations to enable multi-dimensional comparative analysis. Additionally, the g-index algorithm was employed to determine thresholds, with the k value set to 5 and the Top N threshold set to 50, aiming to identify key nodes within the network. The association strength between network nodes (Links) was calculated using the Cosine Similarity algorithm. Based on these parameter settings, this study visualised 1,079 selected articles to reveal the knowledge nodes, development trends, and collaboration networks in the 3D apparel field over the past decade. This analysis aims to delineate the research pathways and knowledge production patterns in this academic domain.

BASIC RESEARCH AND PROGRESS IN THE 3D APPAREL FIELD

Temporal distribution of literature

The volume and timeline of published literature reveal the evolutionary characteristics of a specific academic field. As shown in figure 2, the research in the 3D apparel field can be divided into three development stages. The first stage (2011–2015) represents a period of slow growth, with an average annual publication of approximately 38 articles. The second stage (2016–2020) marks a phase of steady growth, with the average annual publication rising to 80 articles. Entering the third stage (2021–2024), the field experienced rapid development, with the average annual publication significantly increasing to 146 articles. Overall, the publication volume in the 3D apparel field exhibits a steady and sustained growth trend. Notably, since 2020, there has been a significant surge in research output, likely driven by two main factors: first, the growing emphasis on 3D technology in the apparel industry as a mainstream trend in fashion; second, the impact of the COVID-19 pandemic, which disrupted offline international apparel trade. Consequently, 3D technologies enabled virtual garment displays for online selection, presentation, and transactions, playing a crucial role in international apparel trade. This period saw a positive correlation between market feedback and academic

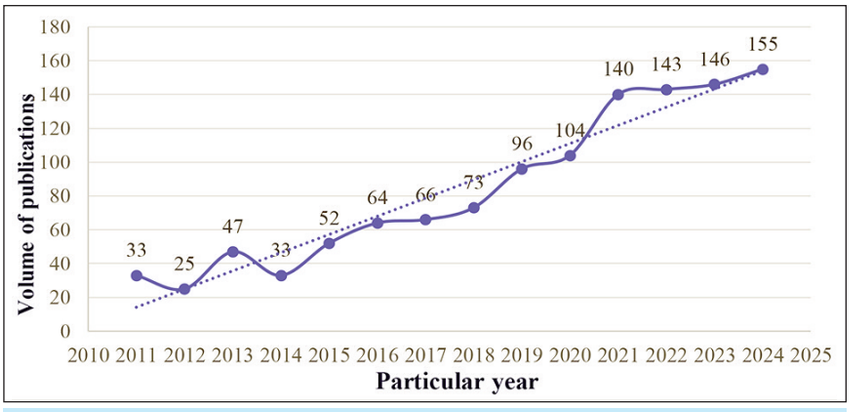

Fig. 2. Annual number of publications

research, leading to a significant increase in studies in the field.

Spatial distribution of literature

National and institutional distribution characteristics

An analysis of the global distribution of research on 3D apparel reveals contributions from 74 countries, with the top 10 countries by publication volume listed in table 1. Countries with high betweenness centrality often serve as key nodes in specific research fields, marked in CiteSpace with purple rings (betweenness centrality > 0.1) to highlight their importance in the domain (figure 3). Based on publication volume and centrality rankings (table 1), China ranks as the leading country in terms of research output and influence in this field, with 490 publications and a betweenness centrality of 0.37, far surpassing other nations. Following China are the United States, South Korea, the United Kingdom, France, and others. The results indicate a positive correlation between publication volume and the development level of the apparel industry.

According to the latest statistics, China maintained its global leadership in apparel production and export in 2024. The China National Textile and Apparel Council reported that from January to December 2024, China's textile and apparel exports totalled USD 301.1 billion, a 2.8% increase year-on-year. Of this, textile exports amounted to USD 141.96 billion (a 5.7% increase), and apparel exports reached USD 159.14 billion (a 0.3% increase).

Additionally, from January to November 2024, China's apparel industry enterprises above a designated size produced 18.569 billion garments, a 3.94% increase year-on-year.

As the world's largest apparel producer and exporter, China's vast industry scale provides ample market demand and practical platforms for the research and application of 3D technology in the apparel field.

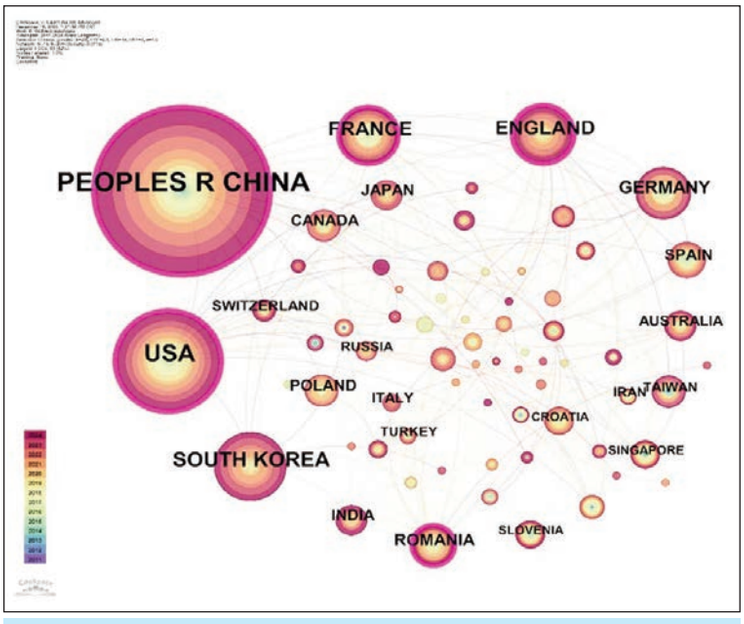

Fig. 3. Country distribution of relevant studies

Table 1

RANKING OF NATIONAL IMPACT OF RELEVANT RESEARCH

Mark	Country	Volume of publications	Centrality
1	China	490	0.37
2	USA	201	0.27
3	England	74	0.22
4	Romania	35	0.18
5	France	76	0.15
6	Germany	54	0.07
7	Turkey	17	0.07
8	Australia	25	0.06
9	South Korea	104	0.05
10	Switzerland	22	0.05

Simultaneously, China's apparel industry is accelerating its transformation toward higher quality and increased digitalisation, with a growing demand for digital technologies. The government has introduced a series of policies supporting smart manufacturing and the digital economy, such as the "14th Five-Year Plan for Digital Economy Development". These factors collectively position China as a global leader in 3D apparel research.

National and institutional distribution and collaboration characteristics

However, publication volume alone is not sufficient to measure a country's influence in the field of 3D apparel research. For instance, although South Korea's publication volume exceeds that of the United Kingdom, Romania, and France, its betweenness centrality does not show a positive correlation with publication volume. This indicates that while South Korea has an advantage in terms of publication output, its academic influence in the field may not be as significant as that of the United Kingdom, Romania, and France.

Further analysis using CiteSpace software on the effective samples produced the institutional distribution map of 3D apparel research, shown in figure 4. A total of 1079 papers involved 336 research institutions, encompassing universities and research organisations. Based on centrality rankings (table 2), the top five influential institutions are Donghua University (79 papers), Hong Kong Polytechnic University (38 papers), Tsinghua University (21 papers), the Chinese Academy of Sciences (29 papers), and Zhejiang University. All of these institutions are based in China, underscoring China's leading position in the field of 3D apparel research.

In terms of specific research areas, Chinese universities such as Donghua University, Hong Kong Polytechnic

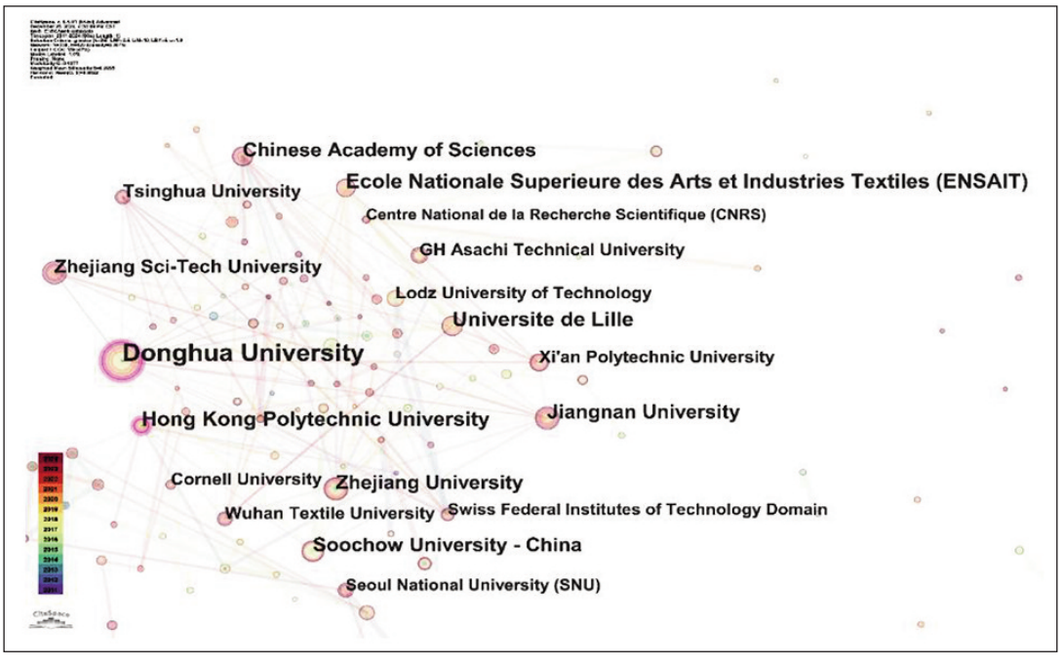

Fig. 4. Institutional distribution of relevant research

University, Jiangnan University, Soochow University, and Xi'an Polytechnic University primarily focus on 3D body modelling, 3D apparel design, and modelling. Meanwhile, Zhejiang University and the Chinese Academy of Sciences concentrate on virtual simulation technologies and computer hardware and software development. Among the 336 nodes, there are 420 connections, resulting in a node density of 0.0075, indicating relatively robust collaboration and tight inter-institutional networks.

Table 2

RANKING OF INSTITUTIONAL IMPACT (TOP 10)

Count	Centrality	Year	Intuition
79	0.18	2011	Donghua University
38	0.15	2011	Hong Kong Polytechnic University
21	0.08	2013	Tsinghua University
29	0.07	2011	Chinese Academy of Sciences
32	0.07	2011	Zhejiang University
13	0.06	2013	Centre National de la Recherche Scientifique (CNRS)
16	0.05	2012	Swiss Federal Institutes of Technology Domain
38	0.05	2013	Université de Lille
3	0.04	2022	University of Alberta
17	0.04	2011	Cornell University

Comparing author and institutional collaboration networks reveals that the top five institutions maintain close cooperative relationships, largely due to their geographic concentration in China. However, certain institutions and authors also engage in international collaborations. For example, as shown in the author collaboration network, the top ten authors include Wang Jianping from Donghua University and Liu Kaixuan from Xi'an Polytechnic University. Both have collaborated with Bruniaux Pascal from ENSAIT (École Nationale Supérieure des Arts et Industries Textiles) in France, reflecting significant international partnerships.

Author distribution characteristics

Analysing authors provides insights into the representative scholars and core research forces in the field. According to the renowned scholar Price (1963), in a given research domain, half of the papers are written by a small group of high-productivity authors. This group's size is approximately equal to the square root of the total number of authors, a principle known as "Price's law":

$$\Sigma_{m+1}^{I} n(x) = \sqrt{N} \quad (1)$$

where $n(x)$ represents the number of authors who have written xxx papers, and $I = n_{max}$ denotes the maximum number of papers authored by a single researcher in the field [4]. Based on the CiteSpace analysis, $n_{max} = 2$, and N is the total number of authors. According to Price's law, the minimum number of papers authored by core authors in this field is calculated as: $m = 0.749 \times \sqrt{n_{max}} \approx 3.82$. Thus, authors with four or more publications are identified as core authors in this field. CiteSpace analysis revealed that there are 46 core authors, contributing a total of 302 apers, accounting for 33.9% of the total publications. Among these, only 24 authors have published more than four papers, and just nine authors have published more than eight papers, indicating that there are relatively few high-productivity authors, leaving significant room for further research. Figure 5 lists the top ten high-productivity authors in this field.

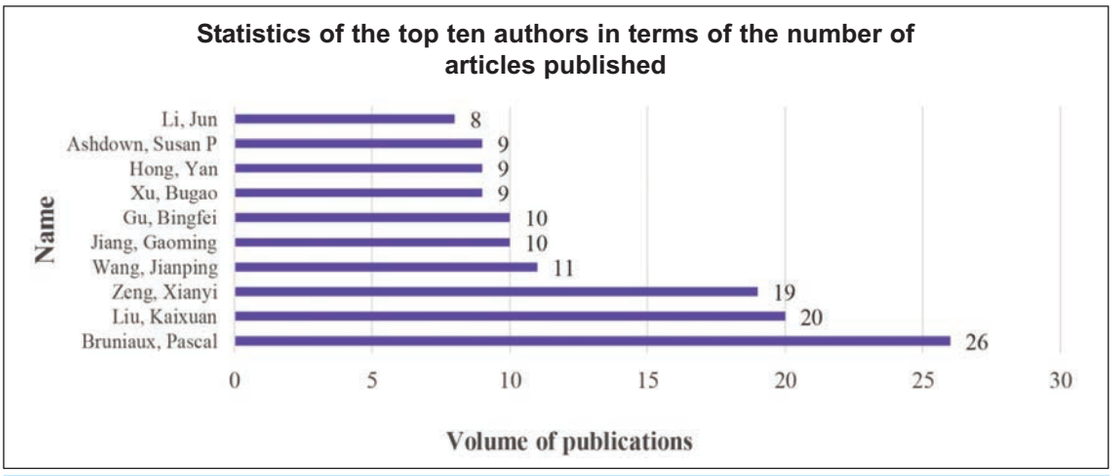

Fig. 5. Top 10 highly productive authors

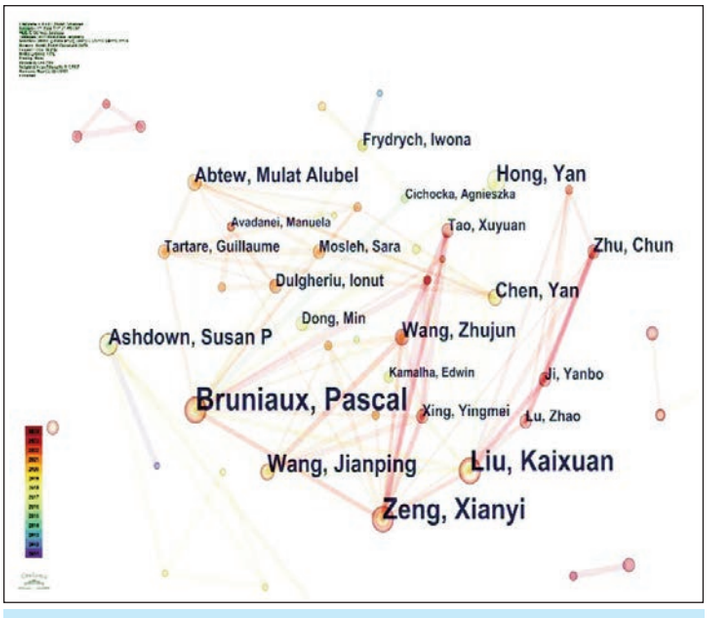

Fig. 6. Core author collaboration network

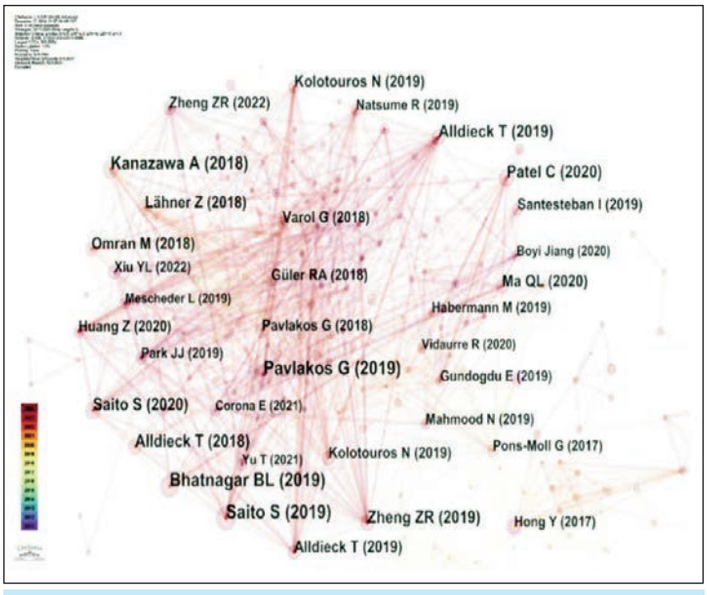

Fig. 7. Co-citation visualisation map of literature in the 3D clothing field

Using CiteSpace to analyse authors as nodes generated a collaborative network of core authors in the 3D apparel field (figure 6). The analysis identified 448 author nodes, 446 connections, a network density of 0.0045, and a modularity Q value of 0.9277. A modularity Q value greater than 0.3 indicates significant clustering, while values approaching 1 reflect strong and well-defined community structures [5]. Figure 6 shows that core authors have numerous and concentrated connections, with high node density, indicating a well-established collaborative network in the 3D apparel research field.

Further analysis of the author and institutional co-occurrence networks reveals that the top five influential institutions have strong collaborative relationships due to their shared location in China. Additionally, some authors from these institutions have established international collaborations. For example, as shown in table 4, Wang Jianping from Donghua University and Liu Kaixuan from Xi'an Polytechnic University have co-authored papers with Bruniaux Pascal from ENSAIT (École Nationale Supérieure des Arts et Industries Textiles) in France, highlighting their significant academic influence in international collaborations.

Highly cited literature analysis

According to Thomas Kuhn's theory of scientific development, scientific progress is often accompanied by significant discoveries, with classic literature serving as pivotal turning points in scientific fields. Betweenness centrality is a crucial structural indicator for evaluating the impact of literature. In CiteSpace, literature with high centrality often acts as a bridge connecting different research areas. These works, referred to as "Turning Points", are marked with purple rings (betweenness centrality > 0.1). By setting the node type to "reference", a co-citation visualisation map of literature in the 3D clothing field was generated (figure 7). Based on the CiteSpace analysis

report, the top 10 documents in terms of betweenness centrality, along with their authors, are listed in table 3.

Citation frequency is another key metric for assessing the impact of academic achievements. To further explore the citation patterns in the 3D clothing research field, we analysed the citation frequencies of high-impact papers (table 1). The findings are that the two most cited papers are *PIFu: Pixel-Aligned Implicit Function for High-Resolution Clothed Human Digitisation* and *Expressive Body Capture: 3D Hands, Face, and Body From a Single Image*, with citation frequencies of 1168 and 1068, respectively. These papers, authored by Shunsuke Saito and G. Pavlakos, were both published within the last five years. Saito's research systematically introduced the Pixel-Aligned Implicit Function (PIFu), a technique that aligns the pixels of 2D images with the global context of 3D objects locally, enabling high-resolution clothed human digitisation from a single image [6].

Among the top 10 most cited papers listed in table 1, five were published after 2015, accounting for 50%. This indicates that the quality of publications in the 3D clothing research field has significantly improved in recent years, making it a growing focus of academic attention.

The authors and institutions contributing to these highly cited papers show a concentration of academic influence within a few core research areas. These areas mainly involve 3D image processing, virtual clothing visualisation, and human digitisation modelling.

Through the combined analysis of betweenness centrality and citation frequency, it is evident that highly influential literature not only bridges different research areas but also provides a solid foundation for technological breakthroughs and academic development in the 3D clothing field. These studies have further advanced the adoption and dissemination of 3D clothing technologies in both academia and industry.

VISUAL ANALYSIS OF RESEARCH HOTSPOTS IN THE FIELD OF 3D CLOTHING

Keyword co-occurrence map analysis

Keywords serve as concise representations of a document's core themes. Analysing high-frequency keywords through bibliometric techniques can effectively reveal research hotspots, emerging trends, and the structural relationships between topics in a scientific domain [7].

Using CiteSpace software, high-frequency keyword analysis was conducted on the valid literature, generating a network with 498 nodes and 2181 connections, achieving a density of 0.016 and a modularity Q-value of 0.511, indicating good clustering. The keyword co-occurrence map for the 3D clothing research field from 2011 to 2024 is shown in figure 8. In figure 8, nodes are presented in the form of Tree Ring Histories. The size of the rings represents the frequency of keyword occurrences: the larger the ring, the higher the frequency. The colour of the rings reflects the active time period of the keywords, with the gradient from the inner to outer rings indicating the timeline of publications. The thickness of the rings is proportional to the frequency of keywords appearing in a specific time interval [3].

It can be observed that "human body", "virtual try-on" and "3D body" are the three core nodes. These keywords occupy a central position in the literature collection and radiate extensively to form a complex network structure. They are primarily connected to keywords such as "3D model", "3D printing", "3D body scanning", "3D reconstruction" and "protective clothes", indicating that the 3D clothing research field has developed a relatively mature thematic framework.

Table 3

MOST INFLUENTIAL LITERATURE STATISTICS (TOP 10)

Mark	Centrality	Frequency	Author	Year	Title of document
1	0.2	8	He KaiMing	2016	Deep Residual Learning for Image Recognition
2	0.12	6	Chen Xiaowu	2015	Garment Modeling with a Depth Camera
3	0.11	15	Hong Yan	2017	Interactive virtual try-on based three-dimensional garment block design for disabled people of scoliosis type
4	0.08	11	Floraine Berthouzoz	2013	Parsing Sewing Patterns into 3D Garments
5	0.07	9	Meng Yuwei	2012	Computer aided clothing pattern design with 3D editing and pattern alteration
6	0.06	48	Shunsuke Saito	2019	PIFu: Pixel-Aligned Implicit Function for High-Resolution Clothed Human Digitization
7	0.06	45	G. Pavlakos	2019	Expressive Body Capture: 3D Hands, Face, and Body From a Single Image
8	0.06	6	Brouet Remi	2012	Design Preserving Garment Transfer
9	0.05	7	Guan Peng	2012	DRAPE: Dressing Any PErson
10	0.04	26	Theimo Alldieck	2019	Learning to Reconstruct People in Clothing From a Single RGB Camera

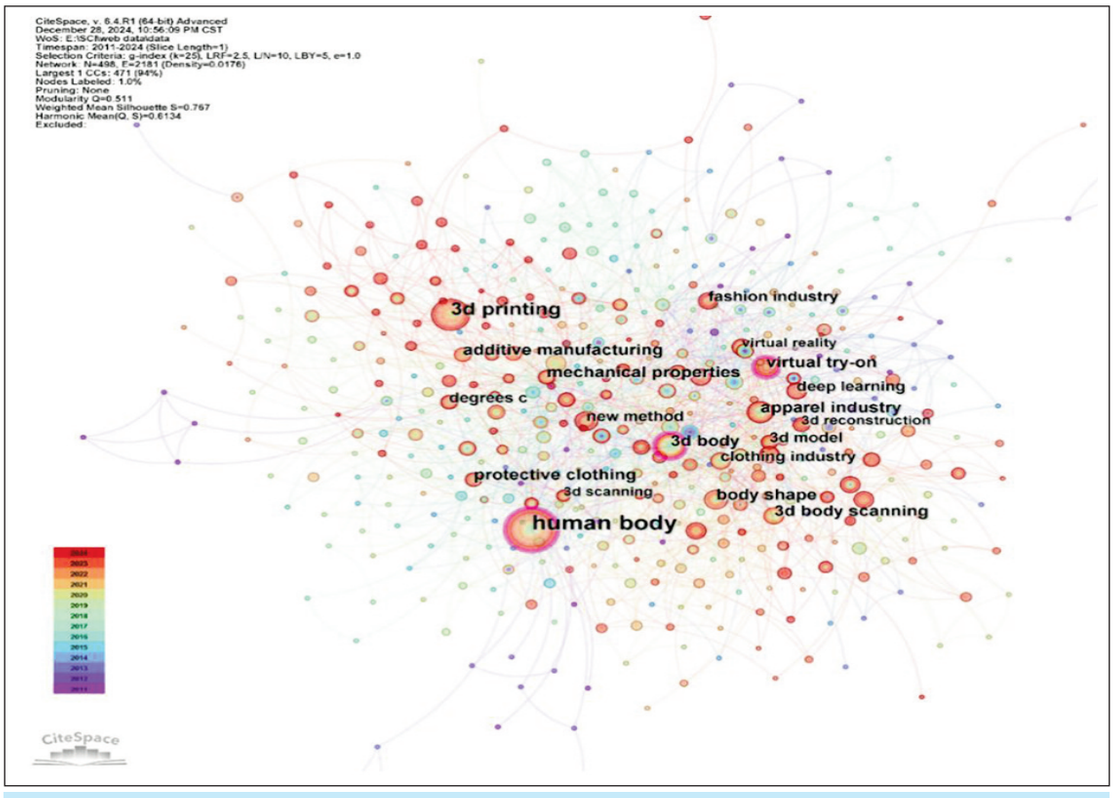

Fig. 8. Keyword co-occurrence map for the 3D clothing research field

Table 4

HIGH FREQUENCY KEYWORD STATISTICS

Count	Centrality	Year	Phrases
150	0.15	2011	human body
84	0.02	2016	3d printing
46	0.11	2011	3d body
45	0.1	2013	virtual try-on
40	0.06	2013	protective clothing
40	0.08	2013	mechanical properties
37	0.08	2015	additive manufacturing
36	0.06	2013	body shape
36	0.09	2011	apparel industry
34	0.07	2011	3d body scanning

As shown in table 4, the most frequently occurring keywords are: “human body”, “3D printing”, “3D body”, “virtual try-on”, “protective clothing”, “mechanical properties”, “additive manufacturing”, “body shape”, “apparel industry” and “3D body scanning”. This demonstrates that substantial research efforts have been devoted to these key topics.

Keyword cluster analysis

Keywords are a highly condensed summary of research in the field and can accurately reflect the primary focus of the literature. By performing co-occurrence clustering analysis of high-frequency keywords in the 3D clothing domain, research hotspots can be clearly visualised. Using CiteSpace software, a common clustering analysis of the keywords in 1,079 articles within the search scope was conducted. Based on the keyword network, the LLR clustering algorithm was applied, and the resulting keyword clustering model is shown in figure 9. In this model, the Q value and S value indicate clustering performance. The Q value reflects modularity, and the S value represents the average silhouette score. When Q>0.3, the clustering structure is significant, and when S>0.5, the clustering is highly reliable. In this study, the Q value is 0.511 (>0.3), and the S value is 0.767 (>0.5), indicating that the clustering structure is reasonable and credible [5].

The keyword clustering analysis yielded nine clusters: #0 3D printing technology, #1 3D body, #2 virtual reality, #3 virtual try-on, #4 design thinking, #5 garment design, #6 3D garments, #7 virtual fitting, and #8 3D body scan (table 5). To further summarise the research hotspots in this field, similar clustering labels were merged. Combined with high-frequency and high-centrality keywords, the primary knowledge groups in the 3D clothing research field were categorised into three main research directions: 3D Body Scanning (Type A), Virtual Clothing Simulation Technology (Type B), and 3D Clothing Printing (Type C).

Cluster A focuses on the 3D human body and includes the primary clustering terms #1 3D body and #8 3D body scan. The research on 3D body scanning extends from capturing body shape data to creating 3D body models, and from controlling overall body morphology to analysing specific body part features. This provides critical technical support and scientific

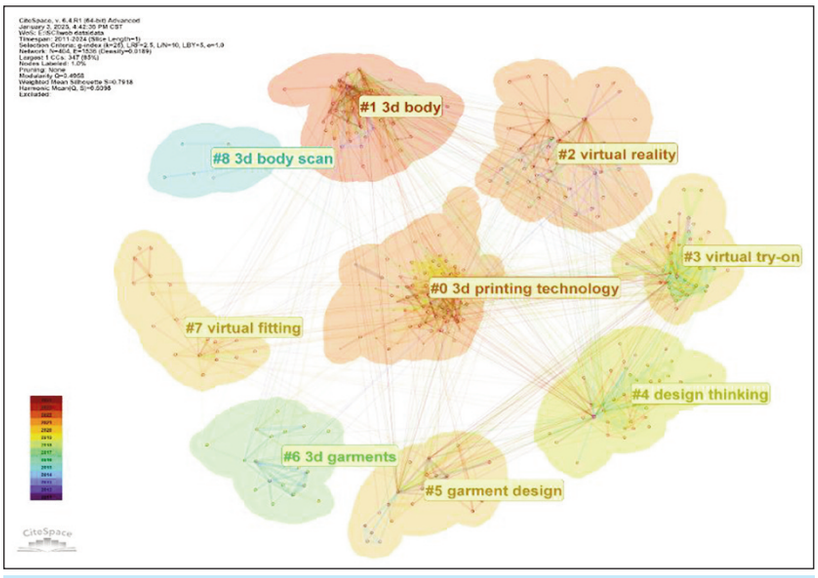

Fig. 9. Keyword clustering model map

foundations for the development of 3D clothing technology [8].

For instance, Wang Jun utilised 3D scanning technology to construct a parametric 3D lower-body model for women with different body types. The study included classifying young female samples by body type, reconstructing characteristic curves, and establishing 3D lower-body models for three distinct body types. This approach offers an effective method for building parametric 3D lower-body models, serving as a reference for parametric virtual human modelling and virtual fitting for pants [9–12]. Moreover, Liu Kaixuan proposed a new research direction that applies artificial intelligence to predict human body dimensions in the apparel industry. The study introduced a new model based on backpropagation artificial neural networks (BP-ANN) to improve the efficiency and accuracy of garment pattern-making [9].

Cluster B focuses on 3D virtual simulation technology for apparel, encompassing the main clustering terms #2 virtual reality, #3 virtual try-on, #7 virtual fitting, and #6 3D garments. The technology for precise simulation of clothing was first developed in 1990 by the MIRALAB Laboratory at the University of Geneva in Switzerland. This innovation combined virtual fabric, human body modelling, and dynamic presentation technologies to enable virtual dressing functionality [10]. Subsequently, the lab developed several iconic virtual fitting systems, such as VirtualTryOn, Fit-me.com [11]. and the MIRA Cloth system, which allows dynamic dressing effects to be demonstrated via interactive devices. Building upon this foundation, recent innovations have introduced deep learning-based 3D modelling, real-time physics-based simulations, and interactive Metaverse environments to deliver highly immersive digital fashion experiences, transforming both consumer engagement and apparel production workflows [13].

Over the past five years, 3D virtual simulation technology for apparel design has gained widespread acceptance and application in the market. Systems such as CLO3D and Style3D dominate the field, enabling comprehensive workflows for clothing design, including fabric selection, colour and pattern design, human modelling, pattern drafting, stitching, fitting, showcasing, and runway presentation. Many designers approach the process by analysing external elements such as colour, fabric, and patterns. They focus on virtual fabric textures and material properties to study the static effects of different

Table 5

CLUSTERING HIGH-FREQUENCY KEYWORD		
Mark	**Cluster**	**High-frequency keywords**
0	3D printing technology	3D printing; mechanical properties; mechanical properties; protective clothing; additive manufacturing; degrees C
1	3D body	3D body; apparel industry; body shape; clothing industry
2	virtual reality	human body; new method; virtual reality; garment fit; fashion design
3	virtual try-on	virtual try-on; 3D model; deep learning; 3D reconstruction; the-art methods
4	design thinking	laser cladding; clothing design; 3D modelling; process parameters
5	garment design	garment design; 3D body scanner; human bodies; apparel design; clothing pressure
6	3D garments	2D patterns; novel approach; 3D simulation; 3D garments
7	fast garment fitting	cloth simulation; first time; effective approach; existing approaches; pose recovery
8	3D body scan	gait recognition; 3D body model; feature extraction; point cloud; clothing variations

materials, glossiness, and pattern designs. Additionally, designers consider planar pattern structures and technical requirements to investigate the 3D dynamic structure of garments, using simulations to quickly showcase dressing effects.

Moreover, 3D apparel showcasing has become a major research direction for scholars. For instance, Liu Fengyi utilised convolutional neural networks (CNN) and virtual reality technology to construct a 3D apparel design model, highlighting the efficiency and accuracy of CNN in 3D garment design and its potential applications in virtual reality [12].

Cluster C centres on 3D apparel printing, encompassing the main clustering keywords #0 3D printing technology and #9 3D fabric. 3D printing technology disrupts the traditional production mode, which involves fabric cutting and garment sewing. Instead, it enables the direct printing of entire garments, making production more convenient and efficient. This breakthrough technology is poised to bring transformative changes to the apparel industry.

To meet the growing demand for personalised and diversified consumer needs, developing soft, comfortable, and wearable 3D-printed textile garments is becoming increasingly critical. Researchers are working to integrate 3D printing technology with traditional fabric structures to create 3D-printed textile products that retain the breathability, flexibility, and comfort of conventional textiles.

For instance, Yu and Kim (2023) utilised a portable 3D body scanner to collect anthropometric data and applied 3D CAD software to model garments and accessories. Subsequently, they employed a fused deposition modelling (FDM) 3D printer to fabricate life-sized dress forms suitable for both standing and seated postures, demonstrating the integration of digital design and additive manufacturing in personalised fashion production [14–16].

ANALYSIS OF RESEARCH HOT SPOTS AND TRENDS

The evolution and challenges of the Technical core layer

The bibliometric findings indicate that the advancement of the 3D apparel field is intrinsically linked to the progression of its Technical core layer, the foundational technologies encompassing 3D body scanning, virtual garment simulation, additive manufacturing, and associated algorithms. The temporal distribution of publications, as depicted in figure 1, delineates three distinct evolutionary phases: an initial period of slow growth (2011–2015), followed by a phase of steady growth (2016–2020), and a recent phase of rapid expansion (2021–2024). The notable surge in research output post-2020 is attributable to two pivotal factors: the growing recognition of 3D technology as a mainstream imperative within the fashion industry, and the critical role of 3D-enabled virtual garment displays in sustaining online apparel commerce amidst the disruptions caused by the COVID-19 pandemic. This trend underscores a positive feedback loop between market demands and academic inquiry in this domain.

The evolution of research foci within this technical core is further illuminated by the keyword timeline analysis (figure 10). The nascent stage (2011–2014) was predominantly characterised by efforts in fundamental data acquisition and geometric modelling,

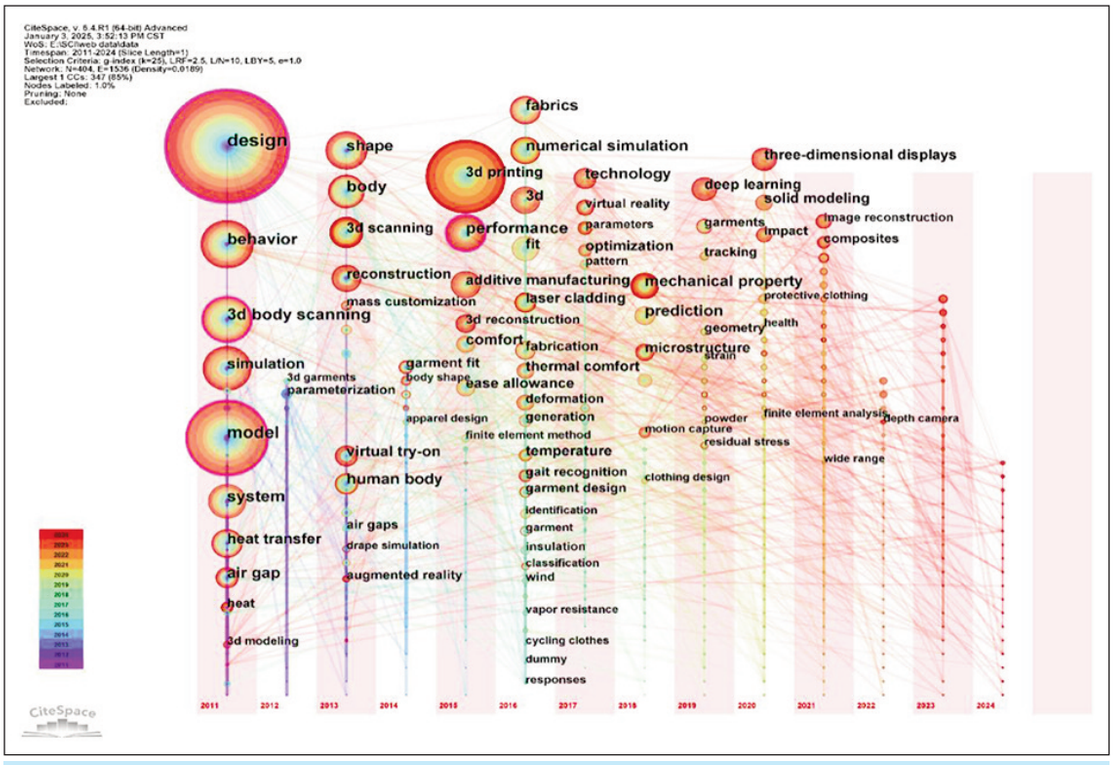

Fig. 10. The evolution of research hotspots in the field of 3D fashion

with keywords such as “3D scanning”, “body”, “3D model” and “shape” emerging as central themes. This focus reflects the field’s primary challenge of accurately capturing and digitally reconstructing the human form, which serves as the essential substrate for all subsequent applications. The subsequent period (2015–2019) witnessed a diversification towards materialisation and preliminary interaction, marked by the rising prominence of keywords like “fabrics”, “3D printing”, “additive manufacturing” and “virtual reality”. This shift signifies a maturation of basic scanning technologies and a growing research impetus to translate digital designs into physical products and rudimentary immersive experiences.

The most recent phase (post-2019) has seen the emergence of keywords such as “three-dimensional displays”, “image reconstruction”, “virtual simulation” and “digital reconstruction”, pointing towards advancements in fidelity and integration. The particularly long duration of activity associated with “virtual simulation”, coupled with its relatively weak co-occurrence links with other terms, suggests that this subdomain is not only a persistent research hotspot but also one experiencing rapid, and often parallel, technological iterations, potentially leading to a fragmented intellectual landscape.

However, despite these significant strides, the Technical core layer confronts persistent and formidable challenges that curtail its broader efficacy and adoption. A primary impediment is the fidelity-realizability gap. Although parametric body modelling has achieved considerable sophistication [8], accurately simulating the nonlinear, dynamic behaviour of complex textiles, such as the drape of silk or the structural integrity of knitted fabrics under mechanical stress, remains a largely unsolved problem. The technical hurdles involve replicating physical properties like buckling, stretching, and collision response in real-time, which are computationally intensive and often simplified to the detriment of realism. Furthermore, while AI-driven solutions for body dimension prediction [9] and garment digitisation [6] offer transformative potential for automation, their performance is frequently constrained by limitations in training data. The reliance on anthropometric datasets that lack diversity in ethnicity, age, and body type can perpetuate biases and hinder the global applicability of these tools. This gap between idealised digital representation and physical reality constitutes a fundamental constraint within the current technical paradigm.

A comparative analysis of the field’s development reveals an intriguing geopolitical dimension. The concentration of high-volume research output and institutionally central contributors in China (as detailed in Section 2.2) appears closely aligned with national industrial policies and the demands of a massive manufacturing sector, emphasising applied technological development and rapid integration. In contrast, several foundational algorithmic breakthroughs, such as the development of the PIFu model for high-resolution clothed human digitisation [6], originated from a more globally diverse research base. This suggests a potential strategic dichotomy wherein research in East Asia may excel in applied engineering, scalability, and integration, while contributions from North America and Europe are more pronounced in pioneering the underlying core algorithms and computer graphics theories. This dynamic not only shapes the global knowledge production network but also influences the types of technical challenges that are prioritised for investigation.

The Application and Integration layer: from technology to solution

The maturation of the Technical Core Layer has directly catalysed the proliferation of solutions within the Application and Integration layer, where foundational technologies are synthesised into practical tools and experiences for both industry and consumers. This layer encompasses the implementation of 3D assets in virtual try-on systems, e-commerce platforms, and most notably, within immersive Metaverse environments. Bibliometric trends from the past three years confirm a decisive shift from purely technological development towards practical application and commercialisation.

Core technological applications: virtual try-on and fitting

A primary manifestation of this layer is in virtual try-on (VTO) and fitting systems. These applications leverage the Technical core, 3D body scanning, modelling, and simulation algorithms, to create realistic garment behaviours on digital avatars. They reconstruct human body models from anthropometric data and apply intelligent algorithms to establish garment-body spatial relationships, enabling accurate virtual try-on

Keywords	Year	Strength	Begin	End	2011 - 2024
garment industry	2011	3.13	**2011**	2013	
parameterisation	2012	5.04	**2012**	2014	
image analysis	2013	2.97	**2013**	2018	
fit	2016	4.03	**2016**	2020	
generation	2016	3.02	**2016**	2017	
insulation	2016	2.89	**2016**	2019	
movement	2017	2.88	**2017**	2018	
computer-aided design	2018	3.22	**2018**	2021	
prediction	2018	3	**2018**	2021	
human body	2013	2.75	**2018**	2019	
garments	2019	2.93	**2019**	2021	
virtual fitting	2020	2.75	**2020**	2021	
3d printing	2015	3.16	**2021**	2022	
three-dimensional displays	2020	5.02	**2022**	2024	
solid modelling	2020	4.36	**2022**	2024	

Fig. 11. Top 15 keywords with the strongest citation burst

experiences [17]. Early systems, such as the My Virtual Model (MVM) developed by a Canadian research team, laid the groundwork by generating dynamic 3D avatars from user data. This innovation has been adopted and advanced by retailers; for instance, brands like H&M have explored online fitting room solutions to enhance user interaction and digital visualisation [11].

The evolution within this sub-domain is increasingly driven by Artificial Intelligence. Recent years have seen the emergence of AI-powered personalised size recommendation systems (e.g., "The Right Size", "Fit Me") that utilise deep learning and pose estimation techniques to improve sizing accuracy in online fashion retail [18]. These systems calculate patterns and infer dimensions based on consumer measurements to recommend suitable garments. Research institutions have also contributed significantly to this field. The University of London's Bidynetics system digitises body dimensions to assess garment-body match [19], while Germany's Fraunhofer Society employs 3D scanning to directly capture body shape features, generating 1:1 scale models for garment recommendation [20, 21].

However, the seamless integration and effectiveness of these applications remain constrained by the limitations of the underlying Technical Core. Although these technologies integrate numerous advanced processes, the challenge of simulating the nonlinear, dynamic behaviour of fabrics, such as precise drape, wrinkles, and collision response in real-time, persists. The computational intensity required often leads to simplifications that detrimentally impact realism. Thus, while the applications are innovative, their fidelity and user trust are ultimately bound by the unresolved challenges of physical simulation.

Emerging commercial paradigms: digital fashion and the Metaverse

The most avant-garde expression of the Application layer is the integration of virtual clothing into the Metaverse and digital ecosystems. This represents a significant evolution in the digitalisation of fashion, moving beyond tools to digital-only end-products themselves. The expansion of the Metaverse and the growing importance of digital identities have spurred a "digital avatar economy", with the fashion industry demonstrating particularly high engagement [21].

Early milestones, such as The Fabricant's sale of the Iridescence digital dress for $9,500 in 2019 [19], marked the emergence of fashion NFTs and validated digital fashion as a valuable asset [20]. This commercial movement has been rapidly adopted by luxury brands. Academic research confirms that for luxury brands, the Metaverse represents a new frontier for experiential marketing and brand storytelling [22–24]. This strategic imperative has led to rapid commercial adoption. Gucci, for example, has launched virtual garment collections on platforms like Zepeto, treating digital fashion as a consumable commodity in its own right [21]. Similarly, Balenciaga partnered with Fortnite to open a virtual retail space [22], and Decentraland hosted the inaugural Metaverse Fashion Week in 2022, featuring collections from major luxury houses.

Academic inquiry is beginning to investigate this phenomenon. Research suggests that immersive fashion experiences, particularly in VR, can foster emotional engagement and enhance brand storytelling, which plays a critical role in shaping consumer loyalty [25–27]. Furthermore, empirical studies confirm that 3D virtual try-on technology in Metaverse environments significantly influences consumers' purchase intentions and acceptance of digital garments [28]. Beyond these specific empirical findings, the broader academic trajectory is becoming clear. The trajectory revealed by this bibliometric analysis, highlighting the Metaverse as a key research frontier, is further explained by comprehensive academic inquiry. Dwivedi et al. posit that the Metaverse will act as a transformative force for marketing, enabling new levels of customer interaction through immersive XR journeys and the rise of a 'digital avatar economy' [26]. This aligns with the observed research focus on virtual try-on and digital fashion, suggesting the industry is not merely responding to hype but is engaging with a complex new paradigm for consumer engagement, identity expression, and value creation. A critical analysis, however, reveals a significant tension between the pace of commercial adoption and scholarly understanding. As Chan et al. systematically reveal, extant literature predominantly still defines digital fashion as a tool for design or marketing [21], largely neglecting its conceptualisation as a digital-only end-product [23]. This gap is exemplified by industry pioneers like The Fabricant and Gucci operating on a fundamentally different paradigm than what is reflected in much of the academic literature. Therefore, a pressing need exists for academic research to reconceptualise digital fashion within a framework that aligns with its current industrial trajectory, exploring its implications for consumption, ownership, and value creation in digital economies.

The Macro-impact layer: broader implications and future frontiers

The advancements and applications within the Technical Core and Application Layers inevitably precipitate profound consequences at the Macro-impact layer, affecting broader industrial practices, consumer societies, and ethical norms. This layer transcends technological specifics to address the sustainability, inclusivity, economic, and experiential paradigms shifted by 3D apparel technologies. The bibliometric analysis underscores that future research must extend beyond technical optimisation to grapple with these larger implications.

Addressing the sustainability paradox and technical bottlenecks

A primary macro-impact is the potential of 3D technologies to advance fashion sustainability, for instance, through virtual sampling that reduces material waste. However, this promise is contingent upon overcoming persistent technical bottlenecks. A major issue remains the difficulty in reproducing highly

realistic fabric drape and dynamic behaviours, particularly for complex textiles like silk or multi-layered garments. While researchers like Wang have demonstrated improvements through parametric human body modelling, significant limitations persist in simulating garments under varied environmental conditions [8]. Similarly, Yu and Kim have emphasised unresolved integration problems between 3D body models and garment geometries, despite advances in scanning and printing technologies [14]. This creates a sustainability paradox: the digital process itself consumes significant energy for computation and data storage. Therefore, a critical future research direction involves conducting comprehensive lifecycle assessments (LCA) to quantify the net environmental benefit of adopting these digital technologies, ensuring that the solution does not inadvertently exacerbate the problem.

Ensuring algorithmic fairness and global inclusivity

The push towards personalisation and AI-driven solutions introduces another macro-level challenge: algorithmic bias and exclusion. Another significant challenge lies in the effectiveness and fairness of AI-powered size recommendation systems. Although applications like “The Right Size” and “Fit Me” have mitigated size uncertainties in online retail, their universal applicability is hindered by data sparsity, cultural diversity in body shapes, and inherent biases in anthropometric datasets [18]. This reliance on non-representative data risks perpetuating discrimination and excluding global populations from the benefits of digital fashion. Future research must, therefore, prioritise the development of inclusive and representative datasets, as well as adaptive algorithms that are culturally and anthropometrically diverse, to ensure that the digital fashion revolution does not leave a significant portion of the world’s population behind.

Governing digital ecosystems and defining value

Furthermore, the integration of 3D fashion technologies into Metaverse platforms introduces complex interdisciplinary questions concerning the governance of new digital ecosystems. Issues of interoperability between closed platforms, intellectual property protection for digital garments, and establishing consumer trust and acceptance of virtual fashion remain largely unaddressed [27]. Moreover, the absence of haptic feedback and multi-sensory experiences in current virtual try-on systems limits their ability to deliver fully immersive and persuasive environments [28]. Addressing these challenges will require unprecedented interdisciplinary collaboration across computer graphics, textile engineering, human-computer interaction, law, and business ethics to establish the norms, standards, and economic models that will define value and ownership in the digital fashion economy.

Future research agenda: a call for interdisciplinary convergence

The future trajectory of 3D apparel technology is poised at the convergence of AI, the Metaverse, and advanced simulation, a shift confirmed by recent studies showing how this fusion transforms consumer engagement and retail models by enhancing customer loyalty through virtual try-on and AI-driven personalisation in immersive environments [29]. Consequently, the findings of this bibliometric review culminate in a clear and interdisciplinary future research agenda. Going forward, scholarly efforts must prioritise developing standardised digital garment formats and materials to ensure interoperability across platforms, whilst also exploring multi-sensory feedback systems, encompassing haptic and auditory elements, to bridge the experiential gap between physical and digital fashion. Furthermore, establishing robust ethical frameworks for AI usage, data privacy, and the environmental claims of digital fashion is paramount. In parallel, there is a pressing need to investigate new consumer behaviours, psychological ownership, and value perception concerning digital-only products. This comprehensive agenda moves beyond solving isolated technical problems towards shaping a responsible, inclusive, and sustainable digital future for the entire fashion industry through concerted interdisciplinary efforts.

CONCLUSION

In conclusion, this study has moved beyond a descriptive bibliometric summary by proposing and applying a three-tier conceptual framework (Technical core, Application & Integration, Macro-impact) to analyse the evolution of 3D apparel technology research. This approach has provided a structured and critical lens through which to interpret a decade of scholarly activity, revealing not only the field’s thematic hotspots but also the dynamic interplays and tensions between technological advancement, practical application, and broader societal implications.

The findings confirm China’s preeminent role, particularly in the applied research and development that characterises the Application and Integration Layer. The analysis further identifies enduring challenges that span across these layers: the fidelity-realizability gap in physical simulation within the Technical Core, the commercial-academic conceptual gap regarding digital fashion as an end-product in the Application layer, and the sustainability paradox and issues of algorithmic bias at the Macro-impact level. Addressing these complex challenges necessitates deeper interdisciplinary collaboration that extends beyond computer graphics and textile engineering to include ethics, social science, and business strategy. Looking forward, the convergence of 3D technologies with the Metaverse, AR, and AI is poised to redefine fashion fundamentally. To navigate this transition responsibly, future research must be guided by the imperatives of this framework: developing standardised formats to ensure interoperability, pioneering multi-sensory experiences to bridge the physical-digital divide, and establishing robust ethical frameworks to ensure inclusivity and sustainability. The adoption of 3D technology is not merely a technical upgrade but a pivotal step toward a more innovative, efficient, and consciously designed future for the global apparel industry.

REFERENCES

[1] Falagas, M.E., Pitsouni, E.I., Malietzis, G.A., Pappas, G., *Comparison of PubMed, Scopus, Web of Science, and Google Scholar: strengths and weaknesses*, In: The FASEB Journal, 2008, 22, 2, 338–342, https://doi.org/10.1096/fj.07-9492LSF

[2] Cobo, M.J., López-Herrera, A.G., Herrera-Viedma, E., Herrera, F., *Science mapping software tools: Review, analysis, and cooperative study among tools*, In: Journal of the Association for Information Science and Technology, 2018, 68, 3, 602–617

[3] Chen, C., *CiteSpace II: Detecting and visualising emerging trends and transient patterns in scientific literature*, In: Journal of the American Society for Information Science and Technology, 2006, 57, 3, 359–377

[4] Price, D.J. de Solla, *Little Science, Big Science*, New York: Columbia University Press, 1963

[5] Chen, C., Ibekwe-SanJuan, F., Hou, J., *The structure and dynamics of cocitation clusters: A multiple-perspective cocitation analysis*, In: Journal of the American Society for Information Science and Technology, 2010, 61, 7, 1386–1409

[6] Saito, S., Huang, Z., Natsume, R., et al., *PIFu: Pixel-aligned implicit function for high-resolution clothed human digitisation*, In: Proceedings of the IEEE/CVF International Conference on Computer Vision, 2019, 2304–2314

[7] Chen, C., *Science mapping: A systematic review of the literature*, In: Journal of Data and Information Science, 2017, 2, 2, 1–40

[8] Wang, J., Li, X., Pan, L., et al., *Parametric 3D modeling of young women's lower bodies based on shape classification*, In: International Journal of Industrial Ergonomics, 2021, 84, 103142

[9] Liu, K., Wang, C.C.L., Zhang, Y., Mak, M.W., *Construction of a prediction model for body dimensions used in garment pattern making based on anthropometric data learning*, In: The Journal of The Textile Institute, 2017, 108, 12, 2107–2114

[10] Protopsaltou, D., Luible, C., Arevalo, M., et al., *A body and garment creation method for an Internet-based virtual fitting room*, In: Advances in Modelling, Animation and Rendering, London: Springer, 2002, 105–122

[11] Cordier, F., Seo, H., Magnenat-Thalmann, N., *Made-to-measure technologies for an online clothing store*, In: IEEE Computer Graphics and Applications, 2003, 23, 1, 38–48

[12] Fengyi, L., Liu, S., *3D garment design model based on convolutional neural network and virtual reality*, In: Computational Intelligence and Neuroscience, 2022, 1, 9187244

[13] Sayem, A.S.M., *Digital fashion innovations for the real world and Metaverse*, In: International Journal of Fashion Design, Technology and Education, 2022, 15, 3, 301–308

[14] Yu, M., Kim, D.E., *The development of dress forms in standing and sitting postures using 3D body scanning and printing*, In: Fashion and Textiles, 2023, 10, 1, 1–25

[15] Chen, C., Dubin, R., Kim, M.C., *Emerging trends and new developments in regenerative medicine: A scientometric update (2000–2014)*, In: Expert Opinion on Biological Therapy, 2014, 14, 9, 1295–1317

[16] Chen, C., *Science mapping: A systematic review of the literature*, In: Journal of Data and Information Science, 2017, 2, 2, 1–40

[17] Lim, K.H., Phang, J.T.S., *Implementation of 2D-to-3D Prediction Network for Point Cloud Clothing Alignment*, In: 2024 IEEE International Conference on Image Processing (ICIP), 2024

[18] Bindu, D.H., Siri, M., Shanvitha, M.S.V.S., *PoseSmart: AI-Driven Dress Recommendations with Pose Estimation*, In: 2025 3rd International Conference on Computer Vision and Image Processing (CVIP), 2025

[19] Särmäkari, N., *Digital 3D fashion designers: Cases of Atacac and the Fabricant*, In: Fashion Theory, 2023, 27, 5, 689–715

[20] Boughlala, A., Smelik, A., *Tracing the history of digital fashion*, In: Clothing and Textiles Research Journal, 2025

[21] Chan, H.H.Y., Henninger, C.E., Boardman, R., Cano, M.B., *The adoption of digital fashion as an end product: A systematic literature review of research foci and future research agenda*, In: Journal of Global Fashion Marketing, 2024, 15, 1, 155–180

[22] LYST Insights, *The digital fashion report*, 2023, Available at https://www.lyst.com/data/digital-fashion-report/ [Accessed on February 202]

[23] Truiz, C.D., Cruz, A., *Unconventional luxury brand collaborations: A new form of luxury consumption among young adults in China*, In: International Marketing Review, 2023, 40, 7, 1–21

[24] Jiang, Q., Kim, M., Ko, E., *The metaverse experience in luxury brands*, In: Asia Pacific Journal of Marketing and Logistics, 2023, 35, 10, 2280–2297

[25] Kim, J., Sullivan, P., *Emotional branding speaks to consumers' hearts: The case of fashion virtual reality (VR) experience in brand storytelling*, In: Fashion and Textiles, 2019, 6, 1, 1–16

[26] Dwivedi, Y.K., Hughes, L., Baabdullah, A.M., Ribeiro-Navarrete, S., Giannakis, M., Al-Debei, M.M., Dennehy, D., Metri, B., Buhalis, D., Cheung, C.M.K., Conboy, K., Doyle, R., Dubey, R., Dutot, V., Felix, R., Goyal, D.P., Gustafsson, A., Hinsch, C., Janssen, M., Wirtz, J., *Metaverse marketing: How the metaverse will shape the future of consumer research and practice*, In: International Journal of Information Management, 2022, 66, 102542

[27] Mu, X., Zhang, H., Shi, J., Hou, J., Ma, J., Yang, Y., *Fashion intelligence in the Metaverse: Promise and future prospects*, In: Artificial Intelligence Review, 2024

[28] Yoon, S., Oh, H.-J., Song, S., *The impact of virtual try-on technology on consumer purchase intention in the Metaverse fashion industry*, In: Journal of Retailing and Consumer Services, 2023, 73, 103276

[29] Schmidt, L., Weber, M., Müller, S., Carter, B., Hoffmann, C., *Redefining Customer Loyalty in the Age of Virtual Experience: An Innovative Model*, In: Journal of Electronic Commerce and Management, 2024

Authors:

XIZHUO CHEN[1], ANDING LIU[1,2], YU HOU[1], BIN LI[1,2]

[1]Wuhan Textile University, School of Fashion, Minzu Avenue in Hongshan District, 430073, Wuhan, China

[2]Wuhan Textile University, Hubei Research Centre of Intangible Cultural Heritage, Minzu Avenue in Hongshan District, 430073, Wuhan, China

Corresponding authors:

ANDING LIU
e-mail: ada20040705@126.com
BIN LI
e-mail: 405586515@qq.com

Effects of elasticity distribution of sports bras on breast support and pressure comfort performance for senior females

DOI: 10.35530/IT.077.03.2025101

XIAOFANG LIU
YUE SUN
XIAOFEN JI

ABSTRACT – REZUMAT

Effects of elasticity distribution of sports bras on breast support and pressure comfort performance for senior females

Sports bras efficient in the reduction of breast displacement (RBD) were always rated low in pressure comfort performance. Elasticity distribution was found to be influential in RBD and pressure distribution in the under-band; however, the effects of other parts have yet to be studied. This study aimed to investigate the effects of elasticity distribution on RBD and pressure comfort for the optimisation of these two performances for senior females. Five sports bras with different elasticity distribution in 5 parts (front strap, back strap, cup, back panel, and under-band) were developed to compare with the one without elasticity distribution. 20 senior female participants were involved, and the RBD, dynamic peak pressure and compressive feelings at four test points were measured and analysed by ANOVA. The results indicated that Bra A, C, and E significantly improved RBD in all three directions (P<0.001), Bra D enhanced RBD in direction Z (P<0.001), while Bra B showed no significant effect in any direction. The effect on pressure varied with the specific placement of the test point relative to the high-Young's modulus part of the sports bra, and the compressive feelings of Bra A and E were below 3 at all four test points. Comprehensively, the elasticity distributions of applying high-Young's modulus in the front straps (Bra A) and under-band (Bra E) were ideal and typical, which significantly enhanced RBD without inducing discomfort, and provided novel information in optimising RBD and pressure comfort for the sports bras industry and the exercising senior females.

Keywords: *senior females, sports bra, elasticity distribution, breast displacement, pressure comfort*

Efectele distribuției elasticității bustierelor sport asupra susținerii bustului și a confortului la presiune pentru persoanele vârstnice de sex feminin

Bustierele sport eficiente în reducerea deplasării bustului (RBD) au fost întotdeauna evaluate ca având un confort scăzut la presiune. S-a constatat că distribuția elasticității are o influență asupra RBD și asupra distribuției presiunii în zona benzii inferioare; cu toate acestea, efectele celorlalte părți nu au fost încă studiate. Prezentul studiu și-a propus să investigheze efectele distribuției elasticității asupra RBD și asupra confortului la presiune, în vederea optimizării acestor două caracteristici pentru persoanele vârstnice de sex feminin. Au fost dezvoltate 5 bustiere sport cu distribuție diferită a elasticității în 5 părți (breteaua frontală, breteaua din spate, cupa, panoul din spate și banda inferioară) pentru a fi comparate cu cel fără distribuție a elasticității. Au participat 20 de persoane vârstnice de sex feminin, iar RBD, presiunea maximă dinamică și senzațiile de compresie în patru puncte de testare au fost măsurate și analizate prin ANOVA. Rezultatele au indicat că bustierele A, C și E au îmbunătățit semnificativ RBD în toate cele trei direcții (P<0,001), bustiera D a îmbunătățit RBD în direcția Z (P<0,001), în timp ce bustiera B nu a prezentat niciun efect semnificativ în nicio direcție. Efectul asupra presiunii a variat în funcție de amplasarea specifică a punctului de testare în raport cu partea cu modulul Young ridicat al bustierei sport, iar senzațiile de compresie ale bustierelor A și E au fost sub 3 în toate cele patru puncte de testare. În ansamblu, distribuțiile elasticității obținute prin utilizarea unui modul Young ridicat la bretelele frontale (bustiera A) și la banda inferioară (bustiera E) s-au dovedit ideale și tipice, ceea ce a îmbunătățit semnificativ distribuția presiunii (RBD) fără a provoca disconfort și a oferit informații noi privind optimizarea RBD și a confortului la nivel de presiune pentru industria bustierelor sport și pentru persoanele vârstnice de sex feminin care practică exerciții fizice.

Cuvinte-cheie: *persoane vârstnice de sex feminin, bustieră sport, distribuția elasticității, deplasarea bustului, confortul la presiune*

INTRODUCTION

The demographic pressure resulting from the ageing population is one of the most pressing global concerns [1]. Encouraging elderly individuals to engage in low-intensity physical activities is beneficial for their health and helps alleviate the burden on the social healthcare system. However, during physical activity, women's breasts experience movement relative to the chest wall due to the limited anatomical support, which may result in exercise-related breast pain, the risk of breast sagging or even breast diseases [2]. And the situation becomes more pronounced in senior females, as the skin covering the breasts loses elasticity, the connective tissues

become less resilient as a result of a decline in reproductive hormones, estrogen [3]. A sports bra is proven to be effective in reducing the range of movement (ROM) of the breast; however, it also exerts pressure on the body due to the fabric's tensile behaviour, which may lead to discomfort, skin irritation or even injuries in cardiopulmonary function [4]. Besides, the sports bras efficient in breast support often generated higher pressure to females, or were rated low in comfort performance, resulting in a contradiction in sports bras design. For example, Lu et al. observed that a cup with a pad decreased the breast movement but also increased contact pressure, compared to the cup without a pad [5]. Celeste et al. found a lower ROM for cross-back straps when compared to the vertical straps; however, it was also rated low in pressure comfort of the shoulder [6].

Moreover, most of the research focused on the reduction of breast displacement (RBD) or pressure comfort, with limited research focused on the optimisation of these two performances. For senior females, whose breast tissue mechanical properties have declined and become more sensitive to pressure, optimising both support performance and pressure comfort is crucial. Elasticity distribution, i.e., using fabrics of different Young's modulus (a property that quantifies fabric deformation under applied external forces) in different parts [7], is a widely utilised approach to enhance pressure comfort. According to Laplace's law, the pressure exerted by the sports bra is determined by fabric tension and the radius of body curvature [5]. Therefore, variations in Young's modulus in different parts, for the same elongation, will lead to differences in fabric tension and, consequently, alter the pressure distribution. Given the variation in pressure comfort thresholds (PCT, defined as the boundary between pressure comfort and discomfort) across different body regions [8], rational pressure distribution may improve pressure comfort. For instance, Liu et al. presented a new computational pipeline for designing and fabricating 4D garments as knitwear by careful control of elasticity distribution to reduce pressure and fabric sliding [7]. Zheng et al. found that the seamless bras knitted with different loop lengths in different regions provided better comfort to wearers than commercial bras [9]. Recently, researchers found that applying knitting structures with high Young's modulus in the side area of the under-band was effective both in RBD and pressure comfort performance of 4 points covered by the under-band [10]. However, this research predominantly focused on the under-band, while the effects of the elasticity of the whole sports bra have yet to be studied.

In addition, most existing studies on RBD or pressure comfort focused on young women and the movements of running and jumping. The change in anatomical structure and mechanical properties for breast tissues associated with ageing may lead to differences in the results of RBD and pressure comfort. Besides, due to the decline of physiological and psychological exercise capabilities of the elderly, they are encouraged to participate in some low-intensity activities, rather than high-intensity activities such as running and jumping.

This study aimed to explore the effect of the elasticity distribution of sports bras on RBD, pressure distribution and pressure comfort, searching for an optimal elasticity distribution which was effective in improving the support performance without decreasing the pressure comfort of the sports bra for senior females. Consequently, five sports bras with different elasticity distribution (applying high-Young's modulus fabric in front strap, back strap, cup, back panel, and under-band respectively) and one without elasticity distribution (as a control bra) were designed. Forwards-backwards stepping, i.e., a typical movement of square dancing (a widely popular and highly recommended low-intensive exercise for senior females in China, which was proven to be effective in delaying the ageing process), was selected as the experimental movement. RBD, dynamic peak pressure, and psychological pressure comfort sensations of these six sports bras were measured and compared. It was hypothesized that: (1) the elasticity distribution of these five sports bras would significantly improve the reduction of breast displacement (RBD), compared to the control bra; (2) the elasticity distribution of these five sports bras would generate significantly higher dynamic peak pressure, compared to the control bra; (3) based on variations in pressure comfort threshold (PCT) across different body regions, sports bras with rationally designed elasticity distribution would improve the reduction of breast displacement (RBD) without inducing pressure discomfort.

METHODOLOGY

Participants

Following institutional ethical approval, twenty healthy Chinese senior females (aged 60–65 years) from three cities of China (Hangzhou, Shanghai, and Nanjing) were recruited as participants. It has been observed that breast morphology changed in the ageing process, primarily manifesting as increased breast volume, ptosis, and lateral extension, which might affect the breast movement and contact pressure. Therefore, eight anthropometric items of the participants were measured (as shown in table 1), and the participants were selected according to the average anthropometric measurements of Chinese senior females (mean bust girth: 96.70 ± 7.41 cm, mean under-bust girth: 84.23 ± 7.82 cm, mean bust to under-bust difference: 12.47 ± 2.82 cm, mean bust point width: 18.50 ± 1.30cm, mean length from front neck point to bust point: 23.13 ± 2.22 cm, most common cup size: 85B), derived from a survey of 115 Chinese senior females, to minimize the potential between-participant effect in RBD and pressure comfort. The 3D body scanner $(TC)^2$ (US) was used to measure the subjects, and all participants were professionally fitted with an 85B bra size. All subjects had gone through pregnancy, breastfeeding, and

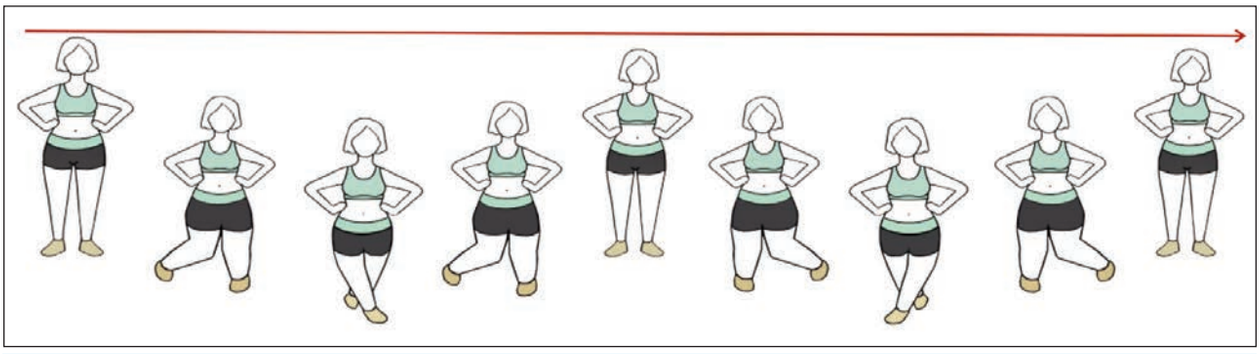

Fig. 1. The illustration of forward-backwards stepping

menopause, experienced no surgical procedures to the breasts, and undertook ≥30 min of exercise more than 4 times a week.

Forwards-backwards stepping, i.e., a typical movement which accounts for 94% of all motions in square dance, was chosen as the experimental movement (figure 1).

Table 1

ANTHROPOMETRIC MEASUREMENTS OF THE SUBJECTS	
Anthropometric measurements	**Mean (Std. D)**
Age (years)	62.60 (1.31)
Height (cm)	158.64 (1.28)
Weight (kg)	61.83 (1.52)
Bust girth (cm)	97.43 (0.56)
Under-bust girth (cm)	84.62 (0.46)
Bust to under-bust difference (cm)	12.81 (0.43)
Bust points width (cm)	18.57 (0.41)
Length from front neck point to bust point (cm)	23.31 (0.41)

Experiment samples

Research showed that well-fitting bras for senior females typically incorporate features such as wide straps, sufficient vertical cup length, higher gore and underarm height, and a rigid under-band, due to morphological changes [11]. Therefore, a compression sports bra with the design features mentioned above was used as the prototype for the experiment samples.

The elasticity distribution of the samples was based on four pressure test points, namely the peak point of shoulder (Point a), the midpoint of the upper scapular region (Point b), the intersection point of under-bust line with the lateral line (Point c), the midpoint between lateral root and the bottom of the breast (Point d), as shown in figure 2, *c*. Point a and c were often reported for pressure discomfort [6]. Points b and d of the elderly women may experience higher pressure compared to young women, due to a forward bending curvature, which is commonly observed in senior females, resulting from kyphosis, and the sagging and lateral extension of breasts [3]. Therefore, the sports bra was divided into 5 parts (front strap, back strap, cup, back panel, and under-band) based on these four test points, to ensure each test point was covered by a different part. To avoid the potential slippage of the peak point of the shoulder (Point a) between the front strap and back strap during physical activity, the front strap was extended 2 cm backwards to ensure continuous coverage of this point by the front strap, as shown in figure 2, *a*.

Two commonly used rib-knitting fabrics with different levels of Young's modulus (F_3~F_4) were selected for the elasticity distribution of the under-band, and two popular weft-knitting fabrics with different levels of Young's modulus (F_1~F_2) were chosen for the front straps, back straps, cups and back panels. The under-band was made of double layers of fabrics, while the other parts were made of a single layer, based on the common types of compression sports bras in the market. The control bra (Bra F) was made

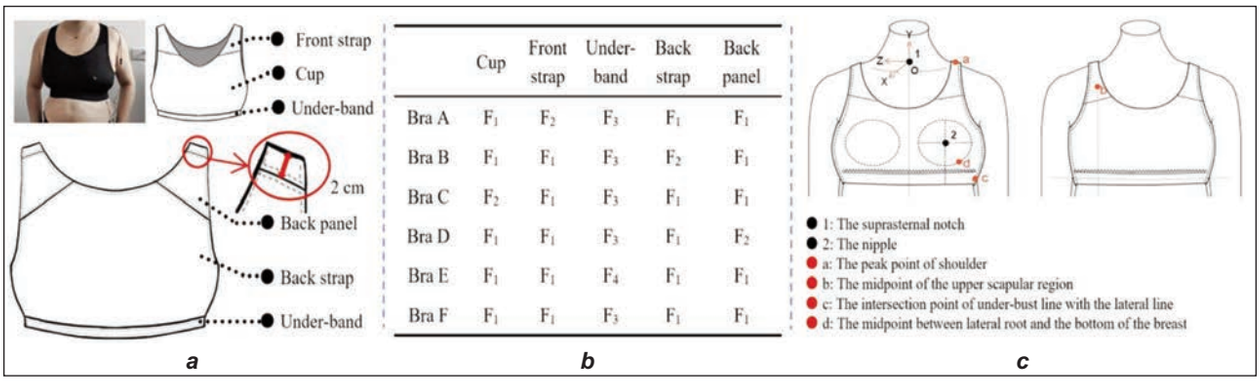

Fig. 2. Experiment details: *a* – structure details of the experimental sample; *b* – elasticity distribution details of the experimental samples; *c* – the trunk local coordinate system (LCS) and the pressure test points

Table 2

PHYSICAL PROPERTY SUMMARY OF THE FABRICS SAMPLES

Fabric	Fabric content	GSM (g/m^2)	Thickness (mm)	E (MPa)	p
F_1	55.1% polyester, 31.7% polyamide, 13.2% spandex	233.60	0.817	1.7235	0.21
F_2	88.7% polyester, 11.3% spandex	315.90	0835	2.8179	0.16
F_3	66.1% polyester, 20.7% polyamide, 13.2% spandex	552.30	1.579	2.3191	0.08
F_4	82.8% polyester, 17.2% spandex	565.10	1.623	3.3563	0.07

Note: The results of F_3 and F_4 were obtained from the tests in which fabrics were folded into double layers to simulate the real wearing conditions of the under-bands.

of fabrics with lower Young's modulus (F_3 for under-band, F_1 for other parts), while the elasticity distribution bras were made of higher Young's modulus in one certain part, and lower Young's modulus in the other four parts, as shown in figure 2, *b*. As the thickness may affect the contact pressure, fabrics were selected with limited differences in thickness between F_1 and F_2, F_3 and F_4. The only differences among these six sports bras were the elasticity distribution; other features, such as style, structure, size, and production methods, were kept the same.

The tensile test was conducted with a tensile testing machine (Instron, USA), according to the Standard FZ/T 70006-2004. The Gramme per Square Meter (GSM) was measured using an electronic balance (XingYun, China) based on the Standard GB/T 4669-2008. The thickness test was carried out with a fabric thickness tester (YG, China) according to the Standard GB/T 3820-1997. The Poisson's ratio (p) was tested with the tensile testing machine (Instron, USA) and a high-definition camera (SONY, Japan). All tests were repeated five times, and the mean value was taken as the average of five test results. The physical properties of the fabrics (F_1~F_4) were summarised in table 2.

Experiment protocol

Motion capture

The breast motion when wearing six sports bras and when naked was captured by the motion capture system (Qualisys, Sweden). A parallel, randomised, blinded design wear trial was carried out. The temperature of the lab was set as 20±2°C, with an average relative humidity of 65±3%. During forward-backwards stepping, as the torso mainly moves in vertical and anterior-posterior direction, the suprasternal notch was chosen as the reference point, while the nipple was chosen as the measuring point for breast movement. A trunk local coordinate system (LCS) based on these two points was established (x: anterior-posterior, y: vertical, z: medial-lateral), which had demonstrated high accuracy in exercises characterised by predominant trunk translation in previous research [5, 6, 12–14]. Two retro-reflective markers were attached to these two points (the suprasternal notch and the nipple, as shown in figure 2, *c*). The relative displacement of the breast was calculated by subtracting the displacement data of the suprasternal notch from that of the nipple, and ROM was determined by the differences between the peak and the trough of the relative displacement curves in gait cycles.

A 30-cycle duration at a frequency of 23 cycles/minute was chosen for the experiment. The middle consecutive 10 gait cycles (the 11^{th}~20^{th}) were selected for analysis. Each sample was tested 3 times, and the mean ROM after wearing each sports bra was taken as the average of the ROM in 30 gait cycles (10 gait cycles multiplied by 3 times). 5-min rest was taken between two test times for each sports bra, and 20 min rest was taken before wearing the next sports bra. Based on ROM, the reduction of breast displacement (RBD) was calculated (breast displacement (braless) minus breast displacement wearing a bra, divided by breast displacement (braless)) [15].

Dynamic peak pressure test

The dynamic peak pressure test was carried out simultaneously with the motion capture, using a pressure testing system (MFF, China), with the pressure sensors (FlexiForce, USA) attached to 4 test points as previously described, as shown in figure 2, *c*.

Similarly, the middle consecutive 10 gait cycles (the 11^{th}~20^{th}) of the total 30 gait cycles were chosen for analysis, and the mean dynamic peak pressure was taken as the average of the peak pressure in the total 30 gait cycles (10 gait cycles multiplied by 3 times).

Subjective pressure comfort test

The pressure comfort was assessed by surveying the wearers regarding their subjective compressive feelings at these 4 test points, using a compressive feeling scale (rated 1~5) developed by Liu et al. [16] and modified according to the samples and pressure test points of this study. Where 1, 2, 3, 4, and 5 represented compressive feelings of extremely weak, weak, neutral, strong, and extremely strong, respectively, and the dynamic peak pressure rated as 3 or below 3 was deemed appropriate, indicating the pressure was acceptable and unlikely to induce discomfort. Compressive feelings were evaluated immediately after the motion capture and pressure test. The test for each sports bra was also repeated 3 times, and the mean compressive feeling when wearing each sports bra was calculated as the average of the three test results.

RESULTS AND DISCUSSION

The effects of elasticity distribution on breast displacement

The multi-planar displacement of the breast when wearing six sports bras of a representative subject (S_1) during one typical gait cycle of forwards-backwards stepping is exhibited in figure 3. The maximum breast displacement occurred in direction Y, followed by direction Z and X. The breast displacement curve in all three directions undergoes four phases, consistent to four stages of the trunk displacement curve in vertical direction (labelled as phases A, B, C, and D in figure 3, *a*), indicating that breast displacement was mainly affected by the trunk movement in direction Y during forwards-backwards stepping, which was much larger than the other two directions.

RBD of 6 sports bras in 3 directions were exhibited in figure 3, e, which showed the highest RBD in the vertical direction (RBD_y: 53.19 ± 1.11% ~ 64.51 ± 0.92%), followed by the medio-lateral direction (RBD_z: 39.69 ± 0.85% ~ 51.23 ± 1.24%) and the anterior-posterior direction (RBD_x: 30.41 ± 1.14% ~ 41.11 ± 1.09%). The data of RBD in three directions when wearing these six sports bras were found to be parametric (Kolmogorov–Smirnov and Shapiro–Wilk, $p>0.05$), and significant differences in bra by direction interaction effect ($F = 524.799$, $P < 0.001$, $\eta^2_{partial} = 0.958$) in RBD were detected by repeated-measures analysis of variance (ANOVA). Bra A performed best in direction X (41.11 ± 1.09%) and Y (64.51 ± 0.92%), while Bra C performed best in direction Z (51.23 ± 1.24%). Bra A, C and E exhibited significantly higher RBD than Bra F in all three directions ($P < 0.001$), Bra D significantly enhanced RBD in direction Z ($P < 0.001$), while Bra B showed no significant difference in RBD with Bra F in any direction, rejecting the first hypothesis.

The results indicated that applying fabrics with high Young's moduli in the front strap (Bra A), cup (Bra C) and under-band (Bra E) achieved significant effects in improving RBD in all three directions. High Young's modulus in the under-band may result in the increasing of contact pressure and body-bra friction, reducing under-band slippage [10], while high Young's modulus in the cup may lead to high fabric tension, effectively limiting breast movement and consequently enhancing RBD. Specifically, researchers have shown that a high Young's modulus of the entire strap contributed to improved RBD [17]. However, the differences between the front and back parts were not detected. The results of this study revealed that high Young's modulus in the front strap effectively improved RBD, rather than the back strap.

The effects of elasticity distribution on dynamic peak pressure

The data of dynamic peak pressure at four test points when wearing six sports bras were found to be parametric (Kolmogorov–Smirnov and Shapiro–Wilk, $p > 0.05$), and significant differences in bra by test point interaction effect ($F = 77.079$, $P < 0.001$, $\eta^2_{partial} = 0.772$) in dynamic peak pressure were detected by repeated-measures analysis of variance (ANOVA). Compared to Bra F, Bra A showed significantly higher pressure at Points a, b, and d ($P < 0.001$), while Bra B exhibited significantly higher

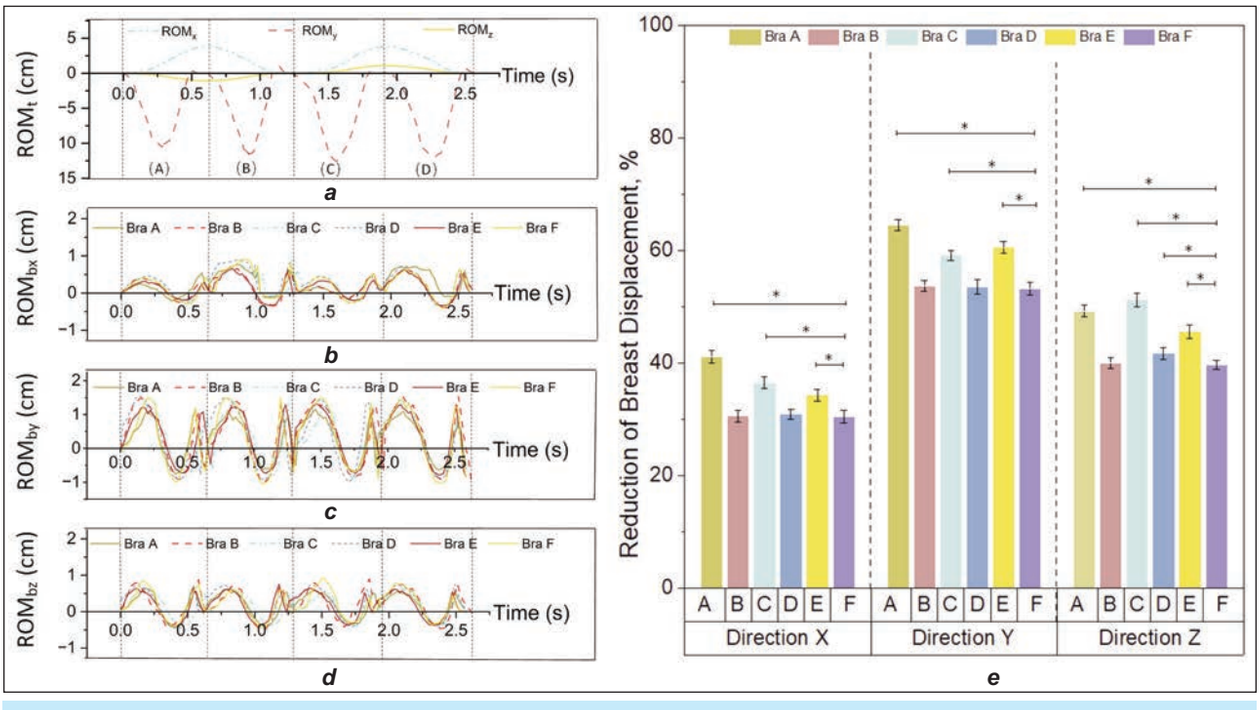

Fig. 3. The displacement of trunk and breast of a representative subject (S_1) during one typical gait cycle of forwards-backwards stepping: *a* – range of trunk movement (ROM_t); *b* – range of breast movement in direction X (ROM_{bx}); *c* – range of breast movement in direction Y (ROM_{by}); *d* – range of breast movement in direction Z (ROM_{bz}); *e* – reduction of breast displacement (RBD)

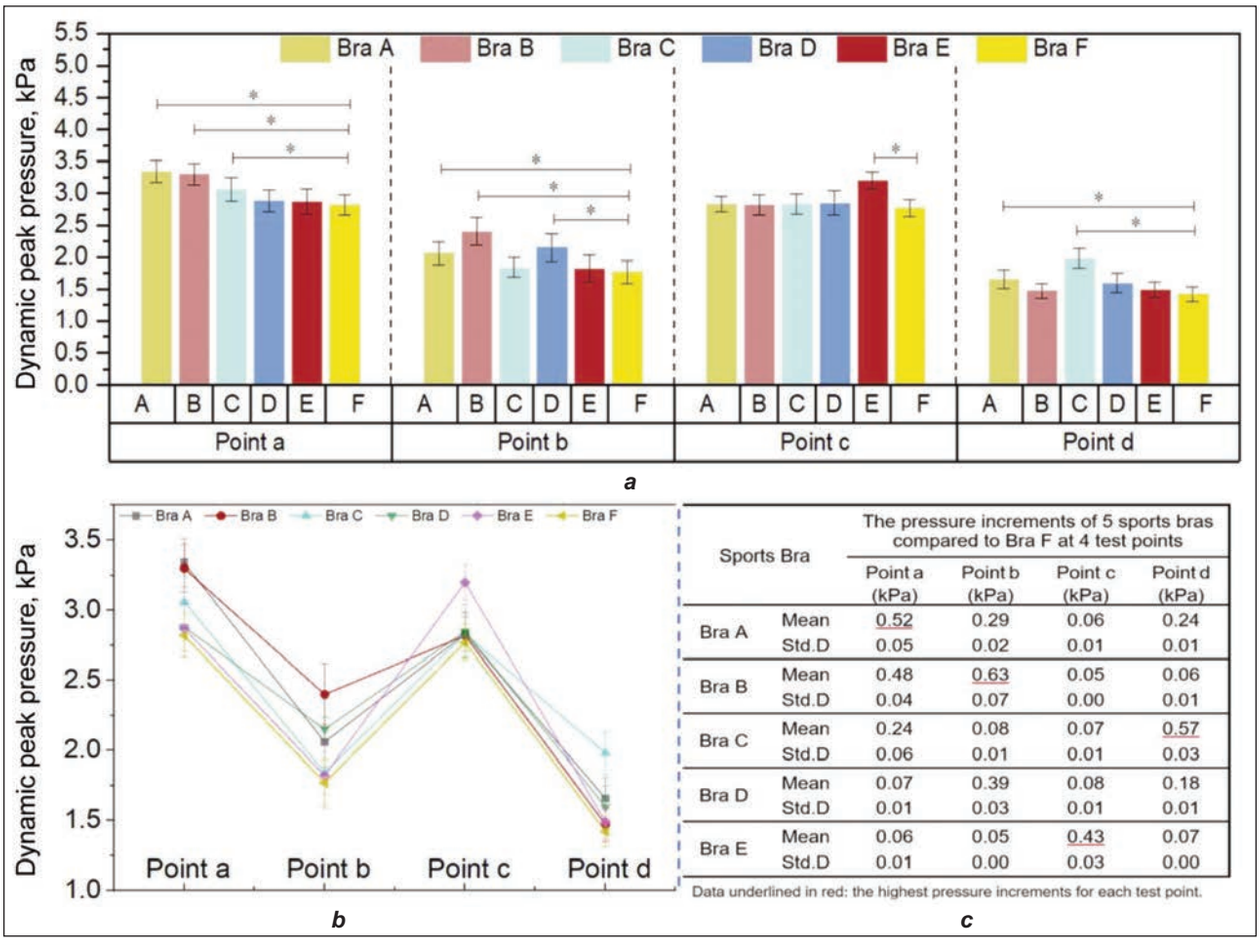

Sports Bra		The pressure increments of 5 sports bras compared to Bra F at 4 test points			
		Point a (kPa)	Point b (kPa)	Point c (kPa)	Point d (kPa)
Bra A	Mean	0.52	0.29	0.06	0.24
	Std.D	0.05	0.02	0.01	0.01
Bra B	Mean	0.48	0.63	0.05	0.06
	Std.D	0.04	0.07	0.00	0.01
Bra C	Mean	0.24	0.08	0.07	0.57
	Std.D	0.06	0.01	0.01	0.03
Bra D	Mean	0.07	0.39	0.08	0.18
	Std.D	0.01	0.03	0.01	0.01
Bra E	Mean	0.06	0.05	0.43	0.07
	Std.D	0.01	0.00	0.03	0.00

Data underlined in red: the highest pressure increments for each test point.

Fig. 4. The comparison of mean dynamic peak pressure between samples: *a* – the differences in the mean dynamic peak pressure; *b* – the pressure distribution; *c* – the pressure increment of Bra A, B, C, D, E, compared to Bra F

pressure at Points a and b ($P < 0.001$). Bra C significantly increased pressure at Point a and d ($P < 0.001$), Bra D generated significantly higher pressure at Point b ($P < 0.001$), while Bra E significantly increased pressure at Point c ($P < 0.001$), as shown in figure 4, *a*. All five sports bras generated significantly higher dynamic peak pressure at certain test points, but no significantly differences were found at other test points, compared to bra F. Therefore, the second hypothesis was partially accepted.

Concerning pressure distribution, crossed curves of 6 sports bras were observed (figure 4, *b*), indicating varied pressure distribution of each bra. Compared to bra F, the pressure at each point of the other 5 bras increased (figure 4, *c*), suggesting that applying a high Young's modulus in any part of the sports bra resulted in pressure increase at all test points. However, the pressure increment at each point varied across different elasticity distributions. For points a, b, and d, bras with high Young's modulus in the parts covering the test point and the part adjacent to the test point in the stretching direction showed greater pressure increments, while bras with high Young's modulus in the parts far away from the test point exhibited smaller increments. For example, Bra A (with high Young's modulus in front strap covering Point a) demonstrated the highest dynamic pressure increment at Point a (0.52 ± 0.05 kPa), followed by Bra B and Bra C (0.48 ± 0.04 kPa and 0.24 ± 0.06 kPa respectively, with high Young's modulus in back strap and cup), while Bra D and E (with high Young's modulus in back panel and under-band) exhibited the lowest dynamic peak pressure increment (0.07 ± 0.01 kPa and 0.06 ± 0.01 kPa respectively) as shown in figure 4, *c*. This might have been because a high-modulus section would promote greater stretching in the adjacent areas, resulting in larger elongation, and thus higher pressure, which was also observed in previous research [7]. For Point c, only Bra E with a high Young's modulus in the under-band significantly increased the dynamic peak pressure; this effect could be attributed to the end-to-end structure of the under-band, which was weakly influenced by other parts.

The effects of elasticity distribution on compressive feeling

As shown in figure 5, the compressive feelings of Bra A ($2.20 \pm 0.10 \sim 2.72 \pm 0.13$), E ($1.93 \pm 0.14 \sim 2.83 \pm 0.15$) and F ($1.75 \pm 0.12 \sim 2.01 \pm 0.11$) were all below 3 at all four test points, indicating that the pressure is appropriate and acceptable, while that of Bra B (3.78 ± 0.26) and D (3.46 ± 0.29) at Point b, and Bra C at Point d (3.85 ± 0.18) exceeded 3, indicating that

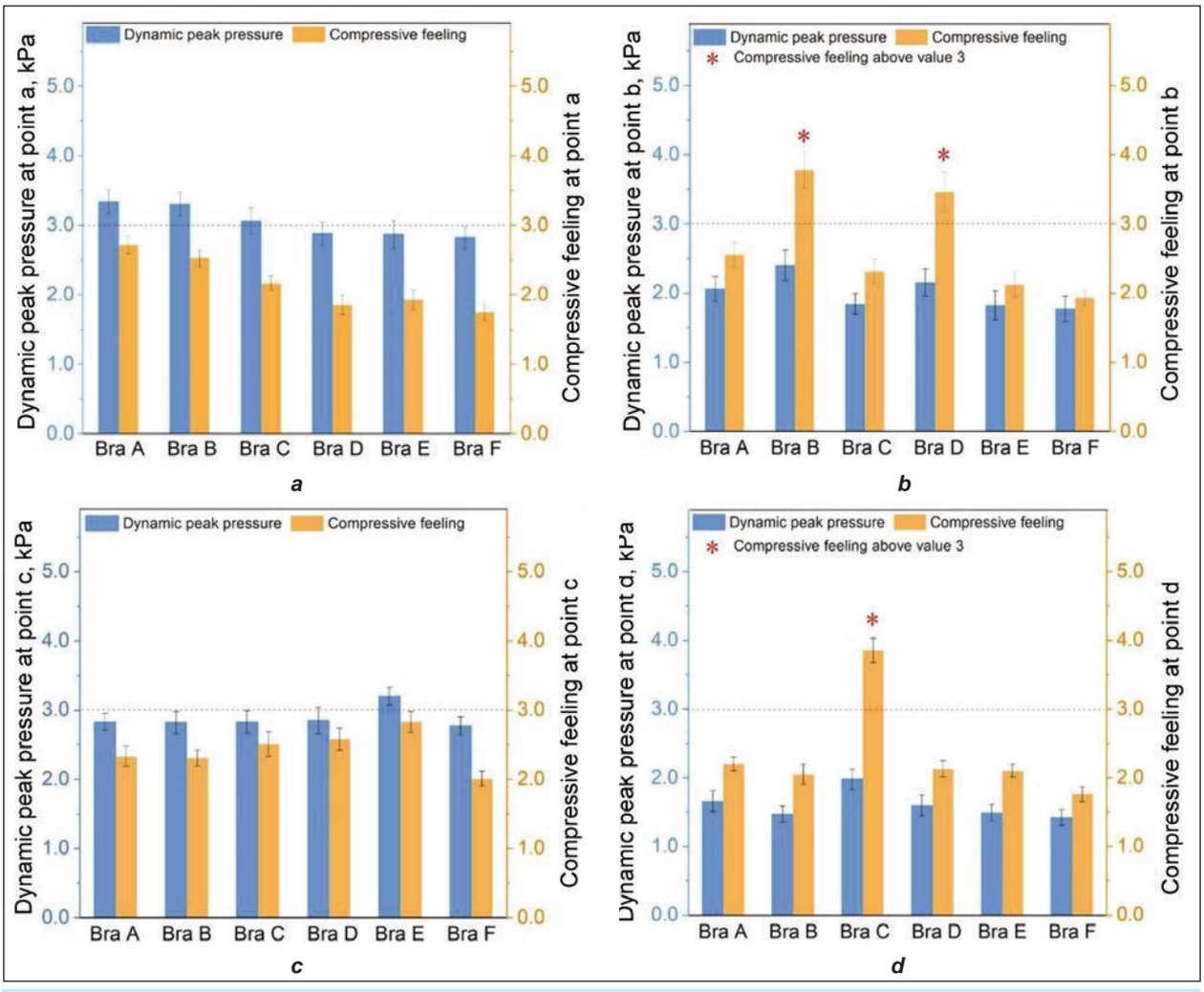

Fig. 5. The dynamic peak pressure and compressive feeling of six sports bras at: *a* – Point a; *b* – Point b; *c* – Point c; *d* – Point d

the pressure is excessively high and might contribute to discomfort. Therefore, although Bra A and E significantly increased the dynamic peak pressure at Point a, b, d (for Bra A), and Point c (for Bra E, as shown in figure 4, *a*), they would not induce pressure discomfort.

The results might have been due to the differences in pressure comfort thresholds (PCT) across body regions, which were also reported in previous researches [8], resulted from the differences in human anatomical structure, such as local shape, subcutaneous soft tissue properties and bone structure or the differences in body deformation under external pressure, which had been suggested closely related to the clothing pressure comfort [18]. The bone-next-to-skin areas (e.g., Point a and c) always exhibited a higher PCT, while the areas where remarkable fat accumulated always showed a lower PCT (e.g., Point d) [8]. In addition, a wider, thicker, and more curved upper back, the increased back pain, and discomfort in the levator scapulae muscle caused by the additional burden of the breasts observed in senior females [19] might contribute to a lower PCT in the upper scapular area (Point b).

Summarily, Bra A and E performed best, which significantly enhanced RBD without inducing pressure discomfort, accepting the third hypothesis. Bra C also effectively improved RBD; however, it exerted excessive pressure at point d, while Bra D significantly improved RBD in direction Z but led to excessive pressure at point b. Bra B showed no significant effect on RBD but generated excessive pressure at point B, resulting in pressure discomfort.

Consequently, the elasticity of applying high-Young's modulus fabric in front straps (Bra A) and under-band (Bra C) was suggested to optimise both RBD and pressure comfort for senior females.

CONCLUSION

This study provided novel information in optimising the breast support and pressure comfort performance of sports bras for senior females, by applying elasticity distribution in front strap, back strap, cup, back panel and under-band. The findings revealed that elasticity distribution significantly affected RBD, pressure distribution, and compressive feeling of senior females during the typical movement of square dancing, i.e., forwards-backwards stepping.

The effect on RBD varied with elasticity distributions and directions. Bra A, C, and E significantly improved RBD in all three directions ($P < 0.001$), Bra D only enhanced RBD in direction Z ($P < 0.001$), while Bra B showed no significant effect in any direction. The effect on pressure varied with the specific placement of the test point relative to the high-Young's modulus part of the sports bra. For Points a, b, and d, bras with high Young's modulus in the parts covering and adjacent to the test points generated higher pressure than the others, while for Point c, only Bra E with high Young's modulus in the under-band significantly raised the dynamic peak pressure. The compressive feelings of Bra A and E were all below 3 (neutral compressive feeling and the pressure is considered appropriate) at all four test points, while those of Bra B, C, and D exceeded 3 at certain test points. Comprehensively, the elasticity distributions of applying high-Young's modulus fabric in the front straps (Bra A) and under-band (Bra E) were ideal and typical, which significantly enhanced RBD without inducing discomfort, and were suggested to optimise both RBD and pressure comfort for senior females.

It is suggested that future research may include a wider range of Young's modulus, more elasticity distribution cases, test points, and more low-intensive activities to provide a comprehensive and in-depth understanding of the effects of elasticity distribution for senior females. Additionally, A large-scale experiment with stratified depth randomisation will be needed for future research to benefit more exercising senior females of different ages, body mass, breast morphology and breast size.

FUNDING INFORMATION

1. High-level talents research start-up project of Jinling Institute of Technology (jit-b-202368).
2. General project of philosophy and social science research in Jiangsu universities (2024SJYB0423).
3. General Project of Humanities and Social Sciences Research of the Ministry of Education of China (24YJCZH268).

REFERENCES

[1] Zhang, J., Lau, N., Huang, T.-C., et al., *Identifying key evaluation criteria and design attributes to optimise sports bra design for senior females*, In: Fashion and Textiles, 2025, 12, 1, http://doi.org/10.1186/s40691-025-00413-2

[2] Brisbine, B.R., Steele, J.R., Phillips, E.J., et al., *Breast pain affects the performance of elite female athletes*, In: Journal of Sports Sciences, 2020, 38, 5, 528–533, http://doi.org/10.1080/02640414.2020.1712016

[3] Coltman, C.E., Steele, J.R., McGhee, D.E., *Effects of age and body mass index on breast characteristics: a cluster analysis*, In: Ergonomics, 2018, 61, 9, 1232–1245, http://doi.org/10.1080/00140139.2018.1481229

[4] Macintyre, L., *Designing pressure garments capable of exerting specific pressures on limbs*, In: Burns, 2007, 33, 5, 579–586, http://doi.org/10.1016/j.burns.2006.10.004

[5] Lu, M., Qiua, J., Wang, G., et al., *Mechanical analysis of breast–bra interaction for sports bra design*, In: Materials Today Communications, 2016, 6, 28–36, http://doi.org/10.1016/j.mtcomm.2015.11.005

[6] Celeste, E.C., Deirdre, E.M., Julie, R.S., *Bra Strap Orientations and Designs to Minimse Bra Strap Discomfort and Pressure during Sport and Exercise in Women with Large Breasts*, In: Sports Medicine-Open, 2016, 2, 5, 1–8, http://doi.org/ 10.1186/s40798-015-0014-z

[7] Liu, Z.S., Han, X.J., Zhang, Y.C., et al., *Knitting 4D Garments with Elasticity Controlled for Body Motion*, In: ACM Transactions on Graphics, 2021, 40, 4, http://doi.org/10.1145/3450626.3459868

[8] Wang, Y.R., Liu, Y., Luo, S.L., et al., *Pressure comfort sensation and discrimination on female body below waistline*, In: Journal of Industrial Textiles, 2018, 109, 8, 1067–1075, http://doi.org/10.1080/00405000.2017.1399498

[9] Zheng, R., Yu, W., Fan, J., *Pressure evaluation of 3D seamless knitted bras and conventional wired bras*, In: Fibers and Polymers, 2009, 10, 1, 124–131, http://doi.org/10.1007/s12221-009-0124-7

[10] Liu, X., Ji, X., Yan, Y., et al., *The elasticity distribution of under-band based on pressure comfort and breast support performance for seamless sports bras*, In: Industria Textila, 2023, 74, 3, 278–285, http://doi.org/10.35530/IT.074.03.202244

[11] Zhang, S.C., Yick, K.L., Yip, J., et al., *An understanding of bra design features to improve bra fit and design for older Chinese women*, In: Textile Research Journal, 2021, 91, 3–4, 406–420, http://doi.org/10.1177/0040517520944253

[12] Liu, X., Ji, X., Ocran, F.M., *Effects of ventilation design on thermal comfort performance and breast displacement for sports bras*, In: Textile Research Journal, 2023, 93, 3–4, 519–537, http://doi.org/10.1177/00405175221122508

[13] Liang, R., Yip, J., Yu, W., et al., *Numerical simulation of nonlinear material behaviour: Application to sports bra design*, In: Materials & Design, 2019, 183, http://doi.org/10.1016/j.matdes.2019.108177

[14] Coltman, C.E., McGhee, D.E., Steele, J.R., *Bra strap orientations and designs to minimise bra strap discomfort and pressure during sport and exercise in women with large breasts*, In: Sports Medicine-Open, 2015, 1, 1, 21, http://doi.org/10.1186/s40798-015-0014-z

[15] Zhou, J., Yu, W., Ng, S.-p., *Identifying effective design features of commercial sports bras*, In: Textile Research Journal, 2012, 83, 14, 1500–1513, http://doi.org/10.1177/0040517512464289

[16] Liu, H., Chen, D.S., Wei, Q.F., et al., *An investigation into the bust girth range of pressure comfort garment based on elastic sports vest*, In: Journal of the Textile Institute, 2013, 104, 2, 223–230, http://doi.org/10.1080/00405000.2012.714940

[17] Yan, Y.X., Gao, J., Jin, Z.M., et al., *Research on the relationship between clothing pressure developed by women's basketball sports bra and heart rate variation indexes*, In: International Journal of Clothing Science and Technology, 2014, 26, 6, 500–508, http://doi.org/10.1108/ijcst-12-2013-0143

[18] Dan, R., Shi, Z., *Numerical simulation of the area shrinkage mass for the waist of elastic pantyhose by using FEM*, In: International Journal of Clothing Science and Technology, 2019, 32, 2, 244–254, http://doi.org/10.1108/ijcst-05-2019-0069

[19] Ryan, E.L., *Pectoral girdle myalgia in women: a 5-year study in a clinical setting*, In: Clinical Journal of Pain, 2000, 16, 4, 298–303, http://doi.org/10.1097/00002508-200012000-00004

Authors:

XIAOFANG LIU[1], YUE SUN[2], XIAOFEN JI[3]

[1]Jinling Institute of Technology, College of Art, No.99 Hongjing Avenue, Jiangning District, Nanjing 211169, Jiangsu Province, China
e-mail: fongfonghz@163.com

[2]Zhejiang Sci-Tech University, School of Fashion Design and Engineering, No.8 Kangtai Road, Linping District, Hangzhou 311199, Zhejiang Province, China
e-mail: sunyue@zstu.edu.cn

[3]Zhejiang Sci-Tech University, School of International Education, No.8 Kangtai Road, Linping District, Hangzhou 311199, Zhejiang Province, China

Corresponding author:

XIAOFEN JI
e-mail: xiaofenji@zstu.edu.cn

Innovative application of batik patterns in Cheongsam design

DOI: 10.35530/IT.077.03.202541

ZHANG YU JUN JUNG JUNG HO

ABSTRACT – REZUMAT

Innovative application of batik patterns in Cheongsam design

To explore the sensory imagery differences in Cheongsam styling resulting from the combination of various batik pattern themes, this study selected four different thematic categories of batik patterns and used commonly worn Cheongsams as the research carrier. By integrating these elements, 24 Cheongsam research samples were developed, along with six pairs of Kansei words forming the semantic space for evaluation. A survey questionnaire was designed to collect consumers' sensory evaluation of the Cheongsam samples. Subsequently, data analysis was conducted using SPSS 26.0. The results indicate that two primary Kansei factors influence the appearance of batik-patterned Cheongsams, which were identified as the style factor and the temperament factor based on their characteristics. Different batik pattern themes combined with Cheongsam exhibit distinct sensory imagery in their appearance. Cluster analysis further revealed that Cheongsam samples within different clusters possess unique sensory evaluation characteristics, while those within the same cluster show a high level of consistency in overall sensory evaluation of appearance. This study proposes design methods and recommendations for the integration of batik patterns with traditional Cheongsam, expanding the development path for the application of batik patterns in traditional garment design. It contributes to the preservation and development of batik culture from the perspective of intangible cultural heritage and provides insights into the innovative design of traditional handicrafts.

Keywords: *batik, Cheongsam, factor, Kansei engineering, sensory imagery, SPSS*

Aplicarea inovatoare a modelelor Batik în designul rochiilor Cheongsam

Pentru a explora diferențele de imagistică senzorială în stilul rochiilor Cheongsam rezultate din combinarea diverselor teme de modele Batik, acest studiu a selectat patru categorii tematice diferite de modele Batik și a utilizat rochiile Cheongsam purtate în mod obișnuit ca suport de cercetare. Prin integrarea acestor elemente, au fost create 24 de probe de rochii Cheongsam pentru cercetare, împreună cu șase perechi de cuvinte Kansei care formează spațiul semantic pentru evaluare. A fost conceput un chestionar de sondaj pentru a colecta evaluarea senzorială a consumatorilor cu privire la probele de rochii Cheongsam. Ulterior, analiza datelor a fost efectuată utilizând SPSS 26.0. Rezultatele indică faptul că doi factori Kansei primari influențează aspectul rochiilor Cheongsam cu modele Batik, care au fost identificați ca factorul stil și factorul temperament pe baza caracteristicilor lor. Diferitele teme ale modelelor Batik combinate cu Cheongsam prezintă imagini senzoriale distincte în ceea ce privește aspectul lor. Analiza cluster a relevat, de asemenea, că probele Cheongsam din cadrul diferitelor clustere dețin caracteristici unice de evaluare senzorială, în timp ce altele din cadrul aceluiași cluster prezintă un nivel ridicat de consistență în evaluarea senzorială generală a aspectului. Acest studiu propune metode de design și recomandări pentru integrarea modelelor Batik cu Cheongsam-ul tradițional, extinzând astfel perspectivele de dezvoltare pentru aplicarea modelelor Batik în designul vestimentar tradițional. Acesta contribuie la conservarea și dezvoltarea culturii Batik din perspectiva patrimoniului cultural imaterial și oferă perspective asupra designului inovator al meșteșugurilor tradiționale.

Cuvinte-cheie*: Batik, Cheongsam, factor, inginerie Kansei, imagini senzoriale, SPSS*

INTRODUCTION

As an important part of China's traditional culture, Batik holds a unique status and plays a significant role in Chinese heritage. It also serves as a valuable resource for contemporary cultural innovation. Batik, historically known as wax-resist dyeing, is recognised as one of the four major traditional Chinese dyeing and weaving techniques, alongside clamp-resist dyeing, tie-dyeing, and ash-resist dyeing [1]. Batik is a traditional Chinese folk handcrafted printing and dyeing technique that mainly uses wax knives and liquid wax as tools and materials, and natural fibre fabrics such as cotton and linen as creative carriers. Through the processes of indigo solution dyeing and boiling-water dewaxing, batik creates patterns with strong ethnic and regional characteristics, embodying historical depth and artistic value [2]. In 2006, Miao batik was included in the first batch of national intangible cultural heritage representative projects [3]. Regarding batik craft, many scholars have taken Miao batik techniques and patterns as research objects, analysing their unique cultural connotations, artistic characteristics and innovative design applications in modern products. For example, Tian et al. [4] proposed an automatic generation method for batik floral patterns based on the Iterated Function System within fractal geometry. This method aims to facilitate

the digitalisation and innovative design of the printing and dyeing industry while supporting the spread and development of intangible cultural heritage, such as batik. By incorporating fractal theory, designers and users can achieve the automatic generation and transformation of batik patterns. Chen et al. [5] proposed a method to extract batik fabric patterns and elements. The method preprocesses digital images of batik fabrics using morphological preprocessing, extracts pattern elements, and generates independent element images. The Canny algorithm extracts the overall contours of batik elements. This method enables efficient digital storage and promotes the further development of batik patterns. To promote the inheritance of batik techniques among young people, Zheng et al. [6], from the perspective of user experience, established the Kano model to classify and optimise the demand factors generated by users during the batik experience, and proposed new ideas such as the re-creation of the pattern of batik, finished product carrier, and experience process. Finally, they designed a batik technique process that meets the user experience of young users. Bao et al. [7] analysed the artistic expression techniques of batik fabrics and conducted innovative research on the method of combining batik and other handicraft printing and dyeing techniques by examining the artistic expression of batik fabrics. They broadened new perspectives for the preservation and development of the traditional art of handmade printing and dyeing. Li et al. [8] combined batik patterns with clothing design, segmented and reorganised batik patterns and colours, and created derivative patterns by combining the three-dimensional craftsmanship of fabrics, enriching the cultural heritage and artistic connotation of modern fashion and protecting the continuation and inheritance of batik culture. This approach is guided by the interests and aesthetic preferences of modern people.

However, the above research mainly focuses on the digital generation and preservation of batik patterns, the user experience of batik techniques, batik process innovation and the design of modern products, but there is a lack of research on the innovative application of batik patterns in traditional clothing. The Cheongsam reflects China's historical and cultural tradition, still popular and practical today, and it serves as an ideal medium for integrating batik pattern elements [9]. Based on the existing research results, this paper takes batik patterns as the research subject, the traditional Cheongsam as the design medium, and uses Kansei engineering as the theoretical framework. It uses objective analysis methods such as quantitative analysis and factor analysis to explore the changes in consumers' cognitive perception of different styles of batik patterns combined with Cheongsam. The findings of this study provide a theoretical reference for designers in creating and developing batik Cheongsams that better meet consumers' sensory needs and provide a reference for consumers to choose products that meet their sensory needs. Furthermore, this paper summarises design and application methods for combining batik patterns with Chinese traditional clothing, Cheongsams, based on Kansei engineering. This is to offer practical insights and help for the application of batik folk culture in the innovative design of traditional clothing, and to promote and develop new directions for batik art. At the same time, the integration of batik and Cheongsam fosters symbolic reconstruction and cultural hybridity, revealing aesthetic characteristics typical of the Chinese cultural context and reaffirming the role of dress as a marker of identity construction [10].

DETERMINE THE STUDY PROTOCOL

Theory of Kansei Engineering

The concept of Kansei engineering was first proposed by Kenichi Yamamoto in October 1986 [11]. Kansei refers to the overall perception a person experiences of an artefact, environment, or situation through their senses of sight, hearing, touch, smell, taste, and cognition [12]. Kansei engineering technology is a method that visualises and quantifies the user's sensory imagery and finds the correlation between it and product attributes to guide design and research [13]. While meeting the subjective needs of consumers, it provides designers with a more efficient product design and development approach [14]. Currently, Kansei engineering is involved in clothing style, colour, fabric and function design [15].

Determine the batik pattern

Batik refers to a dyeing process in which wax is melted into liquid form and applied to the preconceived pattern areas of the fabric. The fabric is then immersed in dye to achieve colouration. Due to the water-insoluble properties of wax, the applied wax forms a resist layer on the fabric's surface, protecting the original colour and preventing the dye from penetrating the material. Finally, the wax is removed through washing, revealing the desired pattern [16]. From an overview of the current batik product market, the rapid development of the market economy has driven the transformation of batik production from traditional handmade family workshops to mechanised factory-based production. To some extent, this shift has increased the production volume of batik products and expanded production channels. However, challenges remain, such as the lack of diversity in patterns, motifs, and the types and properties of substrates used in batik production. However, batik products still face challenges such as a lack of diversity in patterns, motifs, and the types and properties of carriers used.

Batik patterns, as an embodiment of artisans' aesthetic consciousness, are characterised predominantly by stylised visual forms and composition [17]. In this study, extensive batik patterns were collected and systematically classified through market surveys and website research. Subsequently, expert consultations, interviews, and literature reviews were conducted to categorise the collected batik designs into four categories based on their subject matter and stylistic features: plant patterns, animal patterns,

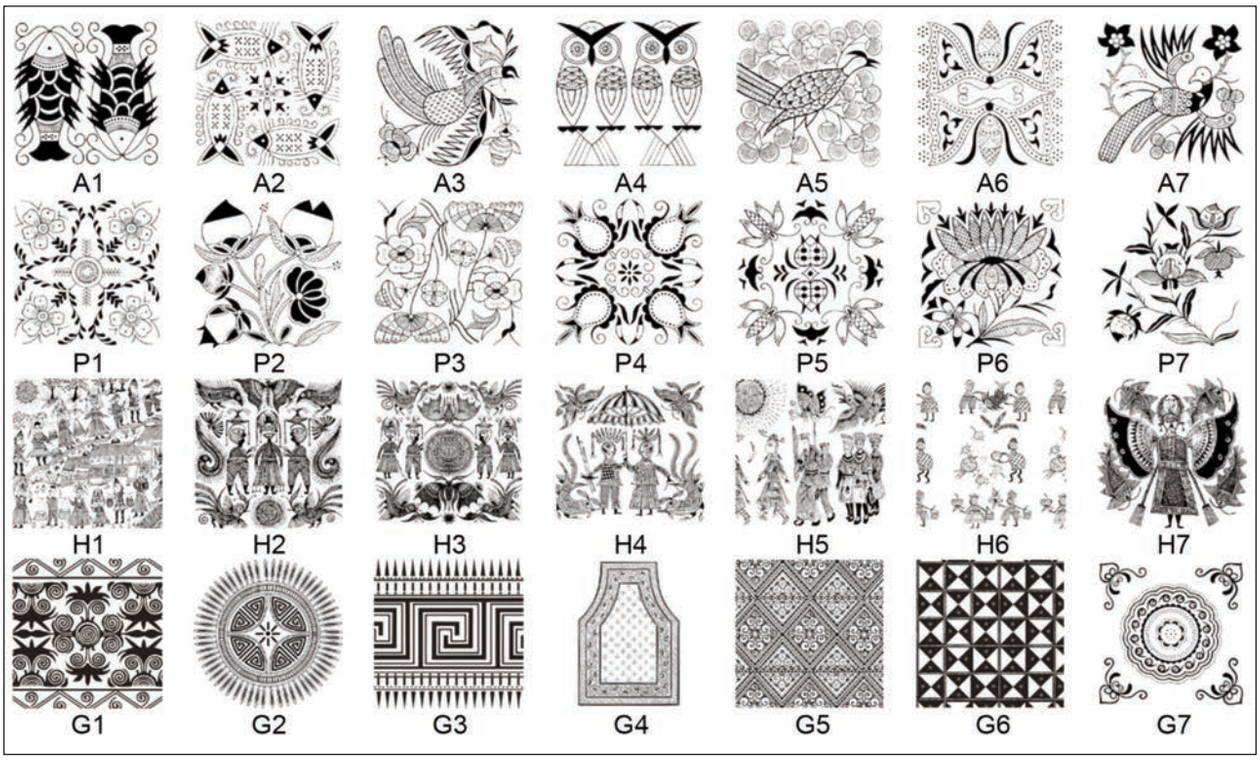

Fig. 1. Study sample of the batik pattern

geometric patterns, and human figure patterns. Through field research and the examination of physical artefacts, the collected patterns were further analysed and categorised. Ultimately, seven representative patterns were extracted from each category, resulting in a total of 28 batik patterns selected as representative samples for subsequent pattern analysis. To ensure that the subsequent sensory evaluations were not influenced by fabric material, colour, clarity, or size, the 28 selected batik patterns were standardised using Adobe Photoshop 2021. The images were subjected to correction, desaturation, sharpness adjustment, and parameter modification. All pattern samples were converted into black-and-white vector graphics with identical settings, and the image dimensions were uniformly set to 2.0 cm × 2.0 cm. In addition, batik patterns with high similarity were arranged separately to improve differentiation. The specific styles of batik patterns are shown in figure 1. Patterns No. A1-A7 are animal batik patterns, No. P1-P7 are plant batik patterns, No. H1-H7 are human figure batik patterns, and No. G1-G7 are geometric batik patterns. The numbering system includes a visual key in which the letter before each number serves as an index to differentiate the pattern categories.

Determine the Cheongsam sample

Using CorelDraw software, the batik patterns from figure 1 were individually applied to a stand-up collar basic Cheongsam design of the same size, with adjustments made to their arrangement, combination, and orientation as needed. All samples were then standardised as black-and-white vector graphics with dimensions of 5.0 cm in height and 2.0 cm in width, yielding 28 final images. Cheongsam samples No. a_1–a_7 incorporate animal batik patterns; p_1–p_7 incorporate plant batik patterns; h_1–h_7 incorporate human figure batik patterns; and g_1–g_7 incorporate geometric batik patterns. The 28 samples were randomly coded, as shown in figure 2.

QUESTIONNAIRE INVESTIGATION AND ANALYSIS

Determine the Kansei word pair

A large collection of adjectives describing the style and design of batik-patterned Cheongsams was first compiled. Subsequently, a focus group consisting of 40 participants was invited to discuss and refine the adjective set. The group included: ten senior practitioners with over 20 years of experience in traditional ethnic hand-dyeing and garment craftsmanship; ten university faculty engaged in teaching and research on ethnic textile printing and apparel design, with an average teaching tenure of more than 10 years, several of whom have 15–20 years of academic experience; ten professional designers specializing in ethnic hand-dyeing clothing with substantial practical experience in the industry; and ten Cheongsam enthusiasts who consistently purchase, collect, and wear Cheongsams and have a deep understanding of their stylistic attributes. All participants had close connections with either batik or Cheongsams and long-term exposure to batik Cheongsam design, enabling them to make informed judgments. This

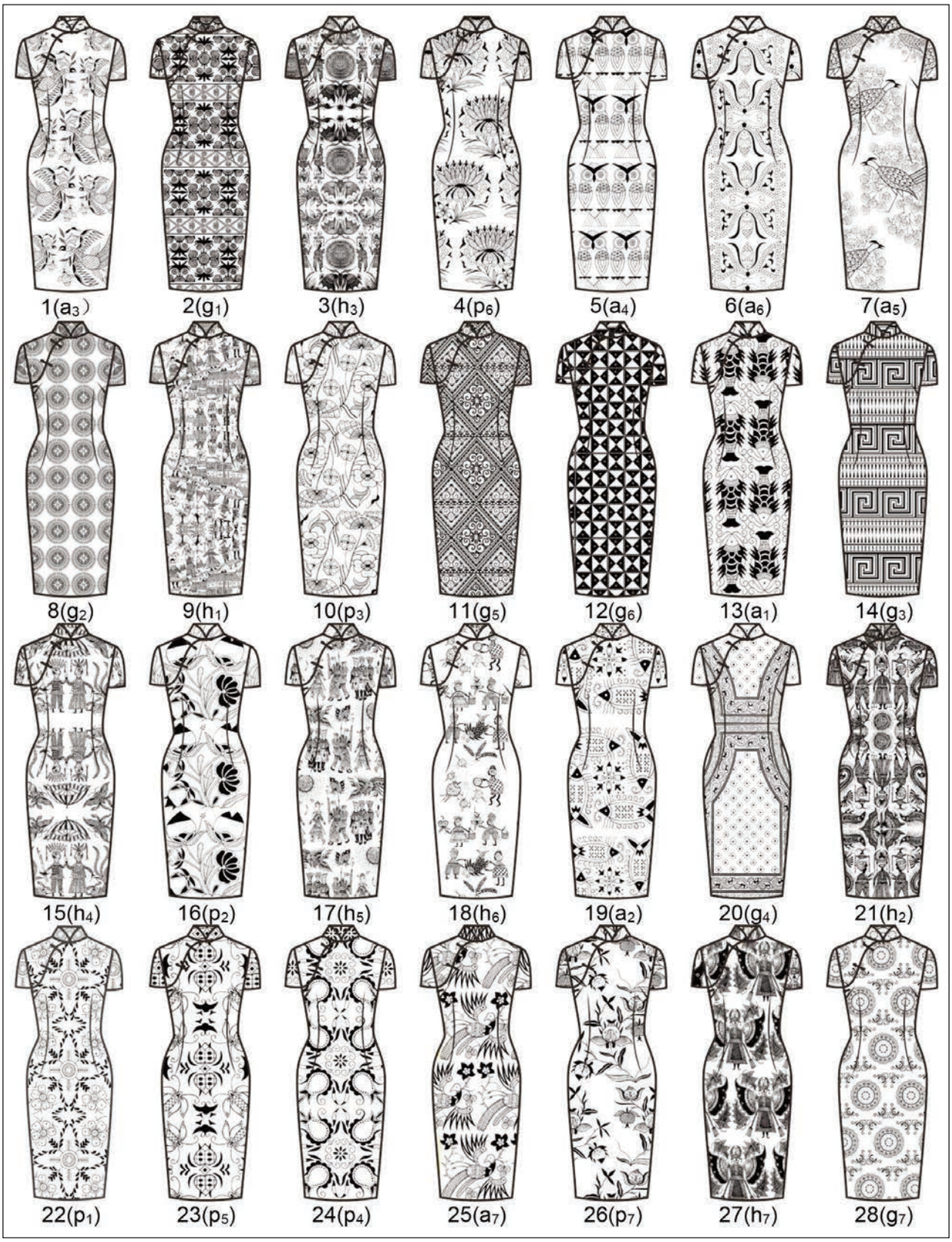

Fig. 2. Cheongsam study sample

composition ensured the reliability and validity of the adjective selection process. Through a structured screening process, less commonly used, redundant, and semantically similar adjectives were eliminated. Ultimately, six pairs of high-frequency, semantically opposite adjectives were identified as Kansei words for subsequent research. The final six pairs of Kansei words are as follows: Simple - Complex, Modest - Luxurious, Reserved - Expressive, Traditional - Avant-garde, Orderly - Disorderly, and Youthful - Mature.

To further ensure the reliability and objectivity of the adjective selection process, both Cronbach's alpha

and the Intraclass Correlation Coefficient (ICC) were employed for dual verification. Cronbach's alpha was used to assess the internal consistency of the 40 evaluators' ratings regarding the "validity of the Kansei adjectives". A coefficient of Cronbach's alpha ≥ 0.70 was considered indicative of acceptable reliability. The ICC was used to examine the inter-rater agreement on the "priority ranking of Kansei adjective pairs", where ICC ≥ 0.60 was considered acceptable, and ICC ≥ 0.75 was regarded as excellent. The results demonstrated high reliability across both indicators. For Cronbach's alpha, the coefficient for "relevance ratings" was 0.82, and the coefficient for "semantic clarity ratings" was 0.79, both exceeding the acceptable threshold of 0.70. This indicates strong internal consistency among the 40 evaluators and the absence of substantial subjective discrepancies. Regarding inter-rater agreement, the ICC calculated from the "adjective priority ranking" data was 0.81 (95% CI: 0.72–0.88), surpassing the 0.75 benchmark for excellent reliability. These results confirm that the six selected Kansei adjective pairs were recognised with a high degree of consensus and were not affected by evaluator background differences. Accordingly, they can be considered a reliable semantic basis for subsequent Kansei evaluation.

Questionnaire survey

The survey questionnaire was designed using a five-point semantic differential scale. Participants evaluated the research samples based on the meanings of six pairs of Kansei words, assigning sensory ratings accordingly. The assigned scores indicate the degree of association between each Kansei word pair and the corresponding Cheongsam sample. The five scale points were set as follows: –2, –1, 0, 1, and 2. For example, considering the Kansei word pair "Simple - Complex", a score of –2 indicates that the sample is perceived as highly simple, 1 represents moderately simple, 0 signifies a neutral perception (neither simple nor complex), 1 suggests moderately complex, and 2 indicates highly complex. The specific evaluation format of the questionnaire is shown in table 1.

Table 1

QUESTIONNAIRE EVALUATION FORM

Kansei word	Scale points					Kansei word
	–2	–1	0	1	2	
simple	-	-	-	-	-	complex
modest	-	-	-	-	-	luxurious
reserved	-	-	-	-	-	expressive
traditional	-	-	-	-	-	avant-garde
orderly	-	-	-	-	-	disorderly

Questionnaire distribution

The respondents of this survey were all drawn from professional groups closely related to the research topic. The sample included: undergraduate students majoring in fashion design (junior year or above) with coursework in Kansei Engineering; university faculty with academic and practical backgrounds in ethnic hand-dyeing and apparel design; professional designers engaged in ethnic batik and garment development; and Cheongsam consumers with extensive experience in purchasing and wearing such garments. A total of 80 valid participants were included. The demographic characteristics of the respondents are presented in table 2. Due to the specialised nature of this study, the questionnaire content is relatively complex. The survey includes 28 Cheongsam samples, each assessed with six questions, resulting in a total of 168 questions. The questionnaire was conducted through a combination of online and offline methods. A total of 80 questionnaires were distributed, with 78 valid responses collected, achieving an effective response rate of 97.5%, which meets the sample size requirements for the study. The participants provided subjective evaluations of 28 batik-patterned Cheongsam samples. Each questionnaire generated 168 scores (28 Cheongsam sample images × 6 pairs of Kansei words). The average sensory evaluation scores for the 28 Cheongsam samples were calculated based on the valid responses. The specific average sensory evaluation scores for the Cheongsam research samples are shown in table 3.

Table 2

DEMOGRAPHIC CHARACTERISTIC OF THE RESPONDENTS

Demographic	Characteristic	Frequency	Percentage
Gender	Male	32	40
	Female	48	60
Age	20–29	10	12.5
	30–39	20	25
	40–49	30	37.5
	Above 50 years old	20	25
Occupation	Undergraduate students (junior year or above)	10	12.5
	University faculty	30	37.5
	Professional fashion designer	20	25
	Batik Cheongsam consumer	20	25

To analyse the sensory tendencies of the 28 Cheongsam designs, the origin-point method was applied for further data processing and calculation. The score of 0 was set as the origin point of the evaluation scale. The closer participants' psychological perceptions of the samples align with the meaning conveyed by the Kansei word, the more the Cheongsam sample's average score deviates from 0. In other words, a higher or lower score indicates a

Table 3

MEAN SENSORY RATINGS OF CHEONGSAM SAMPLES

Sample number	Kansei word pairs					
	Simple - Complex	Modest - Luxurious	Reserve - Expressive	Traditional - Avant-garde	Orderly - Disorderly	Youthful - Mature
1(a_3)	0.72	0.22	0.70	–0.24	–0.18	0.96
2(g_1)	0.26	0.18	0.38	–0.44	0.08	0.46
3(h_3)	1.04	0.80	0.78	0.10	0.48	0.50
4(p_6)	0.54	0.62	0.44	–0.24	–0.12	0.60
5(a_4)	0.38	0.44	0.32	0.70	0.00	–0.62
6(a_6)	0.72	0.80	0.48	0.04	–0.10	–1.00
7(a_5)	0.70	0.54	0.56	–0.44	–0.28	–0.66
8(g_2)	–0.02	–0.10	–0.12	–0.24	-0.50	0.62
9(h_1)	1.28	0.96	1.04	0.14	1.14	0.76
10(p_3)	0.68	0.58	0.62	–0.08	0.80	0.84
11(g_5)	–0.18	0.12	0.10	0.00	–0.98	0.08
12(g_6)	–0.26	–0.42	–0.16	–0.08	–0.32	0.10
13(a_1)	0.52	0.62	0.50	–0.08	–0.36	–0.54
14(g_3)	–0.50	–0.48	–0.20	0.58	–0.42	0.02
15(h_4)	1.14	0.96	0.80	0.44	0.48	0.20
16(p_2)	0.18	0.34	0.58	0.00	–0.14	0.14
17(h_5)	1.02	0.94	0.98	0.52	0.80	0.32
18(h_6)	0.46	0.52	0.64	0.12	0.20	0.66
19(a_2)	0.32	0.58	0.42	0.16	0.14	–0.56
20(g_4)	0.92	0.64	0.42	0.22	–0.56	0.34
21(h_2)	0.86	0.76	0.74	0.28	0.66	0.36
22(p_1)	0.68	0.64	0.42	–0.18	0.00	1.02
23(p_5)	0.82	0.64	0.56	–0.06	0.20	0.68
24(p_4)	0.82	0.72	0.72	0.06	0.24	0.76
25(a_7)	0.66	0.62	0.42	–0.18	0.00	1.04
26(p_7)	0.54	0.64	0.44	–0.20	–0.10	0.62
27(h_7)	1.06	0.83	0.78	0.10	0.47	0.54
28(g_7)	0.00	–0.12	–0.14	–0.24	–0.50	0.66

more distinct positive or negative subjective impression. For example, Cheongsam Sample No. 1(a_3) received a score of 0.72 on the "Simple - Complex" Kansei scale, suggesting that it evokes a relatively complicated impression. On the "Youthful - Mature" scale, its average score was 0.96, indicating that its styling characteristics tend to convey a mature image.

As shown in table 3, the combination of Cheongsams with batik patterns of different themes influences individuals' subjective impressions and evaluations of the garments. In other words, the integration of different thematic batik patterns with Cheongsam samples leads to variations in the subjective sensory evaluation of their overall design style. To identify the Kansei words that best characterise the design features of each Cheongsam sample, the ranking method was applied. The absolute values of the sensory scores for all Cheongsam samples were ranked, and the top three Kansei words with the highest absolute scores were extracted for each sample. The main imagery styles of the 28 Cheongsam samples are presented in table 4.

Table 4 indicates that when batik patterns with animal designs are integrated into cheongsam designs, the most prominent imagery style is "Youthful". Firstly, animal patterns are often associated with vitality, energy, and nature [18]. These patterns, characterised by vibrant colours and dynamic forms, evoke positive emotions in viewers, thereby creating a sense of youthfulness and liveliness. Psychological studies have shown that visual stimuli can influence an individual's emotional state and self-perception [19]. The dynamism and wildness conveyed by animal patterns can effectively enhance the wearer's youthful image. Secondly, as a traditional Chinese garment, the cheongsam inherently symbolises elegance and beauty. The integration of animal-themed batik patterns into Cheongsam designs enhances its modern and fashionable appeal. This fusion of traditional and contemporary elements reinforced the youthful effect. When batik patterns with geometric

Table 4

CHEONGSAM SAMPLE MAIN IMAGE STYLE							
Sample number	**Sequencing of Kansei words**			**Sample number**	**Sequencing of Kansei words**		
	1	**2**	**3**		**1**	**2**	**3**
1(a_3)	Mature	Complex	Expressive	15(h_4)	Complex	Luxurious	Expressive
2(g_1)	Mature	Traditional	Expressive	16(p_2)	Expressive	Luxurious	Complex
3(h_3)	Complex	Luxurious	Expressive	17(h_5)	Complex	Expressive	Luxurious
4(p_6)	Luxurious	Mature	Complex	18(h_6)	Mature	Expressive	Luxurious
5(a_4)	Avant-garde	Youthful	Luxurious	19(a_2)	Luxurious	Youthful	Expressive
6(a_6)	Youthful	Luxurious	Complex	20(g_4)	Complex	Luxurious	Orderly
7(a_5)	Complex	Youthful	Expressive	21(h_2)	Complex	Luxurious	Expressive
8(g_2)	Mature	Orderly	Traditional	22(p_1)	Mature	Complex	Luxurious
9(h_1)	Complex	Disorderly	Expressive	23(p_5)	Complex	Mature	Luxurious
10(p_3)	Mature	Disorderly	Complex	24(p_4)	Complex	Mature	Luxurious
11(g_5)	Orderly	Simple	Luxurious	25(a_7)	Mature	Complex	Luxurious
12(g_6)	Modest	Orderly	Simple	26(p_7)	Luxurious	Mature	Complex
13(a_1)	Luxurious	Youthful	Complex	27(h_7)	Complex	Luxurious	Expressive
14(g_3)	Avant-garde	Simple	Modest	28(g_7)	Mature	Orderly	Traditional

designs are integrated into Cheongsam designs, the most prominent imagery styles are “Orderly” and “Simple”. Firstly, the foundation of geometric patterns lies in their well-defined shapes and lines, which create a visually structured composition. Studies have shown that highly symmetrical and regular patterns can evoke a sense of cognitive comfort, leading to an orderly visual experience [20]. Secondly, the minimalist design philosophy has become increasingly valued in modern fashion. Geometric patterns reduce visual interference, emphasising the essence of the design and enhancing its simplicity in form [21]. Therefore, the application of geometric batik patterns aligns with current design trends and allows the Cheongsam to strike a balance between tradition and modernity, presenting a naturally harmonious aesthetic. When batik patterns with human figure designs are integrated into Cheongsam designs, the most prominent imagery style is “Expressive”. The primary reason is that human figure batik patterns often carry rich narratives and cultural symbolism, making them highly evocative in visual storytelling [22]. Studies have shown that human figure patterns with narrative characteristics can convey early human culture, evoking emotional resonance in viewers [23]. Therefore, when batik patterns with human figure themes are applied to Cheongsam design, viewers experience a deeper emotional response due to the cultural stories behind them. Additionally, human figure batik patterns are often depicted in exaggerated and dynamic forms, emphasising movement and emotion. This expressive artistic approach, characterised by striking lines, enhances visual impact and adds a dramatic flair to the overall design. When plant batik patterns are integrated into Cheongsam designs, the most prominent imagery styles are “Intricate” and “Mature”. The primary reason is that plant patterns often exhibit high levels of complexity and intricate craftsmanship [24]. In Cheongsam designs, plant batik patterns, with their fine details, create a rich sense of visual depth. This intricate design language makes the wearer’s image more three-dimensional, enhancing the overall aesthetic effect and creating a complex, profound visual experience. Moreover, plant batik patterns often carry rich cultural symbolism, conveying reverence for nature and admiration for life [25]. In traditional cultures, plants often symbolise growth, prosperity, and the continuity of life. Their cultural significance makes the application of plant patterns not merely an aesthetic pursuit but also a reflection of a profound cultural identity.

KANSEI ENGINEERING ANALYSIS

Factor analysis

To conduct a more in-depth investigation into the sensory differences generated by different thematic batik patterns on Cheongsams, the SPSS 26.0 software was used to perform a KMO validity analysis and Bartlett’s test of sphericity on the mean sensory score of 28 Cheongsam samples. The specific results showed that the KMO validity analysis value was 0.747, which is greater than 0.500, and Bartlett’s test of sphericity revealed a significant P-value of 0.000, which is less than 0.050, indicating a high correlation between the variables and suggesting the suitability for subsequent factor analysis [26].

In this study, principal component analysis (PCA) was applied to reduce the dimensionality of the mean Kansei evaluation scores for the samples. According to the Kaiser criterion, the eigenvalue reflects the explanatory power of a common factor with respect to the original variables. When an eigenvalue exceeds 1, the corresponding factor explains more information than a single adjective pair and thus has value in aggregating multiple variables. Therefore,

Table 5

KANSEI WORD PAIRS EXPLAIN TOTAL VARIANCE						
Ingredient	Initial Eigenvalue			Extraction of the sum of squares of loads		
	Total	Variance (%)	Accumulation (%)	Total	Variance (%)	Accumulation (%)
1	3.520	58.708	58.708	3.522	58.708	58.708
2	1.290	21.497	80.205	1.290	21.497	80.205
3	0.740	12.458	92.663	-	-	-
4	0.280	4.682	97.346	-	-	-
5	0.090	1.592	98.938	-	-	-
6	0.060	1.062	100.000	-	-	-

factors with initial eigenvalues greater than 1 were extracted as common factors, and the total variance explained by the Kansei adjective pairs is shown in table 5.

As shown in table 5, the initial eigenvalue of the first factor is 3.522, which explains 58.708% of the variance in the original 6 pairs of Kansei words. The initial eigenvalue of the second factor is 1.290, which explains 21.497% of the variance in the original 6 pairs of Kansei words. The cumulative contribution rate of the two factors is 80.205%, and since the eigenvalues are greater than 1, these two common factors can fully represent the meanings of the 6 pairs of Kansei words and reflect the sensory information of the 28 Cheongsam samples. Therefore, two common factors can be extracted. The rationality of the two common factors is verified using a scree plot, as shown in figure 3. The first factor has the highest eigenvalue, and the inflexion point occurs at the third factor, where the line becomes flatter. Since the eigenvalues of the first and second factors are both greater than 1, this confirms that extracting two common factors is reasonable.

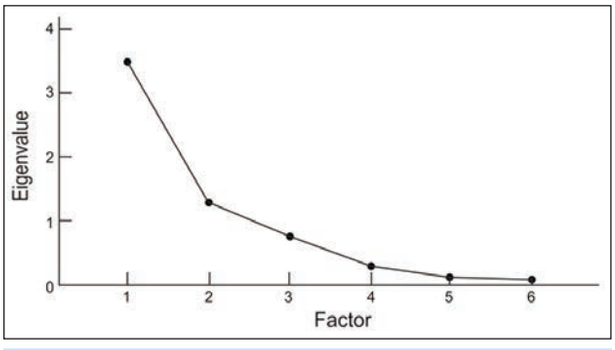

Fig. 3. Scree plot analysis figure

To further investigate the composition of the common factors and assign appropriate names, the core associated variables of the two extracted factors were distinguished. The factor loading matrix was standardised to eliminate potential interference caused by differences in the scoring scale of the Kansei adjective pairs (e.g., some pairs showing larger score variations and others smaller), thereby ensuring the objectivity of the rotation results. The Varimax method with Kaiser normalisation was then applied to obtain the rotated component matrix, as shown in table 6.

Table 6

FACTOR COMPONENT ROTATION MATRIX		
Kansei word pair	Factor	
	1	2
Simple - Complex	0.951	0.066
Modest - Luxurious	0.925	–0.087
Reserved - Expressive	0.959	0.002
Traditional - Avant-garde	0.243	–0.787
Orderly - Disorderly	0.857	–0.010
Youthful - Mature	0.224	0.812

As shown in table 6, the factor loadings reflect the correlation between the factors and the Kansei word pairs. The higher the correlation, the greater the absolute value of the factor loadings. After rotation, the first common factor showed high loadings on the four adjective pairs “Simple - Complex”, “Modest - Luxurious”, “Reserved - Expressive”, and “Orderly - Disorderly”, with loading values of 0.951, 0.925, 0.959, and 0.857, respectively, all above 0.85. The second common factor was associated with the adjective pairs “Traditional - Avant-garde” and “Youthful - Mature”, with loadings of –0.787 and 0.812, both exceeding 0.78. These clear correspondences between factors and variables verify the validity of the rotation method. In the first common factor, the Kansei word pairs with higher absolute factor loadings include “Simple - Complex”, “Modest - Luxurious”, “Reserved - Expressive”, and “Orderly - Disorderly”. This suggests that the first common factor effectively explains the variance of these four pairs of Kansei words, which reflect individual personality traits and preferences. Therefore, this factor can be categorised as the “Style factor”. In the second common factor, the Kansei word pairs with higher absolute factor loadings include “Traditional - Avant-garde” and “Youthful - Mature”. These Kansei word pairs primarily relate to the cheongsam itself and reflect an individual’s dressing style, which can be categorised as the “Temperament factor”. The analysis indicates that consumers’ psychological perception of batik-patterned Cheongsams mainly

Table 7

PEARSON CORRELATION COEFFICIENTS FOR KANSEI WORD PAIRS

	Simple - Complex	Modest - Luxurious	Reserve - Expressive	Traditional - Avant-garde	Orderly - Disorderly	Youthful - Mature
Simple - Complex	1					
Modest - Luxurious	0.920**	1				
Reserve - Expressive	0.900**	0.884**	1			
Traditional - Avant-garde	0.120	0.177	0.175	1		
Orderly - Disorderly	0.709**	0.658**	0.778**	0.304	1	
Youthful - Mature	0.205	0.033	0.155	–0.279	0.265	1

Note: * P<0.05; ** P<0.01

consists of two factors: the style factor and the temperament factor. The contribution rate of the style factor is higher than that of the temperament factor, suggesting that consumers prioritise the appearance and overall style of the Cheongsam when selecting and purchasing one.

Correlation Analysis

To verify the consistency of evaluations among the Kansei adjective pairs and to examine their potential interrelationships, a Pearson correlation analysis was conducted. As shown in table 7, strong positive correlations were found among the pairs "Simple - Complex", "Modest - Luxurious", "Reserved - Expressive", and "Orderly - Disorderly". All correlation coefficients exceeded 0.70 and reached significance at the 0.01 level. For example, the correlations between "Simple - Complex" and "Modest - Luxurious" (r = 0.920), as well as between "Simple - Complex" and "Reserved - Expressive" (r = 0.900), were the highest. This indicates that the simpler the pattern, the more strongly it is perceived as modest, reserved, and orderly; conversely, the more complex the pattern, the more likely it is to evoke associations of luxury, expressiveness, and disorder.

In contrast, the adjective pairs "Youthful - Mature" and "Traditional - Avant-garde" showed relatively weak correlations with the pairs mentioned above, with coefficients generally below 0.30 and without statistical significance. This suggests that these two pairs are relatively independent constructs and are not directly associated with perceptions of pattern complexity or luxury.

Cluster analysis

Analysis results

Based on the similarity among the Cheongsam samples, hierarchical clustering in cluster analysis was applied to analyse 28 Cheongsam samples, grouping those with similar characteristics into the same category. The clustering results under different clustering intensities were obtained, and the specific hierarchical clustering analysis results are shown in figure 4.

As shown in figure 4, when the clustering scale is set to 5, the Cheongsam samples are clustered into 11 categories. When the clustering scale is set to 10, the samples are grouped into 4 categories. When the clustering scale is 15, the samples are clustered into 3 categories. Finally, when the clustering scale ranges from 20 to 25, the Cheongsam samples are classified into 2 categories. Taking the clustering scale of 10 as an example, the Cheongsam samples in cluster 1 include samples numbered 1(a_3), 2(g_1), 4(p_6), 10(p_3), 16(p_2), 18(h_6), 20(g_4), 22(p_1), 23(p_5), 24(p_4), 25(a_7) and 26(p_7). The primary imagery style

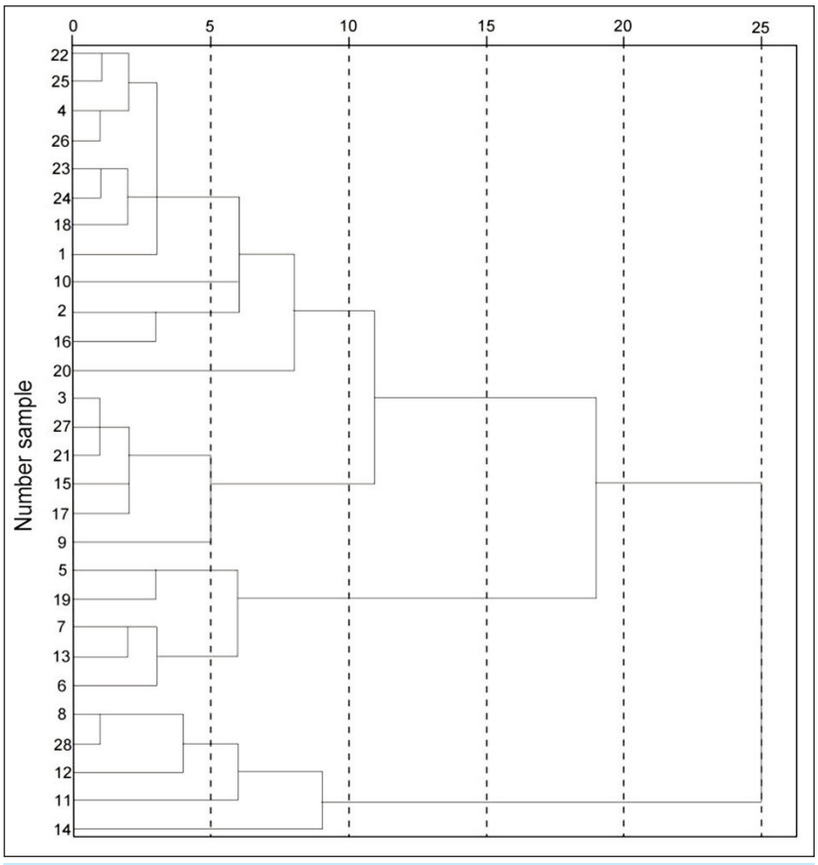

Fig. 4. Results of hierarchical clusteringe

of this cluster is characterised by “mature” and “luxurious”, encompassing all plant-themed batik patterns. According to the previously obtained mean scores of the sensory evaluations, plant patterns generally exhibit soft, delicate, and fluid artistic forms. The depiction of mature fruits and full-bloom flowers symbolises abundance and vitality. Within Cluster 1, the geometric patterns in samples 2(g_1) and 20(g_4) are more compact in composition compared to the other four geometric patterns. These designs incorporate various elements such as curves, dots, and spirals, creating a sense of fluidity and interwoven lines. Sample 18(h_6) features a human figure pattern; unlike other human figure patterns, it minimises the incorporation of animal and plant patterns, resulting in a visually more mature and composed aesthetic. Additionally, samples 1(a_3) and 25(a_7) showcase phoenix patterns. In traditional Chinese culture, the phoenix symbolises prosperity, abundance, and vitality. Therefore, the overall style characteristics of Cluster 1 emphasise opulence, sophistication, and mature elegance. The Cheongsam samples in Cluster 2 are numbered 3(h_3), 9(h_1), 15(h_4), 17(h_5), 21(h_2) and 27(h_7). This cluster is characterised by human figure patterns. The most prominent imagery style of this cluster is “intricate”, followed by “expressive”. The human figure patterns exhibit a unique narrative charm, with diverse and complex compositions. Detailed elements such as hair, clothing textures, accessories, and additional decorative patterns are rendered using meticulous and intricate realism. The depiction of human movements is exaggerated yet dynamic, enhancing the visual appeal. The background of these human figure patterns incorporates elements such as plants and animals, contributing to a visually rich, lively, and engaging aesthetic. The Cheongsam samples in Cluster 3 are numbered 5(a_4), 6(a_6), 7(a_5), 13(a_1) and 19(a_2). This cluster comprises four Cheongsam samples featuring animal batik patterns. The most striking imagery style of this cluster is “Youthful”. This is primarily due to the rhythmic arrangement of animal patterns, which conveys a sense of vitality and dynamism. The Cheongsam samples in Cluster 4 are numbered 8(g_2),11(g_5), 12(g_6), 14(g_3) and 28(g_7). All samples in this cluster feature geometric patterns. The dominant imagery styles of this cluster are “Orderly” and “Minimalist”. The geometric patterns in this cluster are composed of systematically arranged fundamental elements such as continuous sun patterns and meander patterns, forming a structured and repetitive design. These patterns exhibit clean and sharp lines with a symmetrical and balanced composition. The key characteristics of this cluster include balance, symmetry, and repetition. Compared to other Cheongsam samples, those in this cluster emphasise a greater sense of simplicity, restraint, and harmonious order.

Through cluster analysis, it can be observed that although different batik patterns combined with Cheongsams produce varying sensory differences, Cheongsam samples within the same cluster exhibit similar mean values and higher proportions of Kansei word pairs. Additionally, these Cheongsam samples share similar overall appearances and stylistic sensory imagery.

Validation of clustering results

To objectively evaluate the validity of the clustering outcome, a Silhouette Score analysis was conducted using Python. This method was employed to quantitatively verify the clustering performance. The overall silhouette coefficient represents the average silhouette value of all samples and ranges from –1 to 1. It reflects the balance between intra-cluster cohesion and inter-cluster separation. A silhouette value closer to 1 indicates better clustering performance; values near 0 suggest that samples lie on cluster boundaries; and values approaching –1 imply that samples may have been incorrectly assigned to clusters [9]. The silhouette analysis was performed on the clustering result with a set threshold of 10 clusters, and the corresponding results are presented in table 8.

Table 8

SILHOUETTE-BASED EVALUATION OF CLUSTER QUALITY

Cluster	Sample size	Mean Silhouette coefficient	Cluster quality evaluation
1	12	0.81	Excellent
2	6	0.85	Excellent
3	5	0.71	Good
4	5	0.77	Good
Overall mean silhouette coefficient: 0.79		Overall mean silhouette coefficient: 0.79	

As shown in table 8, the average silhouette coefficients of the four clusters were all positive, with an overall mean value of 0.79. This indicates good intra-cluster cohesion and inter-cluster separation. Specifically, Cluster 2 (human figure patterns) exhibited the highest silhouette coefficient (0.85), suggesting that its features were the most distinct and the clustering performance was optimal. Cluster 3 (animal patterns) had a relatively lower coefficient (0.71), but it remained within an acceptable range, implying that some overlap in perceptual features may exist within this group. Overall, the clustering quality was evaluated as “good”, confirming the statistical validity of the Cheongsam sample classification based on Kansei evaluation. This result is consistent with the aforementioned hierarchical clustering analysis and further substantiates the rationality of categorising the 28 Cheongsam samples into four perceptual feature groups.

CONCLUSION

To explore the sensory imagery of Cheongsam appearance after integrating batik patterns, this study, based on the principles of Kansei engineering, selected four categories of pattern themes with typical formal characteristics and combined them with

Cheongsam designs. A total of 28 cheongsam research samples were extracted, along with six pairs of Kansei words with opposite meanings that accurately describe the stylistic characteristics of the samples, forming the semantic space for this study. Subsequently, a five-point scale sensory evaluation questionnaire was designed, and face-to-face surveys were conducted to collect participants' sensory evaluations of the cheongsam samples. The sensory rating absolute values obtained from the questionnaire were analysed using SPSS 26.0, leading to the following conclusions:

- Through factor analysis, two common factors influencing the sensory characteristics of the Cheongsam research samples were extracted, enabling an effective sensory evaluation of the 28 Cheongsam samples. Based on their specific meanings, these factors were named the Style factor and the Temperament factor, respectively. Since the contribution rate of the Style factor is higher than that of the Temperament factor, the sensory style characteristics generated by the Cheongsam's appearance play a decisive role.
- From the perspective of batik patterns, different thematic contents of batik patterns influence the overall appearance characteristics of the Cheongsam when combined. Specifically, cheongsam samples featuring animal patterns predominantly convey the sensory imagery of "Youthful". Those incorporating plant-themed batik patterns most strongly evoke the impressions of "Mature" and "Luxurious". Cheongsam samples with human figure patterns exhibit the most prominent sensory characteristics of "Expressive", followed by "Intricate". Meanwhile, Cheongsam samples with geometric patterns are most frequently associated with the Kansei words "Simple" and "Orderly", carrying the highest weight in evaluation.
- Through cluster analysis, it was determined that when the clustering scale distance is set to 10, the research samples can be grouped into four clusters. Within different clusters, the combination of various batik pattern themes with Cheongsam results in distinct sensory imagery. However, within the same cluster, Cheongsam styles exhibit a high overlap in specific pairs of Kansei words, with similar sensory evaluation scores. This consistency suggests that the Cheongsam samples within each cluster share a certain level of uniformity and regularity in their overall sensory evaluation of appearance.

Due to space limitations, this study still presents certain constraints regarding the selection of batik pattern colours, themes, and Cheongsam silhouette classifications. Future research will expand the sample scope and further refine the methodological design to ensure more rigorous and reliable conclusions. In addition, the findings are subject to cultural contextual limitations. The ethnic symbolism embedded in batik patterns and the cultural connotations of the Cheongsam may influence participants' perceptual judgments of style and temperament. Therefore, the conclusions are primarily applicable within specific cultural contexts, and further verification and adjustment are required when extending the results to other regions or consumer groups. The study employed a research methodology that combines Kansei Engineering theory, quantitative analysis, and user evaluation. The core of this approach lies in extracting product attributes, constructing a semantic space of affective perception, and quantifying the relationships between design features and user responses. This logical framework demonstrates strong general applicability and can be extended to other product design domains to identify the correspondence between product attributes and users' emotional needs, thereby providing a scientific basis for design practice. Based on the discovered relationship between visual imagery and cultural symbolism, future research may further connect these findings with cross-cultural aesthetic theory, incorporating multicultural themes and emotional symbols to interpret the aesthetic characteristics of patterns from the perspective of both cultural commonality and diversity. This approach can also provide a theoretical basis for comparative studies of cultural patterns across regions. From the perspective of cultural heritage, the verification of the integration between batik and Cheongsam demonstrates the feasibility of transforming intangible cultural heritage into practical design applications, contributing to its living transmission. From the perspective of product design, quantifying user affective needs can support precision design, reduce unsold inventory, and enhance product added value and lifecycle sustainability through the creative reinterpretation of cultural symbols. Future work will continue to advance this research through the expansion of study scope, technological enhancement, application extension, interdisciplinary collaboration, and the deepening of user-experience insights. Furthermore, based on the current dataset, a predictive Kansei design model for batik-inspired Cheongsams will be developed to establish a rapid mapping between design parameters and affective imagery, thereby supporting the practical implementation of intelligent design tools.

REFERENCES

[1] Li, B., Jiang, X.W., Zhao, H.Y., Hong, Y., Li, Y.X., Tao, H., *Study on the origin and evolution of the Chinese batik*, In: Industria Textila, 2020, 71, 3, 282–287, http://doi.org/10.35530/IT.071.03.1694

[2] Quan, H., Li, Y., Liu, D., Zhou, Y., *Protection of Guizhou Miao batik culture based on knowledge graph and deep learning*, In: Heritage Science 12, 2024, https://doi.org/10.1186/s40494-024-01317-y

[3] Dong, B., Bai, K., Sun, X., Wang, M., Liu, Y., *Spatial distribution and tourism competition of intangible cultural heritage: take Guizhou, China as an example*, In: Heritage Science, 2023, 11, 64, https://doi.org/10.1186/s40494-023-00905-8
[4] Tian, G., Yuan, Q., Hu, T., Shi, Y., *Auto-Generation System Based on Fractal Geometry for Batik Pattern Design*, In: Applied Sciences, 2019; 9, 11, 2383, https://doi.org/10.3390/app9112383
[5] Chen, D., Cheng, P., *A method to extract batik fabric pattern and elements*, In: The Journal of The Textile Institute, 2020, 112, 7, 1093–1099, https://doi.org/10.1080/00405000.2020.1802885
[6] Zheng, L.X., Wo, C.W., Wang, S.Q., Li, Y., Mao, R., *Experience design of batik art based on Kano model*, In: Journal of Silk, 2022, 59, 1, 102–108
[7] Bao, X.L., Hiu, Y.R., Tan, Y., Ren, X.L., *Research on innovative design of combining batik and related hand dyeing and printing*, In: Wool textile Journal, 2018, 46, 8, 43–46
[8] Li, X.Z., Chen, G., Zhang, J., *Artistic features of Gejia's batik pattern in southeast Guizhou and its application in fashion design*, In: Wool Textile Journal, 2020, 48, 2, 50–54
[9] Jiang, Z.H, Jing, G., Van, H., Wu, B., *Application of Kansei engineering in the innovative design of traditional fashion elements*, In: Industria Textila, 2024, 75, 3, 289–301, https://doi.org/10.35530/IT.075.03.202370
[10] Boero, M., *The language of fashion in postmodern society: A social semiotic perspective*, In: Semiotica, 2015, 207, 303–325, https://doi.org/10.1515/sem-2015-0037
[11] Lin, S., Shen, T., Guo, W., *Evolution and emerging trends of kansei engineering: A visual analysis based on citespace*, In: IEEE Access, 2021, 9, 111181–111202, https://doi.org/10.1109/ACCESS.2021.3102606
[12] Lai, X., Zhang, S., Mao, N., Liu, J., Chen, Q, *Kansei engineering for new energy vehicle exterior design: An internet big data mining approach*, In: Computers & Industrial Engineering, 2022, 165, 107913, https://doi.org/10.1016/j.cie.2021.107913
[13] Ogawa, T., Nagai, Y., Ikeda, M., *An ontological approach to designers' idea explanation style: Towards supporting the sharing of kansei-ideas in textile design*, In: Advanced Engineering Informatics, 2009, 23, 2, 157–164, https://doi.org/10.1016/j.aei.2008.10.001
[14] López, Ó., Murillo, C., González, A., *Systematic literature reviews in kansei engineering for product design – a comparative study from 1995 to 2020*, In: Sensors, 2021, 21, 19, 6532, https://doi.org/10.3390/s21196532
[15] Ge, B., Xue, Y., *Applying a Kansei engineering-based relationship model design approach to developing consumers' sustainability reliance on apparel*, In: Journal of Fashion Marketing and Management, 2024, 28, 5, 1015–1033, https://doi.org/10.1108/JFMM-11-2022-0239
[16] Zhang, Y.Y., *Analysis of design features of home textiles based on traditional dyeing technology*, In: China Dyeing & Finishing, 2023, 49, 10, 99–101
[17] Qin, Z., Ji, T., Liu, Y.H., *The path of introducing embodied knowledge into product design of Miao batik in western Hunan,* In: Packaging Engineering, 2021, 42, 24, 279–285
[18] Greaves, T., *Movement, wildness and animal aesthetics*, In: Environmental Values, 2019, 28, 4, 449-470, https://doi.org/10.1016/j.ecolecon.2021.107055
[19] Benssassi, E.M., Ye, J., *Investigating multisensory integration in emotion recognition through bio-inspired computational models*, In: IEEE Transactions on Affective Computing, 2021, 14, 2, 906–918, https://doi.org/10.1109/taffc.2021.3106254
[20] Hu, H., Liu, Y., Lu, W. F., Guo, X., *A quantitative aesthetic measurement method for product appearance design*, In: Advanced Engineering Informatics, 2022, 53, 101644, https://doi.org/10.1016/j.aei.2022.101644
[21] Wilson, A. V., Bellezza, S., *Consumer minimalism, In: Journal of Consumer Research*, 2022, 48, 5, 796–816, https://doi.org/10.1093/jcr/ucab038
[22] Wen, D., *Analysis of Human Figures, Artistic Value and Enlightenment to Folk Photography in Dunhuang Murals*, In: Mediterranean Archaeology and Archaeometry, 2024, 24, 3, 300–313, https://orcid.org/0009-0004-2131-8509
[23] Oktaviana, A.A., Joannes-Boyau, R., Hakim, B., Burhan, B., Sardi, R., Adhityatama, S., et al., *Narrative cave art in Indonesia by 51,200 years ago*, In: Nature, 2024, 631, 8022, 814–818, https://doi.org/10.1038/s41586-024-07541-7
[24] Han, D., Cong, L., *Miao traditional patterns: the origins and design transformation*, In: Visual Studies, 2021, 38, 3–4, 425–432, https://doi.org/10.1080/1472586X.2021.1940261
[25] Sun, Z., *Excavating the Artistic Value of Tang Dynasty Gold and Silver Decorative Patterns and Its Guiding Significance for Modern Decoration*, In: Mediterranean Archaeology and Archaeometry, 2023, 23, 2, 255–269, https://orcid.org/0009-0008-7828-867X
[26] Song, Y., Wu, T., Zhang, N., *Image evaluation and analysis of fabric with a geometric motif in dress style design*, In: Industria Textila, 2024, 75, 5, 591–598, https://doi.org/10.35530/IT.075.05.2023130

Authors:

ZHANG YU JUN, JUNG JUNG HO

Chonnam National University, College of Arts, Art & Design Technology Cooperation Course,
Interdisciplinary Program of Arts & Design Technology, Room No. 311, College of Arts Bldg. 1,
Chonnam National University, 77 Yongbong-ro, Buk-gu, 61186, Gwangju Metropolitan City, South Korea
e-mail: 17702188109@163.com

Corresponding author:

JUNG JUNG HO
e-mail: vava@jnu.ac.kr

Performance analysis of sustainable fabrics inspired by Ottoman caftan motifs

DOI: 10.35530/IT.077.03.2025131

GENCAL ÖZTÜRK RUKİYE ZEYNEP
SÜNTER EROĞLU NİLŞEN

KOÇAK EMİNE DİLARA

ABSTRACT – REZUMAT

Performance analysis of sustainable fabrics inspired by Ottoman caftan motifs

In this study, sustainable fabrics were developed by taking inspiration from tulips, pomegranate and carnation motifs in the caftan patterns used in the 16th – 17th century Ottoman Empire. In fabric production, sustainable raw materials such as PET and rPET were used for warp yarns. In contrast, polyviscose, Tencel, RO (recycled olefin), organic cotton, and bamboo were used for weft yarns. Yarn counts, yarn strength, elongation and twist properties were analysed. After fabric production, seam opening test, breaking strength, breaking elongation, abrasion, light fastness, abrasion resistance and air permeability tests were performed. The structural characterisation, comfort and durability properties of the fabrics were evaluated. The breaking strength, breaking elongation, and seam opening strength results of the RO-containing K2 are better than those of the natural raw material-containing K1, K3, K4, and K5 fabrics. In tests on fabrics containing natural fibres, it was observed that the K5-coded organic cotton fabric was advantageous in terms of breaking strength, breaking elongation, abrasion resistance, and air permeability. The study revealed that K5 organic cotton fabrics exhibited superior tensile strength, elongation, abrasion resistance, and air permeability, whereas K2 fabrics containing RO showed better seam strength but lower abrasion resistance. All fabrics were transformed into clothing, and modern caftan designs were made. It was concluded that many products could be developed from the patterns of caftan fabrics by considering their usage performance with sustainable materials, and that their applicability in modern textile design and production in different areas would become widespread.

Keywords: *sustainability, pattern design, environmentally friendly, woven fabrics, caftan patterns*

Analiza performanțelor țesăturilor durabile inspirate de motivele caftanelor otomane

În cadrul acestui studiu, au fost create țesături durabile inspirate din motivele cu lalele, rodii și garoafe ale caftanelor utilizate în Imperiul Otoman în secolele al XVI-lea și al XVII-lea. În procesul de producție a țesăturilor, s-au utilizat materii prime durabile precum PET și rPET pentru firele de urzeală, iar pentru firele de bătătură s-au folosit poliviscoză, Tencel, RO (fibră poliolefinică reciclată), bumbac organic și bambus. Au fost analizate finețea, rezistența, alungirea și proprietățile de torsiune ale firelor. După producerea țesăturilor, au fost efectuate teste de rezistență a îmbinării, rezistență la rupere, alungire la rupere, rezistență la abraziune și la lumină, precum și teste de permeabilitate la aer. Au fost evaluate caracteristicile structurale, de confort și de durabilitate ale țesăturilor. Rezultatele privind rezistența la rupere, alungirea la rupere și rezistența îmbinării obținute pentru țesătura K2 cu conținut de RO sunt superioare celor obținute pentru țesăturile K1, K3, K4 și K5, care conțin materii prime naturale. În cadrul testelor efectuate pe țesături care conțin fibre naturale, s-a observat că țesătura din bumbac organic cu codul K5 prezintă avantaje în ceea ce privește rezistența la rupere, alungirea la rupere, rezistența la abraziune și permeabilitatea la aer. Studiul a relevat că țesăturile din bumbac organic K5 prezentau caracteristici superioare de rezistență la tracțiune, alungire, rezistență la abraziune și permeabilitate la aer, în timp ce țesăturile K2 care conțin RO prezentau o rezistență mai bună a îmbinării, dar o rezistență la abraziune mai scăzută. Toate țesăturile au fost transformate în articole vestimentare și s-au creat modele moderne de caftan. S-a ajuns la concluzia că, luând în considerare performanțele de utilizare ale acestora și folosind materiale durabile, se pot dezvolta numeroase produse pornind de la modelele țesăturilor de caftan, iar aplicabilitatea acestora în proiectarea și producția modernă de textile în diverse domenii se va extinde pe scară largă.

Cuvinte-cheie: *durabilitate, proiectare de modele, ecologic, țesături, modele de caftan*

INTRODUCTION

In recent years, the rapidly increasing production and consumption volume in the textile sector, especially under the influence of the “fast fashion” approach, has led to significant problems in terms of environmental sustainability; this has made the textile industry one of the sectors that pollutes the environment the most. Today, environmentally friendly fashion supported by low-carbon production and green growth policies directs individuals to be more conscious and proactive about the protection of natural resources and sustainability [1]. In the sustainable product design process, factors such as raw material supply, production methods, purpose of use, waste management and working conditions should be structured in the light of ecological principles. In this context, environmentally friendly material selection,

application of clean production techniques, extension of the product life cycle and ensuring energy efficiency are among the fundamental strategies of sustainable design.

In material selection, natural fibres such as cotton, linen, hemp, mulberry and ramie offer more sustainable options compared to synthetic fibres due to their technical performance, biocompatibility and low environmental impact [2].

During the Ottoman period, motifs such as tulips, carnations, hyacinths, plane leaves, spring branches, pomegranate leaves, and dagger leaves among curved branches were frequently used in caftan fabrics [3]. Many floral motifs have been adapted and modernised in academic studies. Cihan developed new design suggestions in his thesis study based on tulip, haliç and Chintamani motifs [4]. Similarly, Tekkılıç and his friends created home textile designs using rumi, tulip and spring branch motifs [5]. Tulip and carnation motifs, which are frequently found in plant ornaments and are designed with inspiration from nature, and pomegranate, also known as the fruit of heaven, symbolising fertility and continuity of life, are motifs that are the common denominator of the past and the present. The tulip motif developed as part of a rich visual culture intertwined with the use of floral motifs and aesthetic and symbolic meanings in Ottoman art [6]. The pomegranate motif, on the other hand, is a plant that can remain green throughout the year and has been associated with themes such as immortality, eternal life and fertility [7]. The carnation motif also stands out as a frequently preferred floral pattern in Ottoman art. Indeed, there are studies in the literature on the adaptation of motifs from the Ottoman period to modern design applications. Bağcı and Kiper developed a home textile collection with the theme of "Dynasty" inspired by the pattern and colour harmony in Ottoman caftans and introduced hatayi and leaf motifs to use with the digital printing technique [8]. Gümüşer showed that traditional motifs can be transferred to different textile areas from upholstery fabrics to wall coverings through nine original patterns inspired by 16th-century Ottoman palace fabrics [9]. Although previous studies have investigated the adaptation of Ottoman motifs to modern textiles, few have systematically examined their integration with sustainable fibres, which constitutes the research gap this study addresses.

The study aimed to modernise the motifs used in caftan patterns from the 16th and 17th centuries during the Ottoman period, produce fabrics with sustainable raw materials, and predict the commercial use potential of the fabrics by transforming them into clothing forms. Tulip was chosen for its strong symbolic role in Ottoman art and sustainability symbolism; pomegranate for its association with fertility, continuity, and cyclical life; and carnation for its aesthetic richness and prevalence in caftan ornamentation. In addition to motif adaptation, the sustainability aspect is strengthened by focusing on water consumption, carbon footprint, and potential life cycle assessment (LCA) implications of fibre selection. The fabrics produced were made using sustainable linen, bamboo, RO, Tencel, and organic cotton. All fabrics were woven on jacquard weaving machines. To evaluate the physical and mechanical properties of yarns and fabrics, yarn breaking strength, breaking elongation, twist, fabric breaking strength, breaking elongation, abrasion resistance, seam opening, washing and rubbing fastness, and air permeability tests were performed.

EXPERIMENTAL

Materials

As recycled fibres, polypropylene-based recycled olefin and yarns made of recycled polyester fibre were used in fabric production (table 1). RO yarn is known as the first recycled olefin yarn developed by KETS (local fabric manufacturer) and produced entirely from post-consumer textile waste. RO stands out as an environmentally friendly option since its production process is carried out without the use of water. While traditional textile production processes, particularly in dyeing, finishing, and wet processing stages, consume large amounts of water, the production of RO yarn eliminates water use during the yarn manufacturing stage. RO yarns have approximately 40% lower carbon footprint compared to raw

Table 1

YARN PROPERTIES USED IN FABRICS

Raw materials in used yarns	Weft yarn (denier)	Warp thread denier/filament	Yarn elongation (%)	Yarn tensile strength (cN/tex)	Twist count (t/m)	Yarn twist direction
r-PET	450/145	1062	25.9	27.3	-	s
PET	-	150/50	-	-	-	s
RO	1200	-	17.9	18.0	400	s
Polyviscose	30	-	16.1	12.8	261	s
Tencel	298	-	8	25.9	214	s
Bamboo	298	-	14	14.8	202	s
Organic cotton	298	-	5	17.3	240	s
Linen	30	-	4.2	22.0	-	s

Table 2

FABRIC COMPOSITION AND YARN CONTENTS					
Fabric codes	**Fabric composition**	**Weft yarn (1st weft)**	**Weft yarn (2nd weft)**	**Weft yarn (3rd weft)**	**Warp yarn**
K1	%21 CV %9 LN %41 RO %29 r-PET	Polyviscose	Linen	RO	r-PET
K2	%44 RO %17 r-PET %39 PET	RO	r-PET		PET
K3	%44 Tencel %17 r-PET; %39 PET	Tencel	r-PET		PET
K4	%44 Bamboo %17 r-PET %39 PET	Bamboo	r-PET		PET
K5	%44 OC %17 r-PET %39 PET	Organic cotton	r-PET		PET

polypropylene yarn and approximately 50% lower carbon footprint compared to raw Polyester yarn [10].

Methods

Creation of caftan motifs

In the study, new pattern designs were first developed inspired by tulip, pomegranate and carnation motifs found in the caftan patterns. All pattern designs were created in the Adobe Illustrator 2021 program (figure 1).

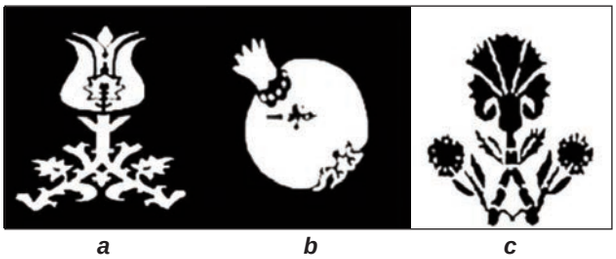

a ***b*** ***c***

Fig. 1. Pattern designs: *a* – Tulip; *b* – Pomegranate; *c* – Carnation

Fabric production

All fabric productions used in the study were made on the Dorier Brand 2008 model jacquard weaving machine. Fabric production was carried out by determining structural parameter values. In fabric production, the average fabric weight of all fabrics in the structural parameters is 294–344 g/m^2, and the fabric width is 140–150 cm. Fabric compositions are given in table 2.

Material tests

Within the scope of the study, breaking strength, breaking elongation (TS 245 EN ISO 2062), and twist tests (TS EN ISO 2061) were applied to yarns, and seam opening (EN ISO 13936-2), breaking strength, breaking elongation (EN ISO 13934-1), rubbing fastness (ISO 105 B06:2020 Cycle(1/3), light fastness (EN ISO 105-B02), abrasion resistance (ISO 12945-4) and air permeability (EN ISO 9237) tests were applied to fabrics. All tests were conducted with at least five replicates (n = 5), and average values with standard deviations were reported.

RESULTS AND DISCUSSION

Yarn count

Yarn counts are given in table 3. Since the 5 fabrics produced in this study had different weft densities, the direct comparison of mechanical properties was interpreted with caution.

Table 3

YARN COUNTS USED IN FABRICS				
Fabric codes	**Weft yarn (1st weft) (denier)**	**Weft yarn (2nd weft) (denier/ filament)**	**Weft yarn (3rd weft) (denier)**	**Warp thread (denier/ filament)**
K1	30	30	1200	1062
K2	1200	450/145		150/50
K3	298	450/145		150/50
K4	298	450/145		150/50
K5	298	450/145		150/50

Yarn tensile strength, elongation at break and twist

Viscose, found in K1 fabric, is a cellulose-based regenerated fibre and offers a natural softness and shine; however, its strength, especially in the wet state, is limited. Polyester, on the other hand, is known for its high strength and durability properties as a synthetic fibre. Although the low strength of viscose in polyviscose fabrics is increased somewhat with the contribution of polyester, it is known that the breaking strength of polyviscose fabric is generally lower than fabrics produced from other natural and regenerated fibres such as organic cotton, Tencel,

and bamboo [11]. The weft yarn belonging to the K4 coded fabric containing Tencel has the highest breaking strength among natural raw material-based fabrics. Tencel, also known as Lyocell, found in the fabric coded K4, is a regenerated cellulose fibre with high crystallisation and orientation. Thanks to these features, the breaking strength and elongation values of Tencel fibres are higher than those of cotton and viscose fibres. The higher tensile strength of Tencel yarns compared to viscose and bamboo can be attributed to their higher crystallinity and orientation, which is consistent with the findings of Bilir and Şardağ [12].

In the warp yarns, yarns containing r-PET and PET raw materials were used. PET is a polymer with high crystallinity. This crystalline structure is supported by strong van der Waals and hydrogen bonds between molecules, which increase the mechanical strength of the material [13]. Despite the recycling process, r-PET largely preserves the crystalline structure of the original PET, which ensures that the breaking strength of r-PET yarns is high. The high strength of the warp yarns creates a factor that increases fabric strength.

For the breaking elongation values, the highest breaking elongation is seen in the RO yarns in the K2 coded fabrics, while the lowest breaking elongation is seen in the organic cotton in the K5 coded fabric. It has the highest breaking elongation value after the polyviscose RO in the K1. Thirdly, the highest value was observed in the 1st weft yarn in the K4 coded fabric, which contained bamboo yarn. In the K2, K3, and K4 coded fabrics, PET was used in the warp direction, and in the K1 coded fabric, r-PET was used. r-PET provides elasticity with the highest elongation rate (25.9%) as the warp yarn in all fabrics (table 4).

When the twist tests of the 1st weft yarns of the fabrics are performed, all yarns are S twisted. The highest twist value belongs to the K2 coded fabrics and is the RO yarns. The lower twist value (240–261 T/m) is the K1, K3, and K4 coded fabrics (table 4).

Structural parameters of fabrics

The structural values of the fabrics are given in table 5. The designs were produced by using the Dornier Brand 2008 model jacquard weaving machine and the EAT program at Kadifeteks Industry.

Table 4

YARN STRENGTH (CN/TEX) AND YARN ELONGATION (%) VALUES USED IN FABRICS

Fabric codes	Yarn strength (1st weft) (cN/tex)	Yarn elongation (1st weft) (%)	Yarn strength (2nd weft) (cN/tex)	Yarn elongation (2nd weft) (%)	Yarn strength (3rd weft) (cN/tex)	Yarn elongation (3rd weft) (%)	Twist (T/m)
K1	12.8	16.1	22.0	4.2	18.0	17.9	261
K2	18.04	17.9	27.3	25.9	-	-	400
K3	25.9	8	27.26	25.9	-	-	214
K4	14.8	14	27.26	25.9	-	-	202
K5	17.3	5	27.26	25.9	-	-	240

Table 5

STRUCTURAL PARAMETERS OF FABRICS

Fabric code	Weft density (weft/may)	Fabric width (cm)	Warp frequency (wire/cm)	Fabric weight (g/m^2)	Fabric view	Pattern view
K1	9	141	68	342		
K2	18	143	67	295		
K3	32	148	65	312		
K4	42	148	65	310	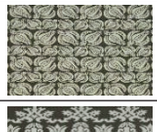	
K5	52	148	65	301		

Fabric seam opening and abrasion test on fabrics

The seam opening test evaluates the resistance of fabrics to seam slippage under stress. Higher opening values indicate lower resistance, meaning that the fabric is more prone to seam failure during garment use, which negatively impacts durability. In this study, since all warp yarns are used as PET and r-PET, the seam opening values in the warp direction are approximately in the range. When the table is examined, the lowest performance for the opening balance in the warp and weft directions is seen in the K1 fabrics. The polyviscose and linen fabrics in the K1 have the lowest values, especially in the weft seam opening. The reason why the seam opening strength of the polyviscose and linen fabrics in the K1 is lower than that of fibres such as bamboo of the K4 coded fabric, organic cotton of the K5 coded fabric, Tencel of the K3 coded fabric and polyolefin of the K2 fabrics is the low flexibility and strength properties of these fibres. This situation leads to easier opening in the seam areas. On the other hand, bamboo, organic cotton, Tencel and polyolefin fibres increase the seam opening strength thanks to their high flexibility and strength properties [11, 14, 15]. Kutgi and Zervent Ünal observed in their studies that viscose fibre has lower seam opening strength than bamboo [16]. Similarly, K1 fabrics gave lower seam opening values than K4 fabrics. While Tencel and bamboo blends showed higher weft direction opening, organic cotton showed a lower weft direction opening value (figure 2).

Abrasion is basically the mechanical deterioration of fabric components by rubbing against another surface. In the abrasion cycle results applied to the fabrics, the most notable measurement (figure 3) is the low abrasion cycle values of the K2 RO-containing fabrics. The RO in these groups is produced from polymers such as polypropylene and polyethylene. These fibres are known for their low density and low melting point. Low density can cause the fibres to be less compact and less durable. In addition, the low melting point increases the possibility of damage to the fibres during thermal processes, which negatively affects the abrasion resistance [17–21]. These results agree with Arora (2020), who reported that lower-density polymers exhibit reduced durability under repeated friction [22].

Fabric tensile strength and elongation at break test

It is seen in the graph that the warp breaking strength values in the warp direction are very close to each other in the fabrics with codes K4 and K5. It was determined that the warp breaking strength values in the fabrics with codes K1 and K2 are low, and the strength is high in the fabric with code K5. The first weft yarn is used as the organic cotton, and the second is for the fabric's breaking strength. It is seen in the graph that the fabric with the lowest breaking strength is among the fabrics with codes K1 and K3 (figure 4).

In the measurements of the breaking strength and breaking elongation (figure 5) of the fabric containing organic cotton in the K5, a good breaking strength. The crystalline structure of the organic cotton fibres in the K5 increased the durability of the fibres and provided an increasing effect on the breaking strength [21]. Thus, it shows higher strength than fabrics belonging to other groups containing Tencel, bamboo and polyviscose. When the breaking elongation values are examined, the fabrics containing Tencel in the K3 gave the lowest results. This situation is associated with the fact that Tencel fibres contain a high percentage of crystalline regions, which increases the strength of the fibres while reducing their flexibility. In addition, the low microfibril angle of Tencel fibres has a limiting effect on the elongation capacity of the fibres [17–20]. All fabric breaking elongation values of the fabrics were measured. Since PET and r-PET are used in the warp

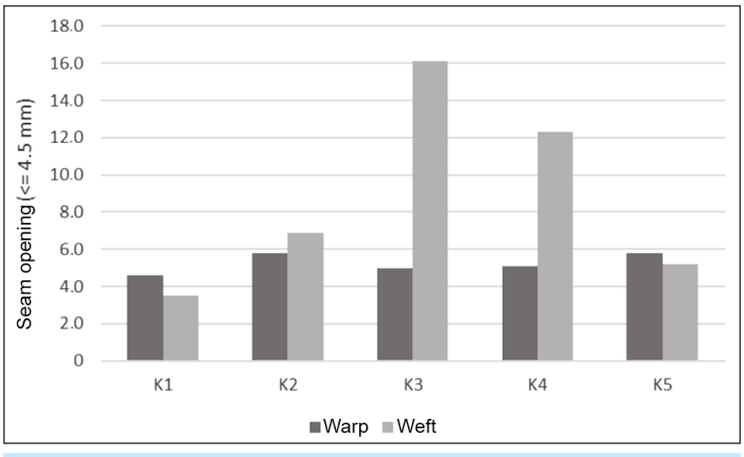

Fig. 2. Fabric seam opening results

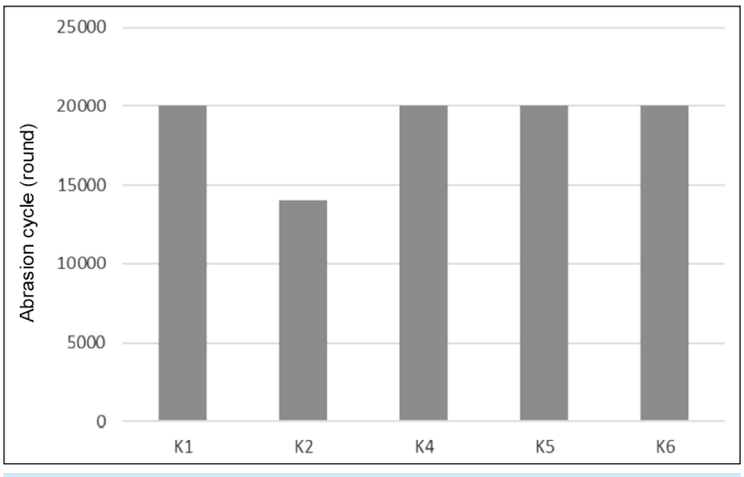

Fig. 3. Abrasion cycle test results of fabrics

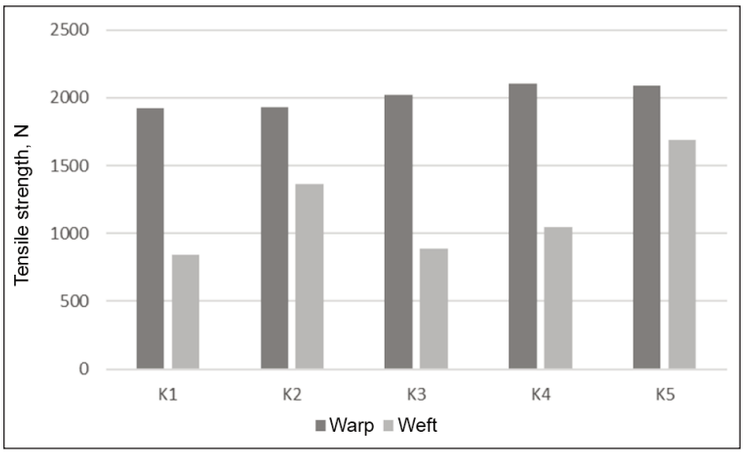

Fig. 4. Fabric tensile strengths results

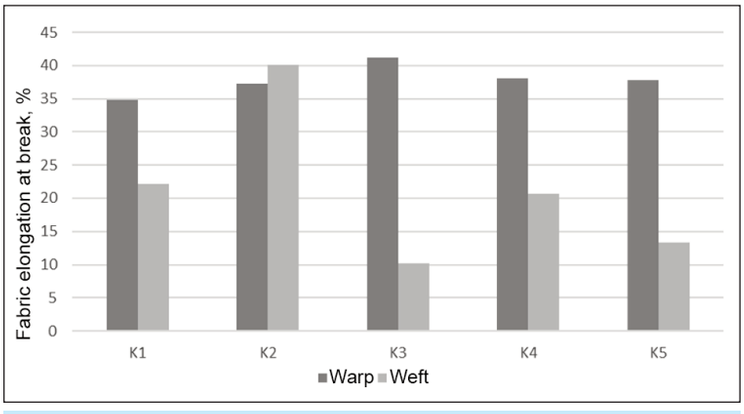

Fig. 5. Elongation at break test results

yarns, the elongation values in the warp direction are more consistent and vary in a narrow range (34.8–41.25%). It was determined that the fabric with the lowest weft breaking elongation was the K3-coded fabric with Tencel in it.

Rubbing and light fastness test of fabrics

Dry rubbing and wet rubbing fastness were evaluated between 4–4/5 for all fabrics. For light fastness, all fabrics have a 4/5 rating. In general, it is seen that all fabrics show high performance in terms of rubbing and light fastness values. When the rubbing and light fastness results of the fabrics were evaluated, it was seen that the fabrics had good light resistance and showed colour fastness against long-term light exposure. In terms of fastness performance, all fabrics were found to be suitable for commercial use and at a reliable level.

Measurement of the air permeability of fabrics

The desired air permeability level in fabric design is optimised according to the application area. Fabrics with high air permeability can provide a comfort-enhancing effect by allowing moisture and heat transfer. Air permeability values in K1 and K2 fabrics are relatively lower than those of other fabrics. (20.1–11.25; 20,42–11,75 Pa-L/min). Air permeability measurements were made at the highest level for K3 coded fabrics (23–11.0 Pa-L/min). Tencel, bamboo and organic cotton fabrics in K4 and K5 exhibit medium-level air permeability values (22–10.75 Pa-L/min; 21–10,5 Pa-L/min). Air permeability values were significantly higher in fabrics containing natural fibres (K3, K4, K5) compared to those with polyviscose/ linen or recycled olefin, which correlates with the porous microstructure of natural fibres. This is consistent with Adamu and Gao (2022), who observed that fabrics with thicker yarns and lower density exhibited increased permeability [19].

Transforming fabrics into clothing form and creating styles

First, sketch drawings of the designs were made. Modelling was done with sketch drawings, and style studies were detailed, and the form, aesthetic lines and details of the design were visually concretised (figure 6).

Various stages of the design process, such as style details, layered arrangements and colour studies,

Fig. 6. Design I and Design II sketch, Design I and II Modelling

Fig. 7. Front and right view of blouse and pants models

were modelled using the lartbook program and the design development process was completed. In the Design I model, the fabrics with pattern motifs were combined with the patchwork technique and turned into a sleeveless top, and in the Design II model, into a long vest product (figure 7). The fabrics obtained were made into three different forms of clothing: a sleeveless blouse, trousers and three skirts. The conversion of fabrics into garments demonstrated that performance characteristics influenced design choices; for example, the high breathability of K5 fabrics made them suitable for summer tops and skirts.

In addition to the mechanical and comfort-related evaluations, the sustainability dimension of the fabrics requires a more detailed discussion. Life Cycle Assessment (LCA) studies have shown that conventional textile fibres such as virgin polyester and polypropylene are associated with high carbon emissions and significant water use, particularly during dyeing and finishing processes [2]. r-PET bottles supply both emissions and fossil fuel consumption reductions ranging from 12% to 82%, respectively, on a cradle-to-grave basis compared to fossil fuel-derived PET bottles, assuming PET bottles are landfilled [23]. Similarly, the production of RO yarn, which is based on post-consumer textile waste, eliminates water usage at the yarn manufacturing stage and demonstrates a lower carbon footprint compared to conventional polyolefin fibres.

Among the natural fibres tested, organic cotton and bamboo provide distinct ecological advantages. Organic cotton cultivation avoids synthetic pesticides and fertilisers, thereby reducing eutrophication potential and soil degradation [24]. Bamboo, on the other hand, is known for its rapid renewability and lower irrigation needs compared to conventional cotton, offering additional environmental benefits. Tencel (Lyocell) fibres are also noteworthy due to their closed-loop production process, in which more than 99% of the solvent is recovered and reused, making it one of the most environmentally friendly regenerated cellulose fibres [21].

Considering these factors, the integration of Ottoman caftan motifs with sustainable fibre compositions not only preserves cultural heritage but also aligns with the global agenda of reducing carbon emissions, water footprint, and energy consumption in the textile sector. The superior seam strength of RO-based fabrics and the enhanced breathability of organic cotton and bamboo blends indicate that these materials could be applied in apparel manufacturing where durability and comfort are prioritised. Moreover, the use of jacquard weaving with sustainable fibres demonstrates compatibility with current industrial looms, supporting scalable production without process modification. Therefore, beyond aesthetic and mechanical performance, the fabrics developed in this study have the potential to contribute to a circular textile economy by lowering the environmental load associated with raw material selection and production processes.

CONCLUSION AND RECOMMENDATIONS

This study highlights the dual contribution of reviving Ottoman caftan motifs and employing sustainable fibres to create fabrics with favourable performance and comfort properties. In this study, pomegranate, tulip and carnation motifs from the caftan patterns of the Ottoman Empire from the 16th and 17th centuries were used in the patterning of fabrics to keep traditional values alive. Fabric compositions were created with natural and recycled fibres such as polyviscose, linen, RO, Tencel, r-PET, bamboo and organic cotton. A total of 5 different fabric compositions were used. The physical test, comfort and fastness properties were determined for each fabric and the yarns contained in the fabrics were measured. In the measurements made for the yarns, yarn count, breaking strength, breaking elongation and twist measurements were made. In the measurements made for the fabrics, breaking strength, breaking elongation, seam opening, abrasion cycle, rubbing and washing fastness and air permeability tests were applied. PET or r-PET were used in the warp yarns in all fabrics. Natural or recycled yarns were used in the weft yarns. Therefore, the observed performance changes are due to the weft yarns.

K1 polyviscose linen containing fabrics showed the lowest values in seam opening, breaking strength and elongation at break tests. This situation is related to the fact that viscose fibres have low strength due to their low crystalline regions, despite having a cellulosic structure, and that linen fibres have a hard and brittle structure despite having a high crystalline

structure. Apart from K1, K3 Tencel containing fabrics showed low value results. It is thought that this situation is because Tencel fibres contain high crystalline regions and thus increase the strength of the fibres while decreasing their flexibility. Among the tested fabrics, K5 organic cotton was the most advantageous in terms of mechanical strength, abrasion resistance, and air permeability, while K2 recycled olefin fabrics performed better in seam strength. All fabric structures were found to be suitable for commercial use and reliable in terms of friction and light fastness performance. When evaluated in terms of air permeability, it was observed that fabrics containing natural raw materials coded with K3, K4 and K5 had higher air permeability. The porous structure of natural fibres exhibited a good performance in terms of air permeability.

Within the scope of the study, as a result of the tests applied to the fabrics produced from the sustainable textile fibres used, textile garments with high physical and comfort properties were produced. All fabrics produced were created with modern kaftan designs and transformed into clothing forms. Fabrics have versatile usage potential both commercially and in terms of design. As in many studies [25, 26], combining traditional design approaches with material functionality features will contribute to design efficiency. From a circular textile economy perspective, this study contributes to closing material and cultural loops by combining recycled synthetics and renewable natural fibres with the reinterpretation of Ottoman caftan motifs. The use of r-PET and recycled olefin reduces dependence on virgin polymers and diverts post-consumer waste from landfills, while organic cotton, bamboo, and Tencel represent renewable and biodegradable resources. From a life cycle perspective, the combination of recycled and renewable fibres used in this study contributes to measurable reductions in environmental burdens. Literature-based [27, 28] LCA data show that r-PET and RO lower greenhouse gas emissions and water use by up to 60% and 100%, respectively, compared to virgin synthetics, while Tencel and bamboo minimise chemical and irrigation demands. Thus, the integration of Ottoman motif-inspired design with eco-efficient fibre systems supports both cultural continuity and life-cycle-based sustainability. Future studies should extend this work by integrating other traditional motifs, applying digital printing techniques, and conducting full LCA analyses to evaluate environmental impacts.

REFERENCES

[1] Park, Y.M., Park, K.S., *Fashion textile planning by eco-friendly fabrics with traditional patterns*, In: Korean Journal of Human Ecology, 2009, 18, 5, 1103–1113

[2] Islam, M.T., Jahan, R., Jahan, M., Howlader, M.S., Islam, R., Islam, M.M., Hossen, M.S. Kumar, A., Robin, A.H., *Sustainable textile industry: An overview*, In: Non-Metallic Material Science, 2022, 4, 2, 15–32

[3] Öztürk, H., Yazar, T., *Ottoman Padishah Knobs and Codes as a Symbolic Value for Weaving and Motific Properties*, In: Researcher, 2017, 5, 3, 148–168

[4] Cihan, N., *New Desıgn Offers on Ceramıc Surfaces (Inspıred By Tulıp, Golden Horn Work and Chıntomanı) Patterns on Ottoman Kaftans in the 17th Century,* Master's thesis, Erciyes University, Türkiye, 2012

[5] Tekkılıç, E.İ., Soysaldı, A., Kılıç, Ö., *Areas of Traditional Turkish Motifs in Home Textile Design*, In: Akademik Sanat, Journal of Art, Design and Science, 2016, 1, 1, 12–19

[6] Obidovna, M.Z., *History of Textiles During the Ottoman Empire Fabric Analysis*, In: Ijodkor O'qıtuvchı, 2024, 4, 40, 51–56

[7] Darvishi, N., Narimani, S., *The Symbolic Role of Tulip and Pomegranate Flowers in the Tiling Art of Iran and Ottoman Turkey,* In: Journal of Art and Civilization of the Orient, 2022, 10, 23–28

[8] Bağcı, V., Kiper, E., *Home Textile Designs Inspired by 16th and 17th Century Ottoman Kaftans with Leaf and Hatayi Motifs and Sample Application*, In: Afyon Kocatepe University Journal of Social Sciences, 2023, 25, 4, 1479–1508

[9] Gümüşer, T., *Motifs in contemporary Turkish textile designs influenced by Ottoman court fabrics in 16th century*, Master's thesis, İzmir Ekonomi University, Türkiye, 2011

[10] Kets, *Rolefin Recycle Yarn*, 2024, Available at: https://kets.com.tr/rolefinrecycledyarn/ [Accessed on 22 October 2024]

[11] Elibüyük, U., Bulut, M.O., Üçgül, İ., *Comparison of Some Physical and Dyeing Properties of Bamboo-Cotton and 100% Cotton Fabrics*, In: Journal of Technical Sciences, 2018, 8, 2, 11–16

[12] Bilir, T.B., Şardağ, S., *The Investigation of Performance Properties of Tencel Cotton Blended Yarn,* In: Uludag University Journal of the Faculty of Engineering, 2017, 22, 1, 13–27

[13] Doğmuş Yılmaz, N., *Investigation of mechanical properties of polyethylene terephthalate (PET) yarns having ultraviolet resistant properties after outdoor weathering tests*, Master's thesis, Bursa Uludağ University, Türkiye, 2020

[14] Sundaresan, S., Ramesh, M., Sabitha, V., Ramesh, M., Ramesh, V., *A detailed analysis on physical and comfort properties of bed linen woven fabrics,* In: International Journal of Advanced Research and Innovative Ideas in Education, 2016, 2, 2, 1649–1658

[15] Okur, N., *Comparative analysis of bamboo fiber and yarn properties with performance properties of other fibers and yarns*, Master's thesis, Istanbul Technical University, Türkiye, 2006

[16] Kutgi, M., Zervent Ünal, B., *Comparison of Cotton-Viscose and Cotton-Bamboo Blended Fabrics According to Selected Parameters*, le Congress, 26-27 September 2019, Adana, Türkiye

[17] Kumpikaitė, E., Tautkutė-Stankuvienė, I., Redeckienė, D., *Interrelation between tensile properties of yarns and woven fabrics with these yarns*, In: AUTEX Research Journal, 2019, 19, 4, 235–241

[18] Li, X., Yang, K., Yuan, Z., Liu, S., Du, J., Li, C., Meng, S., *Recent advances on the abrasion resistance enhancements and applications of superhydrophobic materials,* In: The Chemical Record, 2023, 23, 4, e202200298.

[19] Adamu, B.F., Gao, J., *Comfort related woven fabric transmission properties made of cotton and nylon*, In: Fashion and Textiles, 2022, 9, 1, 8

[20] Medar, R., Mahale, G., *Quality characteristics of cotton, polyester, bamboo and Tencel yarns*, In: Indian Journal of Pure & Applied Biosciences, 2020, 8, 1, 127–134

[21] Baig, S., Hussain, T., *Comparison of mechanical and thermal comfort properties of Tencel blended with regenerated fibers and cotton woven fabrics*, In: AUTEX Research Journal, 2019, 19, 1, 23–30

[22] Arora, A., *Effect of abrasion resistance on the woven fabric and its weaves*, In: International Journal of Sciences: Basic and Applied Research (IJSBAR), 2020, 50, 2, 9–19

[23] Benavides, P.T., Dunn, J.B., Han, J., Biddy, M., Markham, J., *Exploring comparative energy and environmental benefits of virgin, recycled, and bio-derived PET bottles,* In: ACS Sustainable Chemistry & Engineering, 2018, 6, 8, 9725–9733

[24] Textile Exchange, 2025, Available at: www.textileexchange.org [Accessed on 22 August 2025]

[25] Chen, H., Shen, L., Zhang, X., Ren, X., Wang, M., Min, X., Li, X., *Digital design of regional characteristic apparel pattern driven by GAN*, In: Industria Textila, 2022, 73, 3, 233–240, http://doi.org/10.35530/IT.073.03.202117

[26] Carp, M., Popp, A., *The influence of traditional art in the current fashion design*, In: Industria Textila, 2013, 4, 217–221

[27] Shen, L., Worrell, E., Patel, M.K., *Open-loop recycling: A LCA case study of PET bottle-to-fibre recycling*, In: Resources, Conservation and Recycling, 2010, 55, 1, 34–52

[28] La Rosa, A.D., Grammatikos, S.A., *Comparative life cycle assessment of cotton and other natural fibers for textile applications*, In: Fibers, 2019, 7, 12, 101

Authors:

GENCAL ÖZTÜRK RUKİYE ZEYNEP[1], SÜNTER EROGLU NİLSEN[1,2], KOÇAK EMİNE DİLARA[3]

[1]Halic University, Institute of Graduation Studies, Textile and Fashion Design,
34060, Istanbul, Türkiye
e-mail: ozozturk99@gmail.com

[2]Marmara University, Design Department, Fashion Design Programme, Vocational School of Technical Sciences,
34722 İstanbul, Türkiye

[3]Marmara University, Technology Faculty, Textile Engineering Department,
34854, İstanbul, Türkiye
e-mail: dkocak@marmara.edu.tr

Corresponding author:

SÜNTER EROGLU NİLSEN
e-mail: nilsensunter@gmail.com

How digital factors lead to sustainability through circular economy practices: empirical evidence from the textile sector

DOI: 10.35530/IT.077.03.202586

KUN HU
WANHUA KUANG
QUANDE QIN
JIANUO WANG
MD BILLAL HOSSAIN

ABSTRACT – REZUMAT

How digital factors lead to sustainability through circular economy practices: empirical evidence from the textile sector

The transition toward sustainable manufacturing requires integrating digital innovation with environmental responsibility. In the textile sector, the adoption of Industry 4.0 technologies has become essential for achieving circular and sustainable operations. However, the mechanisms linking digitalisation to sustainability remain underexplored. This study examines how five Industry 4.0 technologies, Big Data (BD), Smart Factory (SF), Cyber-Physical Systems (CPS), Internet of Things (IoT), and Interoperability (IP) influence sustainability performance in China's textile industry, with Circular Economy Practices (CEP) acting as a mediating factor.
Adopting a quantitative, cross-sectional design, data were collected through structured questionnaires distributed to 523 professionals in textile manufacturing firms across mainland China. Using purposive sampling, firms that have either adopted or shown interest in adopting 4.0 technologies or circular practices are selected.
The analysis conducted using Structural Equation Modelling (SEM) reveals that BD and CPS exert significant direct effects on sustainability performance, while SF and IoT contribute indirectly through CEP. Interoperability shows no significant impact, indicating that integration does not lead to sustainability gains unless strategically aligned with circular principles. The results confirm that circular practices act as a key mechanism transforming digital capabilities into environmental benefits. These outcomes highlight the strategic role of digital technologies, guided by the Resource-Based View (RBV), in enabling a sustainable and circular transformation of China's textile industry.

Keywords: *Smart Factory, Big Data, IoT, Cyber-Physical Systems, Interoperability, Industry 4.0, circular economy, sustainability*

Modul în care factorii digitali contribuie la sustenabilitate prin practicile economiei circulare: dovezi empirice din sectorul textil

Tranziția către o producție durabilă necesită integrarea inovației digitale cu responsabilitatea față de mediu. În sectorul textil, adoptarea tehnologiilor Industriei 4.0 a devenit esențială pentru realizarea unor operațiuni circulare și durabile. Cu toate acestea, mecanismele care leagă digitalizarea de durabilitate rămân insuficient explorate. Acest studiu examinează modul în care cinci tehnologii din cadrul Industriei 4.0, Big Data (BD), Smart Factory (SF), Sistemelor ciber-fizice (CPS), Internetului obiectelor (IoT) și Interoperabilității (IP) influențează performanța în materie de sustenabilitate în industria textilă din China, cu Practicile economiei circulare (CEP) acționând ca factor de mediere. Adoptând un design cantitativ, transversal, datele au fost colectate prin chestionare structurate distribuite către 523 de profesioniști din firme de producție textilă din China continentală. Folosind eșantionarea intenționată, sunt selectate firmele care au adoptat sau au manifestat interes în adoptarea tehnologiilor 4.0 sau a practicilor de economie circulară. Analiza efectuată utilizând modelarea ecuațiilor structurale (SEM) relevă faptul că BD și CPS exercită efecte directe semnificative asupra performanței în materie de sustenabilitate, în timp ce SF și IoT contribuie indirect prin intermediul CEP. Interoperabilitatea nu are un impact semnificativ, ceea ce indică faptul că integrarea nu conduce la îmbunătățiri în materie de sustenabilitate decât dacă este aliniată strategic la principiile economiei circulare. Rezultatele confirmă faptul că practicile circulare acționează ca un mecanism-cheie de transformare a capacităților digitale în beneficii pentru mediu. Aceste concluzii evidențiază rolul strategic al tehnologiilor digitale, ghidate de perspectiva bazată pe resurse (RBV), în facilitarea unei transformări durabile și circulare a industriei textile din China.

Cuvinte-cheie*: Smart Factory, Big Data, Internetul obiectelor (IoT), Sisteme ciber-fizice, Interoperabilitate, Industria 4.0, Economia circulară, sustenabilitate*

INTRODUCTION

The contemporary manufacturing landscape is undergoing a profound transformation, driven by the integration of advanced digital technologies and an escalating global focus on sustainable development. The global industries are also being pressured to strike a balance between economic growth and environmental responsibility, which makes them seek innovative solutions that can optimise the resources and reduce the waste [1]. The implementation of

Fourth Industrial Revolution (4.0) technologies can be considered one of the most promising answers to these demands. These are technologies, including smart manufacturing, data analytics, cloud computing, and real-time connectivity, that are revolutionising the functioning of industry, allowing new levels of efficiency, responsiveness, and sustainability [2]. With companies going digital in order to stay competitive, a similar focus on sustainability, especially in the form of the circular economy (CE), is transforming supply chains across the globe.

At the global level, 4.0 technologies are identified as potentially helpful in contributing to sustainability goals because they allow monitoring data in real-time and optimising resources [3]. These aspects are particularly important in industries such as textiles, which have a high environmental footprint, in terms of water and energy usage, pollution, and linear, wasteful operations that have long been the hallmark of such industries [4]. The CEP paradigm provides a way out of these problems, as it encourages recycling, reuse, remanufacturing, and minimising resource input throughout the supply chain processes [5]. The implementation of 4.0 technologies in CEP systems can support closed-loop supply chains, which would make sure that materials and products remain in use as long as possible, which will help reduce their environmental footprint [6].

These technological improvements are especially important in the textile industry. Being one of the largest producers of textiles in the world, China has a serious problem with environmental and operational issues in this industry [7]. The use of traditional manufacturing processes causes inefficiency and high ecological degradation in the industry, such as overconsumption of fossil fuels and dumping of chemicals in water bodies. Although the Chinese government is making efforts to make the industrial sector go digital and sustainable, as demonstrated by the digital China vision and green industrial policies, the uptake of 4.0 technologies in the textile industry is still small and scattered [8]. The majority of companies are still working with old systems and low technology integration, which prevents the attainment of sustainable and circular supply chain models.

Despite the increasing number of evidence of 4.0 technologies' potential to enhance the degree of circularity and sustainability in the world, the dynamics of this relationship within the framework of the Chinese textile industry have not been examined to a substantial degree [9]. The application of 4.0 technologies may have a significant beneficial impact on the sustainability of the supply chain, making it more visible, enabling it to be circular, and more efficient [10, 11]. These studies emphasise that 4.0 technologies may enable sustainable transitions, but also point out that other aspects, including CEP practices that enable the recycling of materials, influence such outcomes greatly. This has not been extensively covered by these previous studies, creating a gap in the empirical literature. This gap should be filled in, as the textile industry in China has a crucial strategic role in the economy and environment [12]. The industry not only makes a significant contribution to the GDP and the labour market of the country, but it also determines its environmental impact [13]. The inability to modernise and shift to sustainable and circular supply chains can undermine the competitiveness of the industry in the long term in the world market that is becoming more sustainability-focused. The textile supply chains in China can provide useful information to policymakers regarding how 4.0 technologies can be used to promote sustainable practices, to allow industry leaders and academics to facilitate the digitalisation of the textile industry and environmental change.

The proposed research aims to analyse the role of Industry 4.0 technologies in the sustainability performance of the Chinese textile industry, both directly and indirectly, as a result of the circular economy practices. This study is especially important as it takes a complex research model that places the circular economy as an intermediary variable in the correlation between 4.0 technologies and sustainability performance. This research will address five technological factors: Big Data (BD), Smart Factory (SF), Cyber-Physical Systems (CPS), Internet of Things (IoT), and Interoperability (IP). All these technologies have their peculiarities of opportunities, which could be utilised as far as the process of implementing the circular practices into manufacturing activities is concerned. The practical example of the BD analytics application in the work with big data to simplify the use of resources on the process and supply chain levels is practical [14, 15]. Creative factory arrangements make a highly dynamic, computerised manufacturing room to assist in setup in real-time and efficient flow of materials [16]. CPS is digital and physical in nature, which can dynamically control and monitor processes, which is essential to the circular operations. The IoT can also provide the connectivity infrastructure that allows machines, products, and nodes in the supply chain to communicate and exchange data in real time, enhancing the visibility of the supply chain and tracking material [17]. IP guarantees that various technological systems and platforms have the capability to share information with each other and increase the level of integration and effectiveness of circular strategies [18]. This study focuses on the overall effects of these technologies on sustainability performance in the textile industry, both directly and indirectly via the use of CEP. This research can help in understanding the impact of technological changes on the environment and sustainability by modelling the mediating role of CE. The literature has tended to assume that technology and sustainability are directly related in a linear form, but this paper suggests that the introduction of circular practices is an obligatory step through which the sustainability potential of 4.0 technologies can be achieved.

The study contributes to theory and practice. Theoretically, the work is well based on the Resource-Based View (RBV) that states that the

internal resources and capabilities of an organisation play a central role in attaining sustained competitive advantage [19]. In this context, the 4.0 technologies, including BD, SF, CPS, IoT, and IP, may be theorised as valuable, rare, inimitable, and non-substitutable (VRIN) assets that enable companies to build unique capabilities. When these high-technological assets are properly combined with the use of the circular economy, they can become strategic resources that cannot be easily imitated by competitors. The RBV points out that having such technologies does not necessarily result in competitive advantage, but rather the capability of firms to use them in a manner that generates synergies with circular strategies results in high levels of sustainability performance [19, 20]. This view is specifically applicable to the textile industry in China, where the heterogeneity of technological usage and capability building among the companies can be attributed to the differences in the sustainability levels. This study identifies internal resource configuration as a strategic element of attaining circular and sustainable supply chains by integrating the RBV lens. In practice, the results will provide information to the managers and policymakers. The determination of the technologies that contribute to the strongest circularity and sustainability can be used to guide firms on the types of investments they should make (e.g., investing in IoT sensors or data analytics) and government agencies on the type of support programs they should prioritise. Effectively, the analysis will demonstrate how digital improvements and circular solutions can produce a greener production. A report on a digital and sustainable transformation in the textile industry can be used as an example to other textile-producing areas that need to modernise in a responsible way [21]. This paper is very useful in offering insights on how the textile industry and other industries in the emerging economies can use Industry 4.0 and circular strategies to have a more sustainable future.

RESOURCE-BASED VIEW (RBV)

Resource-Based View (RBV) may be used to provide theoretical explanations that can help understand how the implementation of Industry 4.0 technologies may be associated with the sustainability of the textile industry. The RBV explains that a sustainable competitive advantage is achievable, and firms can be able to exploit viable, rare, inimitable and non-substitutable (VRIN) resources [19]. In this context, Big Data (BD), Smart Factory (SF), Cyber-Physical Systems (CPS), Internet of Things (IoT), and Interoperability (IP) may be viewed as essential internal resources that can empower the capacity of firms and enhance their general performance. The technologies would facilitate advanced processing of the data, predictable processes when empowered, and multiple functions throughout the production and supply chains [2]. With the effective integration, they can increase the resource utilization, minimize a waste, and stimulate the shift to more circular and sustainable production systems [1]. The significance of the RBV to this study is in the fact that these technological instruments are not just the tools of operation but rather the key internal resources of long-term performance that are considered in factory sustainability [22].

The translation of such technological resources into sustainability outcomes can be achieved successfully due to the complementary organisational capacity, namely, the application of the practices of the circular economy (CEPs). The role of CEPs in the context of the present study is as follows: CEPs are the channels through which the Industry 4.0 technologies are exerting their impact on the sustainability performance. These technologies, in combination with the cyclic processes such as recycling, remanufacturing, and reusing, allow companies to create closed-loop systems that minimise the quantity of waste and the recovery of resources [22]. This insight is consistent with the perception of natural resources, as developed by Hart (1995), which emphasises that a mixture of technological and environmental forces enhances sustainable competencies of firms. Digital technologies can help textile companies to improve the use of the circular production process, as they guarantee the optimal material management, waste reduction, and real-time control [6]. Based on the empirical evidence, the usage of technological capabilities coupled with the applications of the circular economy is far more likely to rise in both the environmental and economic performance [6]. The RBV indicates that the Chinese textile companies can be made sustainable by obtaining technology by combining it successfully with a circular economy practice.

HYPOTHESES DEVELOPMENT

The emergence of Big Data as a core component of Industry 4.0 has transformed how firms manage operations, particularly in resource-intensive industries. Big Data analytics enables companies to collect, analyse, and determine huge quantities of organised and undefined data to optimise decision-making and improve the effectiveness of operations [23]. Within the textile manufacturing industry, in which lengthy and ecologically stressful production processes are involved, the application of BD can open up the possibility of real-time tracking of the use of energy and water, the minimisation of material waste, and supply chain streamlining [24]. Evidence-based information enables proactive maintenance, quality decrease, and improved inventory administration, all of which play a role in enhancing sustainability performance (Xi et al., 2025). According to the RBV, the ability to create and/or implement this technology might be regarded as a valuable and rare resource in increasing the competitiveness of a firm at the firm level, primarily as a consequence of sustainability [19]. According to Bag et al. (2023), companies using smart analytics will demonstrate better

environmental performance because of resource-informed use and waste minimisation plans. Therefore, based on these insights, the following hypothesis is proposed:

H1: Big Data has a significant positive impact on sustainability performance in the textile sector.

The integration of smart factory systems within textile manufacturing processes is rapidly reshaping the landscape of industrial sustainability. A smart factory is a completely digitalised production area in which the machines, systems, and humans acquire a connection via cyber-physical infrastructure, facilitating the optimisation of the processes dynamically and autonomously [16]. Such settings allow real-time decision-making, adaptive control, and flexible manufacturing to become feasible and result in enormous efficiency of resources used and reduction of waste [25]. In textile industries, smart factories enable tracking and streamlining the process of dyeing, weaving and finishing, which could previously be characterised by the inefficient use of water, energy and chemicals. Such capability enables manufacturers to minimise the use of material and minimise emissions to the environment, which shape the goals of sustainability [26]. In the RBV, a smart factory system can be regarded as a worthy and inimitable source of competitive advantage in terms of increased performance in environmental responsibility [19].

Therefore, the following hypothesis is proposed:

H2: Smart Factory systems have a significant positive impact on sustainability performance in the textile sector.

CPS serve as the backbone of Industry 4.0 by tightly integrating physical production processes with computational control systems. These systems have embedded sensors, real-time communication, and an autonomous feedback loop that ensures constant monitoring and adjustment of the manufacturing operations [27]. In the textile industry, CPS allows the accurate control of temperature, humidity, and performance of machines as well as the flow of materials, reducing the inefficiencies that cause waste and gases. Spinning or dyeing machines fitted with smart sensors are able to sense the deviations and automatically adjust the spinning of the machine to prevent overusage of water or energy. CPS also helps in predictive maintenance, minimising the chances of sudden shutdown and loss of resources [28]. The functionalities will make the production environment more sustainable by improving the effectiveness of the system with regard to its reliability and responsiveness [29]. In terms of the RBV theory, CPS can easily be treated as an inimitable asset, which allows a firm to match its operational control to its sustainability ends [22]. Thus, the following hypothesis is posited:

H3: Cyber-Physical Systems (CPS) have a significant positive impact on sustainability performance in the textile sector.

The IoT has emerged as a transformative tool in enabling sustainable manufacturing. IoT brings together the machines, sensors, products, and humans in a networked infrastructure that enables the exchange of real-time data and vocational visibility across a system [30]. IoT technologies in the textile industry encourage the smooth tracking of water consumption, energy efficiency, emissions, and logistics of the supply chains. This can be done through the placement of sensors onto fabric dyeing systems that measure the amount and rate of chemicals and make finer adjustments that would decrease the unnecessary amount used and waste [12]. With IoT, the entire supply chain can be traced, which would enable responsible sourcing, reuse of material, and resourceful management of inventory [31]. According to RBV, when the IoT infrastructure is present in firm-specific systems that minimize resources consumption and environmental cost, the infrastructure turns out to be a strengthened capability that is hard to replicate [32]. Consequently, a hypothesis is presented:

H4: Internet of Things (IoT) has a significant positive impact on sustainability performance in the textile sector.

IP is an important facilitator of sustainable production. It makes sure that different technologies, including ERP systems, machines, cloud platforms, and analytics tools, can be used in synergy [33].

Interoperability can also be used in eliminating silos and promoting coordinated decision-making in the textile industry, where operations involve different functions that would include fibre processing, logistics, etc. One of them is to link the machine data with environmental tracking systems to enable firms to align the production specifications with sustainability indicators [34]. Interoperability provides real-time coordination and consequently enables effective scheduling, reduced downtimes and improved resource utilisation that contributes to the reduction of environmental footprints [35]. Interoperability in the RBV is not described as a technology capability but a strategic capability that can enhance the utility of available technology resources by maximising the synergistic nature of the resources [36]. It is often firm-specific and hard to imitate, hence it satisfies valuable RBV criteria [19]. Based on these insights, the following hypothesis is formulated:

H5: Interoperability has a significant positive impact on sustainability performance in the textile sector.

Recent discourse in sustainability and industrial innovation highlights that the relationship between Industry 4.0 technologies and sustainability outcomes is not merely direct but often occurs through enabling organisational capabilities, particularly CEP. A strategy that has the capacity to convert the technological potential into real sustainability is the circular economy principles, after stripping resources, reuse and recycle outputs [37]. CEP is not merely an environmental program but an active operating system to achieve an innovative use of technological resources, to reduce waste and emissions and to maximise efficiency and lifespan of used materials. Although 4.0 technologies can maximise valuable features of managing data intelligently, automated

as well as machine integration, and having a system-wide visibility, the impact of the technology on sustainability is immense when applied in line with the circular processes matching the resource-conscious production and closed value chains [38].

Under the RBV, these technologies can be seen as valuable, rare, inimitable, and non-substitutable (VRIN) resources; however, to extract their full potential, firms must develop complementary capabilities [19, 22]. CEP acts as such a capability, integrating technological assets into routines and systems that deliver environmental benefits. BD analytics provides the insights needed to redesign processes for lower material usage; CPS and IoT enable real-time monitoring for efficient waste recovery and reuse; and SF systems, when combined with circular logic, can support flexible remanufacturing or energy optimisation. IP enhances CEP by facilitating communication across systems involved in reuse, recycling, or eco-design. Without such integration into circular frameworks, the environmental value of 4.0 technologies may remain underutilised [39]. Therefore, this research proposes that the circular economy mediates the relationship between these five industries' 4.0 technologies and sustainability performance, acting as the mechanism through which digital transformation leads to environmental improvement (figure 1). Based on the above discussion, the following hypotheses are proposed:

H6–H10: Circular Economy mediates the relationship between industry 4.0 factors (Big Data, Smart Factory systems, Cyber-Physical Systems, Internet of Things and Interoperability) and sustainability performance in the textile sector.

METHODOLOGY

This study adopts a quantitative, cross-sectional research design to investigate how Industry 4.0 technologies influence sustainability performance in the textile sector of mainland China, with circular economy practices acting as a mediating variable (figure 2). The quantitative approach is suitable for testing theoretical hypotheses and generalising findings based on numerical data [40]. A cross-sectional design is chosen as it captures a snapshot of firms' technological and sustainability practices at a single point in time, which is appropriate given the stable nature of technological infrastructure and policy environment in China's textile industry during the data collection period. The textile sector in mainland China was selected for this study due to its substantial contribution to China's economy and its representation of the broader national textile landscape. Mainland China hosts a significant portion of textile manufacturing firms. These firms are currently facing mounting pressure to adopt sustainable and digital practices, making them ideal units of analysis for this study. The target population comprises operational managers, production heads, and sustainability officers in textile manufacturing firms across mainland China. Using purposive sampling, firms that have either adopted or shown interest in adopting 4.0 technologies or circular practices are selected. This technique is suitable for exploratory models involving emerging concepts, such as Industry 4.0 and CE, in developed economies [41].

To ensure statistical power and model robustness in Structural Equation Modelling (SEM), an appropriate sample size is crucial. Following recommendations by Hair et al. (2021), a minimum sample size of 10 times the number of indicators in the most complex construct is adequate. A 20-to-1 ratio has also been suggested [42]. In this study, the total number of items was 34 and 680 respondents were needed. However, to account for non-response and incomplete data, the survey will be distributed to 600 potential respondents, aiming for at least 523 usable responses. Two software tools will be used for data analysis. SPSS Version 26 will be employed for initial

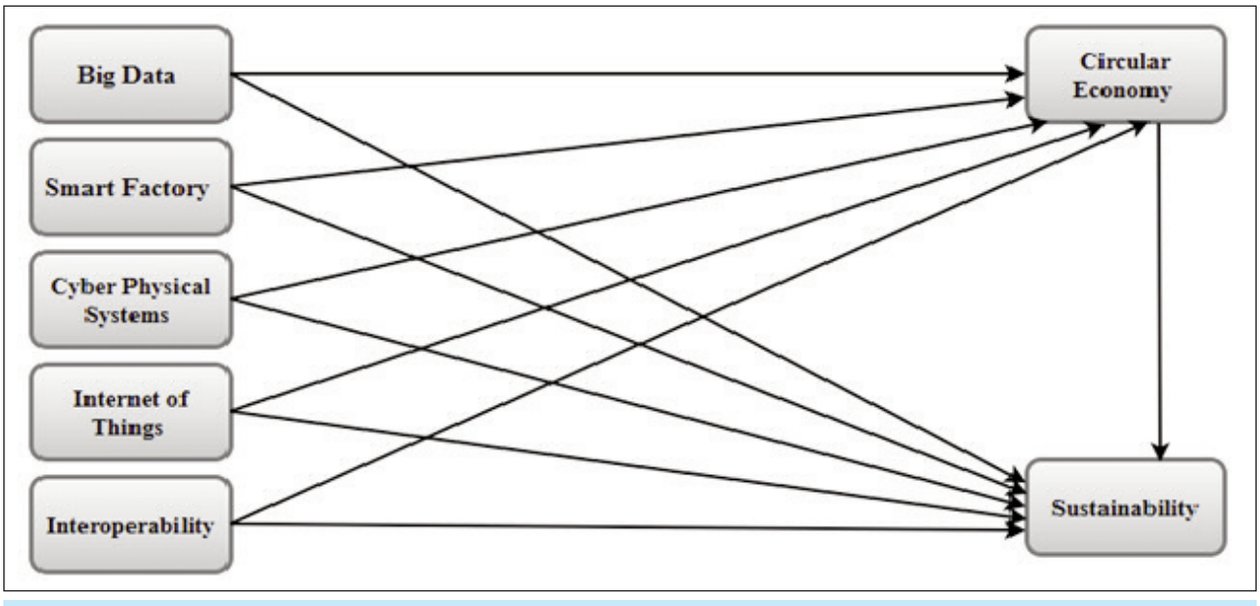

Fig. 1. The relations between the proposed hypothesis

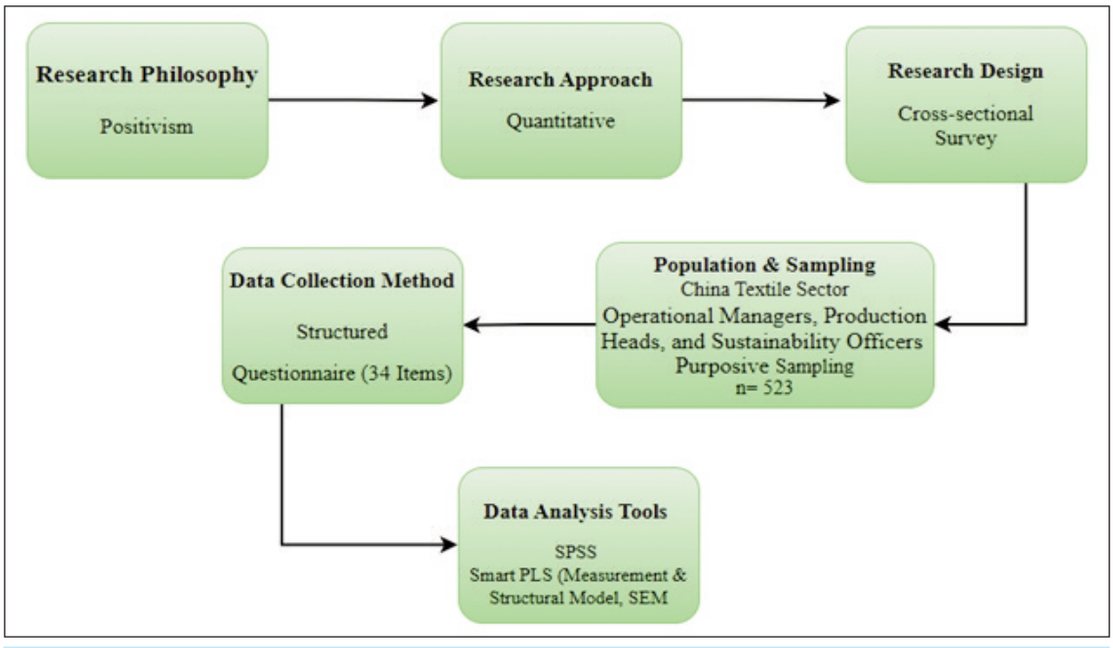

Fig. 2. Flow chart of methodology

data screening and descriptive statistics, while SmartPLS 4.0 will be used to test the structural model [43]. Data were collected using a 7-point Likert scale, ranging from "strongly disagree" (1) to "strongly agree" (7). A Likert scale is most suitable for examining the opinions and views of respondents [44].

Data analysis

Primarily analysis

The research conformed to the criteria provided by Sekaran (2003) and did not contain any missing values in the data. The CMV was measured using the single-factor test by Harman, and it was found that the single factor explained only 45.10 percent of the variance, which is lower than the standard value of 50 percent variance [45], therefore, the CMV issue was not considered serious. Hair et al. (2012) [46] and Bryne (2010) [47] are convinced that data is deemed normal when the skewness is between –2 and +2 and the kurtosis is between –7 and +7. Moreover, all the values are within range. The KMO value of 0.952 indicates an outstanding sampling adequacy for factor analysis, implying that the variables possess common factors [43]. To determine multicollinearity, the value of the variance inflation factor (VIF) is employed [48]. As the existence of multicollinearity is generally ignored when the value of the VIF is lower than 10 [48], it means that the independent variables do not reflect multicollinearity. All the values were lower than 10, hence no issue of multicollinearity.

MEASUREMENT MODEL

The measurement model was assessed to get the reliability and validity of the constructs (table 1). First factor loadings of all the items in the model are adequate, having more than the minimum acceptable value of 0.50 [46]. Although a loading factor of above 0.7 is recommended [49], researchers usually obtain poorer outer loadings (<0.70) in social science research analysis. Instead of deleting the indicators blindly, the impacts of delinking the item on the reliability of the composite, content, and convergent validity should be checked. In general, the suggested criterion should be met; thus, items (outer loading is between 0.40 and 0.70) can be discussed only in those cases when deletion leads to composite reliability or the average variance extracted (AVE) being increased more than the recommended [46]. SS5 contains fewer factor loadings, and it was eliminated in order to improve the reliability statistics. Reliability was estimated by measuring Cronbach's Alpha, rho_a are both greater than the recommended level of 0.700 [50]. An interval between values of Cronbach's Alpha and composite reliability is presented as the value of rho a, and shows a value of more than 0.70, which indicates that it was a good reliability [51].

Discriminant validity

Convergent validity also met expected levels because AVE was greater than 0.5. The Method to test the values of discriminant validity was to contrast the correlation rate of the latent variables with the square root of the AVE [52], heterotrait monotrait ratio of correlation [51], the value of which is lower than the 0.85 scores about discriminant validity, or it is conservative. Thus, the discriminant validity was established (table 2).

Structural equation modelling (SEM)

The structural model results reveal the degrees of influence of different Industry 4.0 technologies factors on sustainability performance (table 3 and figure 3). BD shows a significant and positive relationship with sustainability performance (B=0.214,

Table 1

REGRESSION WEIGHTS AND RELIABILITY STATISTICS						
Variables	**Items**	**Factor loadings**	**Cronbach's alpha**	**(rho_a)**	**(rho_c)**	**(AVE)**
Big Data (BD)			0.828	0.831	0.879	0.593
	BD1	0.790				
	BD2	0.761				
	BD3	0.753				
	BD4	0.788				
	BD5	0.756				
Circular Economy (CEP)			0.951	0.953	0.960	0.775
	CEP1	0.898				
	CEP2	0.889				
	CEP3	0.803				
	CEP4	0.906				
	CEP5	0.856				
	CEP6	0.929				
	CEP7	0.877				
Cyber-Physical Systems (CPS)			0.871	0.881	0.912	0.721
	CPS1	0.801				
	CPS2	0.861				
	CPS3	0.893				
	CPS4	0.838				
Internet of Things (IoT)			0.955	0.956	0.966	0.849
	IoT1	0.914				
	IoT2	0.936				
	IoT3	0.897				
	IoT4	0.915				
	IoT5	0.943				
Interoperability (IP)			0.960	0.963	0.974	0.926
	IP1	0.960				
	IP2	0.965				
	IP3	0.963				
Smart Factory (SF)			0.922	0.930	0.942	0.764
	SF1	0.891				
	SF2	0.925				
	SF3	0.923				
	SF4	0.829				
	SF5	0.797				
Sustainability (SS)			0.945	0.948	0.961	0.860
	SS1	0.955				
	SS2	0.953				
	SS3	0.954				

p<0.000), indicating that data-driven insights strongly contribute to sustainable operations in textile firms. CPS also showed a positive and statistically significant impact (B=0.178, p<0.000), reinforcing the role of real-time automation and intelligent process control in enhancing environmental outcomes. SF systems showed an insignificant effect on sustainability (B=0.034, p=0.676). IoT also showed an insignificant relationship with sustainability (B= –0.048, p=0.570), while IP also has an insignificant impact (B=0.003, p=0.962).

To see whether the model is good or not, the strength of each structural path can be determined by the value of R^2 of the dependent variable, and the value of R^2 is expected to be at least 0.1. Table 4 results indicate that all the R^2 exceed 0.1. Therefore, predictive ability is attained. F^2 value must be varied at ≥ 0.02, ≥ 0.15 and ≥ 0.35, which indicates small, medium, and huge effect sizes of exogenous construct on endogenous [53]. Table 4 shows that BD and CPS had an impact not large (>0.02) on sustainability. Whereas SF, IoT and IP did not influence

Table 2

FORNELL LARCKER AND HTMT RATIO							
Constructs	**BD**	**CEP**	**CPS**	**IOT**	**IP**	**SF**	**SS**
Fornell Larcker							
Big Data (BD)	***0.770***						
Circular Economy (CEP)	0.275	***0.881***					
Cyber-Physical Systems (CPS)	0.384	0.266	***0.849***				
Internet of Things (IOT)	0.266	0.820	0.289	***0.921***			
Interoperability (IP)	0.237	0.573	0.434	0.658	***0.962***		
Smart Factory (SF)	0.250	0.743	0.372	0.836	0.742	***0.874***	
Sustainability (SS)	0.405	0.552	0.382	0.466	0.387	0.456	***0.928***
HTMT (Heterotrait-Monotrait)							
Big Data (BD)							
Circular Economy (CEP)	0.308						
Cyber-Physical Systems (CPS)	0.438	0.292					
Internet of Things (IOT)	0.296	0.858	0.320				
Interoperability (IP)	0.260	0.602	0.479	0.687			
Smart Factory (SF)	0.282	0.785	0.427	0.883	0.799		
Sustainability (SS)	0.455	0.581	0.418	0.490	0.407	0.487	

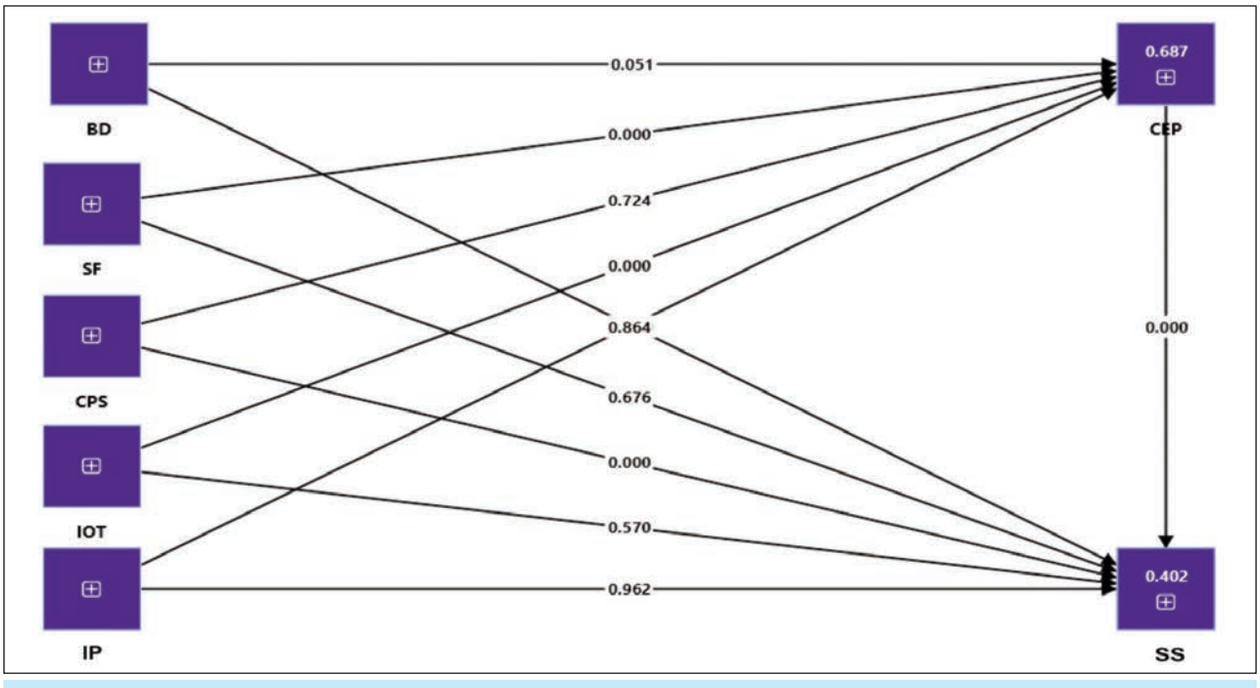

Fig. 3. Structural model results

Table 3

HYPOTHESES RESULTS					
	Original sample	**(M)**	**Standard deviation**	**T statistics**	**P values**
BD → SS	0.214	0.215	0.040	5.296	0.000
SF → SS	0.034	0.034	0.082	0.418	0.676
CPS → SS	0.178	0.178	0.047	3.766	0.000
IOT → SS	–0.048	–0.048	0.085	0.568	0.570
IP → SS	0.003	0.003	0.059	0.048	0.962

Note: BD (Big Data), SS (Sustainability), SF (Smart Factory), CPS (Cyber-Physical Systems), IOT (Internet of Things), IP (Interoperability).

Table 4

STRUCTURAL MODEL PREDICTIVE AND EXPLANATORY POWER			
Variable	**R^2**	**F^2**	**Q^2predict**
Circular Economy Practices (CEP)	0.687		0.679
Sustainability (SS)	0.402		0.318
Big Data (BD)		0.063	
Cyber-Physical Systems (CPS)		0.038	
Internet of Things (IOT)		0.001	
Smart Factory (SF)		0.000	
Interoperability (IP)		0.000	

sustainability. Q^2 determines how well the endogenous constructs are predictive. A Q^2 greater than 0 indicates that the model is relevant in prediction. The outcomes demonstrate that all the constructs have significance in their prediction (table 4). The model fitness was achieved by measuring the standardised root mean square residual. Standardised root square residual was equal to 0.065; it has the necessary value of 0.10, which reflects the suitability of the model [53].

MEDIATION ANALYSIS

The mediation analysis examines how the Industry 4.0 technologies impacted the sustainability performance indirectly using CEP. The findings denote that the IoT has a statistically significant mediation value (B=0.297, p<0.000), indicating that the effect of IoT on the sustainability performance is enhanced by CEP. The effect of SF systems on sustainability is strong through CEP (B=0.090, p=0.001), indicating the role of the latter in the support of the resource-efficient and circular production tool. Another aspect of sustainability, BD has a significant impact regarding CEP (B=0.028, p=0.045), which suggests that its role in promoting sustainability is partly achieved with the help of the process of facilitating circular practices such as waste reduction and resource optimisation in real-time. While CPS demonstrate a negative and statistically non-significant indirect effect (B= –0.007, p=0.725) and IP shows a non-significant indirect impact (B=–0.004, p=0.866), indicating that technological integration alone does not enhance sustainability unless aligned with circular practices.

DISCUSSION

The findings reveal a detailed and complex relationship between Industry 4.0 technologies and sustainability performance in China's textile sector. BD demonstrates a significant positive direct effect on sustainability, supporting the idea that data-driven insights enhance operational efficiency and reduce environmental burdens [54]. The ability to collect, process, and act on large volumes of production data facilitates real-time decision-making and resource optimisation, promoting greener manufacturing practices [24, 55]. The mediation analysis confirms that BD indirectly contributes to sustainability through CEP. This suggests that firms using analytics for material flow tracking, waste detection, and predictive maintenance are better equipped to implement CEP strategies like recycling and resource minimisation [6]. The dual direct and indirect effects of BD affirm its role as a strategic resource in line with the RBV [19, 22].

The direct effect that SF systems had on sustainability was not that significant, meaning that the sustainability of the environment cannot be secured in automated and digitised environments; there have to be other factors to consider. This result aligns with current insights that smart systems need to be deliberately associated with sustainability goals in order to create value. Nevertheless, the indirect effect of SF was significant and high, which means that by combining it with circular processes, including but not confined to the remanufacturing process, energy recapture or closed-loop material utilisation, smart factories can contribute to sustainability [16, 26]. This

Table 5

INDIRECT EFFECT					
	Original sample	**(M)**	**Standard deviation**	**T statistics**	**P values**
BD → CEP → SS	0.028	0.028	0.014	2.002	0.045
SF → CEP → SS	0.090	0.090	0.026	3.435	0.001
CPS → CEP → SS	–0.007	–0.007	0.019	0.352	0.725
IOT → CEP → SS	0.297	0.296	0.050	5.921	0.000
IP → CEP → SS	–0.004	–0.004	0.021	0.169	0.866

Note: BD (Big Data), SS (Sustainability), SF (Smart Factory), CPS (Cyber-Physical Systems), IOT (Internet of Things), IP (Interoperability).

affirms the perspective that technological possibilities should be powered by process-focused structures in a bid to release their potential on the environment.
The direct impact of CPS was high, although CEP did not have an influence on sustainability. This implies that CPS, as a means of providing real-time access to control over physical processes, influences the enhancement of production efficiency and minimises environmental damage even without a formal integration of CEP [27, 56]. Nevertheless, such limited mediation by CEP can suggest that there is a deficit in how the textile companies apply CPS to the higher-end circular processes, such as adaptive reuse or reverse logistics [22]. Therefore, CPS helps to sustain a business in the operating sense, but its capabilities related to circular change in the entire system are unexploited.
The IoT did not exert any direct impact but was highly mediated by CEP. This means that the sustainability advantages of IoT are achieved only when integrated into the models of circles. The ability of IoT to deliver real-time information throughout the supply chain, such as monitoring the use of water, energy, and materials, can be useful in the recycling process, eco-design, and lifecycle monitoring [11]. Thus, IoT itself might not be a sustainability driver, but its combination with CEP plays a key role in the achievement of resource circularity and environmental performance [12, 17].
IP did not have any significant direct or mediated effect on sustainability. Although it is viewed as a fundamental and necessary supporting factor of integrated systems, its ability to impact environmental outcomes seems to be minimal unless it is strategically connected to the idea of the circle or green. This finding indicates that companies can have interoperable platforms but fail to use them to drive sustainability-based cooperation, which is an aspect of maturity or implementation gap.

CONCLUDING REMARKS

Theoretical implications

This study makes several important contributions to the theoretical understanding of sustainability and digital transformation in the context of emerging economies, specifically within the textile industry. The research helps to prove that advanced technologies like BD, CPS, and IoT may be considered as useful, rare, inimitable, and non-substitutable (VRIN) resources due to the use of the RBV [19, 22]. The study builds upon RBV by showing that the entire potential of these technologies in creating sustainability is achieved when they are incorporated into complementary capabilities, which is CEP. This emphasises the fact that technology is not the only answer to high environmental performance, but organisational routines and systems, including those relating to circularity, are essential intermediaries. The substantial mediation of CEP in the connection between such technologies as IoT and sustainability also contributes to the development of knowledge regarding the interactions between the elements of Industry 4.0 in the organisational settings. Moreover, the paper contributes to the empirical complexity of the discussion on digital sustainability by examining an industry and a geographic area that has been under-researched, the textile industry in China. The previous research concentrated more on developed economies; therefore, the current research offers contextual information that can expand the applicability of digital-sustainability theories to developing economies. Though several studies have been conducted on Industry 4.0 and sustainability in the automotive, electronics, and energy sectors in China, the textile industry is a different scenario. The fact that textile manufacturing involves the intensive use of water, chemicals, and energy, and massive production of waste, is unlike these high-tech or capital-intensive industries. It is also characterised by a more fragmented supply chain that has many small and medium-sized businesses that do not always have developed digital infrastructure [7, 8]. The textile industry is both urgent and tricky to investigate the issue of how Industry 4.0 technologies can facilitate sustainable and circular change due to these structural and environmental issues.
This observation is in line with the more general evidence that the practices of the circular economy, especially recycling and the use of secondary raw materials, are significant processes that can be used to attain sustainable industrial development.
Vuckovski et al. (2025) [57] attest to the fact that the implementation of circular processes in the European industries is a highly effective way to increase the efficiency and sustainability outcomes of resources. This supports the conclusion of the current study that the combination of digital technologies and the practices of a circular economy can enhance environmental and operational performance in the manufacturing industries like textiles [58–60].

Practical implications

The findings of the study are practical recommendations to the managers of the textile industries, technology suppliers, and policymakers who are interested in enhancing sustainability through the digital transformation. To begin with, the results indicate that the investment in technologies, including BD and CPS, can directly lead to changes in sustainability, in particular, when they are implemented in order to monitor the utilisation of resources, decrease the quantity of waste, and enhance real-time decision-making. It means that these technologies should be prioritised by the companies regarding budgetary allocation for digitalisation. However, the strategic integration is needed based on the indirect, yet beneficial effect of SF and IoT on CEP practices. Not only are managers expected to adopt technologies, but they are expected to redesign business processes in a way that will promote recycling, reuse, and management of products and product life cycles. This integration plays a critical role towards the achievement of the environmental goals and should be

included in the training and operation planning. The lack of importance of interoperability demonstrates that simple linking of systems is not enough; the companies should ensure that digital linkage is aligned with sustainability goals. The policymakers can promote these changes by providing incentives, regulatory support, and digital infrastructure that would respond to the green industrial practices. This is especially true in the instance of developing economies like China, where the inefficiencies in resources and the outdated manufacturing systems are prevalent. The incentive to use technology with the help of subsidies or tax relief can accelerate the shift to the production that is circular and green production, and sustainability audits can help to accelerate this process. The suppliers of technology will have to develop solutions, which would not only make the productivity more productive, but also enable tracking the environment, and it will be easier to correlate the digital strategy of the firms with the indicators of sustainability.

Limitations and future directions

Although the current research offers significant information on how Industry 4.0 technologies and CEP can be used to improve sustainability in the Chinese textile industry, several shortcomings must be acknowledged. The research was cross-sectional, and this limits the ability to establish a cause-and-effect relationship between variables. The longitudinal research would also give an additional perspective on the transformation of the technological adoption and sustainability performance. The study had only covered textile firms in mainland China, and this might have limited the extension of the findings to other regions or industries. Further research can expand the geographical scope or focus on other sectors with similar environmental and digitalisation concerns, such as the leather, ceramics, or agro-processing sectors. Although the study has covered five key Industry 4.0 technologies, it has not taken into account the other emerging digital technologies, such as blockchain, artificial intelligence, or digital twins, which can also make a more significant contribution to sustainability. The digital transformation knowledge base would be improved through the introduction of more technologies in future models. The study was founded on self-reported survey data that may be influenced by response bias or social desirability. The reliability of the data would be enhanced by the mixed-method approach or by the third-party assessments. Even though the CEP was a mediator, other organisational capabilities such as green innovation, dynamic capabilities, or environmental leadership may be required as key mediators or moderators. These variables should be researched in the future to come up with a more comprehensive framework. The constraints will be discussed to advance the degree of theoretical understanding and applied research of digital sustainability, particularly in the context of the developed economies.

REFERENCES

[1] Sharma, H.B., Vanapalli, K.R., Samal, B., Cheela, V.S., Dubey, B.K., Bhattacharya, J., *Circular economy approach in the solid waste management system to achieve UN-SDGs: Solutions for post-COVID recovery*, In: Science of the Total Environment, 2021, 800, 149605

[2] Andronie, M., Lăzăroiu, G., Ștefănescu, R., Uță, C., Dijmărescu, I., *Sustainable, smart, and sensing technologies for cyber-physical manufacturing systems: A systematic literature review*, In: Sustainability, 2021, 1, 3, 10, 5495

[3] Jamwal, A., Agrawal, R., Sharma, M., Giallanza, A., *Industry 4.0 technologies for manufacturing sustainability: A systematic review and future research directions*, In: Applied Sciences, 2021, 11, 12, 5725

[4] Rathore, B., *Textile Industry 4.0 transformation for sustainable development: prediction in manufacturing & proposed hybrid sustainable practices*, In: Eduzone: International Peer-Reviewed/Refereed Multidisciplinary Journal, 2022, 11, 1, 223–241

[5] Hazen, B.T., Russo, I., Confente, I., Pellathy, D., *Supply chain management for circular economy: conceptual framework and research agenda*, In: The International Journal of Logistics Management, 2021, 32, 2, 510–537

[6] Liu, L., Song, W., Liu, Y., *Leveraging digital capabilities toward a circular economy: Reinforcing sustainable supply chain management with Industry 4.0 technologies*, In: Computers & Industrial Engineering, 2023, 178, 109113

[7] Jianguo, D., Solangi, Y.A., *Sustainability in China's textile industry: analyzing barriers and strategies for green supply chain management implementation*, In: Environmental Science and Pollution Research, 2023, 30, 20, 58109–58127

[8] Bibi, S., Khan, A., Fubing, X., Jianfeng, H., Hussain, S., *Integrating digitalization, environmental innovations, and green energy supply to ensure green production in China's textile and fashion industry: environmental policy and laws optimization perspective*, In: Environment, Development and Sustainability, 2024, 1–41

[9] Hassan, N.M., Khan, S.A.R., Ashraf, M.U., Sheikh, A.A., *Interconnection between the role of blockchain technologies, supply chain integration, and circular economy: A case of small and medium-sized enterprises in China*, In: Science Progress, 2023, 106, 3, 00368504231186527

[10] Karmaker, C.L., Al Aziz, R., Ahmed, T., Misbauddin, S.M., Moktadir, M.A., *Impact of industry 4.0 technologies on sustainable supply chain performance: The mediating role of green supply chain management practices and circular economy*, In: Journal of Cleaner Production, 2023, 419, 138249

[11] Kamble, S.S., Gunasekaran, A., *Analysing the role of Industry 4.0 technologies and circular economy practices in improving sustainable performance in Indian manufacturing organisations*, In: Production Planning & Control, 2021, 34, 10, 887–901, https://doi.org/10.1080/09537287.2021.1980904

[12] Abbas, S., Halog, A., *Analysis of Chinai textile industry: recommendations towards circular and sustainable production. In Circular economy: assessment and case studies,* Singapore: Springer Singapore, 2021, 77–111
[13] Imran, S., Mujtaba, M.A., Zafar, M.M., Hussain, A., Mehmood, A., Farwa, U.E., Saleel, C.A., *Assessing the potential of GHG emissions for the textile sector: A baseline study*, In: Heliyon, 2023, 9, 11
[14] Mageto, J., *Big data analytics in sustainable supply chain management: A focus on manufacturing supply chains*, In: Sustainability, 2021, 13, 13, 7101
[15] Bag, S., Dhamija, P., Luthra, S., Huisingh, D., *How big data analytics can help manufacturing companies strengthen supply chain resilience in the context of the COVID-19 pandemic*, In: The International Journal of Logistics Management, 2023, 34, 4, 1141–1164
[16] Ryalat, M., ElMoaqet, H., AlFaouri, M., *Design of a smart factory based on cyber-physical systems and Internet of Things towards Industry 4.0.* In: Applied Sciences, 2023, 13, 4, 2156
[17] Jayashri, N., Rampur, V., Gangodkar, D., Abirami, M., Balarengadurai, C., Kumar, A., *Improved block chain system for high secured IoT integrated supply chain*, In: Measurement: Sensors, 2023, 25, 100633
[18] Turskis, Z., Šniokienė, V., IoT-Driven Transformation of Circular Economy Efficiency: An Overview. Mathematical and Computational Applications, 2024, 29, 4, 49
[19] Barney, J., *Firm resources and sustained competitive advantage*, In: Journal of Management, 1991, 17, 1, 99–120
[20] Wernerfelt, B., *A resource-based view of the firm*, In: Strategic Management Journal, 1984, 5, 171–180
[21] Petrillo, A., Rehman, M., Baffo, I., *Digital and Sustainable Transition in Textile Industry through Internet of Things Technologies: A Chinai Case Study*, In: Applied Sciences, 2024, 14, 13, 5380
[22] Hart, S.L., *A natural-resource-based view of the firm*, In: The Academy of Management Review, 1995, 20, 4, 986–1014, https://doi.org/10.2307/ 258963
[23] Niu, Y., Ying, L., Yang, J., Bao, M., Sivaparthipan, C.B., *Organizational business intelligence and decision making using big data analytics*, In: Information Processing & Management, 2021, 58, 6, 102725
[24] Malik, S., *Data-Driven Decision-Making: Leveraging the IoT for Real-Time Sustainability in Organizational Behavior*, In: Sustainability, 2024, 16, 15, 6302
[25] Ulhe, P.P., Dhepe, A.D., Shevale, V.D., Warghane, Y.S., Jadhav, P.S., Babhare, S.L., *Flexibility management and decision making in cyber-physical systems utilizing digital lean principles with Brain-inspired computing pattern recognition in Industry 4.0,* In: International Journal of Computer Integrated Manufacturing, 2024, 37, 6, 708–725
[26] Sharifian, H., Abedi, Z., Amidpour, M., Hemmasi, A., Ghaffarzadeh, H., *Energy footprint assessment in oil refineries based on green productivity techniques and tools, case study: Iran*, In: International Journal of Environmental Science and Technology, 2021, 1–18
[27] Oks, S.J., Jalowski, M., Lechner, M., Mirschberger, S., Merklein, M., Vogel-Heuser, B., & Möslein, K.M., *Cyber-physical systems in the context of industry 4.0: A review, categorization and outlook*, In: Information Systems Frontiers, 2024, 26, 5, 1731–1772
[28] Aron, C., Sgarbossa, F., Ballot, E., Ivanov, D., *Cloud material handling systems: A cyber-physical system to enable dynamic resource allocation and digital interoperability*, In: Journal of Intelligent Manufacturing, 2024, 35, 8, 3815–3836
[29] Ilieș, D.C., Safarov, B., Caciora, T., Ilieș, A., Grama, V., Ilies, G., Huniadi, A., Zharas, B., Hodor, N., Sandor, M., Zsarnóczky, M.B., Pantea, E., Herman, G. V., Dejeu, P., Szabo-Alexi, M., Denes David, L., *Museal Indoor Air Quality and Public Health: An Integrated Approach for Exhibits Preservation and Ensuring Human Health*, In: Sustainability, 2022, 14, 4, 2462, https://doi.org/10.3390/su14042462
[30] Qiu, F., Kumar, A., Hu, J., Sharma, P., Tang, Y.B., Xu Xiang, Y., Hong, J., *A Review on Integrating IoT, IIoT, and Industry 4.0: A Pathway to Smart Manufacturing and Digital Transformation*, In: IET Information Security, 2025, 1, 9275962
[31] Chauhan, S., Singh, R., Gehlot, A., Akram, S.V., Twala, B., Priyadarshi, N., *Digitalization of supply chain management with industry 4.0 enabling technologies: a sustainable perspective*, In: Processes, 2022, 11, 1, 96
[32] Larabi, C., *Linking intangible resources to predict firm performance through technology innovation and strategic flexibility: leveraging the resource-based view of the manufacturing firms*, In: Journal of Strategy and Management, 2025
[33] Ameri, F., Sormaz, D., Psarommatis, F., Kiritsis, D., *Industrial ontologies for interoperability in agile and resilient manufacturing*, In: International Journal of Production Research, 2022, 60, 2, 420-441
[34] Getahun, S., Kefale, H., Gelaye, Y., *Application of precision agriculture technologies for sustainable crop production and environmental sustainability: A systematic review*, In: The Scientific World Journal, 2024, 1, 2126734
[35] Olatomiwa, L., Ambafi, J.G., Dauda, U.S., Longe, O.M., Jack, K.E., Ayoade, I.A., Sanusi, A.K., *A review of Internet of Things-based visualisation platforms for tracking household carbon footprints*, In: Sustainability, 2023, 15, 20, 15016
[36] Urbani, R., Ferreira, C., Lam, J., *Managerial framework for evaluating AI chatbot integration: Bridging organizational readiness and technological challenges*, In: Business Horizons, 2024, 67, 5, 595–606
[37] Gül, H., Çağatay, S., Gartner, W.C., *Fossil fuel and resource use impacts of raw material substitution and recycling in tourism sector in Türkiye: Evidence from circular economy adjusted input-output matrix*, In: Current Issues in Tourism, 2025, 28, 15, 2480–2499
[38] Ramani, V., De Giovanni, P., *Circular economy business strategies and public schemes: a game theory-based survey*, In: International Transactions in Operational Research, 2025
[39] Singh, R., Joshi, A., Dissanayake, H., Nainanayake, D., Kumar, V., *Harnessing artificial intelligence and human resource management for circular economy and sustainability: A conceptual integration*, In: Sustainability, 2025, 17, 15, 7054
[40] Creswell, J.W., Inoue, M., *A process for conducting mixed methods data analysis*, In: Journal of General and Family Medicine, 2025, 26, 1, 4–11

[41] Pittri, H., Godawatte, G.A.G.R., Esangbedo, O.P., Antwi-Afari, P., Bao, Z., *Exploring barriers to the adoption of digital technologies for circular economy practices in the construction industry in developed countries: A case of Ghana*, In: Buildings, 2025, 15, 7, 1090
[42] Costello, A.B., Osborne, J., *Best practices in exploratory factor analysis: four recommendations for getting the most from your analysis*, In: Practical Assessment, Research, and Evaluation, 2005, 10, 7, 1–9
[43] Hair, J.F., Astrachan, C.B., Moisescu, O.I., Radomir, L., Sarstedt, M., Vaithilingam, S., Ringle, C.M., *Executing and interpreting applications of PLS-SEM: Updates for family business researchers*, In: Journal of Family Business Strategy, 2021, 12, 3, 100392
[44] Sekaran, U., *Research methods for business: A skill building approach (4th ed.)*, Hoboken, NJ: John Wiley and Sons, 2003
[45] Podsakoff, P.M., MacKenzie, S.B., Podsakoff, N.P., *Sources of method bias in social science research and recommendations on how to control it*, In: Annual Review of Psychology, 2012, 63, 1, 539–569
[46] Hair, J.F., Sarstedt, M., Ringle, C.M., Mena, J.A., *An assessment of the use of partial least squares structural equation modeling in marketing research*, In: Journal of the academy of marketing science, 2012, 40, 414–433
[47] Byrne, B.M., *Structural Equation Modeling With AMOS: Basic Concepts, Applications, and Programming*, New York: Routledge, 2010
[48] Oke, J., Akinkunmi, W.B., Etebefia, S.O., *Use of correlation, tolerance and variance inflation factor for multicollinearity test*, In: GSJ, 2019, 7, 5, 652–659
[49] Vinzi, V.E., *Handbook of partial least squares*, 2010
[50] Wasko, M.M., Faraj, S., *Why should I share? Examining social capital and knowledge contribution in electronic networks of practice*, In: MIS Quarterly, 2005, 35–57
[51] Henseler, J., Ringle, C.M., Sarstedt, M., *Testing measurement invariance of composites using partial least squares*, In: International Marketing Review, 2016, 33, 3, 405–431
[52] Fornell, C., Larcker, D.F., *Evaluating structural equation models with unobservable variables and measurement error,* In: Journal of Marketing Research, 1981, 18, 1, 39–50
[53] Hair, J.F., Black, W.C., Babin, B.J., Anderson, R.E., *Multivariate data analysis*, New Jersey: Prentice Hall, 2010
[54] Di Maria, E., De Marchi, V., Galeazzo, A., *Industry 4.0 technologies and circular economy: The mediating role of supply chain integration*, In: Business Strategy and the Environment, 2022, 31, 2, 619–632, https://doi.org/10.1002/bse.2940
[55] Bag, S., Dhamija, P., Singh, R.K., Rahman, M.S., Sreedharan, V.R., *Big data analytics and artificial intelligence technologies based collaborative platform empowering absorptive capacity in health care supply chain: An empirical study*, In: Journal of Business Research, 2023, 154, 113315
[56] Sheikh, Z.A., Singh, Y., Singh, P.K., Ghafoor, K.Z., *Intelligent and secure framework for critical infrastructure (CPS): Current trends, challenges, and future scope*, In: Computer Communications, 2022, 193, 302–331
[57] Vučkovski, B.G., Ćurčić, N.V., Gheorghe, I.G., *Circular Economy as a Driver of Sustainable Growth: Quantitative Analysis of the Role of Recycling and Secondary Raw Materials in the EU*, In: Sustainability, 2025, 17, 11, 5181, https://doi.org/10.3390/su17115181
[58] Apostu, S.A., Hussain, A., Kijkasiwat, P., Vasa, L., *A comparative study of the relationship between circular economy, economic growth, and oil price across South Asian countries*, In: Frontiers in Environmental Science, 2022, 10, 1036889, https://doi.org/10.3389/fenvs.2022.1036889
[59] Junejo, I., Hossain, M.B., Abid, S., Janjua, Q.R., Ejaz, S., Vasa, L., *Supply chain integration and supply chain performance: evidence from the textile industry*, In: Industria Textila, 2024, 75, 4, 396–404, https://doi.org/10.35530/IT.075.04.2023110
[60] Chopra, R., Agrawal, A., Sharma, G. D., Kallmuenzer, A., Vasa, L., *Uncovering the organizational, environmental, and socio-economic sustainability of digitization: evidence from existing research*, In: Review of Managerial Science, 2024, 18, 2, 685–709, https://doi.org/10.1007/s11846-023-00637-w

Authors:

KUN HU[1,2], WANHUA KUANG[2], QUANDE QIN[3], JIANUO WANG[4], MD BILLAL HOSSAIN[5]

[1]College of Modern Tourism Industry, Guizhou University of Finance and Economics, Guiyang 550025, Guizhou, China

[2]School of Finance, City University of Macau, Macau 999078, China
e-mail: evakhong@gmail.co

[3]School of Humanities and Social Sciences, Macao Polytechnic University, Macau 999078, China
e-mail: qinquande@gmail.com

[4]Huace Film Academy, Communication University of Zhejiang, Hangzhou 310018, Zhejiang, China
e-mail: ericyewu2020@163.com

[5]Sustainability Competence Centre, Széchenyi Istvàn University, 9026, Győr, Hungary

Corresponding authors:

KUN HU
e-mail: hukun202411@163.com
MD BILLAL HOSSAIN
e-mail: hossain.md.billal@sze.hu